Locating Services In Hybrid *Ad Hoc* Cellular Network

Jung Houn Yap

Submitted for the Degree of
Doctor of Philosophy
from the
University of Surrey

Centre for Communication Systems Research
School of Electronics and Physical Sciences
University of Surrey
Guildford, Surrey GU2 7XH, U.K.

July 2003

Abstract

The growing applications of mobile locating have received wide spread attention in recent years. For instance, the positioning of the mobile user equipment could provide a range of services like location-based services, location-sensitive billing, fraud detection, cellular network design and resource management, fleet management and intelligent transportation systems.

A novel user equipment positioning method in the hybrid *ad hoc* cellular system was investigated and its performance evaluated. This method is designed for the applications of the **LoCating Services** for the future wireless cellular system. In the hybrid ad hoc network, the UEs are able to perform peer-to-peer communications and interoperation with the cellular network. Allowing nearby UEs with geo-location information to function as a positioning element, this will mitigate the visibility problem usually encountered in the fixed infrastructure network-based positioning methods. Moreover, it also improves the accuracy of the estimated UE position. Therefore, a different UE positioning approach is derived and verified. The proposed locating method uses the time of arrival of signals transmitted by the cellular Node-B or nearby user equipments for ranging observations. The time of arrivals from the positioning elements is then used to estimate the position of the user equipment.

Additionally, it is known that the LoCating Services does not limit itself to external users and at the same time it is able to assist in network planning, better allocation of the valuable resources in the network, and improves on the present mobility management schemes. Therefore, two position enhanced mobility management algorithms are proposed. They are the position enhanced soft handover algorithm, and path selection algorithm in a relaying cellular network.

Key words: positioning, *ad hoc*, soft handover, relaying

Acknowledgements

I would like to acknowledge my supervisors Prof. Rahim Tafazolli and Prof. Barry Evan, for their guidance and support during my Ph.D program. Due to the nature of this research, having supervisors who are the leading experts in this field was invaluable.

Over the past three years financial support for this research has come from a number of sources. These sources include the Overseas Research Scholarship, Mobile VCE and University of Surrey.

Many thanks to my colleagues in Centre for Wireless Communication Systems Research (CCSR) at the University of Surrey. In particular, I would like to acknowledge the help of Dr. Shahram Ghaheri-Niri for his many constructive advices and discussions during the initial stage of my research program.

In addition, to my parents and sister for their never ending support and encouragement.

Contents

List of Figures

List of Tables

Glossary of Terms

2D	Two Dimensions
3D	Three Dimensions
3G	Third Generation
ActS	Active Set
A-GPS	Assisted GPS
AMP	Advance Mobile Phone
AoA	Angle of Arrival
AVM	automatic vehicle monitoring
AWGN	Additive White Gaussian Noise
CLOS	cellular LOS
CNLOS	cellular NLOS
CoDiT	Code Division Multiple Testbed
DoA	Direction of Arrival
DSP	digital signal processing
E-911	Enhanced-911
E-OTD	Enhanced Observe Time Difference
FCC	Federal Communications Commission
FDD	frequency division duplex
GCC	generalized cross-correlation
GPS	Global Positioning System
GSM	Global System for Mobile Communication
HAHCP	Hybrid *Ad Hoc* Cellular Positioning
HHO	hard handover

IPDL	Idle Period Downlink
ISM	Industrial Scientific and Medical
LAR	Location Aided Routing
LCS	LoCating Services
LLOS	local LOS
LMU	Location Measurement Unit
LNLOS	local NLOS
LOS	line-of-sight
MAC	Medium access control
MAHO	mobile assisted handover
MAI	multiple access interference
MCHO	mobile control handover
MonS	Monitored Set
NB	Node B
NLOS	non-line-of-sight
ODMA	Opportunity Driven Multiple Access
OTDoA	Observed-TDoA
PBRA	Position-based relaying algorithm
pCPICH	Primary common pilot channel
PE	Positioning Element
PERA	Position enhanced relaying algorithm
QoS	Quality of services
RDMAR	Relative Distance Micro-discovery Ad hoc Routing
RSS	Received Signal Strength
SA	Selectivity availability
SHO	soft handover
SQRA	Signal Quality-based relaying algorithm
TA	Timing Advance
TDD	time division duplex
TDoA	Time Difference of Arrival
ToA	Time of Arrival

ToT	time of transmission
UMTS	Universal Mobile Telecommunications System
UTRA	UMTS-terrestrial radio access system
WCDMA	Wideband Code Division Multiple Access
WLANs	Wireless Local Area Networks
α_i	incidence angle
β_i	estimate parameters
Δd	distance difference between two consecutive samples
Δh_b	NB antenna height measured from average roof top level
$\delta(t)$	dirac delta function
η	orthogonality factor
γ_e	environment constant
γ_{th}	matched filter threshold
$\Im$	fourier transform
$\Im^{-1}$	inverse fourier transform
κ	specific attenuation [dBm^{-1}]
λ	wavelength
Ω_i	mean power
ϕ_{sr}	cross-correlation function $r(t)$ and $s(t)$
$\Phi_{sr}(f)$	fourier transform of ϕ_{sr}
$\rho_s(\Delta d)$	shadowing normalized autocorrelation function
σ	standard deviation
$\sigma^2_{tt_{NB_m}}$	timing observation variance between target UE and NB_m
$\sigma^2_{tt_{UE_n}}$	timing observation variance between target UE and assisting UE_n
$\sigma^2_{xy_{UE_n}}$	horizontal coordinates variance of assisting UE_n
σ_n	noise variance
τ	delay
τ_{rms}	root mean square delay spread
Θ	UE moving direction with desired NB

θ	phase shift
ϱ	Gaussian random variable
$\vec{\beta}$	estimate matrix
$\vec{\Psi}$	true covariance matrix
b	observables matrix
$\vec{Q}$	covariance matrix
$\vec{x}$	coefficients matrix
a_{lg}	long-term fading
$a(t)$	amplitude of arrival
c	speed of light
d	distance between the transceivers
d_{cor}	shadowing de-correlation length
e_i	estimation error
$E <>$	expectation operator
err	Euclidean distance
err_{rms}	root mean squared error
$F_{z\|H_0}()$	cumulative distribution function of z under H_0
f_c	carrier frequency
G_{fh}	floor gain
ga	gain of antenna
$h(t,\tau)$	time varying channel of impulse respond
h_{NB}	height of NB
h_{UE}	height of UE
L_{LLOS}	LLOS survival length
m_i	Nakagami-m fading
n	AWGN noise
$N[m,\sigma]$	normal distribution, with mean equals to m and standard deviation equals to σ
P_{FA}	probability of the false alarm
P_{LLOS}	probability of having LLOS
PL	path-loss

R_{bit}	data bit rate
R_{chip}	chip rate
R_s	selected relaying route
rms	root mean square
S_r	sampling rate
$u(t)$	root-raise cosine filter
$U[min, max]$	uniformly distributed within min and max
v	UE velocity

Chapter 1

Introduction

1.1 Introduction

The growing applications of mobile locating have received wide spread attention in recent years. For instance, the positioning of the mobile user equipment (UE) could provide a range of services like location-based services, location-sensitive billing, fraud detection, cellular network design and resource management, fleet management and intelligent transportation systems [1]. For example, imagine you arrive in a new city; it's late and raining hard. You don't speak the language and have no local currency in your pocket. You take out your handset and dial into the location-based services application. Within minutes you have found the nearest cash machine. With money in your pocket, you are able to get a taxi and direct the driver to the hotel that you found from the location-based hotel service. On the way to the hotel, you decided to plan for your next day excursion. You type into a routing service and put together an itinerary that takes you through the countryside, shopping at all the points of historical interest along the way. Such are the promises of location-based services. Along with this explosion of applications has come an ever-increasing demand for improved accuracy and reliability.

1.2 Motivation for Research

The most immediate motivation for the cellular network to provide UE geo-location is Enhanced-911 (E-911) emergency services. In June of 1996, the Federal Communications Commission (FCC) [2] in United States requires all network providers to be able to determine all the UEs locations within an accuracy of 100 meters in 67% of call measurements for network-based system and 50 meters in 67% of call measurements for handset-based system.

Furthermore, in recent years the mobile communications market has been growing rapidly, and therefore there is a need to provide new services in order to capture larger market share. With the introduction of position-based services, the operators can offer new services like locating the nearest service, accessing traffic news, getting help with navigating in an unfamiliar city, obtaining a local street map, and these are just a few of many location-based services that offered a new source of revenue for the operators. It is speculated that by year 2005, the European market for information services would represent a total revenue of US$ 13.5 billion [3].

In addition, the network-based positioning methods could be used as a backup system for the Global Positioning System (GPS). Although a UE equipped with a GPS receiver could achieve highly accurate location reading, but the GPS receiver would suffer from cold start and indoor coverage problems. As a result, network-based methods can assist in positioning when the GPS service is not available.

1.3 Research Objectives

The principle objective of this research is to develop a network-based UE locating method in a hybrid *ad hoc* cellular network. It mitigates the inaccuracy of the estimated UE position and improves the hearability (ability to detect sufficient numbers of positioning transmitters to estimate its location) of the UE. Another objective is to incorporate UE position information for mobility management, such as, handover and relaying algorithms.

These objectives are met through simulations, which are carried out for timing observation in the presence of non-line-of-sight (NLOS) links between the UE and positioning elements (PE), multipath, and position estimation algorithm for the hybrid *ad hoc* network. Simulations were also used to verify the performances of the position enhanced handover and relaying algorithms.

1.4 Research Contributions

In response to the FCC and the LoCating Services (LCS) for the future cellular system, a collaborative research between the Centre of Communication Systems Research (University of Surrey) and Mobile VCE was undertaken to investigate UE positioning in a hybrid *ad hoc* cellular network. The research contributions presented in this thesis can be divided into four categories; covering UE positioning theory characterization and development, inaccuracy reduction of estimated UE position, impact of system parameters on positioning, and applications of UE positioning information on Mobility Management schemes. Lastly, a UK patent was filed for the work in UE positioning in hybrid *ad hoc* cellular network [4].

1.4.1 UE Geo-Locating Development

The first contribution is the characterization and development of UE positioning for the network-based positioning methods. While numerous fixed infrastructure network-based methods have been investigated, the dynamic *ad hoc*-based positioning method for the hybrid network has not been exploited.

In the hybrid network, the UEs are able to perform peer-to-peer communications and interoperation with the cellular network. The technological aspect for a multimode terminal interoperability in a hybrid network could be in different duplex modes, wireless local area networks (WLANs), Bluetooth, home RF networks, and *ad hoc* networks for the peer-to-peer side, GSM and WCDMA networks for the cellular side. Allowing nearby UEs with geo-location information to function as a PE, this will mitigate the visibility problem usually encountered in the fixed infrastructure network-based

positioning methods. Moreover, it also improves the accuracy of the estimated UE position. Therefore, a different UE positioning approach is derived and verified by computer simulation.

1.4.2 Co-relation between system parameters and LCS performance

The quality of services (QoS) of the LCS depends on system parameters, such as line-of-sight (LOS) links between the UE and PEs, the cell size, and physical channel condition. Accurate knowledge of these parameters is critical in effective deployment of LCS. For an example, would there be any effect on the hearability of the network-based positioning methods when the UE resides at the edge or at the centre of the cell? This is not thoroughly investigated because hearability of the UE is of lesser importance than the accuracy of the estimated UE position, which is of primary importance in LCS applications. However, if the UE is not within the transmission range of sufficient PEs, no trilateration can be computed. Therefore, it is important to address any factors that may hinder the performance of the LCS.

1.4.3 Position assisted Soft Handover

Coupled with the UE position information, the distance between the UE and Node B (NB), and UE trajectory can be computed for soft handover in the third generation (3G) wideband code division multiple access (WCDMA) system. The approach is based upon the distance and direction assisted handover algorithms presented by Niri and Tafazolli [5] and Austin and Stüber [6]. In this thesis, an adaptive handover algorithm is derived, using the UE location information approach as presented by these authors. As a further extension to their work, the distance and trajectory of the UE with respect to the desired NB are used to dynamically adjust the hysteresis margins of the handover algorithm, to encourage or discourage adding, dropping or replacing a NB to or from its active set. Using this method, the outage probability improvements are noted as well as the corresponding improvements to the active set update rate and mean active set number.

1.4.4 Position assisted Relaying

Finally, a relaying algorithm, which utilises the UE position information is developed. The earliest introduction of relaying to cellular network is from the Salbu R&D (Pty) Ltd named Opportunity Driven Multiple Access (ODMA) [7]. The basic concept is to use UEs located between the originating UE and the NB as a relay station, to combat coverage dead spots in a typical cellular network. The challenge is to select the most reliable immediate nearby UE to relay the data packet. In order to identify an effective nearby UE as a relayer, the UE position is used to compute the distances between the nearby UEs with the originating UE and its serving NB. The relayer identified can account for the link quality, for it is undesirable to use UE that is remote from the originating UE and its serving NB, and residing from the relaying network, respectively.

1.5 Thesis Overview

This thesis consists of 7 chapters. Chapter 2 is a discussion of the various approaches to cellular positioning and includes a literature review of past and concurrent research efforts. Chapter 3 gives an overview of the position enhanced mobility schemes, introducing the proposed position enhanced soft handover and relaying algorithms. The UE positioning in hybrid *ad hoc* cellular network will be presented in Chapter 4. Furthermore, a model that is suitable for evaluating the performance of locating service is given. In Chapter 5 the performance of position enhanced soft handover is presented under different scenarios. In Chapter 6 the position enhanced relaying algorithm for the hybrid *ad hoc* cellular network is considered to resolve coverage problem in conventional cellular network. Finally Chapter 7 contains the conclusion and proposed future works of the thesis.

Chapter 2

Cellular Positioning Techniques

2.1 Introduction

This chapter consists of three main sections. In the first section, the general methods of cellular positioning are discussed and compared. As each positioning method has its own unique characteristics, advantages and disadvantages. The second section gives an overview of the work already done in the area of mobile positioning. Although there are numerous positioning methods which could be used for LCS, however, emphasis will be placed on the time-based positioning techniques. For it is foresees to be the strongest candidate to be used in mobile positioning. In addition, models used for trilateration, their linearisation, and the mechanism of least-squares for estimating the UE position will be introduced. Finally, the positioning method in a hybrid network, as adopted in this thesis, is presented.

2.2 Approaches to Cellular Positioning

There are several proposed methods in positioning a UE for the cellular networks. However, only those methods that can be practically incorporated in a cellular-type system are discussed. Generally, they can be broadly classified into two categories, as illustrated in Figure 2.1. Those that place the positioning technology in the terminal may be classified as mobile terminal centric. The UE estimates its position and transmits

that information to the network. The biggest drawback of this method is the extra cost involved in reissuing new terminal. Additional hardware and modification may result in the increased weight and size of the terminals, which is contrary to consumer desires. The most obvious example of this type of approach is the inclusion of a GPS receiver in the UE.

The second group of methods is the network centric. In these methods, the positioning technology resides in the network rather than the UE. In this way, no modification in the terminal is necessary and this will be compatible with the UE currently in use. All the changes will be concentrated in the networks infrastructure, i.e., NB and the switching centre. This is by far the greatest advantage of this approach over the mobile terminal centric approach. It is obvious that this approach is the optimum solution for wireless E-911 in the near future, as it would work with the existing UE.

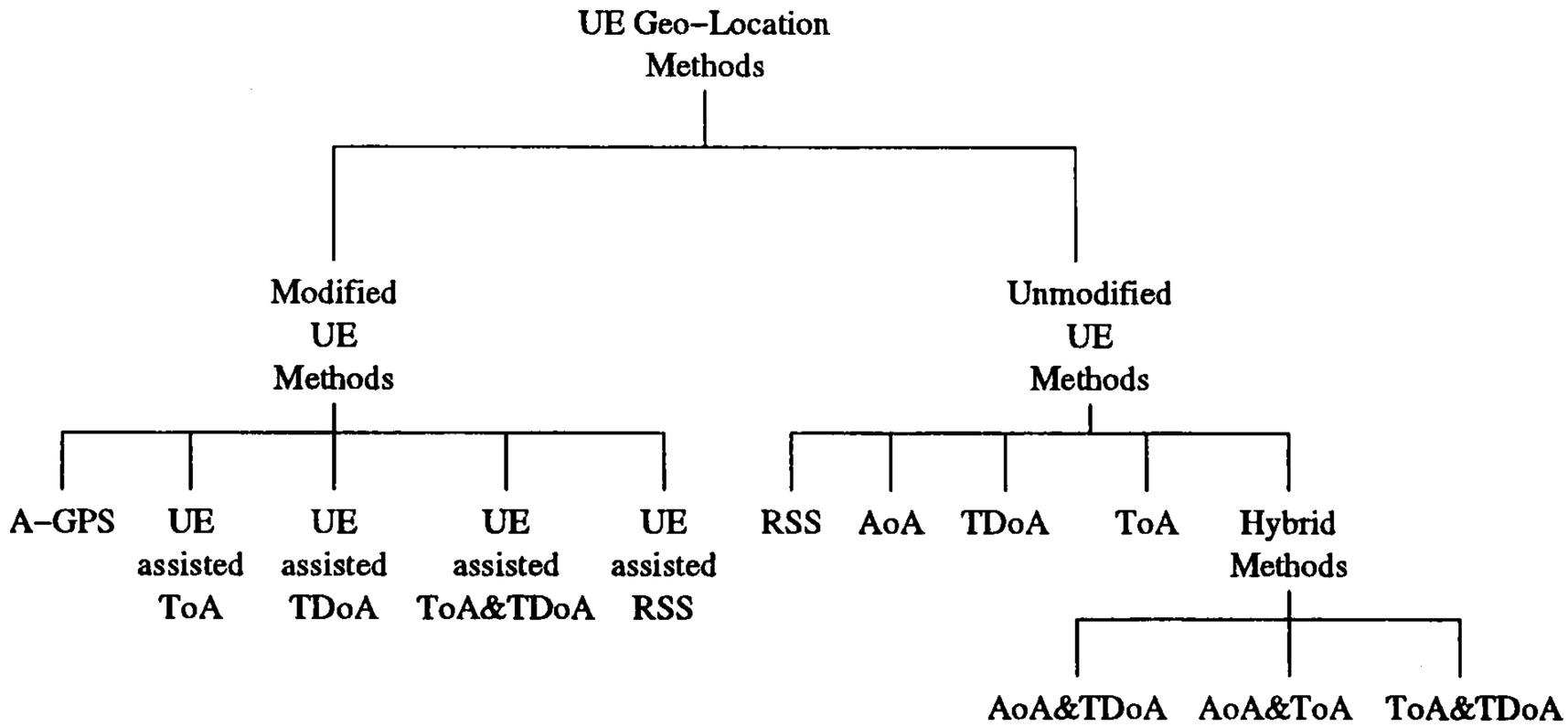

Figure 2.1: UE geo-location methods

2.2.1 Received Signal Strength (RSS)

This method works by measuring the signal strength of the received signal. Consider the scenario in Figure 2.2, the signal strength measurements are related to the path attenuation with respect to distance

$$P_r = P_t + ga - L_p - \gamma_e \log(d) + L_{sha} \tag{2.1}$$

where P_r is received power in dBW, P_t is transmitted power in dBW, ga is the gain of antenna in dBi, L_p and γ_e are environment constants, L_{sha} is lognormal distributed shadowing loss in dB and d is the distance between the transceivers in meters. Position may then be estimated by trilateration. Trilateration refers to the intersection of position lines formed by distances estimated, based on the path-loss equation (2.1). The UE must lie somewhere on a circle with a radius equal to the estimated distance and centred at the NB. Unless the UE is exactly midway between two NBs, the distance circles of two NBs will intersect at two points. Unless prior information is available, it may not be obvious which of the two intersections corresponds to the position estimate. For the cellular application, the distances involved require at least a third range, as in Figure 2.2, to identify the position sought. The fundamental problems associated with signal strength measurement are the multi-path fading, weather and shadowing. Figel et al. [8] suggested that individual estimates varies by 40dB and long term median yield estimates varying by 0.5dB. In addition, due to hearability reason it may not be possible to include large numbers of NBs for positioning. Secondly the signal attenuation has to be converted into distance, and the widely accepted empirical formulae [9] used do not account for local variations caused by actual terrain. So, new algorithm has to be formulated for range estimation using this method.

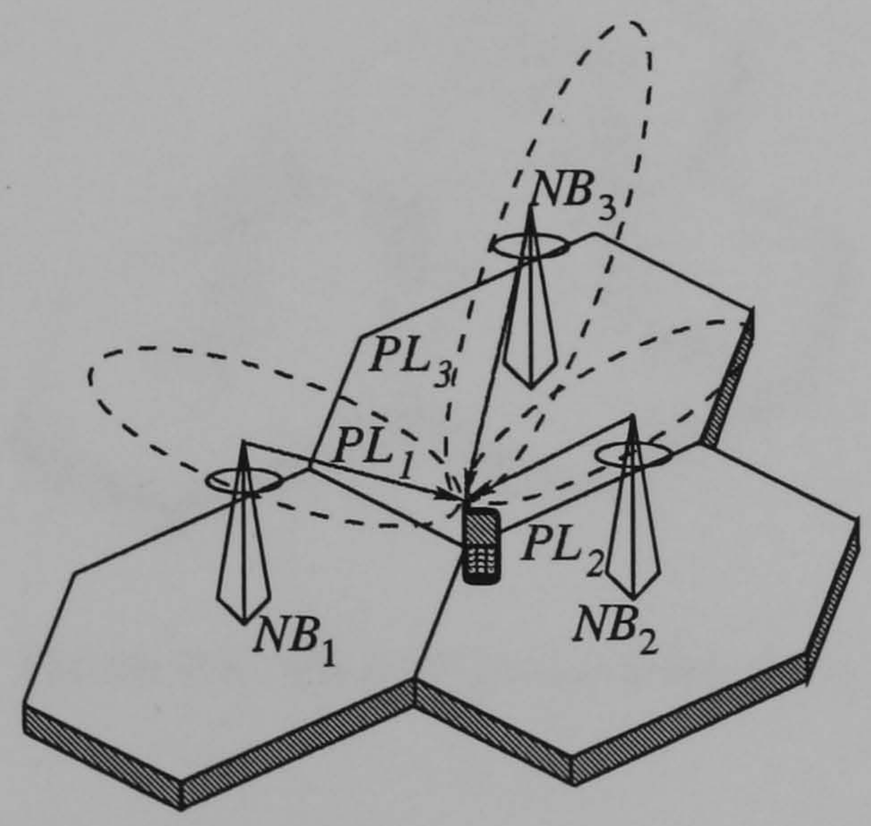

Figure 2.2: UE positioning using Signal Strength

2.2.2 Angle of Arrival (AoA)

This method, also referred to as Direction of Arrival (DoA), works by calculating the displacement angle of the UE at two or three NBs. It utilizes multi-array antennas to estimate the AoA of the signal of interest. A single AoA measurement will restrict the source location along a line in the estimated AoA. If at least two such AoA estimates are available from two antennas at different locations, the position of the signal source can be located at the intersection of the lines bearings from the two antennas [10].

Figure 2.3 shows the method where the UE location is found by triangulation, the intersection of bearings from three antennas array with known location. The drawback of AoA is the cost of installing these antennas, the direction finding antenna is expensive to install and the arrangement of the array have to be calibrated periodically because of winds or storms disturbing the displacement of the array. Another problem using this method is the complexity of signal processing. Usually the algorithms used tend to be highly complex because of the need for measurement, storage and usage of array calibration data and their computationally intensive nature. This method is also restricted to network centric as it is impractical to fix a multi-array antenna on the UE.

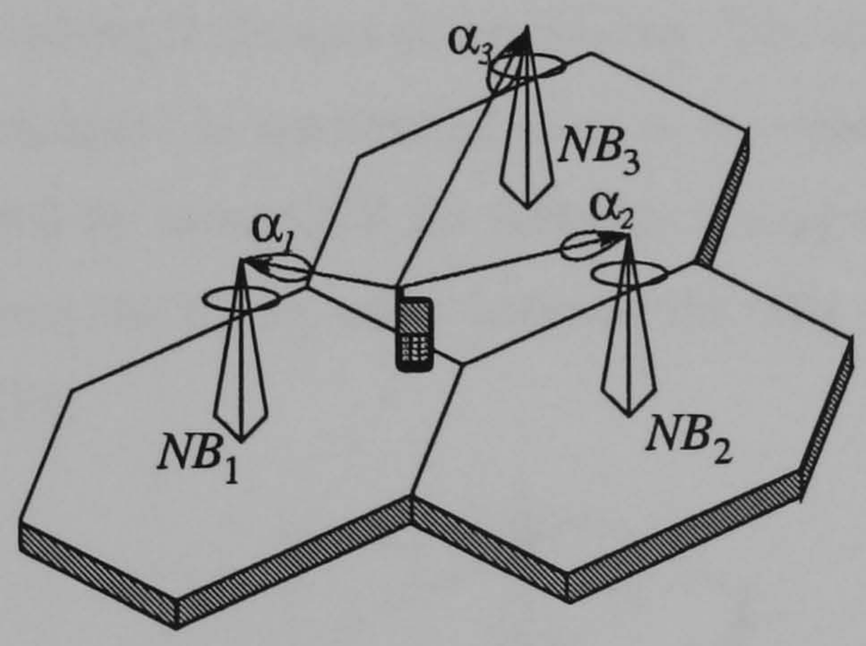

Figure 2.3: UE positioning using AoA

2.2.3 Time of Arrival (ToA)

The ToA works by estimating the propagation delay of the signal from the UE to the NBs or vice versa. As the electromagnetic waves propagate at the constant speed of

light ($c = 3 \times 10^8 \mathrm{m/s}$) in a free space medium, by knowing the Time of Arrival (ToA) of the signal, the distance between the transceiver may be determined by multiplying the propagation time by the propagation velocity c. The trilateration algorithm explained in section 2.2.1 is used to determine the UE position, and in this case the propagation delay of the signal is used to determine the distance between the transceivers.

2.2.4 Time Difference of Arrival (TDoA)

This method uses the difference in the arrival times of the signal from the source to the receiver. The lines of position are then defined as those for which the TDoA between two NBs is a constant, forming a hyperbola between the two NBs on which the UE may exist. This process is repeated with another NB in combination with any of the previously used NBs, the intersection of the two hyperbolas then estimates the position of the UE as illustrated in Figure 2.4. The use of TDoAs in this way is termed hyperbolic trilateration.

This method offers many advantages over other methods; it does not require the absolute time of transmission (ToT) from the transmitter like the ToA or specialized antenna like the AoA, making it cheaper to implement. The only drawback for TDoA is that all the NBs participate in positioning have to be clock synchronized. Nevertheless, this can be solved by using GPS for reference timing or using a receiver with known location to measure the timing offset between the NBs, also known as Location Measurement Unit (LMU).

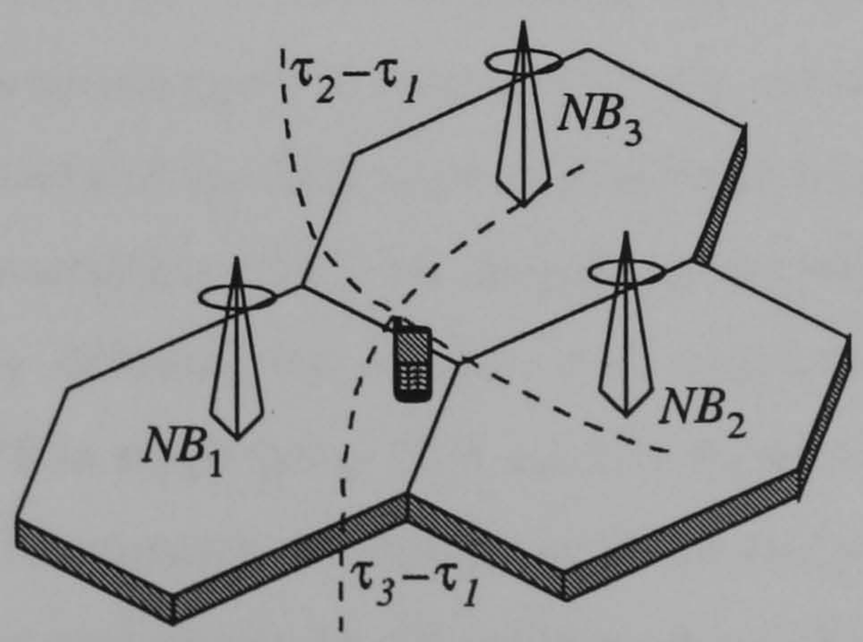

Figure 2.4: UE positioning using TDoA

2.2.5 Hybrid Methods

It is possible to combine methods mentioned in sections 2.2.1 to 2.2.4 into a hybrid positioning method. Using AoA with ToA or RSS only requires one NB to position the UE. This method allows UE to be positioned even when it is only within the transmission range of one NB. Therefore, mitigates the hearability problem. Or a hybrid between the ToA and TDoA suggested by Yost and Panchapakesan [11] would improve location estimation accuracy. However, it is an important issue in such systems to ensure both methods combine synergistically and that the inaccuracies from one method do not adversely affect overall position estimate.

2.2.6 Assisted GPS (A-GPS)

A-GPS is a satellite based positioning system designed to provide three dimensional position and velocity information 24 hours a day, in any weather, anywhere in the world [12]. GPS satellites orbits are circular at a 20,000 km altitude, with a period of 12 hours and at an inclination of 55°. The GPS satellites broadcast signals towards the earth that can be decoded by GPS receivers, enabling users to calculate their three dimensions (3D) positions in real time. The satellites broadcast on two frequencies, L1 at 1.57542GHz and L2 at 1.2276GHz. This allows corrections to be made to compensate for signal delay through the ionosphere. The L1 signal consists of the P-code and C/A code and L2 signal consist only the P-code. The C/A code (Gold code) is a repeated pseudo-random binary sequence of 1023 chips long, running at a rate of 1.023Mchip per second. The P code is encrypted to form the Y code, which cannot be decoded by a civilian user. The position of the GPS receiver is estimated by spherical trilateration. With the Selectivity availability (SA), an intentional degradation of GPS accuracy usually implemented by dithering the satellite clock correction parameters removed, the accuracy of the GPS in single point C/A mode is 10 meters in the horizontal and 30 meters in the vertical component. Although the GPS based system provides excellent positional accuracy, it is undesirable to ask millions of mobile users to purchase a UE (containing a GPS receiver) to ensure compatibility with the LCS. In addition, such a system would suffer from LOS, due to a free space path-loss in excess of 180dB as

GPS signals require a clear unobstructed path between the receiver and the satellites. Furthermore, GPS is also unavailable inside buildings, vehicles, underground, tunnels, etc., which maybe critical from an emergency point of view.

2.3 Previous Work in UE Positioning

Radio navigation systems have evolved in the last 50 years from cameras and star photographs to a satellite and portable receiver systems. The earliest precursor to the GPS is the BC-4 program, which was developed during the 1940s [13]. The BC-4 was an important breakthrough, but it was too fastidious to justify continual development and use, requiring clear skies and large and costly equipment.

The next system developed had fewer limitations that would prevent widespread use. HIRAN was an electromagnetic ranging system used during World War II to determine aircraft position. HIRAN's contribution to the modern GPS lies in studies about the Doppler effect that scientists made during its use. Because of their discoveries, positioning systems are now capable of determining precise positioning for locations all over the globe. The system established after HIRAN was TRANSIT, the Navy's Navigational Satellite System, created to find aircraft and sea-vessel coordinates. Around this time other systems were developed for similar purposes as well. Loran-C, Omega, VOR, Tacan, and VORTAC, were specifically integrated for naval and aircraft uses. These older systems provided valuable information that led to the most advanced system yet, the modern GPS.

In parallel with the development of the GPS, the vehicle location and navigation systems have attracted much attention in the early 1970s [14]. The very first conference that addressed the automatic vehicle monitoring (AVM) system issues is the Public Urban Locator System conference held in Washington DC, on 28 October 1968 [15]. It is to discuss the technologies and applications of AVM, where the positioning of a vehicle can be a stand-alone, satellite based and terrestrial radio based technologies. The UE positioning can be considered a special case of the boarder field of automatic vehicle navigation. One means of automatic vehicle location is positioning of a transmitter or

receiver located in the vehicle. This is similar to the application of UE positioning in that the transmitting or receiving device is now a mobile handset.

In the early 1970s, Turin et al. [16] simulated an urban vehicle monitoring system based on the urban multipath propagation measurement campaign conducted in the San Francisco [17]. Two vehicle navigation systems were considered, in which the ToA measurements were based on estimating the phase of a narrowband (25kHz) phase modulated signal and a wideband (10MHz) pulsed waveform. Simulations of the phase ranging for a dense urban environment resulted in a mean error of 441m and a standard deviation (σ) of 627m, for pulse ranging the corresponding values were 95m and 65m. A least-squares method was used to fit a position to the ToA estimate from a number of fixed reference sites. The resulting location error using four reference sites for phase ranging had a mean error of 202m and a σ of 262m. The corresponding values for pulse ranging were 60m and 50m.

Warren et al. [18] also conducted a vehicle locating experiment, based on the ToA distance measurement and hyperbolic trilateration method. Four position-monitoring stations were chosen to receive the frequency modulated signal emitted from the vehicle. The synchronising pulses from the standard television broadcast were used as a reference signal. The phase of the signal received by the monitoring stations were cross-correlated with the synchronising pulses, and ToA measurements were estimated. It was found that 67% of the two dimension (2D) position of the vehicle estimated having an error of less than 549m.

The estimated two dimension (2D) location of the vehicle was found to have 67% of the estimation having an error of less than 549m.

In recent years, the area of vehicle location, and more specifically cellular UE positioning, has attracted a large amount of interest. The Global System for Mobile Communication (GSM) and CDMA based networks, in particular, were intensively investigated. In the mid 1990s, Silventoinen and Rantalainen [19] conducted a trail for GSM network-based UE positioning. The measurement was carried out in an urban metropolitan city and a rural environment of 350km long route. The Timing Advance (TA) also known as Force Handover method was used to locate the UE position. The

TA method, which is similar to ToA, requires the network to force the UE to make a handover attempt from the servicing NB to one of the adjacent NB. The adjacent NB will measure the TA and then reject the handover request. This will continue until a sufficient number of TA measurements are completed. It was reported that the UE can be located over 92% and 71% of the time in the urban and rural environment, respectively. The mean location error was 500m and 90% of the errors were less than 900m.

Drane et al. [20] also carried out a field test on GSM 900 network-based positioning. A custom built receiver similar to a GSM terminal was used for the field test. They selected 10 sites along a straight section of a street close to downtown Sydney, at intervals of approximately 50m. The TDoA hyperbolic trilateration method was used and the estimated UE positions were found to have an average mean error of 151.2m and σ of 69.34m.

On par with the investigation of UE positioning for GSM, numerous investigation were done for the CDMA networks [21]. Hepsaydir [22] analysed the use of CDMA networks for UE positioning. Four cell sites were selected and the broadcast common pilot channel (CPICH) was used for TDoA measurement. Eight test points were selected amongst the cell sites and all had LOS with the UE. It was reported that the root mean square (rms) error was 182.6m and with a σ of 107.2m. Hepsaydir [22] also suggested pre-filtering the measurements that have large variance, and all measurements were averaged over 25 samples. With this simple filtering method, Hepsaydir [22] was able to reduce the rms error to 138.8m with a σ of 51.2m.

Aatique [23] also evaluated the TDoA method in the CDMA systems. Investing the feasibility and accuracy of TDoA under various system parameters. That includes varying conditions of Additive White Gaussian Noise (AWGN), Multiple Access Interference (MAI), power control and traffic loads. Wang et al. [24] also simulated positioning accuracy using Idle Period Downlink (IPDL) scheme to improve the visibility of adjacent NBs to the UE. The simulated results showed that the IPDL scheme can ease the CDMA near-far problem, but it requires muting the serving NB pilot transmission during the idle period.

The way in which the ranging estimates are processed in order to estimate position has also been investigated. Usually, to obtain a precise location estimate, the Taylor-series algorithm is commonly employed [25]. A set of non-linear equations will be linearised by the Taylor-series expansion. Giving an initial guess of the UE position, the estimate can be improved by iteratively solving the local linear least-squares solution. Smith and Abel [26] developed a closed form non-iterative least-squares algorithm, which compute a reference ToA measurement that minimises the least-squares equation error. The intermediate result is then used to obtain the final UE position. Chan and Ho [27] also proposed a non-iterative algorithm that is effective in locating the UE, based on intersections of hyperbolic curves define by the TDoA measurement. The solution is in closed-form, valid for both distant and close NBs, and is an approximation of the maximum likelihood estimator when the TDoA estimation errors are small.

A number of companies are developing cellular positioning systems. Cambridge Positioning Systems Limited CURSOR^{TM} uses the network-based TDoA, known as Enhanced Observe Time Difference (E-OTD) in GSM, for UE positioning [28]. As opposed to installing an expensive GPS receiver in every UEs. CURSOR^{TM} claims that using E-OTD to achieve a position accuracy of 50m for GSM network, fulfilling the FCC's E-911 regulations. It also offers a range of location-based applications for a wide variety of market sectors, providing operators with the opportunity to offer a range of tailored services, from fleet management to mobile tourist information guides, to their customers.

Cell-Loc Inc is another company which uses network-based TDoA to pin point the geolocation of the UE [29]. The UE will transmit a signal and receive by three or more NBs, where the TOA is estimated. A GPS receiver, operating in time-transfer mode, is located at each cell site to provide time synchronisation between the cells. The ToA estimates are differenced at a central processing sites to produce TDoA measurements. A 2D position is then estimated by hyperbolic trilateration through the use of least-squares method. This allows no changes in the UE since for all measurements are done at the network side. Cellocate^{TM} had conducted field trails on the Advance Mobile Phone (AMP) and CDMA networks, and they too claims that they are able to meet the stringent requirement of the FCC E-911 regulations.

SnapTrack^{TM} [30] is one of those companies that uses A-GPS method for UE positioning. SnapTrack^{TM} has developed a distributed server-aided digital signal processing (DSP)-based processing approach to UE positioning. It uses a reference GPS receiver to garter navigation message and differential correction data for all satellites in view. A location server will store the data and transmit to a UE on-demand basis. These aiding data will assist the GPS enable UE to extract pseudorange information. Enhancing the UE sensitivity, lower time-to-first-fix and power dissipation over the conventional GPS receiver. The SnapTrack^{TM} field test results show that their system is able to achieve 15m error in 68.3% of the estimates in the urban street of Tokyo and 29m error in the urban canyon downtown city of Denver. Achieving accuracy substantially better than the 50m error required by the FCC E-911.

2.4 Timing Estimation

In the previous section, network-based location by timing estimation was presented as a leading candidate to solve the UE geo-locating problem. Correlation of signals was discussed as a common method of estimating the propagation delay between the transceivers. This section will further explain the methods used in particular with the timing estimation by correlation.

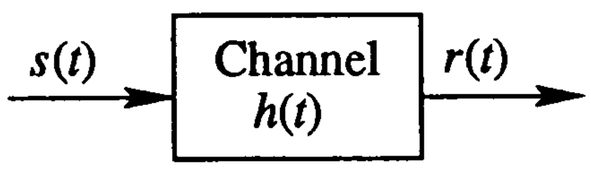

Figure 2.5: Wireless Communication Channel

In a wireless communication system, the signal is transmitted through free space. Hence, it is susceptible to noise corruption and very often, multi-path fading, which is presented in the simple block diagram of Figure 2.5. The multi-path propagation and fading, which are inherent in mobile communications, have a great influence on the UE positioning performance. Due to multi-path, the received signal is the sum of a number of attenuated, phase shifted, and time delayed replicas of the transmitted signal. If the individual arrivals in the impulse response are resolved and the first arrival corresponds

to the LOS path, then multi-path introduces no errors into the timing estimate. Many times, however, the individual arrivals are so close that they cannot be resolved, or the first arrival is too weak to be detected. In such a case, the time delay estimate will skew to the later arrivals, causing errors in UE geo-locating.

2.4.1 Channel Impulse Response

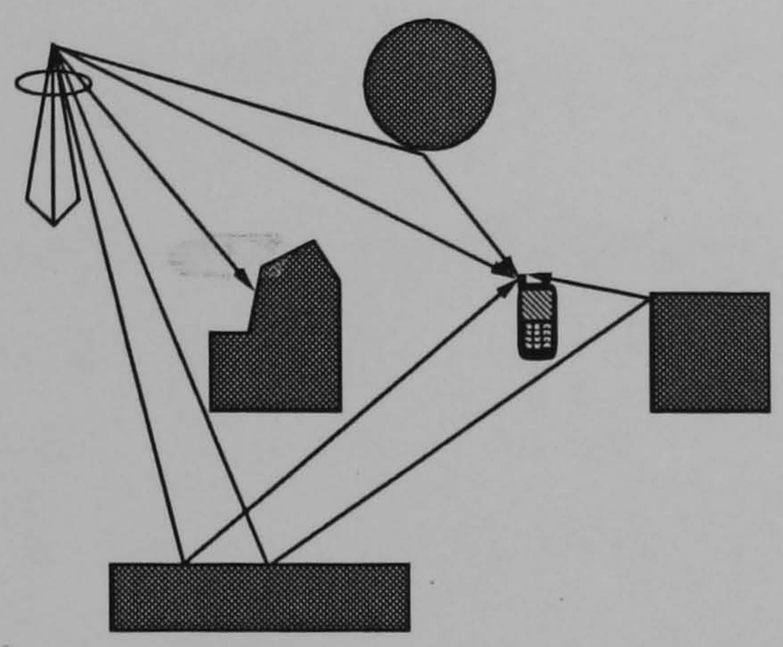

Figure 2.6: Typical multipath environment

Figure 2.6 shows a typical multi-path environment where a transmitter and receiver are surrounded by objects that reflect and scatter the transmitted energy, causing several waves to arrive at the receiver via different routes. Assuming the channel as a linear time-invariant filter, the channel impulse function $h(t)$ can be represented as [31]

$$h(t) = \sum_{i=0}^{L-1} a_i(t) e^{j\theta_i(t)} \delta(t - t_i) \tag{2.2}$$

where L is the number of multi-path arrivals, $a_i(t)$ is the amplitude of arrival i, $\theta_i(t)$ is the phase shift of arrival i, and $\delta(t)$ is the Dirac Delta function, commonly used to represent a unit impulse response. The received signal $r(t)$ can be found from convolving the transmitted $s(t)$ with the impulse response $h(t)$ of the channel, so it can be written as [31]

$$r(t) = \int_{-\infty}^{+\infty} h(\tau) s(t + \tau) d\tau + n(t) \tag{2.3}$$

where $n(t)$ is the additive Gaussian noise.

2.4.2 Impulse Response of Multi-path Channel

In timing estimation, we are not interested in determining the data of $r(t)$, but the first, and hopefully LOS arrival, t_o, which is the timing of interest. The discrete complex received signal of equation (2.3) can be written as the sum of a number of attenuated, phase shifted, and time delayed replicas of the transmitted signal [31].

$$r(t) = \sum_{i=0}^{L-1} a_i s(t - t_i) e^{j\theta_i} + n(t) \tag{2.4}$$

If $s(t) = \delta(t)$, then the magnitude of $|r(t)|$ and hence the magnitude of the impulse response $h(t)$, may appear like Figure 2.7.

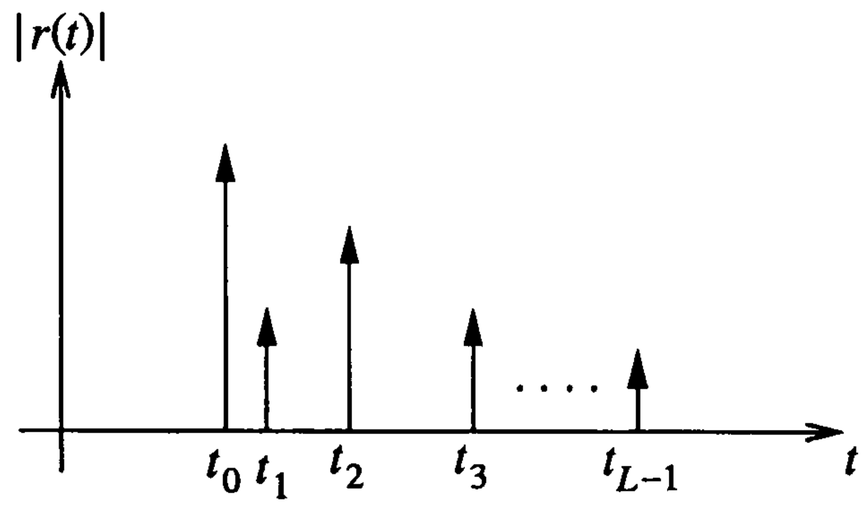

Figure 2.7: Power delay profile consisting of L scatterers

2.4.3 Path Loss and Shadowing

The second important factor of the wireless channel that attributes to the accuracy of UE geo-locating is the attenuation of signal, due to the path-loss associated with the distance between the transceiver. Usually, none of the PEs used for positioning have the same distance apart with the UE. So, it is important to consider only PEs that are within the transmission range of the UE. Okumura et al. [32] was one of the first to provide extensive measurement results made in and around Tokyo city between 200MHz and 2 GHz. Since then, many successive models evolved. By fitting the curves on the diagrams established experimentally by Okumura et al. [32], Hata [33] produced an empirical model in the form of a path-loss equation. This model is valid only for transmission around 150MHz to 1.5GHz, but was later extended to

cover the band of 1.5GHz to 2GHz transmission [34]. The model is further divided into open, suburban, and urban categories. The main parameters that determine the path-loss are the distance between the transceivers, the NB antenna height and carrier frequency. However, a number of correction factors are necessary to account for specific geographical terrain.

A more detail model for the dense urban environments with the NB antenna located above or slightly below the rooftop level for the adjacent buildings is the COST 231 - Walfisch-Ikegami model. This model is based on fairly detailed topographical information such as building density, average building height and street widths. The model works at its best when NB antenna is much higher than the building height because it does not consider the diffraction at street corners. For antenna height below the building roof top, an extended model [35] based on the recursive path-loss model proposed by Berg [36] can be used.

The path-loss models for the UE-to-UE have also been investigated and proposed. Harrold et al. [37] conducted a measurement programme to investigate the propagation issues relating to peer-to-peer communication link in the 2GHz frequency band. The measurements were taken in an indoor open-plan office environment, with both the transmitter and receiver having low height antenna at 2m. To account for the effect of how the terminal location in relation to the human body affects the reception, three different receiver scenarios like receiver held adjacent to the head, at the waist, and in a fabric bag were investigated. In order to represent the sort of terminal proposed for use in 3G network, a continuous wave signal at 2.1 GHz was generated and received by a narrowband receiver. The measurement data was compared with the free space path-loss model, and adjustment for different test scenarios with respect to the free space model is tabulated as follow

The path-loss models described usually assume that path-loss is a function only of parameters such as antenna heights, environment and distance. The predicted path-loss for a system operated in a particular environment will therefore be constant for a given pair of transceiver distance. In practice, however, the particular clutter (buildings, trees) along a path at a given distance will be different for every path, causing variations

		Transmitter					
		LOS			NLOS		
		Head	Pocket	Side	Head	Pocket	Side
Receiver	Head	−2	−1	7	0	5	6
	Pocket	−1	1	0	5	3	5
	Side	7	0	−1	6	5	8

Table 2.1: UE-to-UE path-loss with respect to free space

with respect to the nominal value given by the path-loss models. This phenomenon is called shadowing or slow fading. The spatial autocorrelation of the shadowing is characterised by a Gaussian distribution with zero mean and standard deviation [38], and its normalized autocorrelation function can be described as

$$\rho_s(\Delta d) = \exp^{-\frac{\Delta d}{d_{cor}} \ln 2} \tag{2.5}$$

where d_{cor} is the decorrelation length, and Δd is the distance difference between two consecutive samples. The method for generating correlated shadowing process is

$$L_{sha}(t) = L_{sha}(t-1)\rho_s + \varrho(t)\sqrt{1-\rho_s^2} \tag{2.6}$$

where $\varrho(t)$ is a Gaussian random variable.

2.4.4 Channel Impulse Reponse Estimation

The channel impulse response $h(t)$ is estimated by cross-correlating the input of the channel with the output. This assumes that the input of the channel and the transmitted signal $s(t)$ is known. For joint stationary stochastic process of $r(t)$ and $s(t)$, their cross-correlation function is [39]

$$\begin{aligned}\phi_{sr}(t, t+\tau) &= E[s(t)r(t+\tau)] = E\left[s(t)\int_{-\infty}^{\infty} h(\xi)s(t+\tau-\xi)d\xi\right] \\ &= \int_{-\infty}^{\infty} E[s(t)s(t+\tau-\xi)]\,h(\xi)d\xi \qquad (2.7)\end{aligned}$$

If $s(t)$ is wide-sense stationary, equation (2.7) reduces to

$$\phi_{sr}(\tau) = \int_{-\infty}^{\infty} \phi_{ss}(\tau-\xi)h(\xi)d\xi \qquad (2.8)$$

which is the convolution of $\phi_{ss}(\tau)$ with $h(\tau)$

$$\phi_{sr}(\tau) = \phi_{ss}(\tau) * h(\tau) \qquad (2.9)$$

where $*$ denotes convolution. Again it is easier to implement multiplication in the frequency domain than convolution in the time domain. So equation (2.9) expressed in frequency domain is

$$\Phi_{sr}(f) = \Im\,|\phi_{sr}(\tau)| = \Phi_{ss}(f)H(f) \qquad (2.10)$$

where $\Im$ indicates Fourier transform, $\Phi_{sr}(f)$ is the Fourier transform of $\phi_{sr}(\tau)$, and $\Phi_{ss}(f)$ is the energy density spectrum of the transmitted signal $s(t)$. Hence, cross-correlation of the transmitted and received signal is

$$\phi_{sr}(\tau) = \Im^{-1}[\Phi_{sr}(f)] = \Im^{-1}[S(f)R^*(f)] \qquad (2.11)$$

where $\Im^{-1}$ represents inverse Fourier transform and $R^*(f)$ is the complex conjugate of $R(f)$. From equations (2.10) and (2.11), the impulse response of the channel, and hence the timing estimation, is calculated by

$$h(t) = \Im^{-1}\left[\frac{S(f)R^*(f)}{\Phi_{ss}(f)}\right] \qquad (2.12)$$

This is the conventional correlation method used to solve the problem of timing estimation, also referred as the Generalized Cross-Correlation (GCC) method. The GCC method cross-correlates the received and transmitted signals and the propagation delay is then estimated as the location of the peak of the cross-correlation estimate.

2.4.5 Timing Estimation by Correlation Method

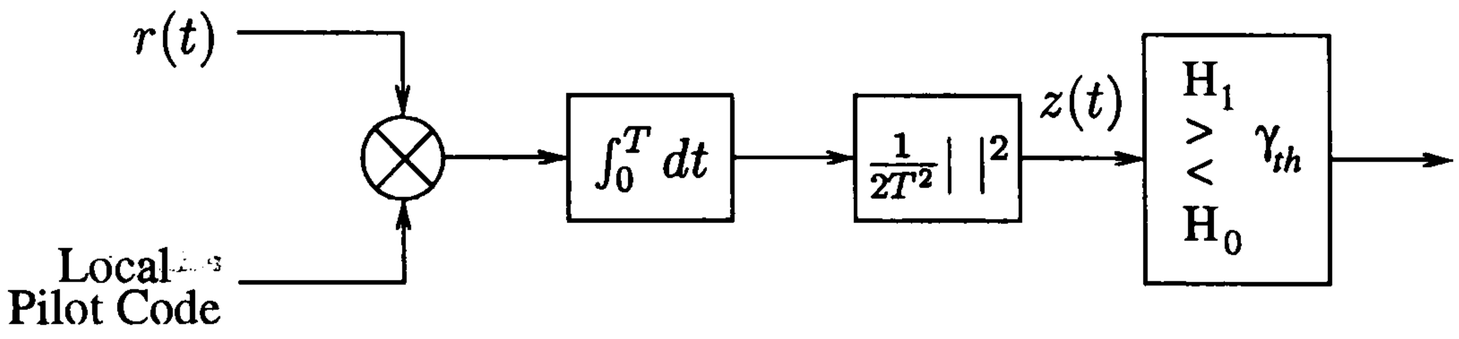

Figure 2.8: Serial search using matched filter

An efficient way to perform timing estimation is to employ a matched filter that is matched to the spreading signal as shown in Figure 2.8. The timing estimation is similar to the initial code acquisition in a spread spectrum system [40]. It is a two-dimensional search; there are the timing and frequency uncertainties, due to the propagation delay and Doppler shift. However, the frequency uncertainty is ignored, and only one-dimensional search in time was performed. Neglecting the presence of noise and multi-path, the received $r(t)$ is only the delay version of the transmitted signal $\sqrt{2A}s(t-\tau)$. The square of the magnitude of the matched filter output is [41]

$$\begin{aligned} z(t) &= \frac{1}{2T^2}\left|\int_0^T r(t)s(t-\hat{\tau})dt\right|^2 \\ &= \frac{A}{T^2}\left|\phi_{ss}(\tau-\hat{\tau})\right|^2 \end{aligned} \tag{2.13}$$

Thus, by continuously observing the matched filter output and comparing it to a threshold γ_{th}, we effectively evaluate different hypothesized delays using the matched filter energy detector.

Matched Filter Energy Detector

The decision statistic z of the matched filter energy detector can be written as [40]

$$
\begin{aligned}
z &= \frac{1}{2T^2}\left|\int_0^T r(t)s(t-\hat{\tau})dt\right|^2 \\
&= \frac{1}{2T^2}\left|\int_0^T \sqrt{2A}s(t-\tau)s(t-\hat{\tau})dt + \int_0^T n(t)s(t-\hat{\tau})dt\right|^2 \\
&= \left|\frac{\sqrt{A}}{T}\phi_{ss}(\tau-\hat{\tau}) + n_z\right|^2 \qquad (2.14)
\end{aligned}
$$

where

$$n_z = \frac{1}{\sqrt{2}T}\int_0^T n(t)s(t-\hat{\tau})dt \qquad (2.15)$$

is a zero mean complex symmetric Gaussian noise with variance σ_n^2. If $z > \gamma_{th}$, the hypothesized code $\hat{\tau}$ matches the actual τ. If $z \leq \gamma_{th}$, we decide otherwise. The decision rule is defined as

H_0 : the hypothesized code delay $\hat{\tau}$ does not match the actual delay τ

H_1 : the hypothesized code delay $\hat{\tau}$ matches the actual delay τ

Since the scrambling code is usually designed to have a small out-of-phase autocorrelation magnitude, under H_0, the signal contribution in the decision statistic is approximately zero. Then from equation (2.14), it is easy to see that under the two hypotheses

$$z = \begin{cases} |n_z|^2 & : H_0 \\ \left|\sqrt{A} + n_z\right|^2 & : H_1 \end{cases} \qquad (2.16)$$

Threshold γ_{th} Determination

The value of the γ_{th} can be determined by [42]

$$\gamma_{th} = 2\sigma_n^2 \ln\left(\frac{1}{P_{FA}}\right) \qquad (2.17)$$

where P_{FA} is the probability of the false alarm. The false alarm probability is given by

$$P_{FA} = Pr\left(z > \gamma_{th} | H_0\right) = 1 - F_{z|H_0}(\gamma_{th}) \tag{2.18}$$

where $F_{z|H_0}(\bullet)$ is the cumulative distribution function of z under H_0. It is central chi-square distributed with two degrees of freedom.

2.5 UE Geo-location Estimation

More generally, almost any problem with a set of sufficient observation data to over-determine a set of parameters calls for some type of approximation method. Most frequently, least-squares is the approximation criterion chosen to obtain the UE position parameters. The general relationship between the observables $b_1, b_2, \ldots, b_I$ and estimate parameters $\beta_1, \beta_2, \ldots, \beta_J$ through an usually implicit and non-linear mathematical model is [43]

$$f(\vec{x}, \vec{\beta}) - \vec{b} = 0 \tag{2.19}$$

where $\vec{x}$ are treated as coefficients matrix. In practice, due to the limited accuracy of measurements or observations, equation (2.19) is not equal to zero. The $\vec{\beta}$ are estimated by finding the numeric values for the parameters that minimize the sum of the squared deviations between the observed responses and the functional portion of the model. Mathematically, the least sum-of-squares criterion, that is minimized to obtain the parameter estimates, is

$$\varepsilon = \sum_{i=1}^{I} Q_i^{-1} \left[f\left(\vec{x}, \vec{\hat{\beta}}\right) - b_i \right]^2 \tag{2.20}$$

where Q_i is the variance of observation b_i, which can be used to weight measurements which are more accurate. If prior information is not known, then the covariance matrix $\vec{Q}$ is replaced with an identity matrix. To emphasize the fact that the estimates of the parameter values are not the same as the true values of the parameters, the estimates are denoted by $\hat{\beta}_1, \hat{\beta}_2, \ldots, \hat{\beta}_J$. In addition, if the observation errors are Gaussian distributed, the least-squares estimates will be a maximum likelihood estimator.

One of the most common methods used to linearise the non-linear model $f(\vec{x}, \vec{\beta})$ is the Taylor-series linearisation, which uses an iterative method to solve the linearised mathematical model. Now, ignoring the 2^{nd} and higher orders terms in the Taylor-series expansion, the linearised model is [25]

$$f\left(\vec{x}, \hat{\vec{\beta}}\right) = f\left(\vec{x}, \vec{\beta}\right) + \sum_{j=1}^{J} \left.\frac{\partial f}{\partial \hat{\beta}_j}\right|_{\vec{\beta}} \delta_j = \vec{b} - \vec{e} \tag{2.21}$$

where
- δ_j is the estimated corrections to the parameters
- $\left.\frac{\partial f}{\partial \hat{\beta}_j}\right|_{\vec{\beta}}$ is the Taylor coefficient
- $\vec{e}$ is the observation residues matrix, $[e_1, e_2, \cdots, e_I]^T$
- $\vec{b}$ is the observation parameters matrix, $[b_1, b_2, \cdots, b_I]^T$

The linearised model can be written in vector form as

$$\vec{A}\vec{\delta} = \vec{Z} - \vec{e} \tag{2.22}$$

where
- $\vec{Z}$ is $\vec{b} - f\left(\vec{x}, \vec{\beta}\right)$
- $\vec{\delta}$ is $[\delta_1, \delta_2, \ldots, \delta_J]^T$
- $\vec{A}$ is $\left[\left.\frac{\partial f}{\partial \hat{\beta}_1}\right|_{\vec{\beta}}, \left.\frac{\partial f}{\partial \hat{\beta}_2}\right|_{\vec{\beta}}, \cdots, \left.\frac{\partial f}{\partial \hat{\beta}_J}\right|_{\vec{\beta}}\right]$

The choice of $\vec{\delta}$ that gives the least-sum-squared error in these relations with the terms in the sum weighted according to the covariance of the observation errors is

$$\vec{\delta} = \left[\vec{A}^T \vec{Q}^{-1} \vec{A}\right]^{-1} \vec{A}^T \vec{Q}^{-1} \vec{Z} \tag{2.23}$$

Calculation starts with an initial guess for $\vec{\beta}$, compute $\vec{\delta}$ with equation (2.23), and update $\vec{\beta}$ with $\vec{\beta} \leftarrow \vec{\beta} + \vec{\delta}$, and repeat the computation. The iterations will converged when $\vec{\delta}$ is essentially zero. Then by the Gauss-Markov theorem, the covariance matrix corresponding to the estimated $\vec{\beta}$ is

$$Q_o = \left[\vec{A}^T \vec{Q}^{-1} \vec{A}\right]^{-1} \tag{2.24}$$

2.5.1 Circular Trilateration

As mentioned, the UE can be positioned using absolute timing TOA method, where the intersection of range circles will be the position of the UE. Given the horizontal coordinates of the UE at $[x, y]$ and the coordinates of the PE_i at $[x_i, y_i]$, the time of travel between the transceivers is τ_i. The circular trilateration equation can be written as

$$\tau_i - \frac{1}{c}\sqrt{(x - x_i)^2 + (y - y_i)^2} = 0 \tag{2.25}$$

with $i = 1, 2, \ldots, I$ numbers of PE. As the TOA observations are not error free, the intersection of the range circles is not at one point. If the numbers of observation is more than the unknown estimate parameters, over-determined, a weighted least squares estimation can be used. Therefore the Taylor coefficient matrix is

$$\vec{A} = c^{-1}\begin{bmatrix} \frac{x-x_1}{r_1} & \frac{y-y_1}{r_1} \\ \frac{x-x_2}{r_2} & \frac{y-y_2}{r_2} \\ \vdots & \vdots \\ \frac{x-x_I}{r_I} & \frac{y-y_I}{r_I} \end{bmatrix} \tag{2.26}$$

where $r_i = \sqrt{(x - x_i)^2 + (y - y_i)^2}$ and the matrix $\vec{Z}$ is

$$\vec{Z} = \begin{bmatrix} \tau_1 - c^{-1}\sqrt{(x - x_1)^2 + (y - y_1)^2} \\ \tau_2 - c^{-1}\sqrt{(x - x_2)^2 + (y - y_2)^2} \\ \vdots \\ \tau_I - c^{-1}\sqrt{(x - x_I)^2 + (y - y_I)^2} \end{bmatrix} \tag{2.27}$$

and the unscaled covariance matrix Q is an identity matrix with dimensions I by I. Thus, the estimated corrections to the parameters of UE horizontal coordinates

$$\vec{\delta} = \begin{bmatrix} \delta_x \\ \delta_y \end{bmatrix} = \left[\vec{A}^T \vec{Q}^{-1} \vec{A}\right]^{-1} \vec{A}^T \vec{Q}^{-1} \vec{Z} \tag{2.28}$$

The iteration starts with an initial guess of UE geo-location $[x, y]$. After each iteration, the estimate for $[x, y]$ is updated to $[x + \delta_x, y + \delta_y]$, and substituted back into equation (2.28). The iteration will stop until $[\delta_x, \delta_y]^T$ converge to zero. The method can be fairly accurate and efficient if the initial guess is sufficiently close to the true value.

2.5.2 Hyperbolic Trilateration

As discussed in section 2.2.4, one of the advantages of using relative time differencing TDoA over TOA is that ToT is not required for timing estimation. Mathematically the time difference model can be formulate as

$$\tau_{i,1} - \frac{1}{c}\left[\sqrt{(x-x_i)^2 + (y-y_i)^2} - \sqrt{(x-x_1)^2 + (y-y_1)^2}\right] = 0 \qquad (2.29)$$

where $i = 2, 3, \ldots, I$, and $\tau_{i,1}$ is the timing difference between PE_i and PE_1, $\tau_i - \tau_1$, with PE_1 as the first arrival and reference PE. Each TDoA estimate will form a hyperbola locus where the UE may exist, and the intersection of the hyperbola loci will determine the UE geo-location. Again due to the errors in the observation, the hyperbolas will not intersect at one point, since a pair of hyperbolas will intersect twice.

Taking the partial derivatives of the unknown $[x, y]$ of equation (2.29), the Taylor-series coefficient is

$$\vec{A} = c^{-1}\begin{bmatrix} \frac{x-x_2}{r_2} - \frac{x-x_1}{r_1} & \frac{y-y_2}{r_2} - \frac{y-y_1}{r_1} \\ \frac{x-x_3}{r_3} - \frac{x-x_1}{r_1} & \frac{y-y_3}{r_3} - \frac{y-y_1}{r_1} \\ \vdots & \vdots \\ \frac{x-x_I}{r_I} - \frac{x-x_1}{r_1} & \frac{y-y_I}{r_I} - \frac{y-y_1}{r_1} \end{bmatrix} \qquad (2.30)$$

The matrix $\vec{Z}$ is

$$\vec{Z} = \begin{bmatrix} \tau_{2,1} - c^{-1}\left(\sqrt{(x-x_2)^2 + (y-y_2)^2} - \sqrt{(x-x_1)^2 + (y-y_1)^2}\right) \\ \tau_{3,1} - c^{-1}\left(\sqrt{(x-x_3)^2 + (y-y_3)^2} - \sqrt{(x-x_1)^2 + (y-y_1)^2}\right) \\ \vdots \\ \tau_{I,1} - c^{-1}\left(\sqrt{(x-x_I)^2 + (y-y_I)^2} - \sqrt{(x-x_1)^2 + (y-y_1)^2}\right) \end{bmatrix} \qquad (2.31)$$

The unscaled covariance matrix $\vec{Q}$ will no longer be the identity matrix, as the TDoA observations are no longer uncorrelated. To account for the correlation between the TDoA observations, the covariance matrix $\vec{Q}$ can be written as

$$\vec{b} = \begin{matrix} \\ \end{matrix} \overset{\vec{U}}{\begin{bmatrix} -1 & 1 & 0 & \cdots & 0 \\ -1 & 0 & 1 & \cdots & 0 \\ \vdots & \vdots & \vdots & \vdots & \vdots \\ -1 & 0 & 0 & \cdots & 1 \end{bmatrix}} \overset{\vec{T}}{\begin{bmatrix} \tau_1 \\ \tau_2 \\ \vdots \\ \tau_I \end{bmatrix}} \tag{2.32}$$

$$\vec{Q} = \vec{U}\vec{U}^T = \begin{bmatrix} 2 & 1 & \cdots & 1 \\ 1 & \ddots & 1 & \vdots \\ \vdots & 1 & \ddots & 1 \\ 1 & \cdots & 1 & 2 \end{bmatrix} \tag{2.33}$$

where $\vec{U}$ has dimensions of $I-1$ by I, and $\vec{Q}$ has dimensions of $I-1$ by $I-1$.

2.5.3 Circular Trilateration with TDoA

As presented in 2.5.2, the hyperbolic trilateration allows UE geo-location to be computed without knowing the absolute ToT of the ranging message. However, it does require that the pair of PEs used to be time synchronised. Furthermore, it may not be possible to isolate the PE causing large residuals, where the TDoA observations are correlated. In addition, there are only $I-1$ TDoA observations, when I PEs are involved in positioning. As residuals are often the useful quantities for testing the quality of observations, therefore, one would wish to have I observation residuals with $I-1$ observations.

Again, consider a UE with horizontal coordinates $[x, y]$, observe $I-1$ of TDoA from I numbers of PEs. The horizontal coordinates of PE_i is at $[x_i, y_i]$, and the ToT of the ranging message is at T_{TOT}. Using the first PE as a reference PE, the observation of the first PE will be

$$\tau_{1,1} = 0 \tag{2.34}$$

Note that this has no additional information, for the additional observation is zero. The TDoA observations written in a circular trilateration model is

$$\tau_{i,1} + \tau_1 - \frac{1}{c}\left[\sqrt{(x - x_i)^2 + (y - y_i)^2}\right] = 0 \tag{2.35}$$

The three unknown parameters to be estimated are the horizontal coordinates of UE $[x, y]$ and τ_1, respectively. Taking the partial derivatives of equation (2.35) with respect to the unknowns, the Taylor coefficient matrix is

$$\vec{A} = c^{-1}\begin{bmatrix} \frac{x-x_1}{r_1} & \frac{y-y_1}{r_1} & 1 \\ \frac{x-x_2}{r_2} & \frac{y-y_2}{r_2} & 1 \\ \vdots & \vdots & \vdots \\ \frac{x-x_I}{r_I} & \frac{y-y_I}{r_I} & 1 \end{bmatrix} \tag{2.36}$$

and the matrix $\vec{Z}$ is

$$\vec{Z} = \begin{bmatrix} \tau_{1,1} + \tau_1 - c^{-1}\sqrt{(x - x_1)^2 + (y - y_1)^2} \\ \tau_{2,1} + \tau_1 - c^{-1}\sqrt{(x - x_2)^2 + (y - y_2)^2} \\ \vdots \\ \tau_{I,1} + \tau_1 - c^{-1}\sqrt{(x - x_I)^2 + (y - y_I)^2} \end{bmatrix} \tag{2.37}$$

Another advantage of circular trilateration with TDoA observation is the correlation in the observations is accounted for by the presence of the third unknown τ_1. As a result, the unscaled observation covariance matrix $\vec{Q}$ is the identity matrix of dimensions I by I.

2.5.4 Chan's Algorithm

Chan and Ho [27] introduced an alternative closed form least squares estimator. It is a non-iterative solution to the hyberbolic trilateration. Since the estimator is a closed

form algorithm, an initial guess of the approximate values for $[x, y]$ is not required. This makes it a prime candidate for caculating an approximate position which may be used to begin the standardized least squares iterative process. Furthermore, it can also take advantage of redundant observations like the Taylor series method. Firstly equation (2.29) can be rewritten as

$$\begin{aligned} r_{i,1} &= c\tau_{i,1} \\ &= r_i - r_1 \\ &= \sqrt{(x - x_i)^2 + (y - y_i)^2} - \sqrt{(x - x_1)^2 + (y - y_1)^2} \end{aligned} \tag{2.38}$$

The squaring of equation (2.38) results in

$$r_{i,1}^2 + 2r_{i,1}r_1 + rr_1^2 = K_i - 2x_i x - 2y_i y + x^2 + y^2 \tag{2.39}$$

where $K_i = x_i^2 + y_i^2$. Subtracting equation (2.25) with $i = 1$ from equation (2.39), gives

$$r_{i,1}^2 + 2r_{i,1}r_1 = -2x_{i,1}x - 2y_{i,1}y + K_i - K_1 \tag{2.40}$$

where $x_{i,1} = x_i - x_1$ and $y_{i,1} = y_i - y_1$.

Following Chan's algorithm, with numbers of PE with $I = 3$, will produce two TDoA timing estimates. The solution of UE $[x, y]$ coordinates is in the form of

$$\begin{bmatrix} x \\ y \end{bmatrix} = -\begin{bmatrix} x_{2,1} & y_{2,1} \\ x_{3,1} & y_{3,1} \end{bmatrix}^{-1} \left(\begin{bmatrix} r_{2,1} \\ r_{3,1} \end{bmatrix} r_1 + \frac{1}{2} \begin{bmatrix} r_{2,1}^2 - K_2 + K_1 \\ r_{3,1}^2 - K_3 + K_1 \end{bmatrix} \right) \tag{2.41}$$

Subsituting the intermediate solution into equation (2.25), with $i = 1$, a quadratic equation in terms of r_1 is produced. The positive root is then substituted back into equation (2.41), resulting in the final solution. In a case when the system is overdetermined, as the number of observations is more than the unknowns, the Taylor-series can again be used. This is achieved by solving the variables $\vec{\beta} = [\ x \quad y \quad r_1\ ]^T$ using the weighted least squares method. From equation (2.39)

$$\vec{x} = -\begin{bmatrix} x_{2,1} & y_{2,1} & r_{2,1} \\ x_{3,1} & y_{3,1} & r_{3,1} \\ \vdots & \vdots & \vdots \\ x_{I,1} & y_{I,1} & r_{I,1} \end{bmatrix} \tag{2.42}$$

and

$$\vec{b} = \frac{1}{2}\begin{bmatrix} r_{2,1}^2 - K_2 + K_1 \\ r_{3,1}^3 - K_3 + K_1 \\ \vdots \\ r_{I,1}^2 - K_I + K_1 \end{bmatrix} \tag{2.43}$$

Given $\vec{Q}$ as the covariance matrix of relative range obsrvations, with $\vec{B} = diag\{r_2^0, \ldots, r_I^0\}$, the true covariance matrix is

$$\vec{\Psi} = \vec{B}\vec{Q}\vec{B} \tag{2.44}$$

where r_i^0 denotes the true value of r_i. In practice, r_i^0 is not known initially, so the approach is to use the least squares method to calculate the $\vec{\delta}$, and usually one iteration is sufficient. It is also assumed that the unknown $\vec{\beta}$ is initially independent, but they are related by equation (2.25), with $i = 1$. To incorporate this relationship and improve the estimate further, let the elements of $\vec{\beta}$ be

$$\vec{\beta} = \begin{bmatrix} x^0 + e_1 & y^0 + e_2 & r_1^0 + e_3 \end{bmatrix}^T \tag{2.45}$$

where e_1, e_2 and e_3 are estimation error of $\vec{\beta}$. Subtracting the first two elements of $\vec{\beta}$ by x_1 and $y_1$and then squaring the elements gives another set of equations

$$\vec{\delta}' = \left[\vec{x}'^T \vec{\Psi}'^{-1} \vec{x}'\right]^{-1} \vec{x}'^T \vec{\Psi}'^{-1} \vec{b}' \tag{2.46}$$

$$\vec{\delta}' = \begin{bmatrix} (x-x_1)^2 \\ (y-y_1)^2 \end{bmatrix}$$

$$\vec{b}' = \begin{bmatrix} (\delta_1 - x_1)^2 \\ (\delta_2 - y_1)^2 \\ \delta_3^2 \end{bmatrix}$$

where $\vec{x}' = \begin{bmatrix} 1 & 0 \\ 0 & 1 \\ 1 & 1 \end{bmatrix}$

$$\vec{\Psi}' = 4B' cov(\delta) B'$$

$$cov(\delta) = (\vec{x}^T \vec{Q}^{-1} \vec{x})^{-1}$$

$$B' = diag\{x^0 - x_1, y^0 - y1, r^0\}$$

The final solution is then obtained from $\vec{\delta}'$

$$\vec{\delta}_p = \pm\sqrt{\vec{\delta}'} + \begin{bmatrix} x_1 \\ y_1 \end{bmatrix} \tag{2.47}$$

The proper solution is selected to be the one which lies in the region of interest.

2.5.5 Measures of UE Geo-locating Accuracy

To meet the FCC requirement, 67 percentile of the estimates must be within 125m and 95 percentile of the estimates must be within 300m. For handset-based methods, this is further reduced to 50m and 150m, respectively.

The estimated UE location accuracy can be measured in terms of the Euclidean distance between the estimate location,$[\tilde{x}, \tilde{y}]$, and the true location, $[x_o, y_o]$.

$$err = \sqrt{(\tilde{x} - x_o)^2 + (\tilde{y} - y_o)^2} \tag{2.48}$$

Or the root mean squared error, which is commonly used to calculate a set of K estimated locations.

$$err_{rms} = \sqrt{E[err^2]} = \sqrt{\frac{1}{K}\sum_{k=1}^{K}[(\tilde{x_k} - x_o)^2 + (\tilde{y_k} - y_o)^2]} \tag{2.49}$$

2.6 UE positioning in Hybrid *Ad Hoc* Cellular Network

The standard network-based positioning methods supported by 3G LCS are the Cell-ID based method and Observed-TDoA (OTDoA) with IPDL [44]. The cell-ID based method is the easiest but the least accurate as the position of the UE is based on the knowledge of the location of the cell it resides in. The accuracy could even degrade further if UE is residing in a large cell or the serving NB is not the nearest because of shadowing fading and handover margin. The OTDoA makes use of hyperbolic trilateration to estimate the position of the UE. It is evident that OTDoA is one of the network-based methods that will meet the requirement of the FCC E-911 service. However, in the cellular communication system, minimum power is transmitted to reduce interferences to other cells and UE. Causing problems in UE positioning, as adjacent NBs are required for trilateration calculation. Moreover, this is more severe when the UE is residing at the centre or in a large cell. Although an IPDL scheme is proposed to improve the visibility of neighbouring NBs to the UE, it will cause data loss and interruption to the networks during the short idle period.

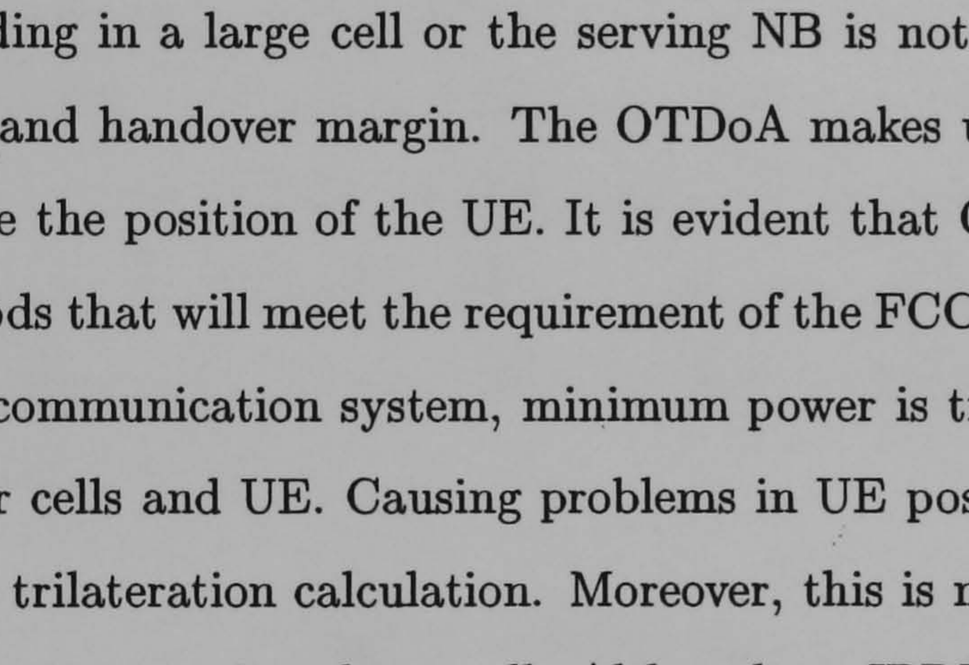

Figure 2.9: Estimated distance d between the UEs is used to mitigate the positioning error

The approach to the proposed positioning method is based on the OTDoA methodology. The proposed method further extends the conventional OTDoA, by including the measured distances between the UEs to mitigate the inaccuracy of the estimated UE geo-location, as illustrated in Figure 2.9. The estimated positions of two UEs will have to be d distance apart. One can easily estimate the d distance if the UEs has peer-to-peer communication functionality, where distance d can be measured using the round trip propagation delay of the signals transmitted between the two UEs. This additional estimated distance between the UEs will provide a better fix for the multi-ranging trilateration least-squares estimator.

In addition, the proposed method can mitigates the hearability problem of conventional OTDoA method. Consider the scenario in Figure 2.10, the UE is only within the transmission range of two NBs. Hence, no trilateration can be performed as a minimum of three NBs are necessary for positioning. Under our proposed method, the UE is not restricted to NB for positioning. Nearby UEs with position information can function as a PE, assisting in UE locating.

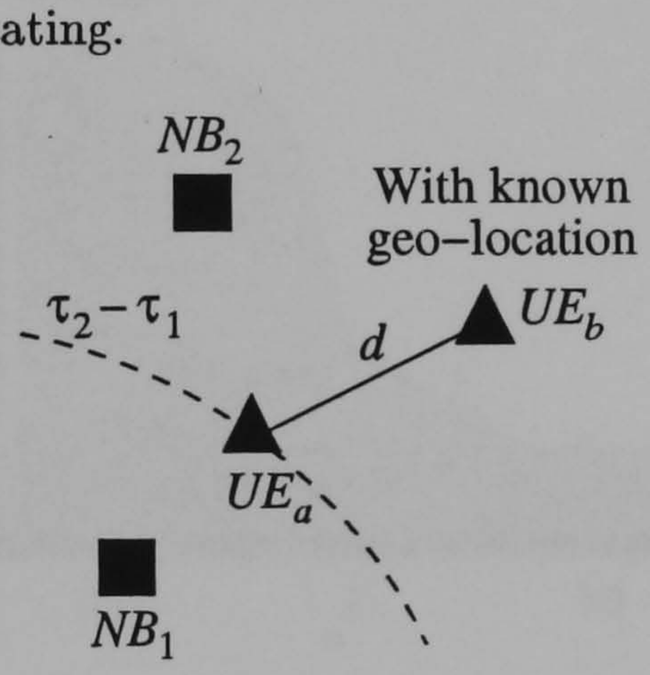

Figure 2.10: Nearby UEs with geo-location information is used to assist in positioning

Since the proposed method is a dynamic *ad hoc* network based method, it is not necessary to induce a GPS receiver into the UE and is also not restricted to NB for trilateration. The nearby UEs with spatial information can function as the PEs, to aid in positioning. Nevertheless, as will be shown later, the performance of the proposed method is dependent on channel conditions and varying system parameters.

2.6.1 The Hybrid *Ad Hoc* Cellular Network

The technological aspect for a multimode UE interoperability in a heterogeneous network could be in different duplex modes, wireless Local Area Networks (WLANs), Bluetooth, home RF networks, *ad hoc* network for the peer-to-peer, GSM and WCDMA networks for the cellular, as illustrated in Figure 2.11. Recent results in literature [45][46][47][48] demonstrate interoperability for heterogeneous network helps to improve cell coverage, increase cell capacity, divert traffic from congested to non-congested cells, enhances reliability of the system, improving UE battery life and supporting higher data rate. It is envisioned, that the potential of the heterogeneous network should not be restricted to the previous studies discussed, but rather, it should be further exploited for other applications. We strongly believe that LCS can benefit from the hybrid ad hoc cellular network, overcoming some of the shortcomings in the conventional network-based positioning methods.

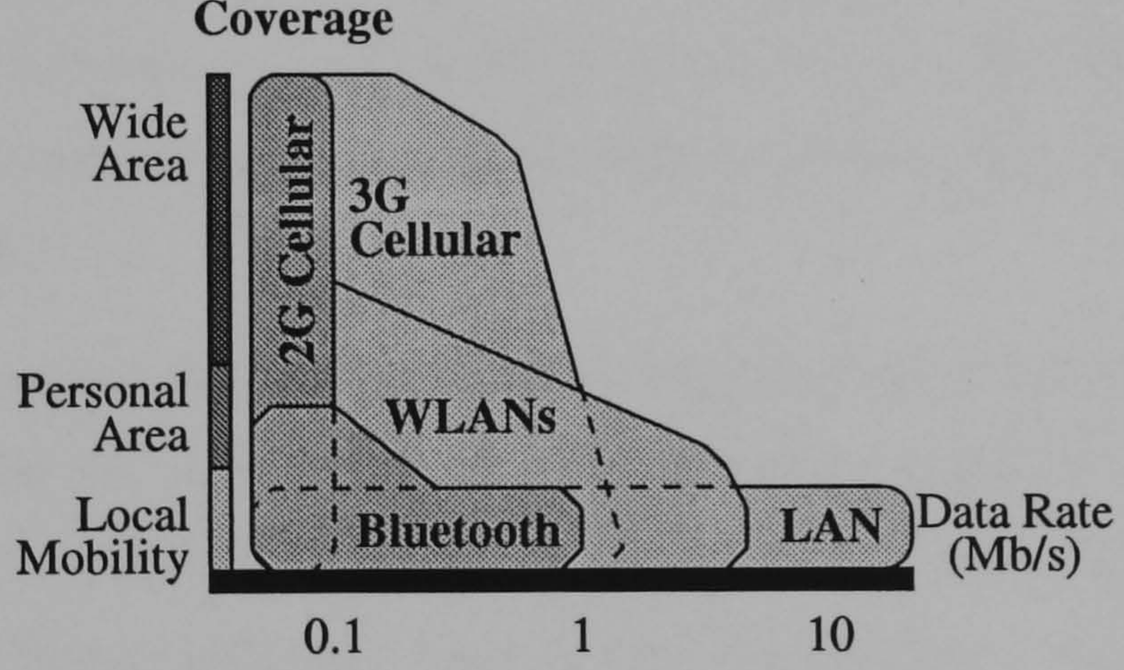

Figure 2.11: Heterogeneous network

The heterogeneous network considered in this work is based on the third generation (3G) Frequency Division Duplex (FDD) WCDMA cellular network with peer-to-peer communication based in Time Division Duplex (TDD) mode, as suggested by Willis et al. [49]. This is to ensure that no adjacent frequency interference between the cellular and peer-to-peer links. As illustrated in Figure 2.12, the FDD mode uplink operates in 1.92 - 1.98 GHz and the downlink operates in 2.11 - 2.17 GHz frequency spectrum, respectively. The TDD mode will operate in 1.90 - 1.92 GHz or 2.01 - 2.025

GHz frequency spectrum, respectively. The TDD also has few other characteristics making it favourable for peer-to-peer communication. It can be implemented on an unpaired band, where the transceivers transmit and receive their signals in the same frequency spectrum. Secondly, based on the received signal, TDD transceivers are able to estimate the fast fading that affect its transmission since the same frequency is used for transmitting and receiving. In addition, the TDD allows flexible capacity allocation between the UEs [50].

Another possible candidate for peer-to-peer communication is the WLANs, operating in the unlicensed 2.40 GHz Industrial Scientific and Medical (ISM) band. The IEEE 802.11b WLANs [51] configured in *ad hoc* mode allows several UEs to get together to form their own wireless network. Through the *ad hoc* mode, the users can share data and devices. The network is typically created spontaneously and is alive until a UE moved out of the coverage area of other UEs. There is no network planning, the UEs configure themselves to act as an access point and as a station. Any of the UE can act as a serve server if connection to a backbone network is required. The server also acts as a bridge or gateway to convert communication protocols from the WLANs to the backbone network.

At the time of writing the thesis, the technology that will be used for peer-to-peer communication has yet to be confirmed. The technology is still in an immature state since current routing algorithms have yet been proven to work under a large size *ad hoc* network. Existing challenges, such as Multicast support, QoS support, power-aware routing have not been dealt with. Moreover, the specific middleware, link and physical layers, including medium access control (MAC), and radio access interfaces required for peer-to-peer have yet to be established. Hence, without introducing more complexity to the heterogeneous network infrastructure and signalling, the Universal Mobile Telecommunications System (UMTS) terrestrial radio access system (UTRA)-TDD mode is selected for peer-to-peer communication. It is assumed that the UE is able to operate in FDD and TDD mode, and no extra WLANs technology would be necessary for peer-to-peer communication. In conclusion, a UE in the hybrid *ad hoc* network will have the ability to interoperate with the cellular network in FDD mode and peer-to-peer network in TDD mode.

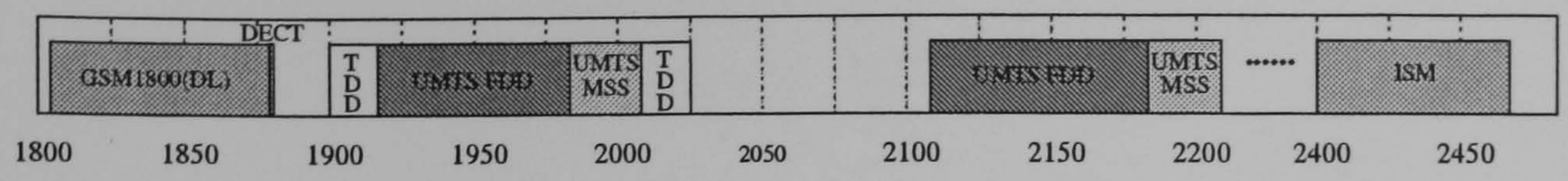

Figure 2.12: IMT-2000 frequency allocations for Europe

2.6.2 Position Estimation

A time-based multi-ranging trilateration is employed to estimate the UE position as discussed in section 2.2.5. It is a hybrid between the ToA and TDoA methods. The time delay measurements from the cellular and peer-to-peer networks will provide the TDoA and ToA to compute the latitude and longitude of the UE. In the case where only the TDoA is available, such as no nearby UE to assist in positioning, the circular TDoA trilateration is used. In contrast, when all PE are the UEs, circular trilateration is used for positioning. If the number of timing measurements exceeds the two unknowns of the UE, latitude and longitude, errors in the observations will prevent a unique solution. A least-squares method is effective in dealing with this redundancy by minimising the sum of square of the residuals.

2.7 Conclusions

In this Chapter, an overview of UE positioning methods is discussed. The emphasis is placed on the developments of UE positioning over the years and notifying the possible approaches for practical implementation. In addition, the pros and cons of each method were highlighted. The previous significant research and work for the development of UE positioning were also described. Although numerous positioning methods are developed, it is clear that the time-based positioning method is the strongest candidate for network-based LCS while the least-squares method is ideally the estimator for estimating the UE position.

Chapter 3

Position Enhanced Mobility Management Schemes

3.1 Introduction

It is known that the LCS does not limit itself to external users and at the same time it is able to assist in network planning, better allocation of the valuable resources in the network, and improves on the present mobility management schemes. Generally, it can be summarised into four different categories as shown in Figure 3.1. In this chapter, the position enhanced Mobility Management schemes, which is the second objective of our works, will be addressed, with much emphasis on the soft handover (SHO) for CDMA-based networks and relaying for hybrid *ad hoc* cellular networks. This chapter will give an introduction to the handover and relaying algorithms, giving an overview of the work already done in this area. Finally, the proposed position enhanced SHO and relaying algorithms as used in this thesis will be introduced.

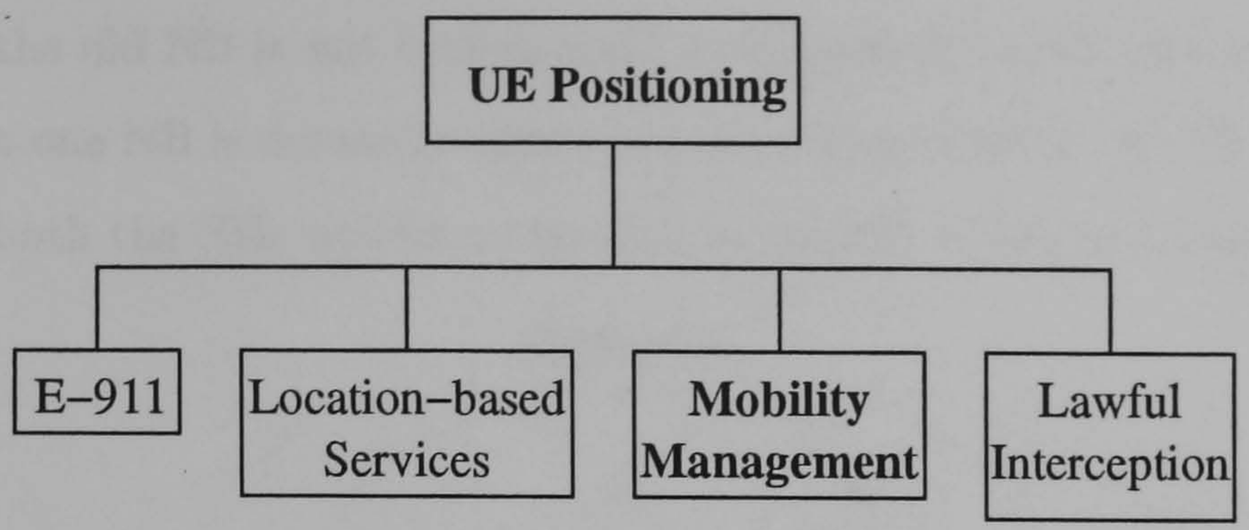

Figure 3.1: Categorisation of LCS services

3.2 Handover in Cellular Network

Handover is the mechanism that transfers an ongoing call from one cell to another as an active UE moves through the coverage area of a cellular network. Allowing the UE to transit from one cell to its neighbouring cells, without losses in the link quality. Figure 3.2 illustrates a typical handover scenario in which an UE travels from NB_1 to NB_2. Initially, the UE is connected to NB_1. The overlap between the two cells is the handover region in which the UE may be connected to either NB_1 or NB_2. At a certain time during the travel, the UE is handed over from NB_1 to NB_2. When the UE is close to NB_2, it remains connected to NB_2. The overall handover procedure can be thought of as having two distinct phases [52]:

- The initiation phase in which the decision about handover is made.
- The execution phase in which either a new channel is assigned to the UE or the call is forced to terminate.

Handover algorithms normally carry out the first phase. Handover may be caused by factors related to radio link, network management, or service options [53][54]. A handover made within the currently serving cell (example, by changing the frequency) is called an intra-cell handover. A handover made from one cell to another is referred to as an inter-cell handover. Handover may be hard or soft. Hard handover (HHO) is "break before make" meaning that the connection to the old NB is broken before a connection to the candidate NB is made. SHO is "make before break" meaning that the

connection to the old NB is not broken until a connection to the new NB is made. In fact, more than one NB is normally connected simultaneously to the UE. For example, in Figure 3.2, both the NBs will be connected to the UE in the handover region.

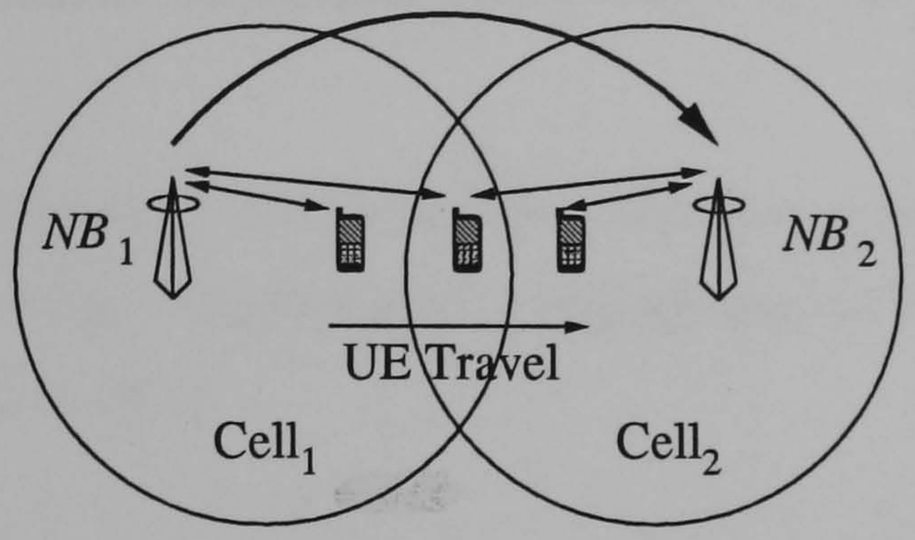

Figure 3.2: Handover scenario in cellular system

3.2.1 Desirable Features of Handover

An efficient handover algorithm can achieve many desirable features by trading different operating characteristics. It should maximise reliability and communication quality, maintain cell boarders and traffic balancing, and minimise number of handovers.

- Handover should be fast so that the user does not experience service degradation or interruption. Service degradation may be due to a continuous reduction in signal strength or an increase in co-channel interference. Fast handover also reduces co-channel interference since it prevents the UE from going too far into the new cell.

- Handover should be reliable. This means that the call should have good quality after handover.

- Handover should maintain the planned cellular borders to avoid congestion, high interference, and use of assigned channels inside the new cell. Each NB can carry only its planned traffic load. Moreover, there is a possibility of increased interference if the NB goes far into another cell site while still being connected to a distant NB because co-channel distance is reduced and the distant NB tends to use a high transmit power to serve the NB.

- The number of handovers should be minimized. Excessive handovers lead to heavy handover processing loads and poor communication quality.

- The target cell should be chosen correctly since there may be more than one candidate NB for handover. Identification of a correct cell prevents unnecessary and frequent handovers.

- The handover procedure should balance traffic in adjacent cells, eliminating the need for channel borrowing, simplifying cell planning and operation, and reducing the probability of new call blocking.

3.2.2 Previous Works in Handover Algorithms

Handover algorithms are distinguished from one another in two ways; handover criteria and processing of handover criteria. The conventional SHO algorithm adopted by UTRA [55] is a dynamic threshold with fixed hysteresis margins, such as, Adding, Dropping, and Replacing based algorithm. With reference to SHO, the UE' *Active Set* (ActS) is defined as a set of the NBs to which the UE is simultaneously connected. All other candidate NBs are defined as *Monitored Set* (MonS). A SHO algorithm is performed to maintain the UE's ActS, in corporation with a set of thresholds such as adding threshold (Th_{ADD}), dropping threshold (Th_{DROP}), replacing threshold (Th_{REP}) and time-to-trigger (T_{trig}). An active moving UE keeps monitoring the signal quality of primary common pilot channel (PCPICH) from each NB, and the SHO is applied to maintain the UE's ActS. The following parameters are used in the algorithm

$Hyst_{ADD}$:	Hysteresis for adding threshold
$Hyst_{DROP}$:	Hysteresis for dropping threshold
$Hyst_{REP}$:	Hysteresis for replacing threshold
$ActS\_Max\_Size$:	Maximum size of the ActS
$Meas\_Sig$:	The measured and averaged PCPICH signal quality
$Best\_NB\_MonS$:	The best measured NB present in the MonS
$Best\_NB\_ActS$:	The best measured NB present in the ActS
$Worst\_NB\_ActS$:	The worst measured NB present in the ActS

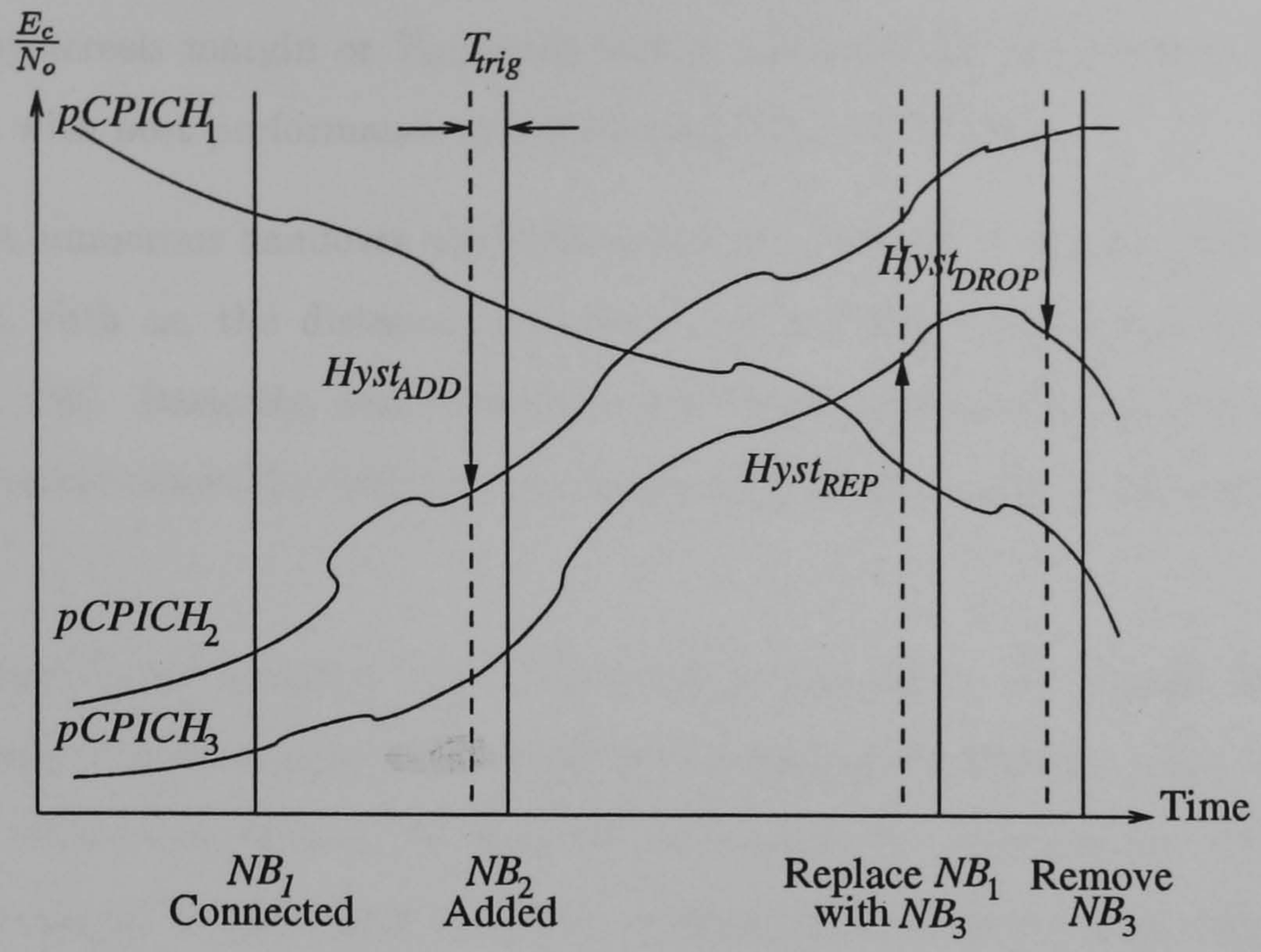

Figure 3.3: An overview of SHO in UTRA

As depicted in Figure 3.3 (where, $ActS\_Max\_Size$ equals to 3), the UTRA SHO is based on a set of dynamic thresholds. The UE's ActS is maintained in the following way

- If $Meas\_Sig$ from the MonS is greater than Th_{ADD} $(= Best\_NB\_ActS + Hyst_{ADD})$ for a period of T_{trig} time and the ActS is not full, add the $Best\_NB\_MonS$ into the ActS.

- If $Meas\_Sig$ from the ActS is below Th_{DROP} $(= Best\_NB\_ActS + Hyst_{DROP})$ for a period of T_{trig} time, remove the $Worst\_NB\_ActS$ NB from the ActS.

- If the ActS is full and $Best\_NB\_MonS$ NB from the MonS is greater than Th_{REP} $(= Worst\_NB\_ActS + Hyst_{REP})$ for a period of T_{trig} time, replace $Worst\_NB\_ActS$ NB with $Best\_NB\_MonS$ NB.

Clearly, the difficulties of relative signal strength-based SHO algorithm for UTRA are to prefix the hysteresis margins and T_{trig} time. If the hysteresis margins and T_{trig} time are not set to the optimum values, it will cause unnecessary handover and call drop to occur. However, it is difficult to base on single criteria and expect the handover algorithm to perform at optimum level in a dynamic wireless cellular environment. As

a fixed hysteresis margin or T_{trig} only makes the handover performance sensitive to situation with best performance at only a particular environment.

Therefore, numerous handover algorithms that are based on multiple criteria are being proposed, such as, the distance, direction, and velocity based handover algorithms [5,6][56,...,59]. Basically, each algorithm tries to determine the mobility of each UE, and adaptively adjust the hysteresis margin or averaging window to suit each individual UE.

The distance-based handover algorithm connects the UE to the nearest NB. The relative distance measurement is obtained by comparing propagation delay times. This criterion allows handover at the planned cell boundaries, giving better spectrum efficiency compared to the signal strength criterion [56]. However, it is difficult to plan cell boundaries in a microcell system due to complex propagation characteristics. Thus, the advantage of distance criterion over signal strength criterion begins to disappear for smaller cells due to inaccuracies in distance measurements.

Austin and Stüber [6] suggested that a direction-based handover algorithm can improve performance in LOS and NLOS scenarios in a multi-cell environment. The basic idea behind this algorithm is that handovers to the NBs towards which the UE is moving are encouraged, by reducing the hysteresis margin. By increasing the hysteresis margin, handovers to the NBs from which the UE is receding is discouraged. This algorithm reduces the probability of dropped calls for HHOs, and the time a UE needs to be connected to more than one NB for SHO, allowing more potential UEs per cell. In this work, absolute direction information is assumed.

Austin and Stüber [57] also proposed a velocity adaptive handover algorithm by adjusting the length of the averaging window to tackle the UE velocity and proposed three methods for velocity estimation: level crossing rate method, zero-crossing rate method, and covariance approximation method. A velocity adaptive handover algorithm can also serve as an alternative to the umbrella cell approach to tackle high velocity UE. Handover is dissuaded to a small cell, as fast moving UE traverse rapidly the coverage of the microcell [58].

Although the signal strength-based SHO for UTRA is less complex than the proposed adaptive handover algorithms, it will never be able to perform at the optimum level for all UEs. Nonetheless, the shortcoming of the works cited above uses complex methods to estimate the mobility of the UE or absolute UE spatial knowledge is considered.

With the LCS available in all cellular networks, UE spatial information can be acquired. So, a more intelligent adaptive SHO algorithm that is based on the position of UE can be derived and practically implemented. The proposed position enhanced SHO is explained in the following section.

3.2.3 Position Enhanced Soft Handover

Using the position estimate, two important parameters with respect to the mobility of the UE can be determined. These are the distance, d, between the UE and the desired NB, and the UE moving direction, Θ, with relevance to the desired NB, as illustrated in Figure 3.4.

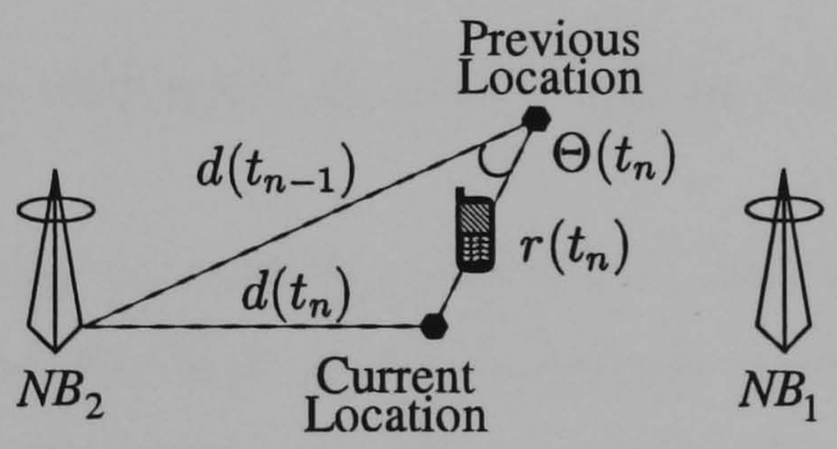

Figure 3.4: Explanation of UE geo-location modelling

From two adjacent estimated positions, the UE moving direction with respect to the desired NB at time t_n can be estimated as

$$\Theta(t_n) = \cos^{-1}\left(\frac{d(t_{n-1})^2 + r(t_n)^2 - d(t_n)^2}{2d(t_{n-1})r(t_n)}\right) \tag{3.1}$$

where $d(t_{n-1})$ is the calculated distance of UE previous estimated geo-location with the desired NB_2, $r(t_n)$ is the calculated distance between previous and current estimated UE geo-location, and $d(t_n)$ is the calculated distance between UE current estimated position and the desired NB_2. These information can be used to adjust the hysteresis

margins for individual UE, in order to support or oppose an NB to be added, dropped or replaced into or from the UE's ActS. With the aforementioned established, the adding, dropping or replacing of the NB into the ActS can be written as

- Lower or raise the $Hyst_{ADD}$ when distance between the UE and the MonS NB reduces or increases. In order to promote or dissuade adding the NB from the MonS to the ActS.

- Raise or lower the $Hyst_{DROP}$ and $Hyst_{REP}$ when distance between the UE and the ActS NB(s) reduces or increases. In order to discourage or encourage dropping the serving NB from it's ActS.

- Lower or raise the $Hyst_{ADD}$ when UE is moving towards ($\Theta < 90°$) or away ($\Theta > 90°$) from the MonS NB.

- Raise or lower the $Hyst_{DROP}$ and $Hyst_{REP}$ when UE is moving towards ($\Theta < 90°$) or away ($\Theta > 90°$) from the ActS NB.

3.3 Relaying in Hybrid *Ad Hoc* Cellular Networks

When it comes to coverage or capacity enhancement solution in a cellular network, significant effort has been placed at the system network or the system infrastructure. In addition, methods like increasing transmitter power, antenna height and gain, cell splitting, sectorised cells, and smart antennas have been investigated to achieve as close as 100% coverage. The above solutions, however, may involve planning, costs, and sometimes a long deployment period.

As an alternative solution, service providers sometimes employ repeaters to extend the coverage to these areas, commonly known as dead spots or coverage holes, that are not covered by the NB [60,...,62]. In order for them to be effective, however, the location for these repeaters must be planned so that a clear LOS to the NB is obtained. Applications of repeaters are useful for extending the coverage to dead spot regions where there is a dense population such as: freeways, tunnels, and convention centres. Nonetheless, the shortcoming is that this method becomes cost-ineffective if

many sparse coverage holes, in which only a few UEs are located, exist. Accordingly, the above will not provide a viable solution.

Conversely, relaying using nearby UEs can be an alternative or complementary method to repeaters. In this case, an individual UE's signal, to whom the NB is intended, but cannot be reached, is relayed by one or more UEs which have a direct or intermediate link to the NB, This process is illustrated in Figure 3.5.

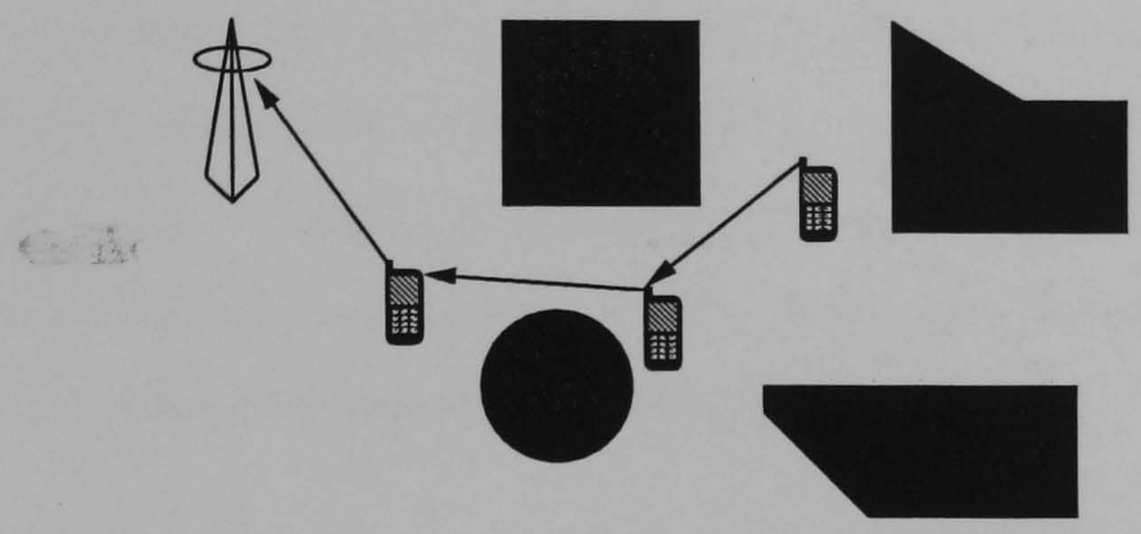

Figure 3.5: Relaying scenario in cellular system

Relaying can be beneficial for both NB-to-UE and UE-to-NB transmissions. Other potential benefits from this relaying include: fast deployment period, fewer infrastructures requirement, increased coverage, and peak power consumption reduction. However, security issue has to be considered when the target UE uses nearby UE(s) to relay the data packets to its NB. Relaying is a common technique used for radio packet data transmission both in commercial and military systems, but not widely used in the cellular systems. The earliest is introduced by SA Patient [7], a multi-hop relaying protocol, named ODMA [59]. The nearby UE(s) is used to relay originating UE data packets to its serving NB when the link quality between them falls below a threshold level. Although it appears to have dropped from the 3GPP standard, as a result of concerns over complexity and signalling overhead issues. Even so, it still remains an attractive prospect for future mobile communication systems due to advantages offered by reduction in transmission power, potentially enhanced coverage and capacity in the extended coverage region [47][60][61].

As a summary, Figure 3.6 illustrates a scenario where the UE at certain locations, in particular at the cell edge, have a poor link to the NB. The dashed arrows indicate

the UE has poor visibility with its serving NB. One of the most common methods is to increase its power transmission. Nonetheless, this will cause interference to other active UE. Another conventional solution used by service providers is to use repeater to extend the coverage to these regions. Then again, numerous of repeaters will be necessary if all UEs with a poor coverage from the NB are to be accommodated via repeaters. Therefore, it will not be cost efficient and slow in deployment.

Figure 3.7 conveys that relaying is one of the solution to the coverage problem presented in Figure 3.6. The nearby UE with a good link to the NB is to act as a relay UE for those with a poor link. Those UEs that suffered from poor visibility with their serving NB will use a nearby UE as a relayer, so call outage could be prevented. As a result, no repeater is required and it is more cost efficient to deploy.

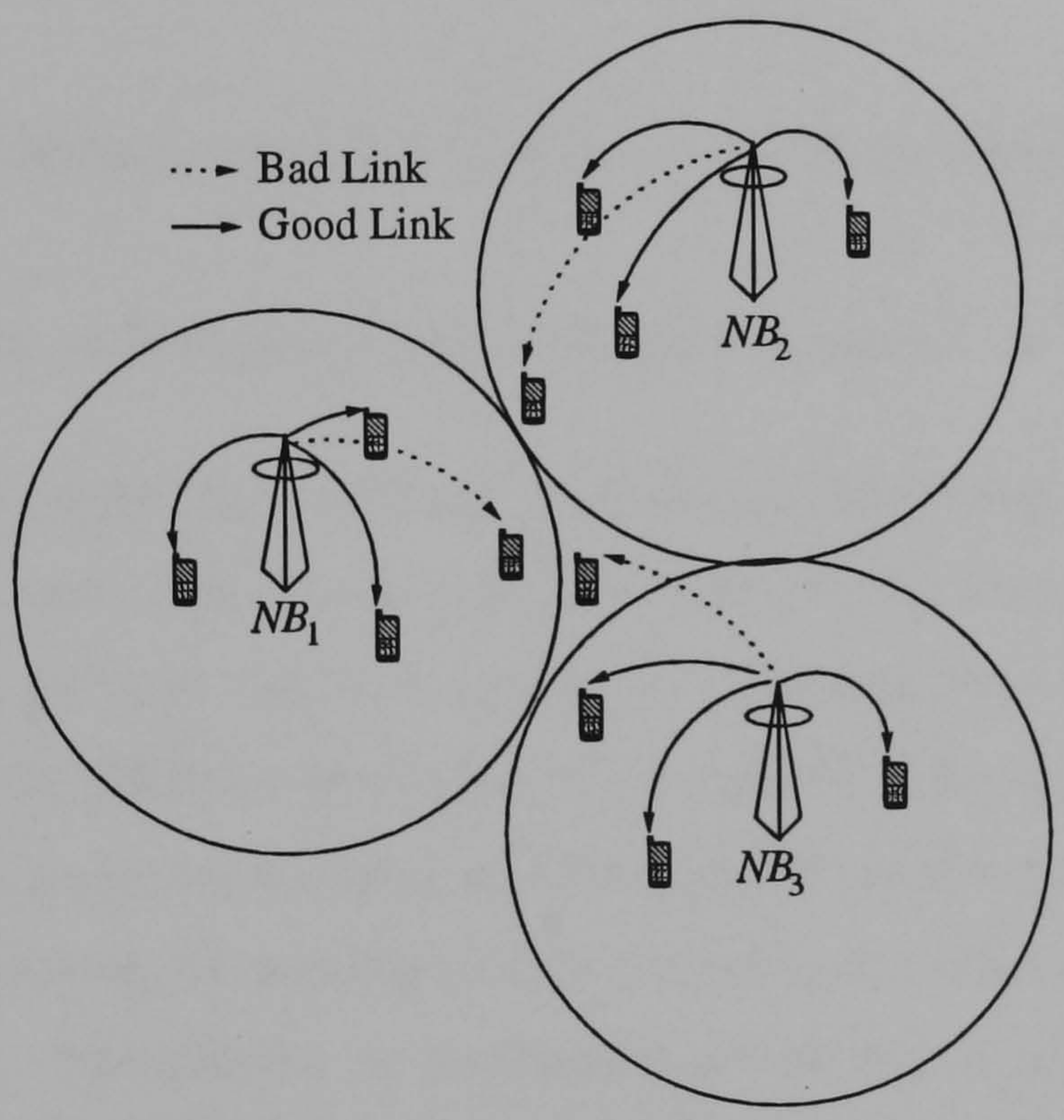

Figure 3.6: A cellular scenario depicting areas of coverage holes or dead spots

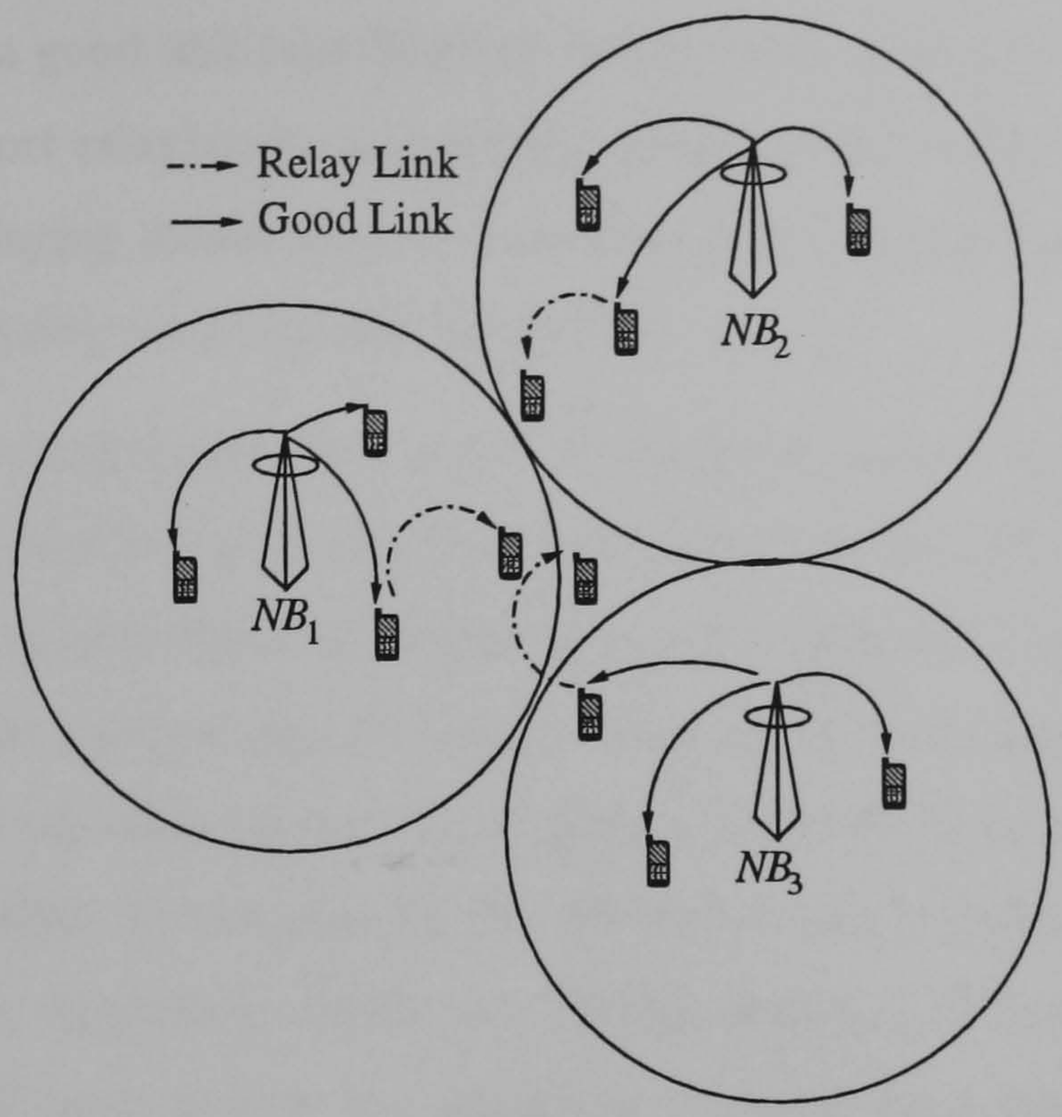

Figure 3.7: Relaying for cellular network to solve the coverage problem

3.3.1 Choosing of Relaying UE or Path Selection

Relaying began in packet radio systems, whereby no infrastructure exists and UEs communicate with each other via intermediate relay UE. Choosing a relaying path is actually a routing problem. As with routing in a wireless radio network involves a trade-off between the efficiency and overhead complexity. They are broadly classified into two categories, proactive and reactive. The proactive algorithms follow the classical approach wherein routes are established upfront and route tables are maintained and updated regularly. The reactive or on-demand algorithms operate on a need-basis and routes are established when needed and there are no periodic updates. On the other hands, the proactive approach is not suitable to the *ad hoc* scenario as high UE mobility mean that link states change frequently, causing an excessively large number of updates [62]. For the scope of this thesis, we will not go details of every routing algorithm and signalling generated for routing, but instead focus on position enhanced routing algorithm and clarify any important routing concepts.

When a relaying is needed, a UE must somehow be informed that such a relaying service is available in the system. It is suggested by Aggelou and Tafazolli [63] that

each UE that has a good link (via direct or intermediate link) to the NB advertise its capability to support relaying by periodically emitting "BEACON" message. So that UEs in need of relaying assistance can listen for these beacons and at the same time assess their link quality to the neighbouring UEs.

As for handover management, two types of handover control are observed; mobile assisted handover (MAHO) and mobile control handover (MCHO) [63]. A MAHO is carried out in a conventional manner whereby the network makes a handover decision for the UE based on the received signal strength measurements reported to it. Meanwhile, a MCHO is carried out solely by the UE, whereby it performs its own link measurements and handover decision. In this process, the NB needs only be informed and instructed by the relay UE(s). According to [63], in a MCHO situation, the handover process can be initiated quickly and requires low signalling overhead since the handover decision does not involve the NB.

The factors for determining whether a certain UE has the capability to support relaying request (assuming it has a good link to the NB) are: buffer space, transmit power, line bandwidth (radio channel) availability and processing time. All of this can be determined at the negotiation time when a request is made. Assuming a UE in need of relaying assistance has already decided on a relay UE, it must then negotiate to determine whether or not its QoS requirements can be satisfied. Otherwise, it may be required to establish a new link with a different relay UE. Unlike the HHO or SHO discussed in section 3.2.2, the relaying algorithm is more complicated and need to consider the handover between the NB-to-UE, and UE-to-UE. As such, three types of handover must be distinguished

- NB-to-relay UE handover
- Relay UE-to-NB handover
- Inter-relay UE handover

Coupled with position information, relay UE discovery can be carried out simply and quickly by the NB for the UE that requires relaying assistance, or by the UE itself. In fact, position information is being proposed in *ad hoc* networks for routing in order to reduce the routing overhead and to maintain a small routing table at the UE. The

Location Aided Routing (LAR) algorithm proposed by Y. Ko [64] suggested that UE position could be used to reduce route discovery overhead. Every UE will use the GPS to obtain their horizontal coordinates and assuming that velocity is known, an expected zone can be defined and route requests are directed to that particular section of the network. Another similar algorithm is the Relative Distance Micro-discovery Ad hoc Routing (RDMAR) algorithm, proposed by Aggelou and Tafazolli [63]. It is based on an algorithm that estimates the relative distance between UEs. This estimate is then used to limit the route discovery area. The relative distance estimation algorithm is executed at the source of route request before route request messages are broadcast. The estimate itself is based on the last known relative distance, the time elapsed since the last distance estimate and the average UE velocity. The relative distance obtained is then converted into actual hop counts using an average UE-to-UE transmission range [65].

3.3.2 Position enhanced relaying algorithm

Similar to the position enhanced SHO algorithm described in section 3.2.3, the position information will be used for path selection as discussed in section 3.3.1. The UE spatial information will be used to persuade the originating UE to select a nearby candidate UE for relaying, as to avoid using UEs that are distanced away. Provided that the candidate UE are within the transmission range between the originating UE and its serving NB.

Figure 3.8 illustrates a scenario where UE_4 is out of the transmission range with its serving NB, and not able to handover to a neighbouring NB. For this reason, it has to use either one of the nearby UE to relay its data packet to the NB. If a signal strength-based relaying algorithm is used to select the best path, UE_3 will be the candidate UE for relaying. On the other hand, if the spatial-based relaying algorithm is used to select the best path, UE_1 will be the candidate UE for relaying. Although path A has the shortest total distance, but it has the weakest $\frac{E_b}{N_o}$. If path C is chosen for its strongest link, there is a high probability that UE_3 may move out of the transmission range with the NB, causing a link breakage.

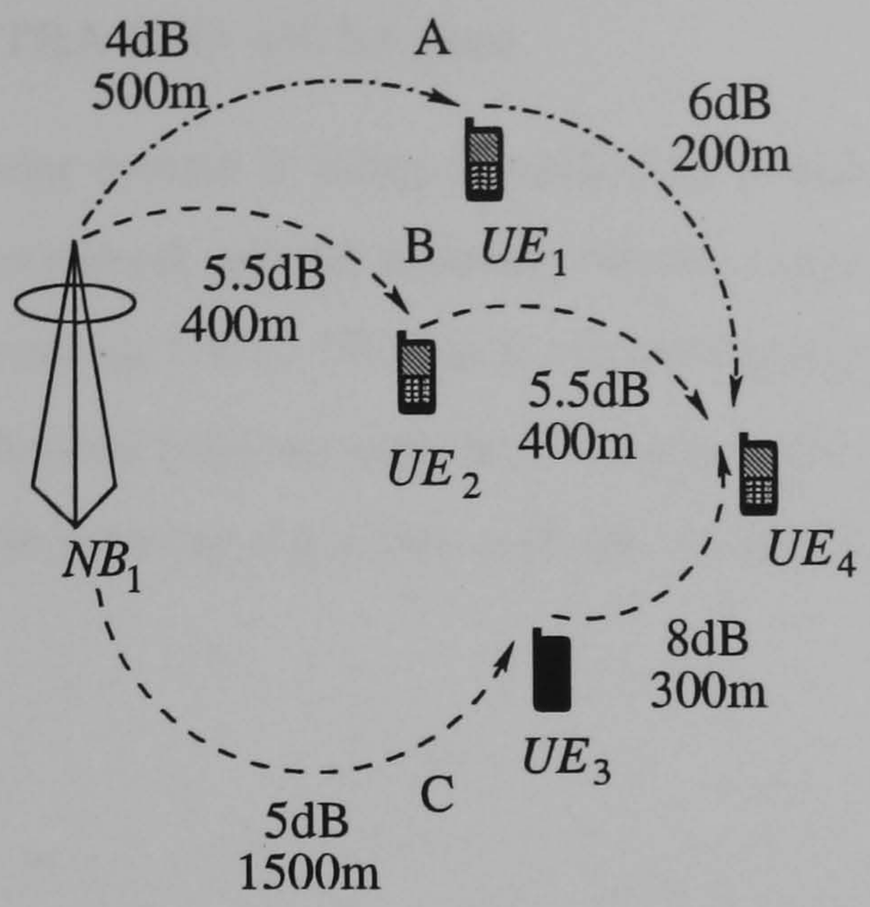

Figure 3.8: Position enhanced path selection

Therefore, a position enhanced relaying algorithm is proposed, where the signal quality and spatial location of the UEs are considered in path selection. The details of this work will be presented in Chapter 6, and an investigation and comparison will be made between the proposed algorithm and above mentioned signal strength-based and position-based relaying algorithms. In addition, a comparison between the relaying and non-relaying cellular network will be carried out.

3.4 Conclusions

In this chapter position enhanced mobility management schemes were explicated and discussed. In particular, to the development of SHO and path selection for the relaying cellular network. The SHO in the cellular network allows a UE to transit from one cell to another cells, without causing losses in the link quality. As a result, it is critical to develop an efficient algorithm that is able to cope with different wireless environments and UE mobility. Numerous adaptive SHO algorithms proposed by numerous researchers were notified and discussed in section 3.2.2. Based on their work, a position enhanced SHO algorithm is proposed. It is suggested to use the UE spatial information to obtain the mobility of the UE, and cleverly adapt the SHO hysteresis margins to suit each individual UE. Details of the work will be presented in Chapter 5, and a

comparison with the UTRA SHO will be given.

On top, a relaying cellular system is being identified to resolve the coverage difficulty encountered in the conventional cellular network. Hence, choosing a reliable candidate UE for relaying will ensure no UE-to-UE link breakage during relaying. In this part of our work, a position enhanced relaying algorithm is proposed to assist in path selection. Further discussion of the relaying algorithm and simulation work will be presented in Chapter 6.

Chapter 4

Performance of UE Positioning in Hybrid Networks

4.1 Introduction

In order to determine the performance of such a location system that utilises the timing measurements taken from the NBs and UEs, as proposed in the thesis, simulations are performed in two stages. The first stage is to simulate the timing estimation between the NBs and UE, and an initial UE position is calculated based on the timing estimated. This preliminary work is done to verify the performance of the conventional OTDoA method. Once this is done, positioning simulations under the hybrid network are undertaken. Coupled with UE-to-nearby UEs distance information, the target UE will re-estimate its location with the assistance of nearby UEs. With the initial assisting UEs spatial information obtained in the first stage of the simulation work. Consequently, all the UEs that participated in the process of positioning will have their positions re-approximated. Thus, better performance is achieved.

4.2 General Structure of the OTDoA Simulation

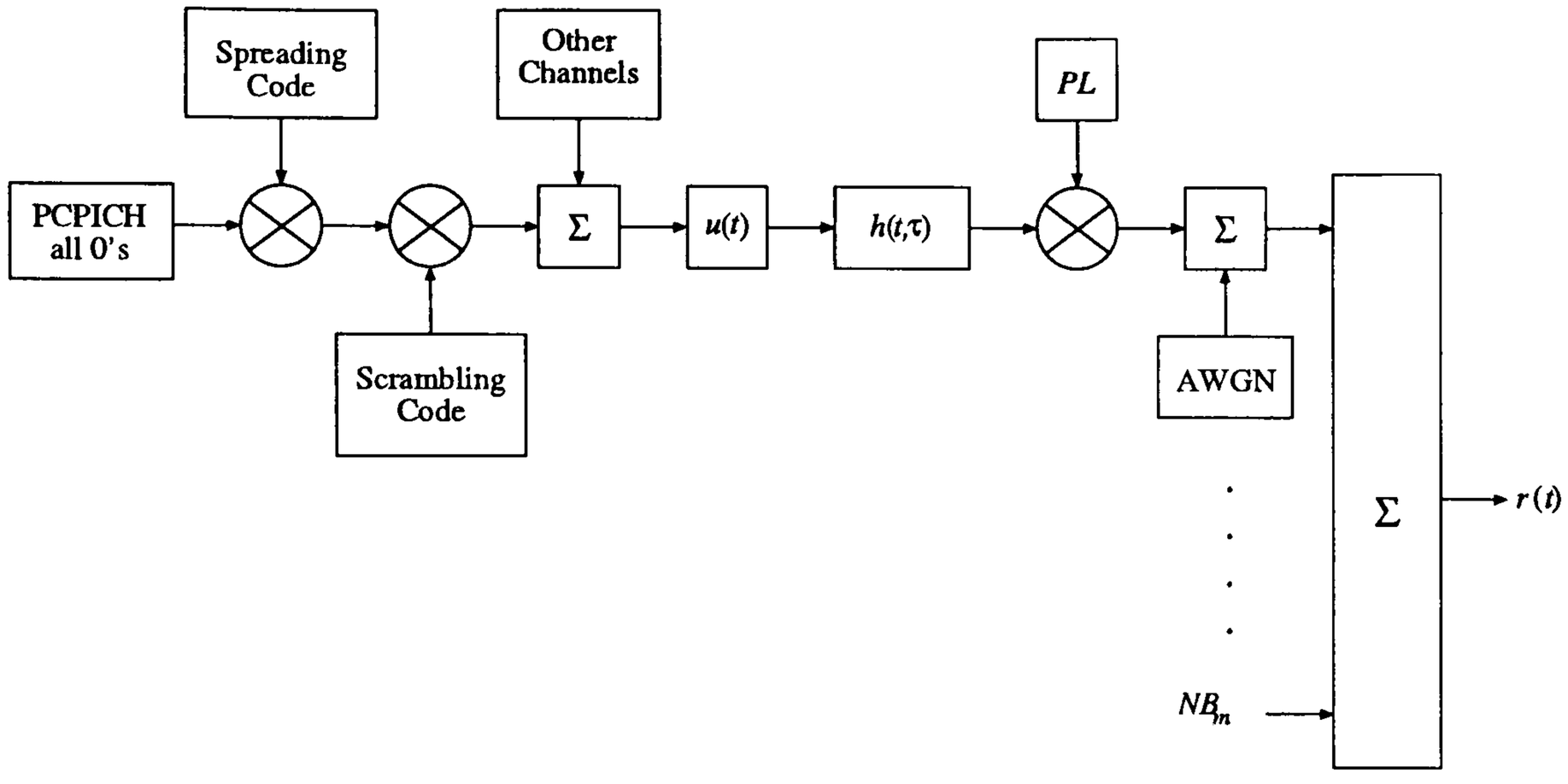

Figure 4.1: Downlink channels of WCDMA cellular network

Figure 4.1 explains the general downlink channels of the WCDMA cellular network. Firstly, the PCPICH channels for each NB are simulated. This channel consists of channelisation Orthogonal Variable Spreading Factor (OVSF) code which is all zeros for PCPICH, and scrambled with a pre-assign primary scrambling code. The primary scrambling code sequences are constructed by combining two real sequences into a complex sequence. Each of the two real sequences is constructed as the position wise modulo-2-sum of 38400 chip segments of two binary m-sequences, generated by means of two polynomials of degree 18. The resulting sequences thus constitute segments of a set of Gold sequences [66]. The next step is to generate a random binary data for different UEs, and is spread using the channel codes of respective UEs. The data and PCPICH will be summed together and pass through a root-raise cosine filter, $u(t)$, with a roll-off rate of 0.22 [67].

The transmitted signal will be corrupted (i.e., delayed and attenuated) with the time varying channel of impulse respond $h(t, \tau)$. The delays (τ) and attenuations (PL) experienced by each NB's downlink signal for each UE, depend on the distance between the transceivers and the path-loss model being used. Then, the spread and sampled signals of the NBs are accordingly delayed and scaled. The AWGN is then added

to the signals depending on the desired $\frac{E_c}{N_o}$. After all the received signals have been computed, the received signals will pass through the matched filter as conversed in section 2.4.5. Lastly, the channel impulse response will be estimated, where the TDoA timing observations will be used to compute the UE position.

4.2.1 Simulation of Multi-path Channel

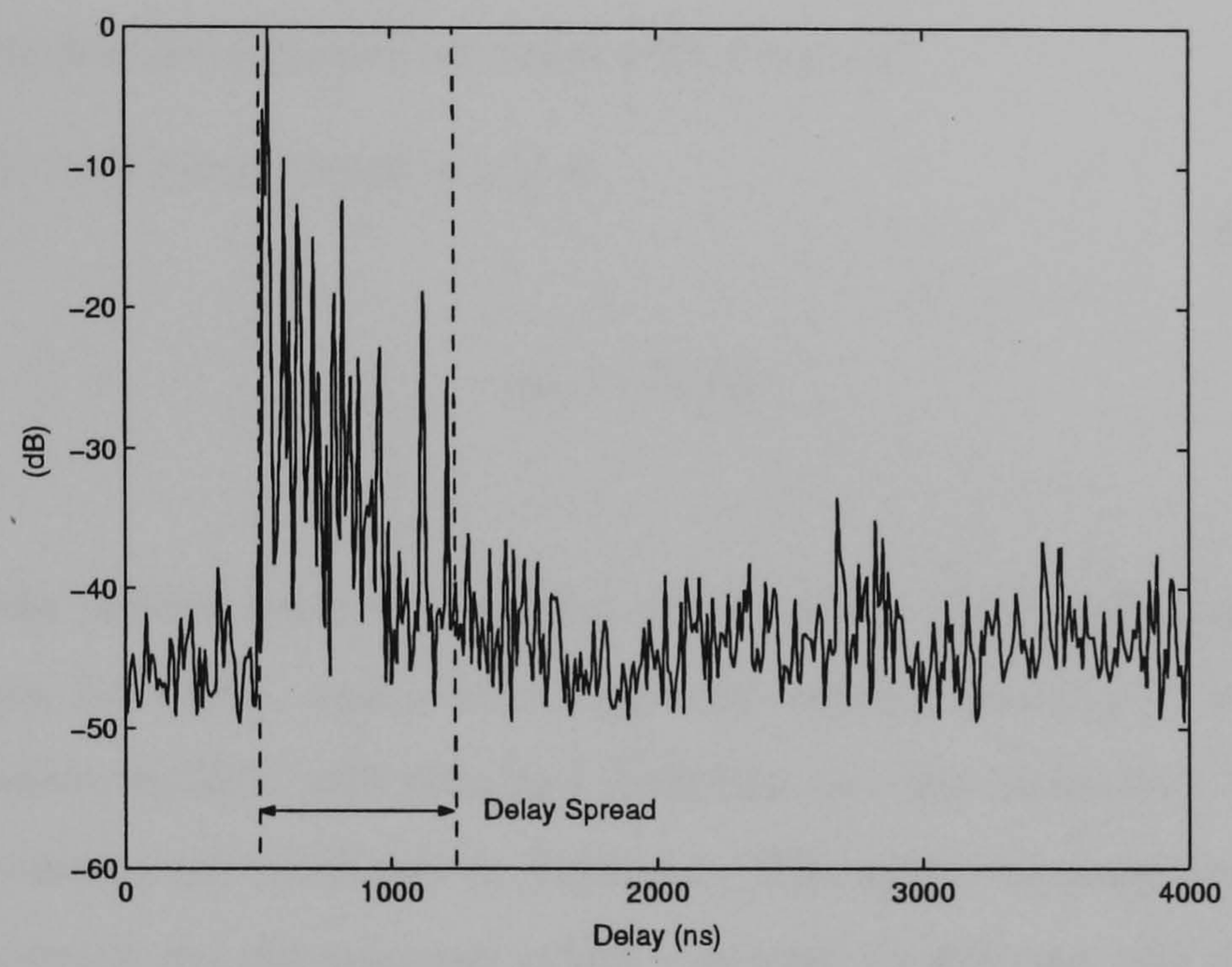

Figure 4.2: Impulse response vs. Excess Delay

Realistic channel models are essential to evaluate the performance of different positioning methods like ToA, OTDoA and DoA. The channel model have to be applicable for different environments including rural, suburban, urban and hilly environments. Relevant channel models are based on real measurement whereby channel characteristics are measured by real time radio channel sounders. Typically, models can be statistical, semi deterministic or totally deterministic. In this work, only statistical and semi deterministic modelling is considered.

Different propagation path lengths of the multi-path signal give rise to different propagation time delays. Delay spread describes to how wide range the power is spread, as illustrated in Figure 4.2. Particularly the accuracy of timing-based methods is very sensitive to delay spread and must therefore be modelled as realistic as possible.

The common channel model employed for evaluating the performance of the positioning methods is the T1P1 channel model proposed by Lundqvist et al. [68]. The channel model delay spread is suggested by Greenstein et al. [69], where the delay spread model is based on following two conjectures

- At any given distance between the transceivers, the delay spread is log-normally distributed.
- The median delay spread increases with distance.

Therefore, the *rms* delay spread (τ_{rms}) is

$$\tau_{rms} = T_1 d^{\epsilon} y \tag{4.1}$$

where T_1 is the median value of the delay spread at $d = 1$km, ϵ is an exponent with values between 0.5 and 1, and y is a lognormal variate, meaning $Y = 10 \log y$ is a Gaussian random variable with standard deviation σ_Y. The parameter values for different environments are tabulated in Table 4.1. The model assumes that there is no correlation between the delay-spread values measured to different NBs from the same UE.

Environment	T_1	ϵ	σ_Y
Urban	0.4 μs	0.5	4 dB
Suburban	0.3 μs	0.3	4 dB

Table 4.1: Delay spread model parameters for the different environments

Given the delay spread, a typical radio channel can be simulated with the Code Division Multiple Testbed (CoDiT) wideband channel model [70], as exemplify in Figure 4.3. The CoDiT model defines different environments such as urban, suburban, and rural environment. In each environment, a number of scatterers are generated and each scatterer is characterized by a mean power Ω_i, mean incidence angle at the UE with respect to LOS direction α_i, an excess time τ_i, and Nakagami-m fading m_i. The

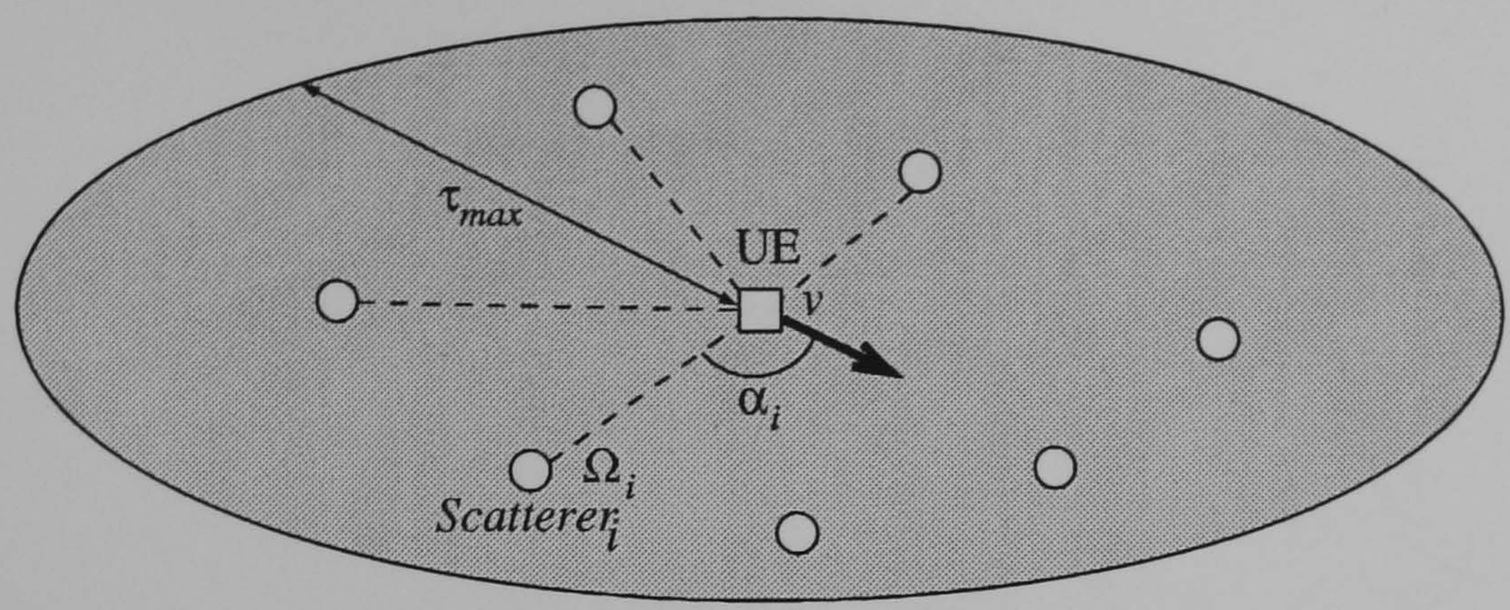

Figure 4.3: CoDiT Spatial scatter model

excess delay is defined as the delay relative to the direct LOS path τ_0. The short-term sinusoidally time varying fading for scatterer i is

$$E_{si}(t) = A_{i0}e^{j\left(\phi_{i0}+\frac{2\pi}{\lambda}vt\cos\alpha_{i0}\right)} + \sum_{l=1}^{N} A_{il}e^{j\left(\phi_{il}+\frac{2\pi}{\lambda}vt\cos\alpha_{il}\right)} \tag{4.2}$$

where

τ_{max} is the maximum delay (s)

N is the number of partial waves

v is the UE velocity (m/s)

λ is the wavelength (m)

A_{i0} is the amplitude of the specular component

A_{il} are the amplitude of the partial waves

ϕ_{i0} is the initial phase of the specular component (radian)

ϕ_{il} are the initial phases of the partial waves, uniformly distributed in the range of $[0, 2\pi]$ (radian)

α_{i0} is the incident angle from the scatterer with respect to the UE route (radian)

α_{il} are the incident angles of the partial waves, Gaussian distributed about the central angle α_{i0}, with variance of 0.15 rad^2 (radian)

The scatterer amplitudes are sorted out from Nakagami-m distribution and the following relation must be fulfilled [71]

$$A_{i0} = \sqrt{\Omega_i \sqrt{1 - m_i^{-1}}} \tag{4.3}$$

$$E\langle A_{il} \rangle = \frac{\Omega_i}{N} \sqrt{1 - m_i^{-1}} \tag{4.4}$$

$$E\left\langle A_{il}^2 \right\rangle = \frac{\Omega_i}{N} \left(1 - \sqrt{1 - m_i^{-1}}\right) \tag{4.5}$$

where m is the Nakagami-m parameter, $E < \bullet >$ and $E < \bullet^2 >$ denote mean and variance respectively. The equation (4.2) models only the short-term fading, so a long-term time variant attenuation factor $a_{lg}(t)$ that models the long-term variation is introduced.

$$E_i(t) = a_{lg}(t) E_{si}(t) \tag{4.6}$$

Therefore, the time varying channel impulse response is the summation of all the scatterers, taking into account that each one is associated to a determined time delay position, which could also depend on time

$$h(t, \tau) = \sum_{i=1}^{L} E_i(t) \delta\left(t - \tau_i(t)\right) \tag{4.7}$$

The parameters for the CoDiT model are listed in Table 4.2. The Nakagami-m parameter, with m_i =1 for Rayleigh and $m_i > 1$ for Rician fading. As its stands, the CoDiT model delay-spread values must be match to the delay-spread model cited earlier. The straightforward method is to rescale the time delay axis by compressing or expending the average power delay profiles to give the desired delay spread. To elaborate, if a given realisation of an average power delay profile has delay spread t_1 and the delay spread model realisation value is t_2, the delays of the average power delay profile scatterers are simply multiplied by $\frac{t_2}{t_1}$.

Environment: Urban					
Scatterer$_i$	Ω_i	m_i	Excess Delay	α_i	Average delay spread to mean excess delay
1^+	$1.5\exp^{(-6\tau/\tau_{max})}$	15	0	0	–
2–20	$(0.5–1.5)\exp^{(-6\tau/\tau_{max})}$	1	$0–\tau_{max}$	$U[0, 2\pi]$	1 : 1
Environment: Suburban					
1^+	4.3	15	0	0	–
2–6	0.1–0.4	1–5	$0–\tau_{max}$	$U[0, 2\pi]$	2 : 1

Table 4.2: Parameter for the average power delay profile and short term fading

where $^+$ denotes UE is having LOS with the NB.

4.2.2 LOS and NLOS Model

When the UE is having LOS with all the NBs, the position estimated will be especially accurate even in the presence of multi-path. On the other hands, if any of the NBs used for positioning is having NLOS with the UE, the accuracy will deteriorate sharply. Since the first arrival path is the reflected or refracted path from the nearby or distance scatterer, the distance estimated will not correspond to the actual distance between the UE and NB. The CoDiT model suggested that the UE will always have LOS with the NBs in the rural and suburban environments and NLOS in the urban environment. However, in actual cellular scenario the UE may not always have LOS or NLOS link with a NB at all time. So, it is necessary to include the LOS and NLOS model to the conventional CoDiT model.

Figure 4.4 illustrates two types of object that could obstruct the LOS path between the UE and NBs. The first type are those obstructors that are near and scattered around the UE, and the second type are the distanced large objects that might cause serve shadowing. The surrounding objects will cause obstruction between the UE and its serving NBs, while the distance objects would generally occur between the UE and its

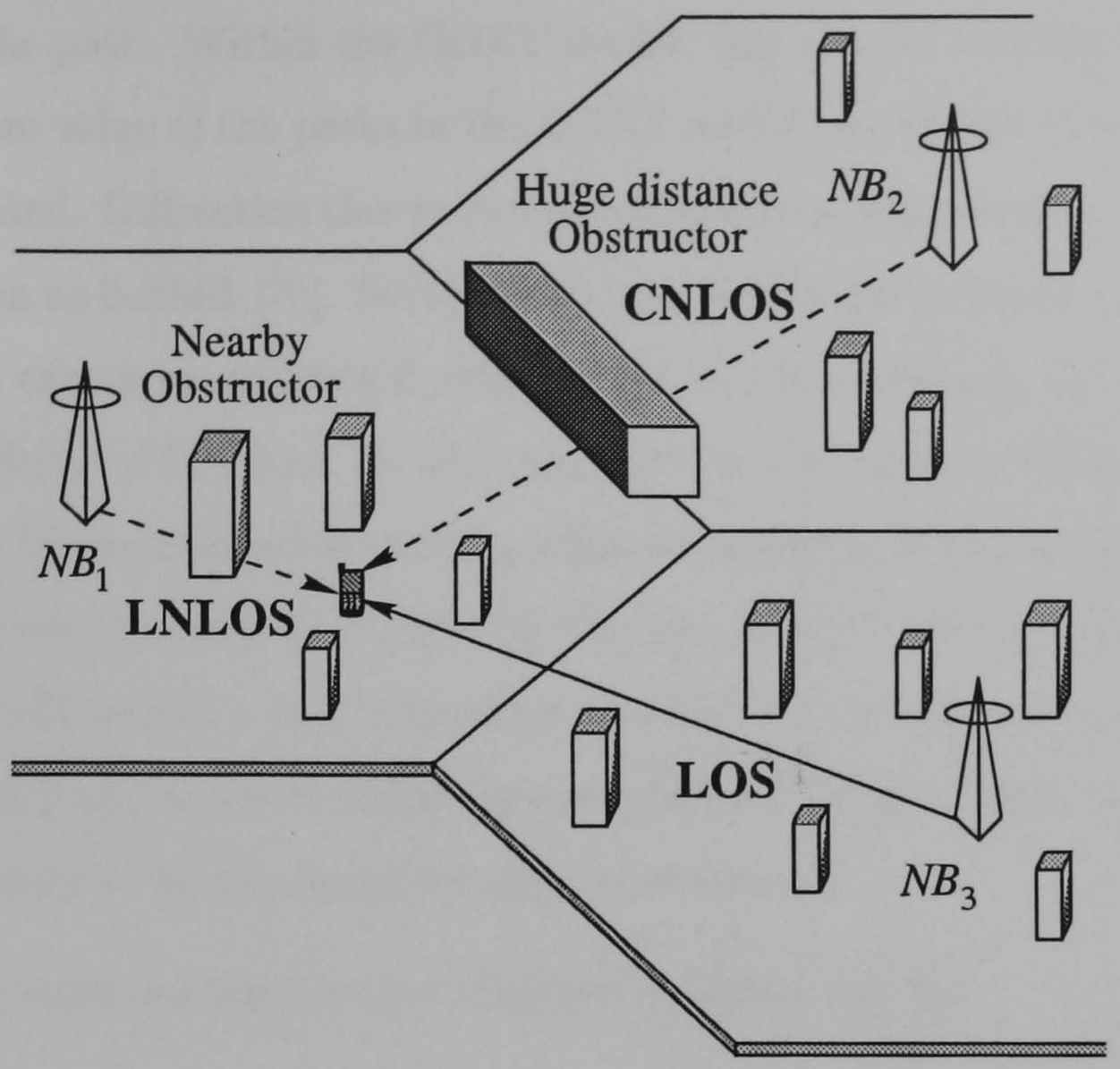

Figure 4.4: Typical cellular environment

neighbouring NBs. Thomas et al. [72] classified these two types of NLOS as the Local and Cellular NLOS, respectively. The surrounding objects will cause the Local-NLOS (LNLOS), and the distance large objects that usually located at the edge of the cell will cause the Cellular-NLOS (CNLOS).

In the LNLOS state, the mechanisms for propagation between the UE and NB will be the reflection off the nearby scatterers, as defined by the CoDiT model. The transverse between the LNLOS to Local-LOS (LLOS) stage will be simulated by the disappearance and appearance of the LOS tap (defined at zero delay) in the CoDiT model. The probability of having LLOS (P_{LLOS}) for rural, suburban and urban environments is 1, 0.8 and 0.2, respectively.

Under the CNLOS state, it is assumed that single path diffraction over the obstructor is the dominant propagation mechanism. The shadow regions caused by CNLOS conditions have four effects on the channel experienced by the UE. There will be loss of coherence as the diffracted path can be assumed to contain a summation of diffuse parts caused by irregularity of the diffraction edge. This has an effect of decreasing the

coherence of the path. Within the CoDiT model, this can be modelled by decreasing the Nakagami-m value of the paths in the CoDiT model. Secondly, all paths to the UE will be attenuated. Diffraction theory and measured data suggests the typical range for this attenuation as 0-30dB [70]. Furthermore, the additional distance travelled around the obstructor causes an additional delay in the signal arriving at the UE. Typically, this will be a delay of 0 to 1μs. In addition, there is a possibility of small angular deflection caused by the obstructor. Hence, it can be modelled by a Gaussian distribution with a mean of zero degrees. It is assumed that due to good cell planning, CNLOS will not exist centrally within a cell. Therefore, the CLNOS would only appear at or near the cell boundary and so affect radio wave propagation between cells. Hence, a serving NB would unlikely to be shadowed by such an obstructor.

Three CNLOS scenarios have been considered and they are the

- Unobstructed: No obstruction between cells
- Partially obstructed: The probability of having CLOS (P_{CLOS}) with the serving cell will be one and the probability of having LOS with neighbouring cell is shown in Figure 4.5, and it is written as

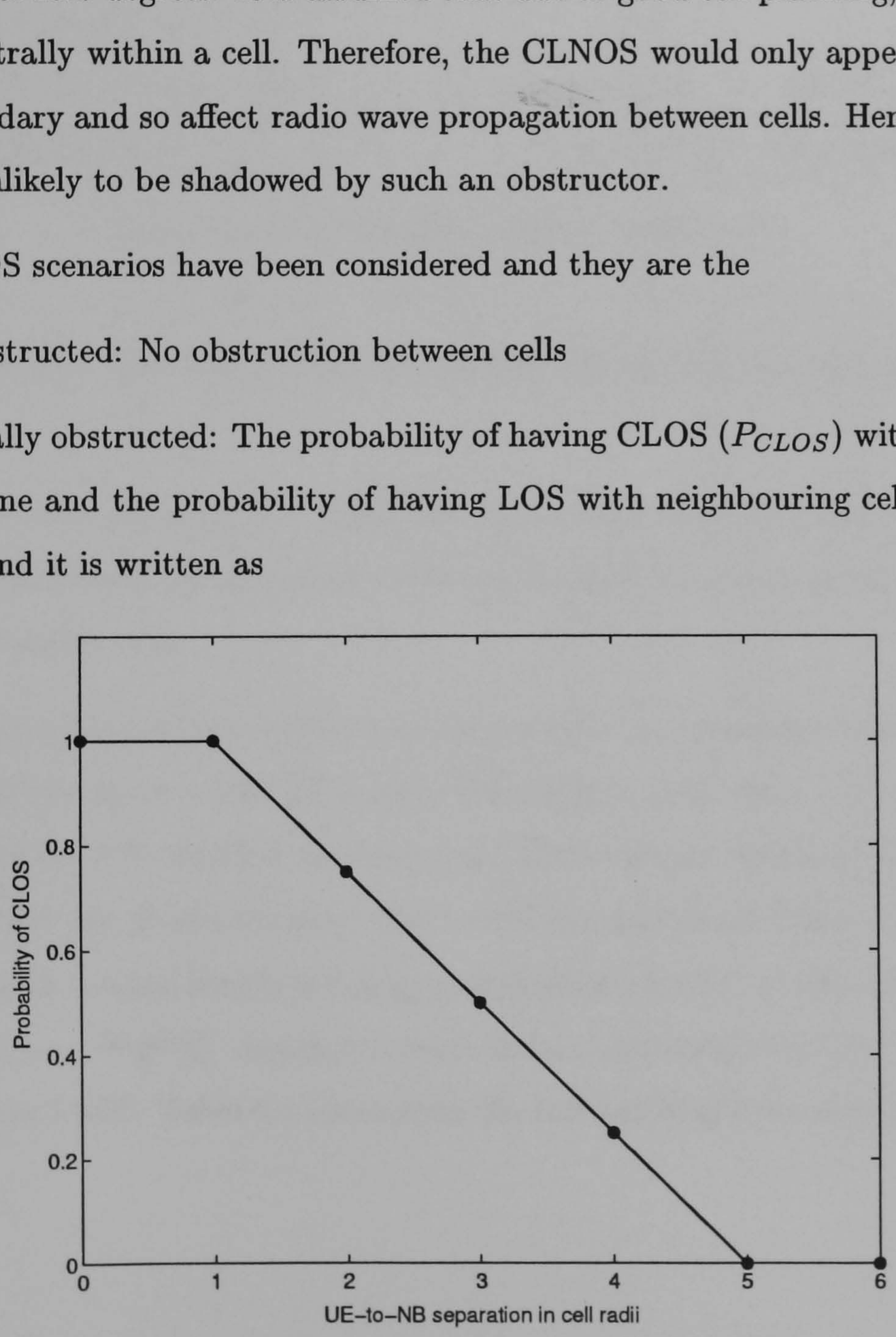

Figure 4.5: P_{CLOS} at difference UE-to-NB distance apart

$$P_{CLOS} = \begin{cases} 1 & ;r < 1 \\ 1 - \frac{r-1}{4} & ;1 \geq r \leq 5 \\ 0 & ;r > 5 \end{cases} \tag{4.8}$$

where r is the distance between the UE and NB, normalised by the cell radius.

Parameter	Unobstructed	Partial	Obstructed
P_{CLOS} (Serving NB)	1	1	1
P_{CLOS} (Other NBs)	1	(4.8)	0
CNLOS shadow (dB)	-	U[0,10]	U[10,20]
CNLOS delay (μs)	-	U[0.0,0.4]	U[0.2,0.8]

Table 4.3: CLOS specific scenario parameters

- Obstructed: The P_{CLOS} with the serving NB will be one and zero for neighbouring NBs.

The additional loss and delay by CNLOS are tabulated in Table 4.3, where U[min,max] denotes the parameter has a uniform distribution with minimum equals to min and maximum equals to max.

As the UE moves around the environment, there will be a transition between the LOS to NLOS and vice versa. The duration a UE exists in each state is modelled as the survival length the UE travelled at each state. The transition decision will occur when the UE travelled out of this distance. The LLOS survival length has a positive normal distribution with a mean length of L_{LLOS} and standard deviation restricted to $\frac{1}{3}$ of the L_{LLOS}, ($N[L_{LLOS}, \frac{L_{LLOS}}{3}]$). Again, to create the survival length for CLOS (L_{CLOS}), is the same as the LLOS. Table 4.4 summaries the survival length for each environments.

Parameter	Suburban	Urban
P_{LLOS}	0.8	0.2
L_{LLOS} (m)	30	15
L_{CLOS} (m)	200	50

Table 4.4: Survival length of LLOS and CLOS

4.2.3 Path-loss Model

Once random excess ranges are generated and added to the LOS distance of each cell site, the propagation losses for the resulting ranges are calculated using the COST-231-Hata model. The equations are considered applicable for the conditions in Table 4.5

Frequency range	1.5GHz ... 2.0GHz
Distance range	1km ... 20km
NB height	30m ... 200m
UE height	1m ... 10m

Table 4.5: Conditions for COST 231-Hata model

The standard formula is

$$PL = 46.3 + 33.9 \log f_c - 13.82 \log h_{NB} - a(h_{UE}) + (44.9 - 6.55 \log h_{NB}) \log d + C_m - K_r \tag{4.9}$$

where

PL is the basic path-loss (dB)

$$a(h_{UE}) \text{ is } \begin{cases} 3.2(\log 11.75 h_{UE})^2 - 4.97 & \text{; Urban} \\ (1.1 \log f_c - 0.7) h_{UE} - (1.56 \log f_c - 0.8) & \text{; Suburban} \end{cases}$$

$$C_m \text{ is } \begin{cases} 3 & \text{; Urban} \\ 0 & \text{; Suburban} \end{cases}$$

$$K_r \text{ is } \begin{cases} 0 & \text{; Urban} \\ 2 \log \left(\left(\frac{f_c}{28} \right)^2 + 5.4 \right) & \text{; Suburban} \end{cases}$$

f_c is the carrier frequency (MHz)

d is the distance between the UE and NB (km)

h_{NB} is the NB height (m)

h_{UE} is the UE height (m)

4.3 Performance of OTDoA Method

Parameters	Values
Cell layout	Hexagonal
Numbers of Cell	19
CNLOS obstruction	Partial obstructed
Chip Rate	3.84Mchip/s
Carrier frequency	2GHz
Spreading Modulation	QPSK
PCPICH Spreading Factor	256
Frame length	10ms
Channel sampling	32 samples/chip
Receiver over-sampling, S_r	4 samples/chip
NB synchronisation offset	0
Roll-off factor for chip shaping	0.22
PCPICH $\frac{E_c}{N_o}$	10dB
Receiver window length	6.67ms (10 time slots)

Table 4.6: UMTS downlink simulation parameters

The UMTS WCDMA FDD downlink channel is simulated. The urban and suburban environments are considered with varying channel model parameters cited in section 4.2.1. The number of UE over an area is selected to be 250 UE/km^2, and each UE is spatially uniform distributed over the simulation area. The cell radius chosen for the urban and suburban environments are 500m and 2000m, respectively. The UEs move around the simulation area and their initial directions are uniformly distributed between 0 to 2π radian, at speed a of 5km/h and 120km/h in urban and suburban

environment respectively. The simulation parameters are listed in Table 4.6 and will be used throughout the simulations, unless stated otherwise.

4.3.1 Effect of $\frac{E_c}{N_o}$ on the OTDoA accuracy

The output of the matched filter will produce a peak when snapshot of the received signal is cross-correlated with the local replica of the transmitted signal. Then again, it is clear that correct estimation of timing delay in this procedure depends on correct estimation of the transmitted chips. Any wrong chips decisions produce bad re-spread replacement in the composite signal. As a result, the timing observations deviate significantly whenever numbers of chips are wrongly estimated. Hence, errors in position estimates don't increase gradually with increasing noise and interference, but increase significantly whenever there are errors in timing estimation.

The first set of results shown in Figures 4.6 and 4.7, exemplify the effect of thermal noise level on the UE position estimator for both urban and suburban environments. Figure 4.6 plots the err_{rms} of UE position estimates, expressed in meters, as a function of $\frac{E_c}{N_o}$. While Figure 4.7 contains the σ of error, also expressed in meters.

Both figures demonstrate the same result of a simulation, which shows increments in positioning error with every increased levels of thermal noise. Figure 4.6 proves that the err_{rms} declines exponentially when the $\frac{E_c}{N_o}$ increased. From the $\frac{E_c}{N_o}$ of 10dB and higher, the improvement of err_{rms} are about 20m or less. The improvement is therefore marginal as compared with low $\frac{E_c}{N_o}$ cases. This is the same for the results plotted in Figure 4.7 when at 10dB and higher, the error σ is 22m or lower. With every increments of 5dB, the error σ only decreased by 10m, so improvement is only 10% or lesser.

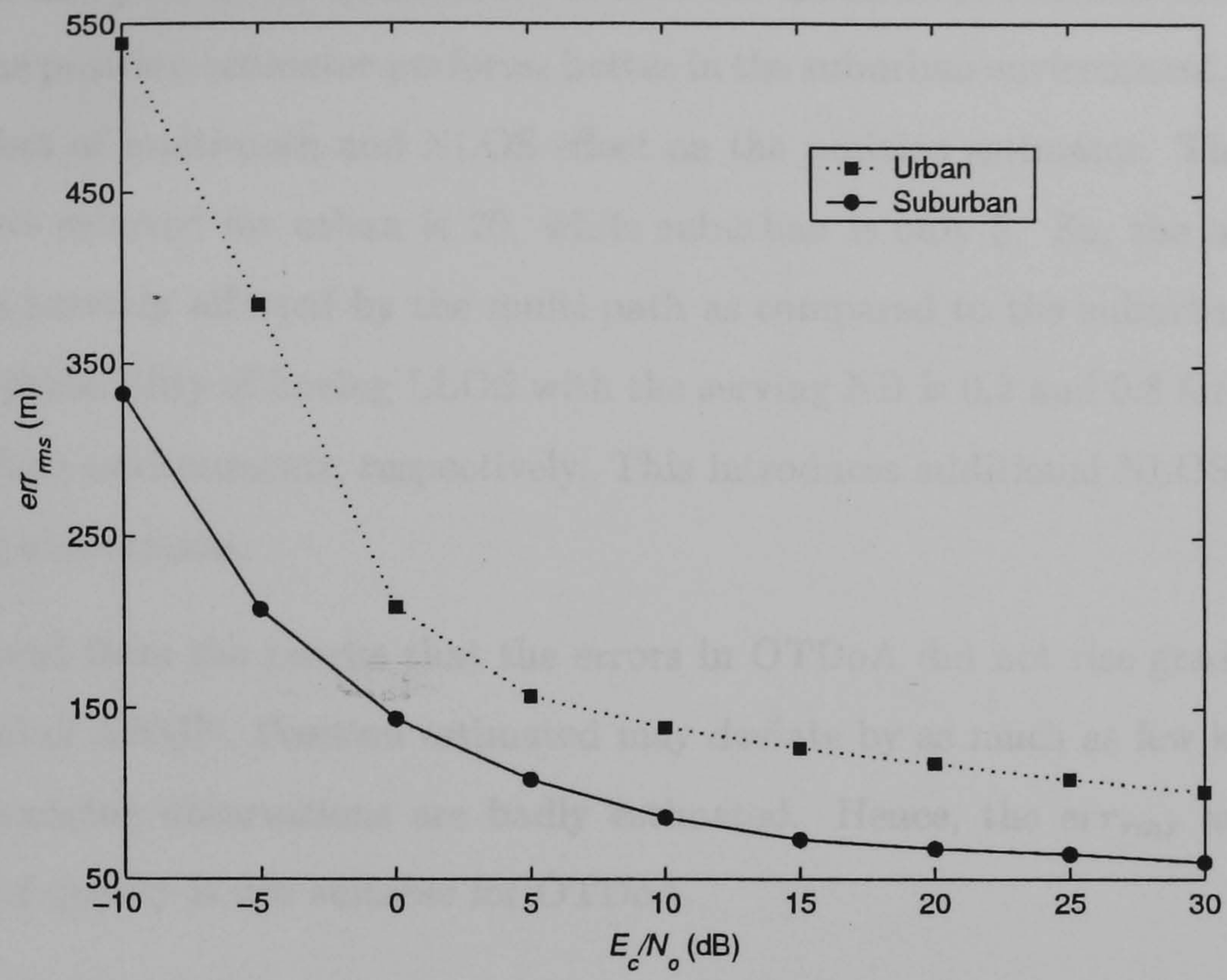

Figure 4.6: OTDoA err_{rms} differences in Urban and Suburban environments

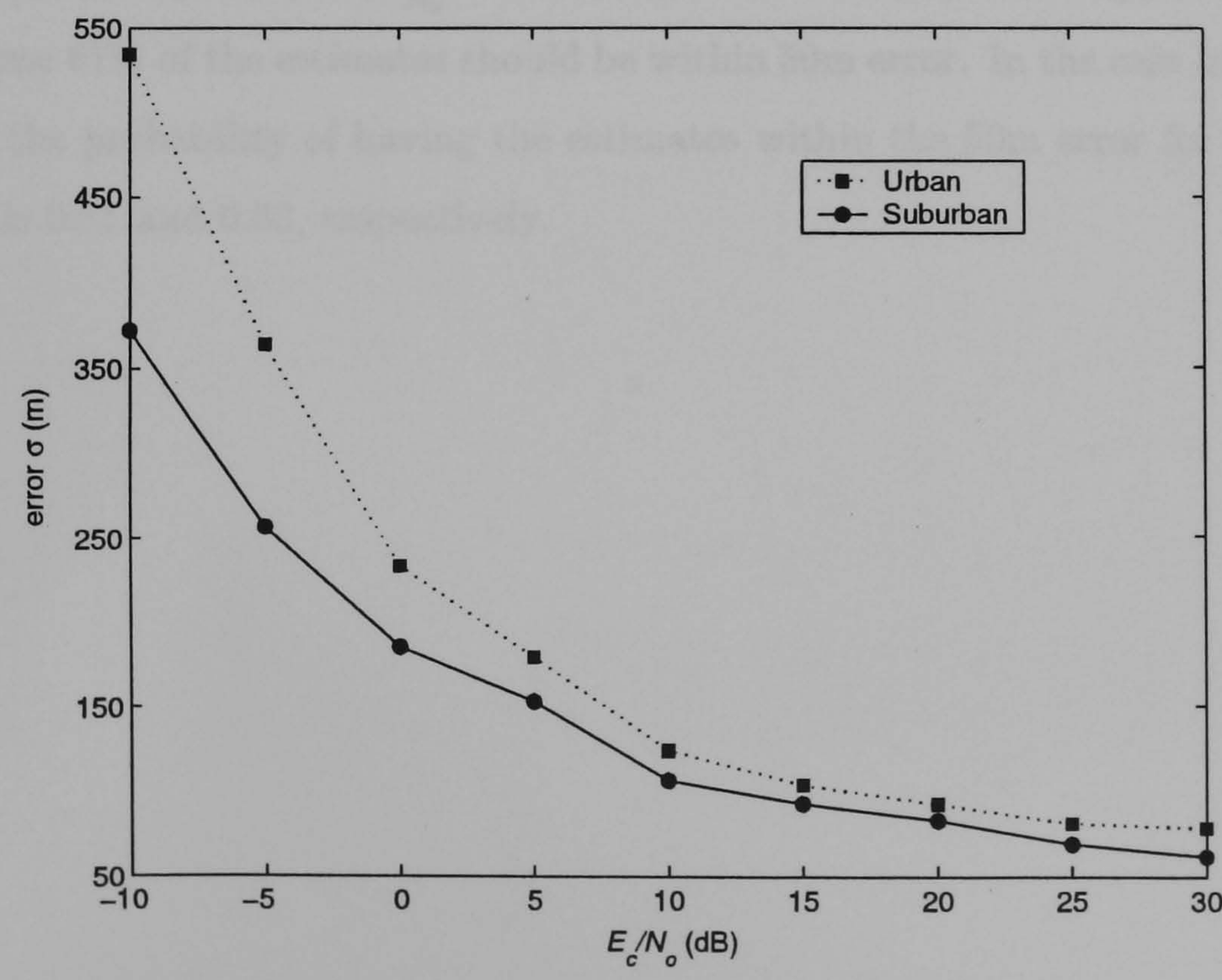

Figure 4.7: OTDoA error σ differences in Urban and Suburban environments

The figures also present the differences between the urban and suburban environments. Notably the position estimator performs better in the suburban environment, representing the effect of multi-path and NLOS effect on the position estimator. The numbers of scatterers selected for urban is 20, while suburban is only 5. So, the urban environment is severely affected by the multi-path as compared to the suburban. What's more, the probability of having LLOS with the serving NB is 0.2 and 0.8 for the urban and suburban environments, respectively. This introduces additional NLOS error into the timing observation.

It is observed from the results that the errors in OTDoA did not rise gradually with higher level of AWGN. Position estimated may deviate by as much as few kms, whenever, the ranging observations are badly estimated. Hence, the err_{rms} and error σ measures of quality is not suitable for OTDoA.

Figures 4.8 and 4.9 demonstrate this point. Both figures present the same results of a simulation that show increased positioning error with increase levels of thermal noise. This simulation measured the Euclidian distance (err) cumulative distribution functions at different levels of $\frac{E_c}{N_o}$. The dashed lines indicate the requirement of the E-911, where 67% of the estimates should be within 50m error. In the case of $\frac{E_c}{N_o}$ equals to 10 dB, the probability of having the estimates within the 50m error for urban and suburban is 0.51 and 0.63, respectively.

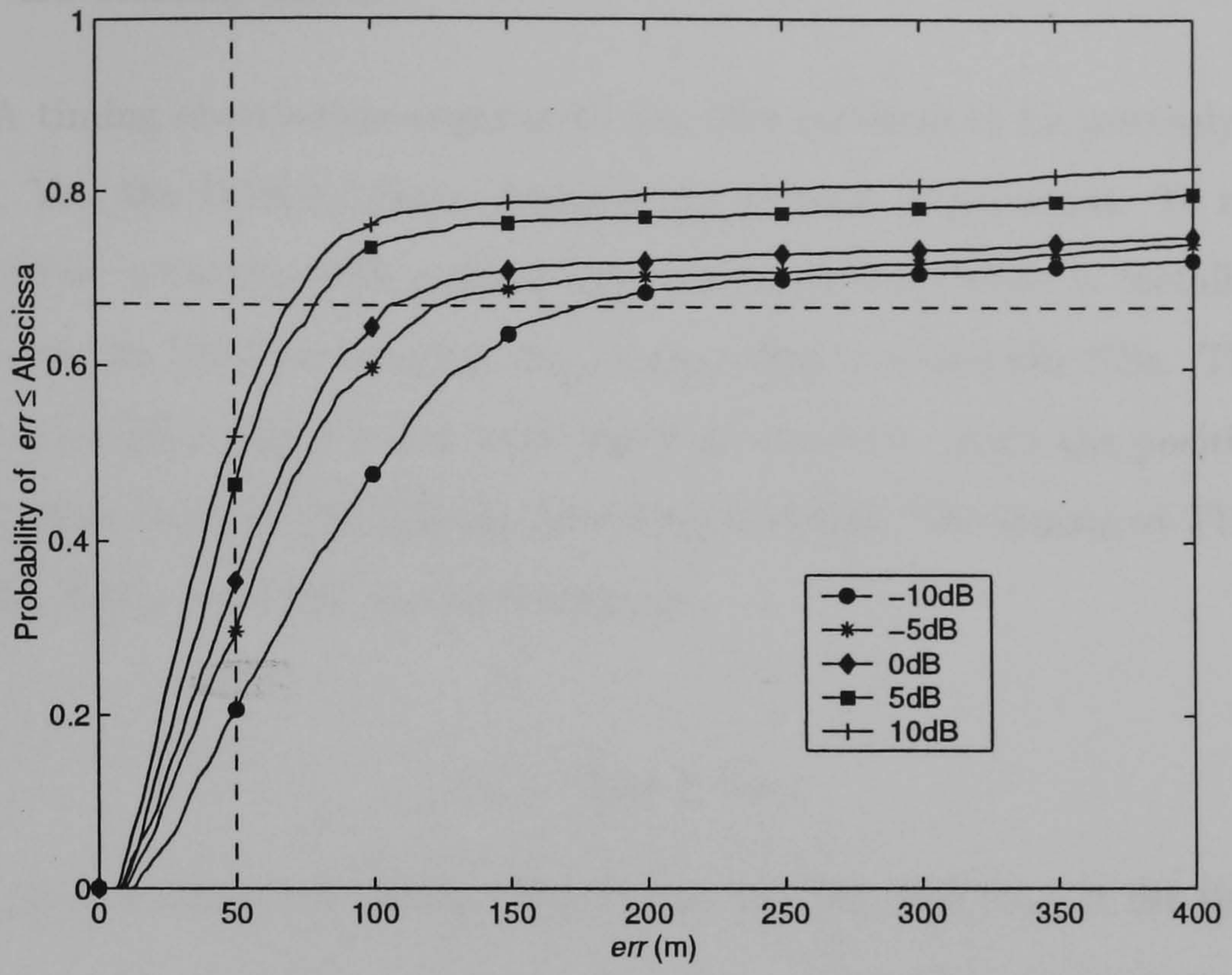

Figure 4.8: OTDoA performance at different levels of $\frac{E_c}{N_o}$ in urban environment

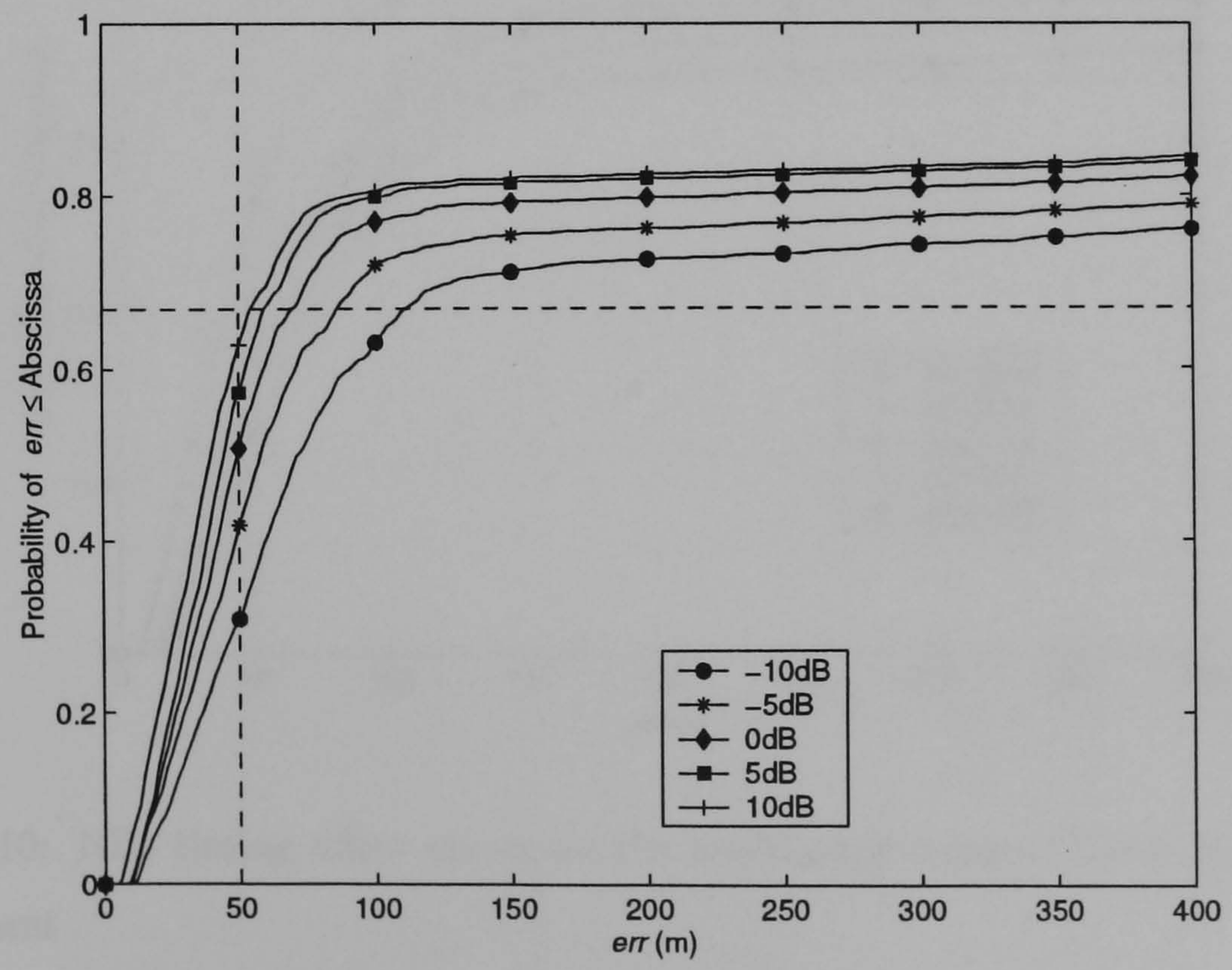

Figure 4.9: OTDoA performance at different levels of $\frac{E_c}{N_o}$ in suburban environment

4.3.2 NBs timing offset

The TDoA timing observation requires all the NBs involved to be precisely time synchronised. Yet, the UTRA cellular network has no such requirement. To resolve this problem, either accurate GPS receiver functioning in time mode is installed in each NB, or to use the LMU to calculate the timing offset between the NBs. The LMU is located at a position where it has LOS link with the NBs. With the position known, the timing offset between the NBs can be determined [44]. The measured TDoA timing between the NB_m and NB_1 can be written as

$$\tau_{m,1} = \tilde{\tau}_{m,1} + O_{m,1} \tag{4.10}$$

where $\tilde{\tau}_{m,1}$ is the measured timing difference at the UE, and $O_{m,1}$ is the timing offset error.

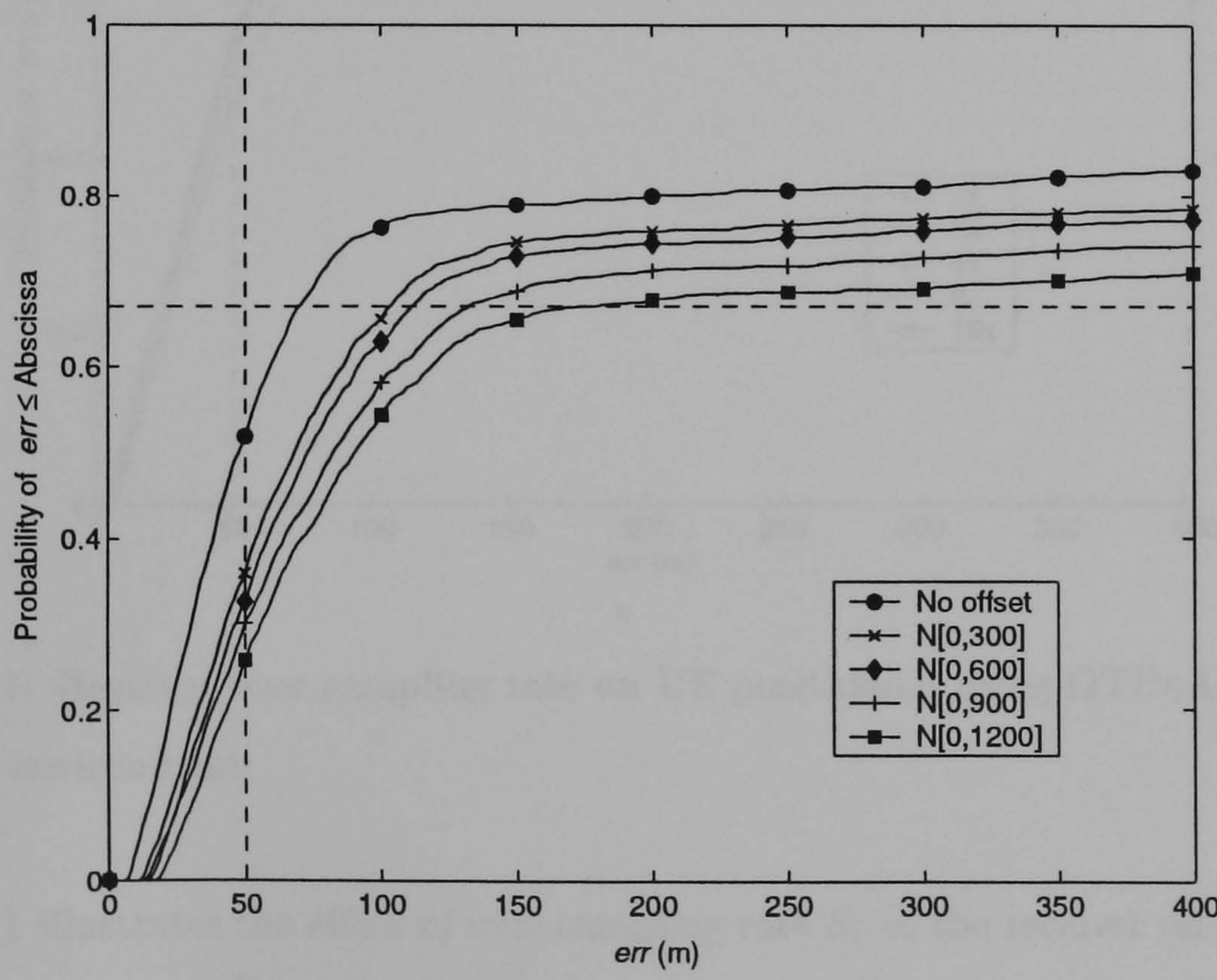

Figure 4.10: NBs timing offset errors on UE positioning using OTDoA in the urban environment

Figure 4.10 shows the effect of varying the synchronisation offset error between the NBs. The synchronisation offset errors for each pair of NBs have a normal distribution

with a mean of zero and σ varied from 0 to 1200ns, respectively. The thermal noise $\frac{E_c}{N_o}$ is fixed at 10dB and the timing offset error is rounded off to the nearest sampling time. It is observed from the cumulative curves that the accuracy degrades as the $O_{m,1}$ error increased. As predicted, when timing offset error is introduced, there is a significant drop in precision. In no timing offset situation, more than 50% of the estimates are within the 50m error, as compared to 35% when $O_{m,1} = N[0, 300]$ is introduced.

4.3.3 Receiver sampling rate

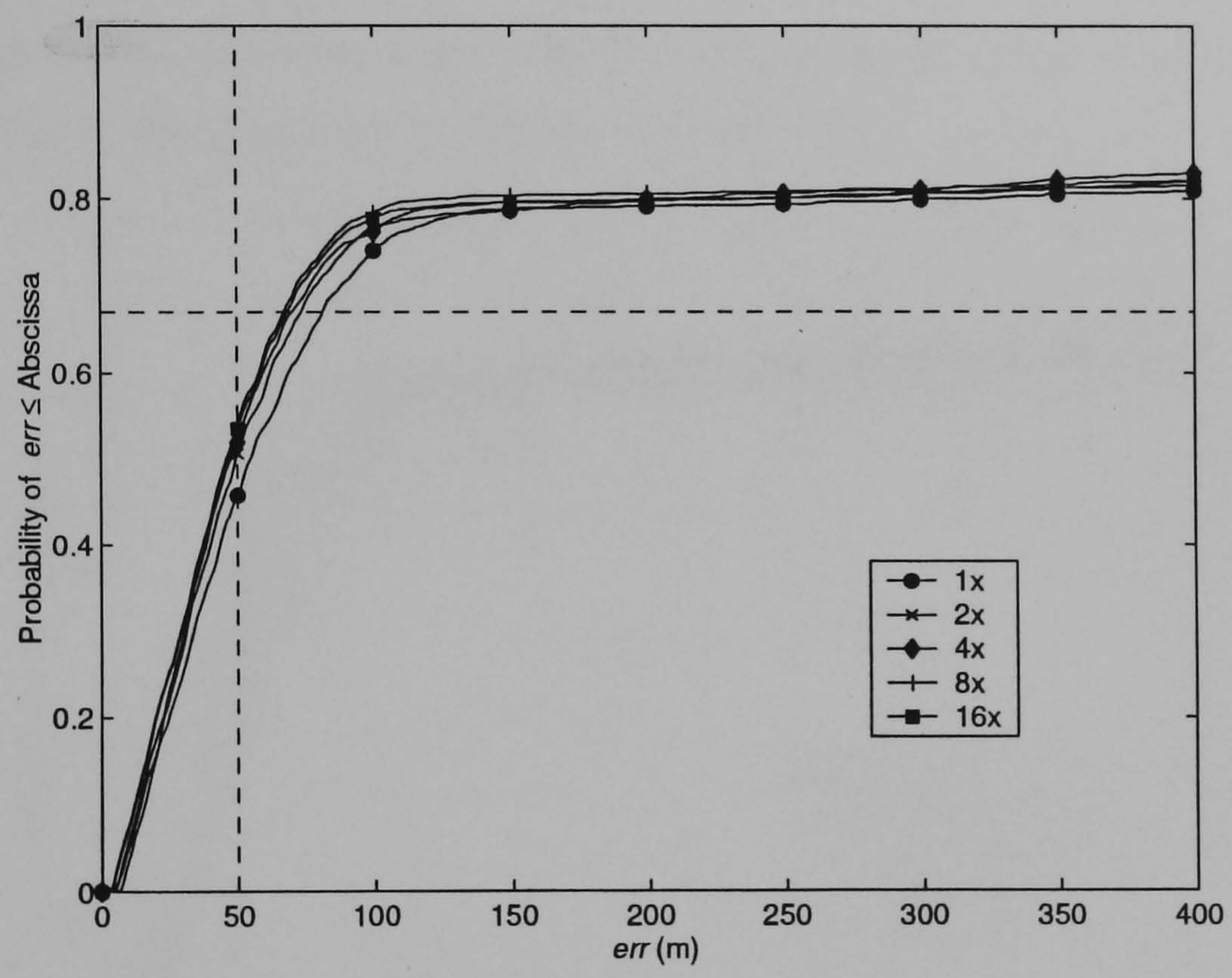

Figure 4.11: Receiver over sampling rate on UE positioning using OTDoA method in the urban environment

Figure 4.11 illustrates the effect of over sampling rate S_r of the receiver on the UE positioning accuracy. A $\frac{E_c}{N_o}$ of 10dB is chosen and perfect NBs timing offset is considered. The accurateness of TDoA timing observation also depends on the over-sampling rate of the receiver, as time quantisation error decreases with higher sampling rate. For $S_r = 1$ corresponds to a quantisation error of 78.125m, and $S_r = 16$ corresponds to 4.883m. Surprisingly, Figure 4.11 conveys that higher S_r does not show much improvement and this may be attributed to the high chip rate of the PCPICH. From the plot,

an over sampling rate $S_r = 4$ is sufficient to produce the desired accuracy.

4.3.4 Distance of UE from its Serving NB

For voice and data applications, satisfactory services are usually met when the UE resides near its serving NB. Falls in QoS usually occurred when it is at the boundary of the cell. However, in UE positioning, the neighbouring NBs are required to locate the UE. The PCPICH from neighbouring NBs will be heavily attenuated when UE resides near the centre of the cell, and this is further aggravated if UE resides in a large cell. That's why poor positioning arises when UE is near to the centre or in a large cell. This scenario is clearly plotted in Figures 4.12 and 4.13.

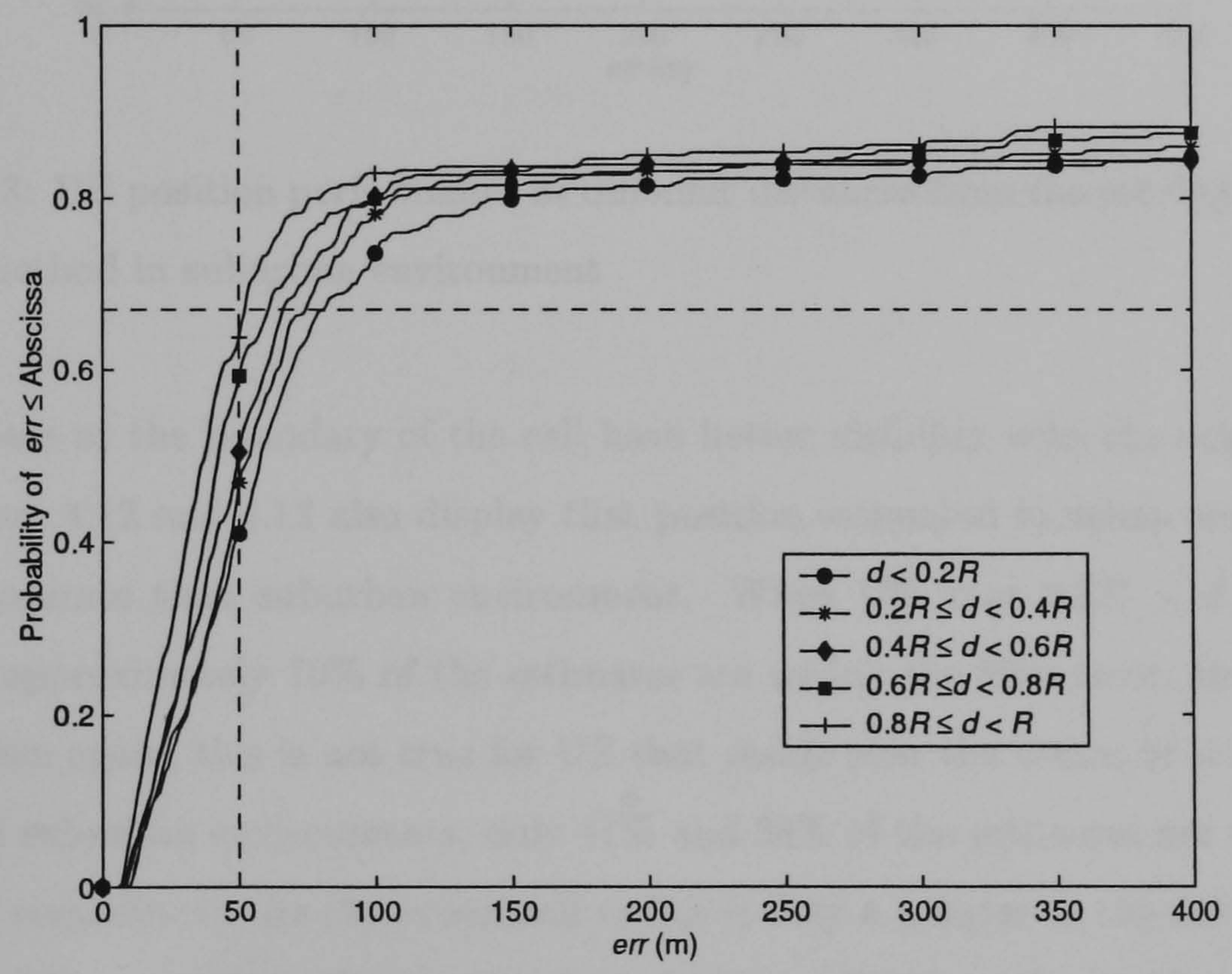

Figure 4.12: UE position performance at different distances from the serving NB using OTDoA method in urban environment

The urban and suburban cells are sectorised into five different rings, and with each ring having a width of 100m and 400m for urban and suburban, respectively. In general, positions estimated are more accurate for the UEs that are located at the boundary of the cell, compare with the UEs that are near their serving NBs. This is because those

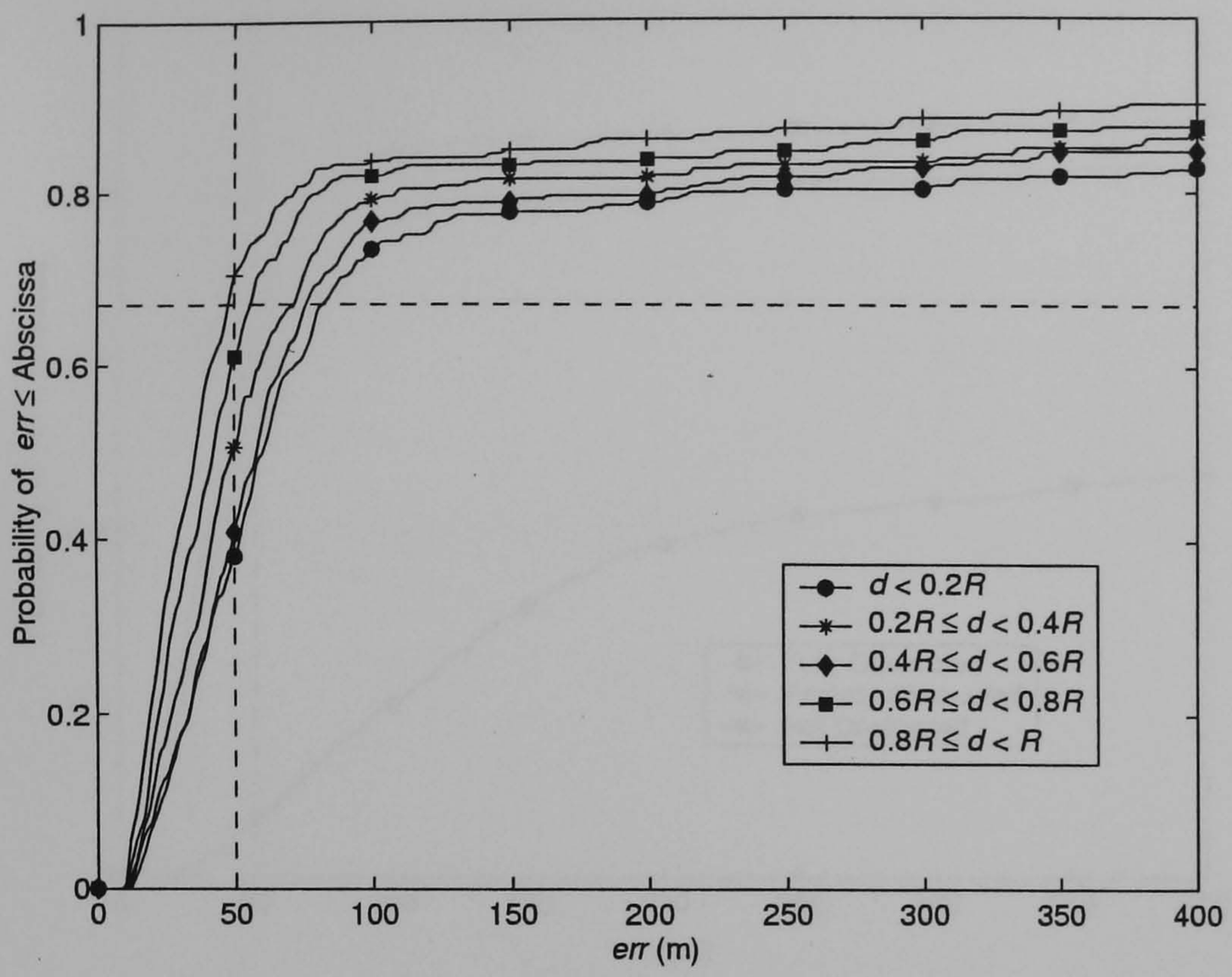

Figure 4.13: UE position performance at different distances from the serving NB using OTDoA method in suburban environment

UEs that are at the boundary of the cell have better visibility with the neighbouring NBs. Figure 4.12 and 4.13 also display that position estimated in urban environment are less accurate than suburban environment. When UE is at $0.8R \leq d < R$, for suburban approximately 70% of the estimates are within the 50m error, and 65% for urban. Then again, this is not true for UE that reside near the centre of the cell. For urban and suburban environments, only 41% and 38% of the estimates are within the 50m error respectively. As the urban cell radius is only a quarter to the suburban cell radius, so UEs in urban cell therefore have better visibility with neighbouring NBs, than UEs in the suburban cell.

4.3.5 Probability of CNLOS on the OTDoA

To investigate the NLOS problem on the LCS, the effect of P_{CNLOS} on the position estimator was investigated. It is discussed that the neighbouring NBs are essential to assist in locating the UE, so the PCPICH signals from neighbouring NBs have

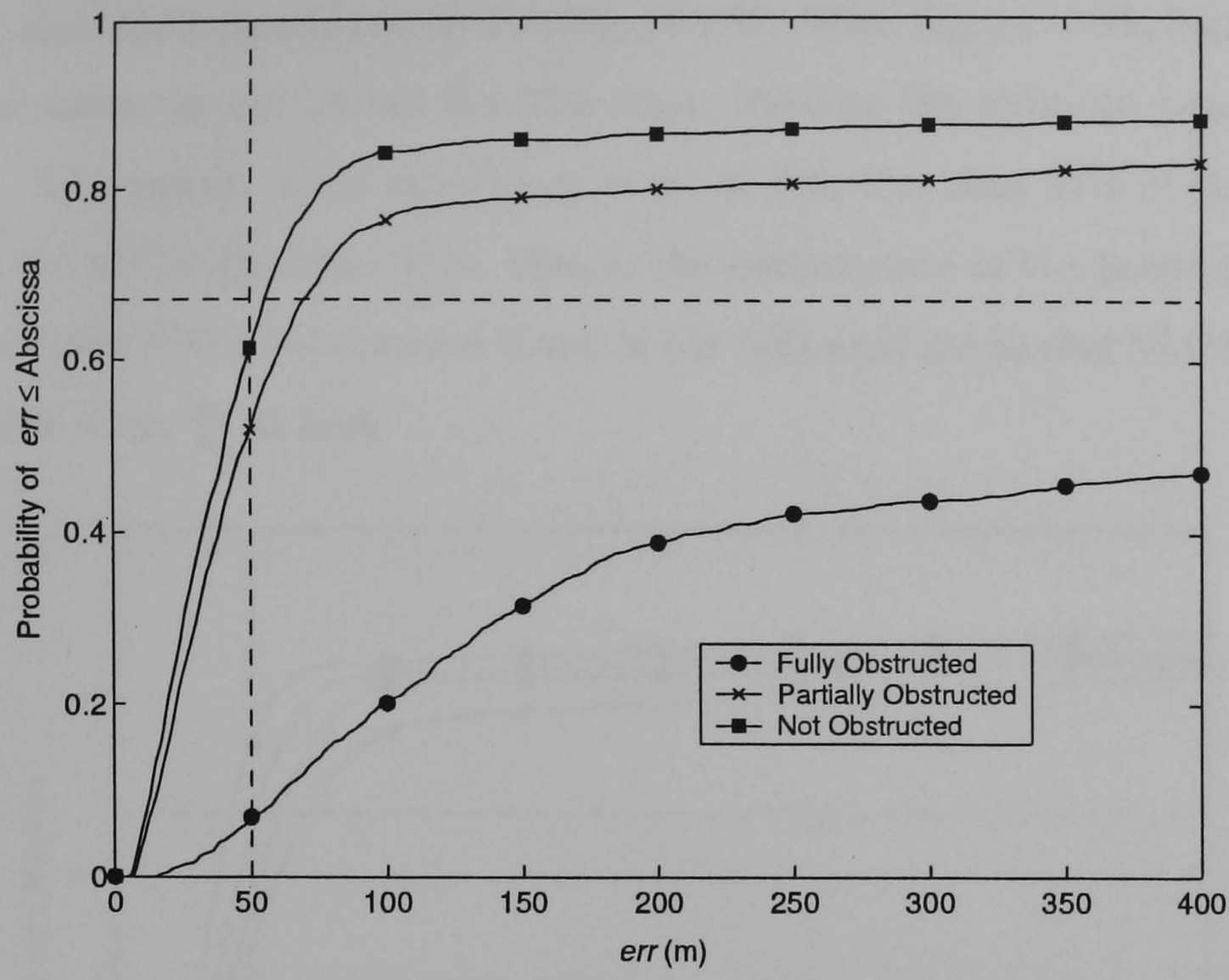

Figure 4.14: CNLOS error on the UE position estimator in urban environment

significant effects on the location services. In this part, three scenarios are studied, the fully, the partially, and no obstruction from the neighbouring NBs. In the simulation work, it is assumed that P_{CLOS} between the UE and its serving NB (nearest to the UE) is always one. The probability of having LOS with neighbouring NBs is always one for no obstruction scenario, zero for fully obstruction scenario, and depends on equation (4.8) for partially obstruction scenario. Figure 4.14 proves that fully obstructed case performed much worse than the others. The result depicts that less than 10% of the estimates are within the 50m error, and 47% of the estimates are within 400m error. For this reason, pre-filtering and appropriate weighting the timing observations which have large variances, are necessary to avoid the position estimator being severely deteriorated by the CNLOS errors.

4.3.6 Probability of LNLOS on the OTDoA

In relation with the previous sub-section, P_{LLOS} is varied from 0.2 to 0.8 and keeping the CNLOS partially obstructed. As expected, the accuracy worsens rapidly when P_{LLOS}

decreased, and this is clearly revealed in Figure 4.15. With $P_{LLOS} = 0.8$, approximately 76% of the estimates are within the 50m error, meeting the stringent requirement of the E-911. Conversely, when the P_{LLOS} is set at 0.6, less than 67% of the positions estimated are within the 50m error. Hence, the performance of the position estimator will not meet the E-911 requirement if any of the NBs used are having NLOS links with the UE, even when $\frac{E_c}{N_o}$ is high.

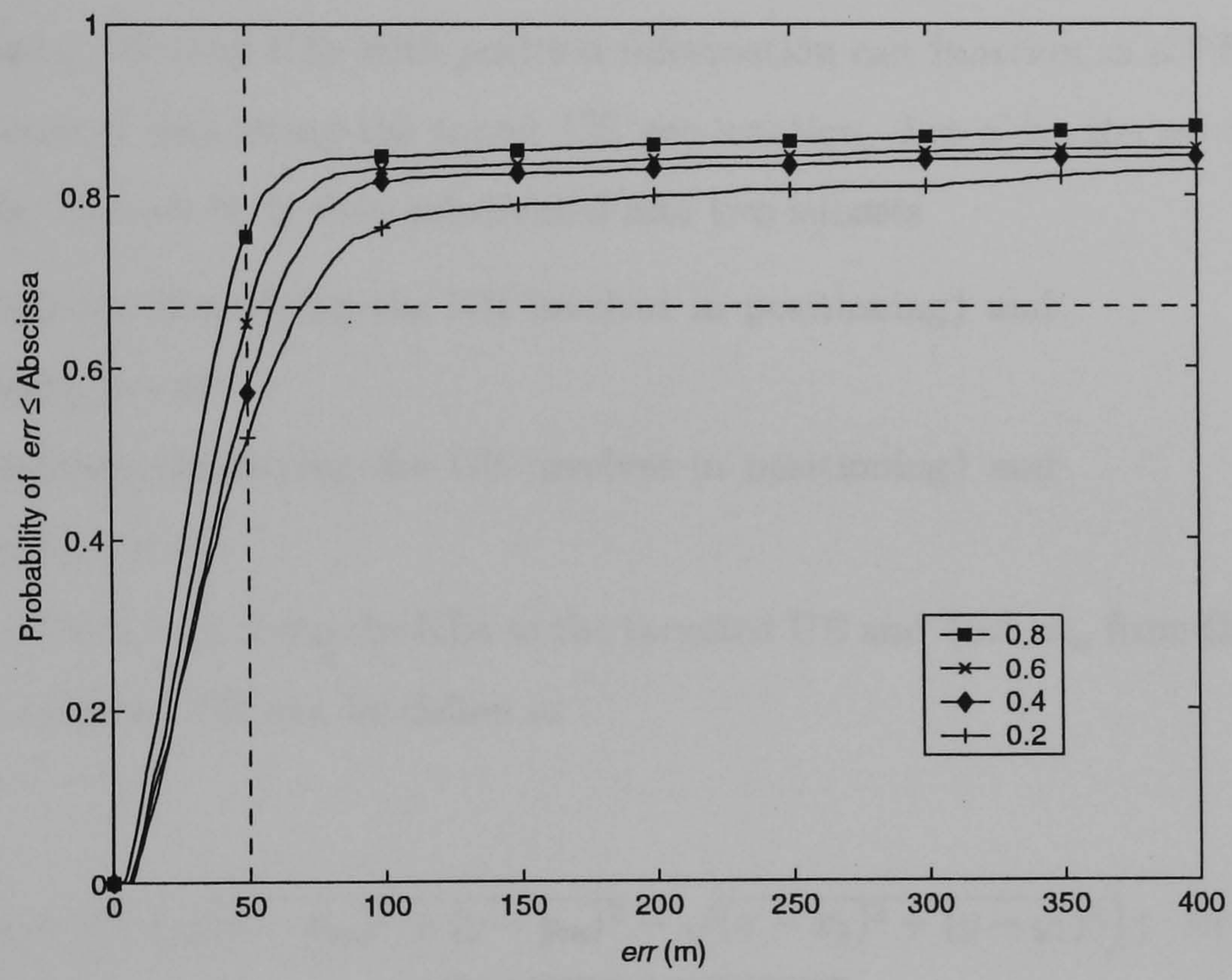

Figure 4.15: LNLOS error on the UE position estimator in urban environment

To sum up, the performance of the UE position estimator depends on the $\frac{E_c}{N_o}$, LOS link between the UE and the NBs, timing offset between the NBs, and the location where the UE resides in a cell. Unpredictably, the time quantisation error has little effect on the accuracy of the position estimates. This is due to the high chip rate of the PCPICH used in UE positioning. However, the NLOS error will deteriorate the accuracy, regardless of the $\frac{E_c}{N_o}$ level. That's why it is desirable for UE to have LOS links with all the NBs that are used for position acquisition, if it is to attain the E-911 requirement. But, it is not feasible in practice to ensure that the UE will have LOS with the NBs at all time. For this reason, methods to improve location accuracy are required. One such method is to exploit the hybrid *ad hoc* cellular network, which will

be investigated in the remainder of this chapter.

4.4 Position Estimator for the Hybrid *Ad Hoc* Cellular Network

In the hybrid *ad hoc* cellular network, the positioning method is not restricted to NB for positioning. Nearby UEs with position information can function as a PE, assisting in the process of estimating the target UE geo-location. Let S be the set identifying all the PEs. The set S, is then subdivided into two subsets

S_m ={indexes identifying the NB involves in positioning} and
$\dim\{S_m\} = M$

S_n ={indexes identifying the UE involves in positioning} and
$\dim\{S_n\} = N$

Then, the TDoA, $\tau_{m,1}$, from the NBs to the targeted UE and ToA, τ_n, from the assisting UE to the targeted UE can be define as

$$\begin{cases} \tau_{m,1} = c^{-1}\left(\sqrt{(x-x_m)^2+(y-y_m)^2} - \sqrt{(x-x_1)^2+(y-y_1)^2}\right); & m \in S_m \\ \tau_n = c{-}1\sqrt{(x-\tilde{x}_n)^2+(y-\tilde{y}_n)^2}; & n \in S_n \end{cases} \tag{4.11}$$

where $[x_m, y_m]$ is the horizontal coordinates of NB_m, and $[\tilde{x}_n, \tilde{y}_n]$ is the estimated horizontal coordinates of UE_n. The targeted UE position $[x, y]$ can be resolved by circular trilateration, as elucidated in section 2.5.3. Ignoring the second and higher order terms in the Taylor series expansion, the equation can now be written as

$$\begin{cases} a_m\vec{\delta} = \tau_{m,1} + \tau_o - c^{-1}\sqrt{(x-x_m)^2+(y-y_m)^2} - e_m \\ a_n\vec{\delta} = \tau_n - \sqrt{(x-\tilde{x}_n)^2+(y-\tilde{y}_n)^2} - e_n \end{cases} \tag{4.12}$$

where $\vec{\delta}$ is $\begin{bmatrix} \Delta x & \Delta y & R_o \end{bmatrix}^T$. Stacking of equation (4.12) results in the cost function of the least-squares estimation, written as

$$\varepsilon = \begin{bmatrix} \vec{Z}_m \\ \vec{Z}_n \end{bmatrix} - \begin{bmatrix} \vec{A}_m \\ \vec{A}_n \end{bmatrix} \begin{bmatrix} \vec{\delta}_m \\ \vec{\delta}_n \end{bmatrix} \tag{4.13}$$

$$\vec{A}_m \quad \text{is } c^{-1} \begin{bmatrix} \frac{x-x_1}{r_1} & \frac{y-y_1}{r_1} & 1 \\ \vdots & \vdots & \vdots \\ \frac{x-x_M}{r_M} & \frac{y-y_M}{r_M} & 1 \end{bmatrix}$$

$$\vec{A}_n \quad \text{is } c^{-1} \begin{bmatrix} \frac{x-\tilde{x}_1}{\tilde{r}_1} & \frac{y-\tilde{y}_1}{\tilde{r}_1} & 0 \\ \vdots & \vdots & \vdots \\ \frac{x-\tilde{x}_N}{\tilde{r}_N} & \frac{y-\tilde{y}_N}{\tilde{r}_N} & 0 \end{bmatrix}$$

where

$$\vec{Z}_m \quad \text{is} \begin{bmatrix} \tau_{m,1} + \tau_o - c^{-1}\sqrt{(x-x_1)^2 + (y-y_1)^2} \\ \vdots \\ \tau_{M,1} + \tau_o - c^{-1}\sqrt{(x-x_M)^2 + (y-y_M)^2} \end{bmatrix}$$

$$\vec{Z}_n \quad \text{is} \begin{bmatrix} \tau_n - c^{-1}\sqrt{(x-\tilde{x}_1)^2 + (y-\tilde{y}_1)^2} \\ \vdots \\ \tau_N - c^{-1}\sqrt{(x-\tilde{x}_N)^2 + (y-\tilde{y}_N)^2} \end{bmatrix}$$

$$r_m \quad \text{is } \sqrt{(x-x_m)^2 + (y-y_m)^2}$$

$$\tilde{r}_n \quad \text{is } \sqrt{(x-\tilde{x}_n)^2 + (y-\tilde{y}_n)^2}$$

Considering the accuracy of timing observations between the NB-to-UE and UE-to-UE, and the calculated assisting UEs positions, the scaled covariance matrix $\vec{Q}$ can be written as

$$\vec{Q} = diag\left[\sigma^2_{tt_{NB_1}}, \ \ldots, \ \sigma^2_{tt_{NB_M}}, \ \sigma^2_{xy_{UE_1}}\sigma^2_{tt_{UE_1}}, \ \ldots, \ \sigma^2_{xy_{UE_N}}\sigma^2_{tt_{UE_N}} \right]$$

$$= \begin{bmatrix} \sigma^2_{tt_{NB_1}} & 0 & \cdots & \cdots & \cdots & 0 \\ 0 & \ddots & 0 & 0 & 0 & \vdots \\ \vdots & 0 & \sigma^2_{tt_{NB_M}} & 0 & 0 & \vdots \\ \vdots & 0 & 0 & \sigma^2_{xy_{UE_1}}\sigma^2_{tt_{UE_1}} & 0 & \vdots \\ \vdots & 0 & 0 & 0 & \ddots & 0 \\ 0 & \cdots & \cdots & \cdots & 0 & \sigma^2_{xy_{UE_N}}\sigma^2_{tt_{UE_N}} \end{bmatrix} \tag{4.14}$$

$\sigma^2_{tt_{NB_m}}$ is the timing observation variance between target UE and NB_m

$\sigma^2_{tt_{UE_n}}$ is the timing observation variance between target UE and assisting UE_n

where

$\sigma^2_{xy_{UE_n}}$ is $\left(c^{-1}\sqrt{\sigma^2_{xx_{UE_n}} + \sigma^2_{yy_{UE_n}}}\right)^2$, the calculated horizontal coordinates variance of assisting UE_n

If the relative variances of the timing and assisting coordinates are unknown, the covariance matrix $\vec{Q}$ will be an identity matrix with dimensions of $M + N$ by $M + N$.

Figure 4.16a illustrates two UEs, UE_1 and UE_2, positioned with trilateration method. Due to the imprecise ranging observations, the positions estimated for the UEs will be within the shaded area, as shown in Figure 4.16a. In order to provide a better location estimate, it will be desirable to minimise the shaded area. It could be achieved by higher ranging observations accuracy or additional NBs to assist in positioning. Then again, if these were not possible, the ranging estimates between the UEs would be used for UE spatial locating. Figure 4.16b demonstrates that the ranging estimate between the UEs is approximately d distance apart, so the shaded area will be the overlap area of the ranging observations between the UE-to-NB and UE-to-UE. In this case, the shaded area is minimised, and better estimates are obtained.

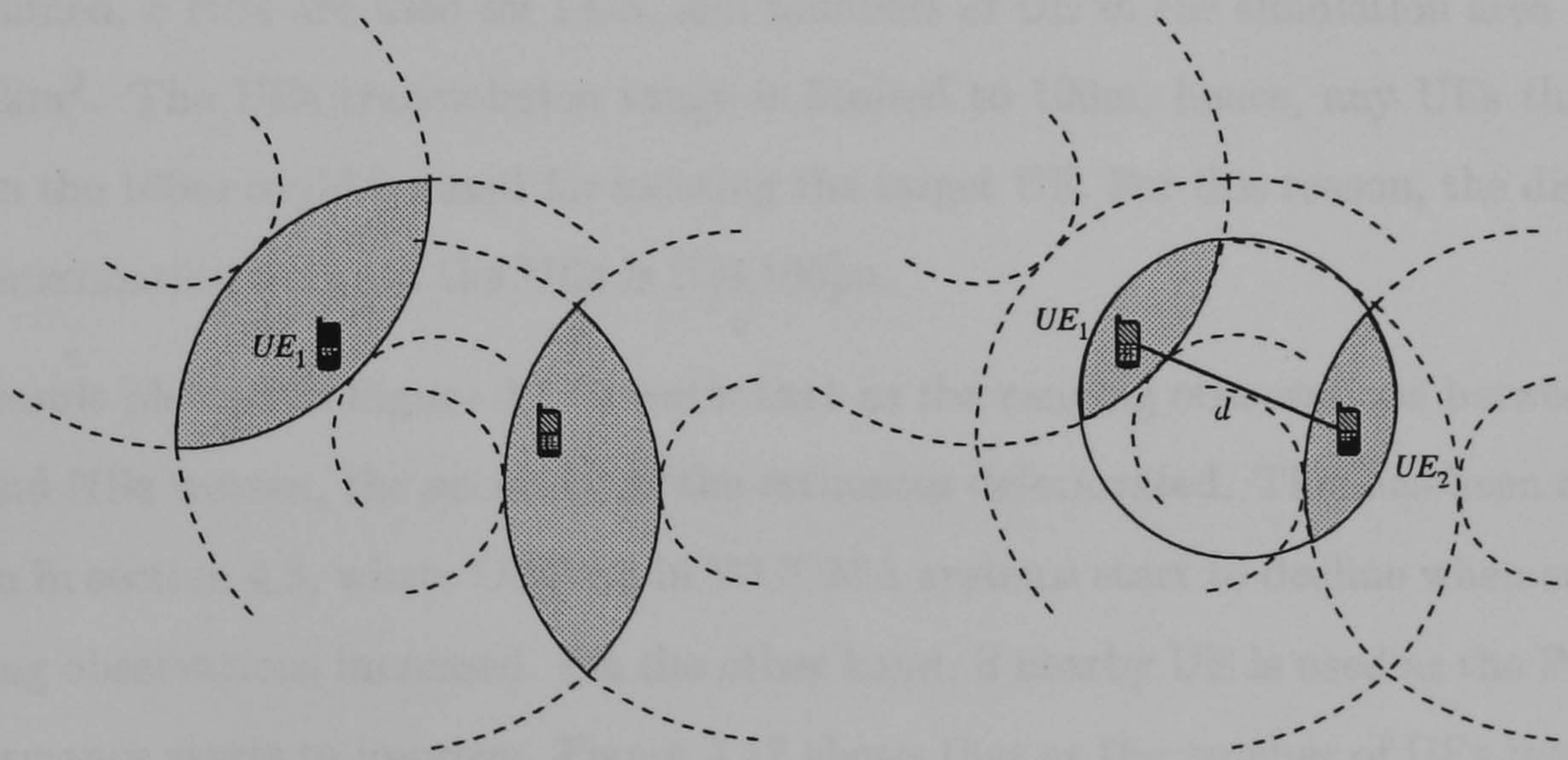

Figure 4.16: Illustration of UE positioning in Hybrid *Ad Hoc* Cellular System

Figure 4.17 shows the err_{rms} of the estimates with ranging observations between the UE and NB varies from N[0,100]m to N[0,1200]m, and numbers of nearby UEs used to

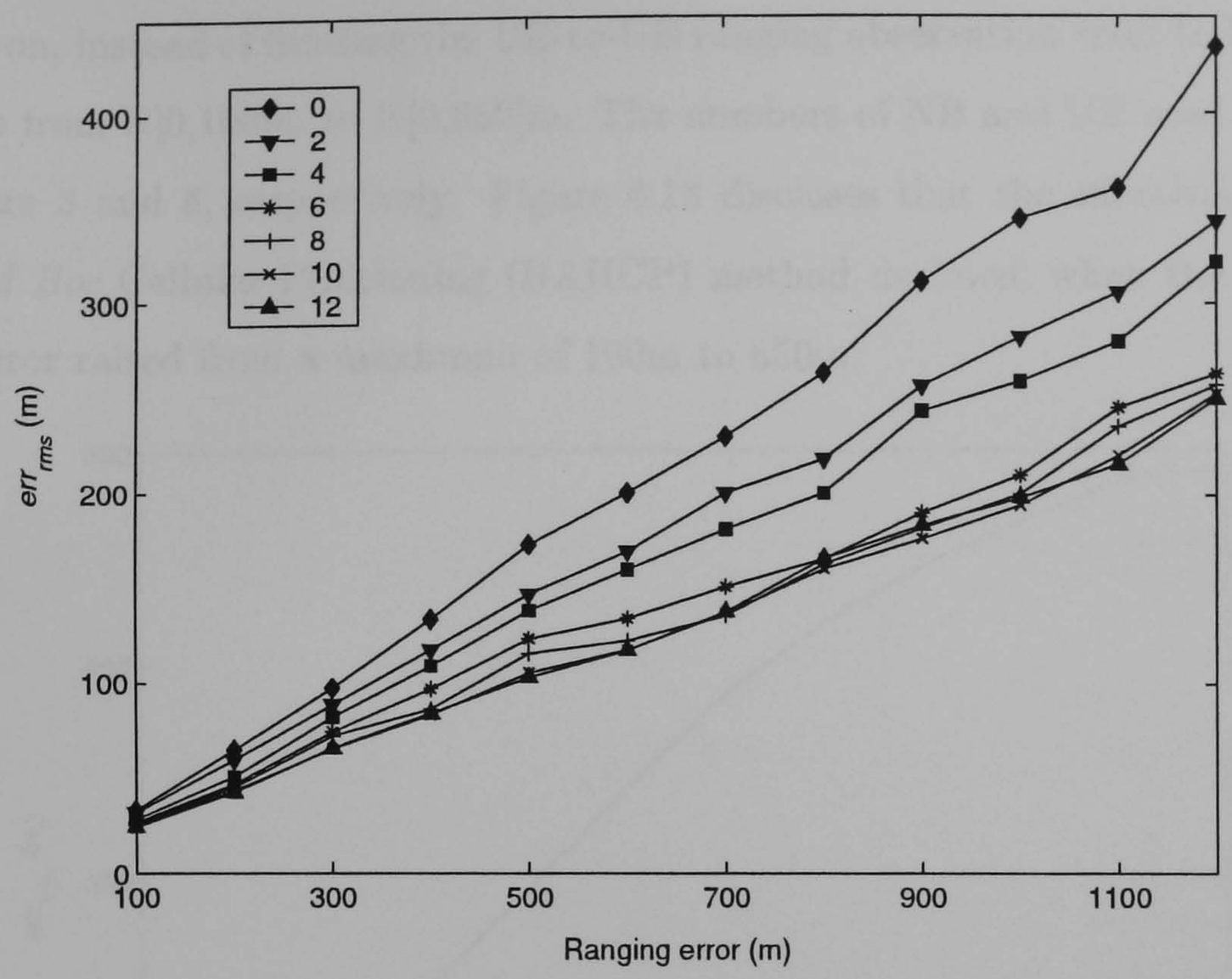

Figure 4.17: The accuracy of LCS with various numbers of nearby UE to assist in geo-location

assist in positioning varies from 0 to 12. In this case, LOS between the NBs and UE is assumed, 3 NBs are used for LCS, and numbers of UE in the simulation area is 250 UEs/km^2. The UEs transmission range is limited to 100m, hence, any UEs that are within the 100m could be used for locating the target UE. For this reason, the distance d approximation between the UEs is N[0,100]m.

The result plotted in Figure 4.17 reveals that as the ranging observations between the UE and NBs worsen, the accuracy of the estimates deteriorated. This has been clearly shown in section 4.3, where OTDoA in WCDMA systems start to decline when error in ranging observations increased. On the other hand, if nearby UE is used as the PE, the performance starts to improve. Figure 4.17 shows that as the number of UEs increased from 0 to 12, with the ranging observations between the UE and NBs at N[0,1200]m, the err_{rms} diminishes by 42%. Clearly, indicates the benefit of using nearby UEs for LCS. On top, the results also show that when the numbers of UE increased from 0 to 6 UEs, considerable improvement is achieved. Further increase in numbers of UE from 6 to 12, only marginal or similar accuracy is attained.

Following on, instead of limiting the UE-to-UE ranging observation error to N[0,100]m, it is varies from N[0,100]m to N[0,650]m. The numbers of NB and UE used for spatial locating are 3 and 6, respectively. Figure 4.18 discloses that the effectiveness of the Hybrid *Ad Hoc* Cellular Positioning (HAHCP) method declined, when the UE-to-UE ranging error raised from a maximum of 100m to 650m.

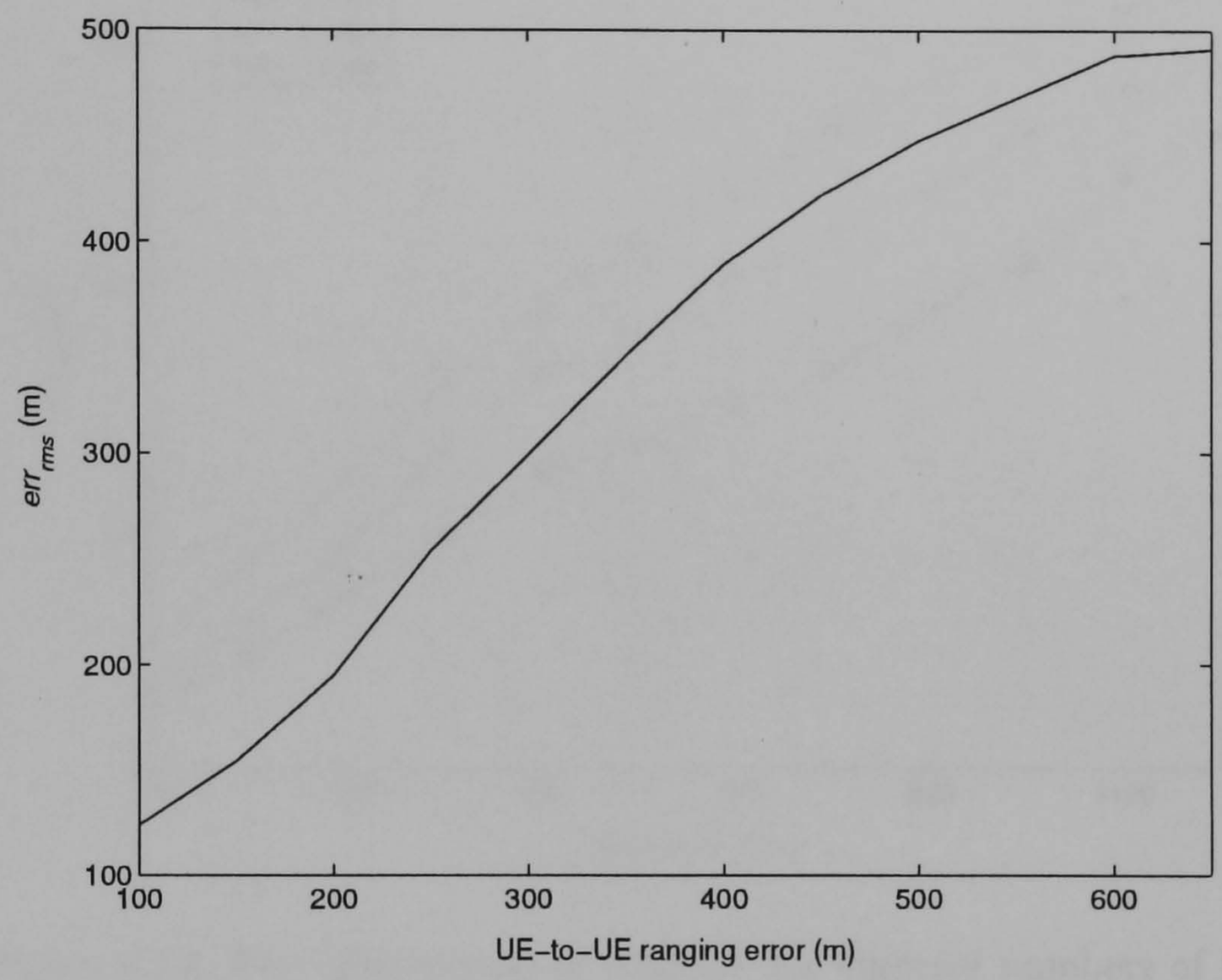

Figure 4.18: The consequences of UE-to-UE ranging imprecision on HAHCP method

One of the drawbacks of HAHCP method is the accurateness of spatial information of nearby UEs used to aid in locating the target UE. The 2D co-ordinates of the NB can be accurately predetermined, while the spatial accuracy of nearby UEs will differ greatly. So it is necessary to study the numbers of NB and UE used for LCS. From Figure 4.17, it is shown that 6 UEs are essential for HAHCP method to provide better performance than the conventional fixed network-based method. In the following, 6 UEs will be used for positioning and the numbers of NB used for LCS varies from 1 to 3. The UE-to-UE ranging observation error is limited to N[0,100]m. Figure 4.19 depicts the err_{rms} of the UE estimates using HAHCP, express in meter, as a function of ranging observation accuracy between the UE and NB. In addition, the number of NB used for LCS varies from 1 to 3. The nearby UE spatial information is obtained

from trilateration method using the NBs, therefore, the accurateness will decline when UE-to-NB ranging error rises. From the results, one can conclude that the HAHCP method would be affected by the ranging error between the UE-to-NB, UE-to-UE and numbers of UE and NB used to aid in geo-location.

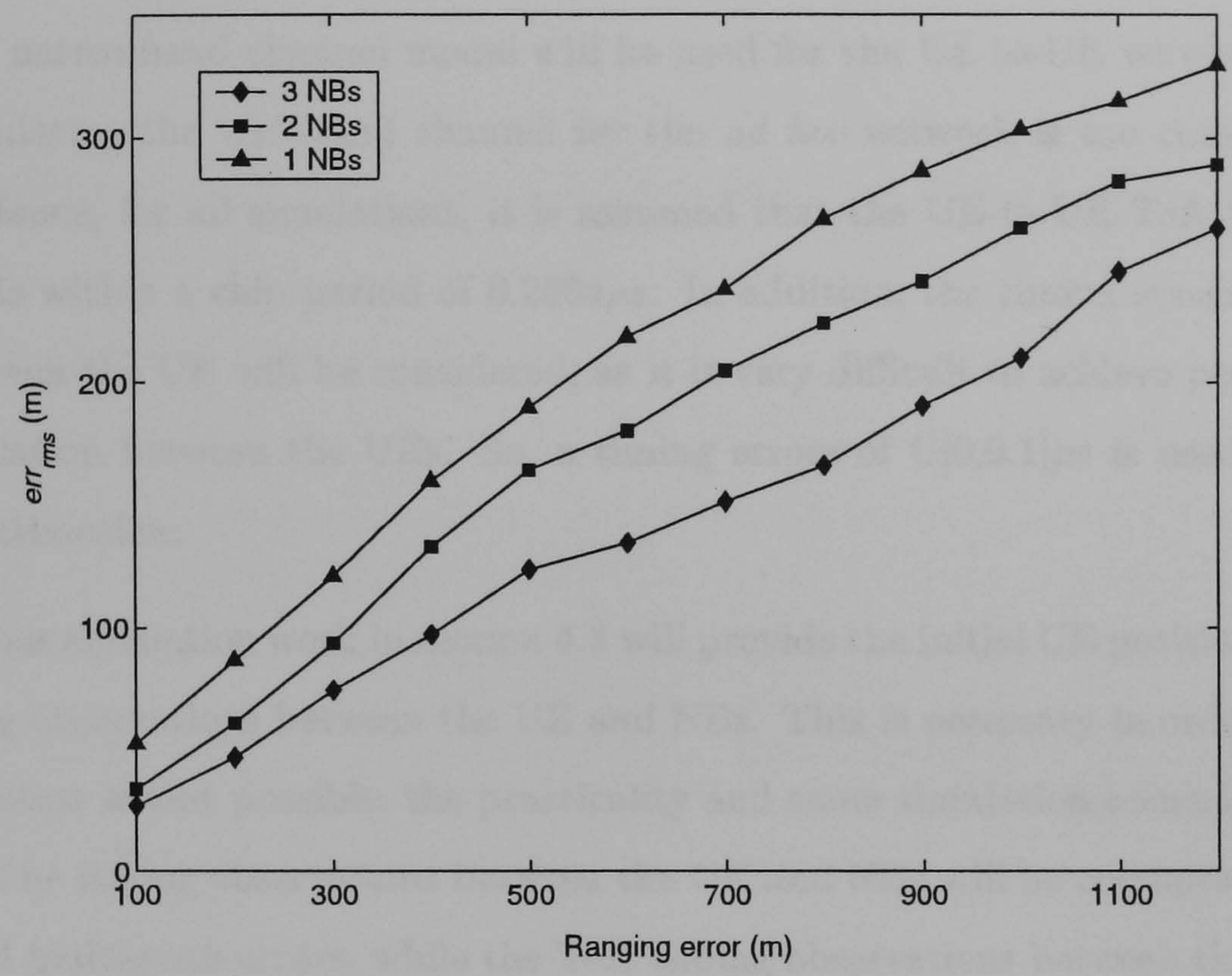

Figure 4.19: The effectiveness of HAHCP for different numbers of NB

In the next section, the HAHCP method is investigated in the WCDMA system, the UE-to-NB air interface will be in FDD mode, while UE-to-UE air interface is in TDD mode. Additionally, the HAHCP method will be compared with the OTDoA method.

4.5 Performance of Hybrid *Ad Hoc* Cellular Positioning Method

The performance on the HAHCP method is tested and compared with the OTDoA results presented in section 4.3. As cited, the technology that will be used for peer-to-peer communication has yet to be confirmed. Therefore, it is assumed that the UE has direct connectivity with the nearby UE, forming a temporary *ad hoc* network. The direct link is achieved using the UTRA-TDD mode, and no adjacent frequency

interference between the peer-to-peer and cellular is considered. Unlike the cellular network, there is no PCPICH from the NBs to obtain the relative timing for positioning. The UE is assumed to estimate the ToA from the probing channels transmitted by nearby UEs [59].

A simpler narrowband channel model will be used for the UE-to-UE wireless link because simulating the wideband channel for the *ad hoc* network is too computing intensive. Hence, for all simulations, it is assumed that the UE-to-UE ToA timing observation is within a chip period of 0.2604μs. In addition, the timing synchronisation error between the UE will be considered, as it is very difficult to achieve perfect clock synchronisation between the UEs. So, a timing errors of U[0,0.1]μs is used for every position estimation.

The previous simulation work in section 4.3 will provide the initial UE position estimate and timing observations between the UE and NBs. This is necessary in order to yield, to the greatest extent possible, the practicality and same simulation scenario with the OTDoA. The timing observations between the UE and NBs will be corrupted with the NLOS and multi-path errors, while the ToA timing observations between the UEs will be kept within the UE-to-UE clock synchronising and chip quantisation errors. For all simulations, it is assumed that the target UE will have LOS with the assisting UE. In reality, this assumption may be practical, as a result of the short distances between them.

The free space path-loss model is used for the peer-to-peer link, with lognormal shadowing of mean and σ of zero and 4dB respectively. The carrier frequency of 2000MHz will be used for all the transmitted signals between the UEs. A $\frac{E_c}{N_o}$ threshold of 10dB is set for the UE-to-UE, any received signals lower than the threshold will not be considered. The simulation scenarios considered are the urban and suburban environments with the same P_{LLOS} and P_{CLOS} between the UE and NBs. The cell radius for the urban and suburban will be fixed at 500m and 2000m. The UEs will be uniformly distributed over 19 cells and the numbers of UE over an area is selected at 250 UE/km^2.

When three or more timing estimations are obtainable, trilateration calculation will produce a fixed for the UE position sought. If only nearby UEs are available for

positioning and each having two ToA timing observations, ambiguity will arise. In this case, the intersection points of UEs that produced the closest to the UE-to-UE distance measured, will be the positions for the target and assisting UEs. If the target UE only has one TDoA estimate from two NBs, the UE position will be the intersection point between the hyperbolic loci and the line connecting the two NBs. In the case when two ToA observations from two assisting UEs are available and no prior information is available, the position of the UE will be the average of the two intersections points. In worst case, if the UE is only within the transmission range of one UE or NB, the position of the UE will be the position of the PE.

4.5.1 Accuracy of the Estimated UE Positions at Different $\frac{E_c}{N_o}$ Levels

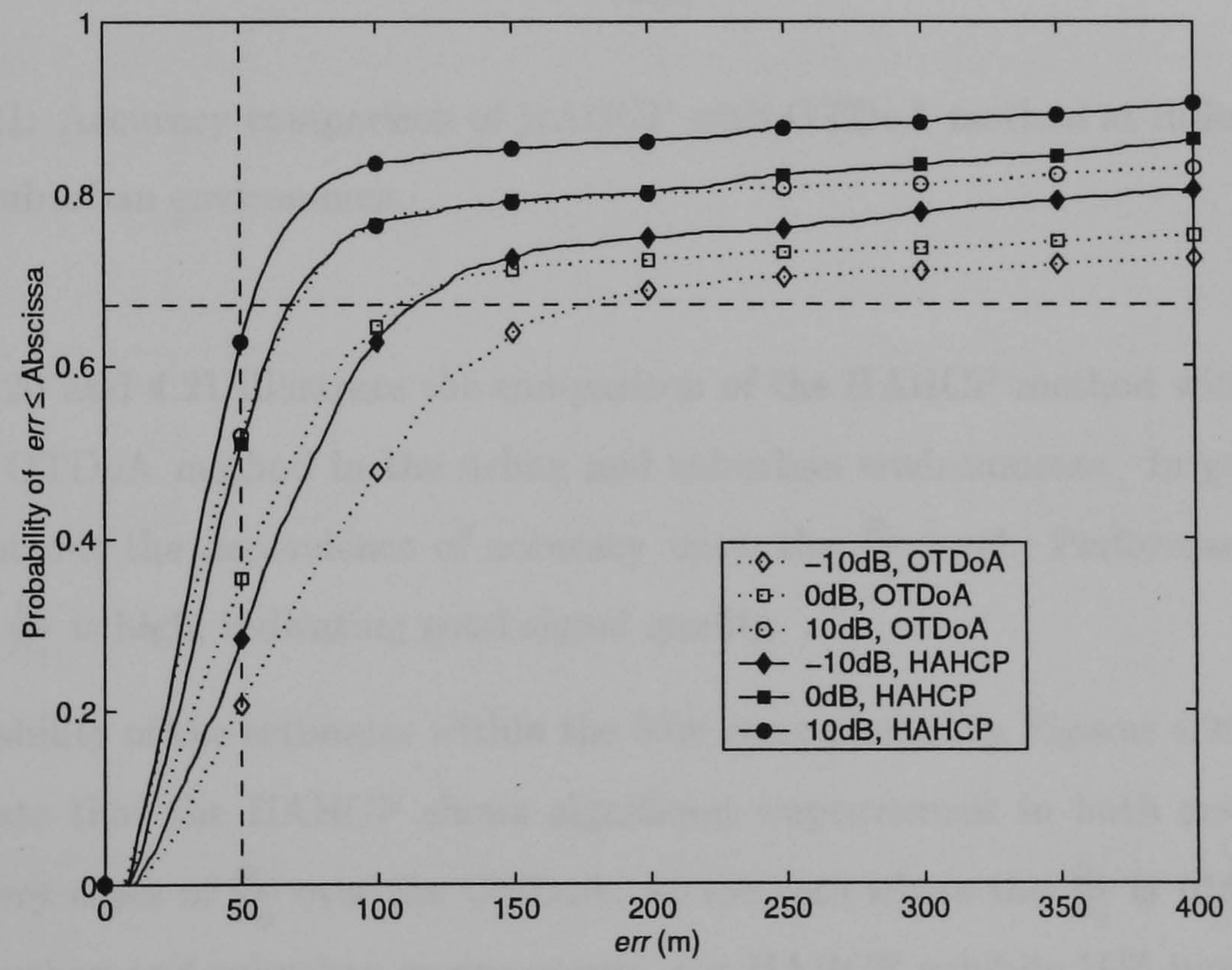

Figure 4.20: Accuracy comparison of HAHCP with OTDoA method at different levels of $\frac{E_c}{N_o}$ in urban environment

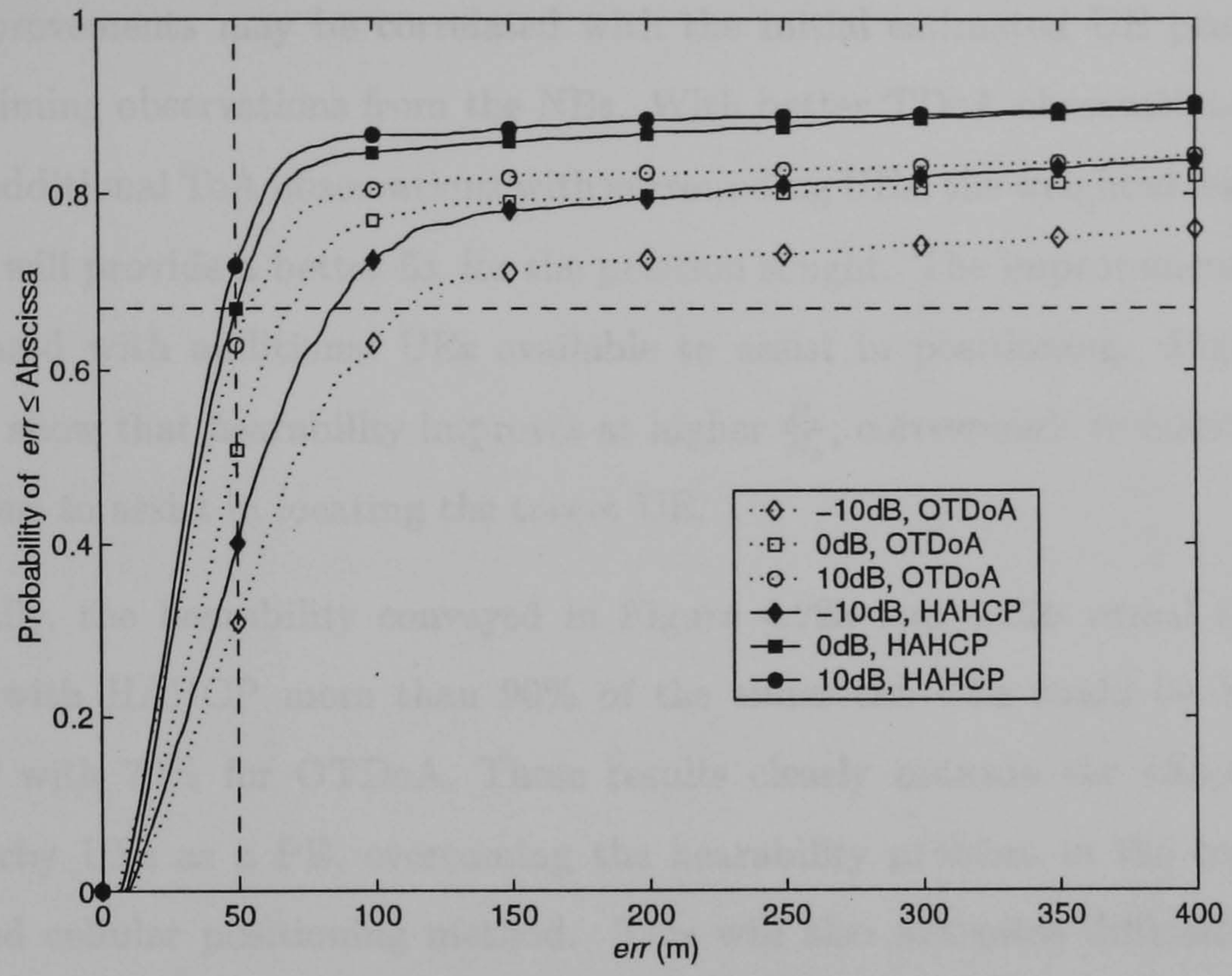

Figure 4.21: Accuracy comparison of HAHCP with OTDoA method at different levels of $\frac{E_c}{N_o}$ in suburban environment

Figures 4.20 and 4.21 illustrate the comparison of the HAHCP method with the conventional OTDoA method in the urban and suburban environments. In general, the plots point out the dependence of accuracy upon the $\frac{E_c}{N_o}$ level. Performance is best when the $\frac{E_c}{N_o}$ is high, indicating good signal quality.

The probability of the estimates within the 50m error plotted in Figures 4.20 and 4.21, demonstrate that the HAHCP shows significant improvement in both environments and at every cases of $\frac{E_c}{N_o}$ over the OTDoA. At the case where the $\frac{E_c}{N_o}$ is 10dB, at 50m error, for urban and suburban environments, the HAHCP exhibits 10% improvements over the OTDoA method.

These improvements may be correlated with the initial estimated UE positions and accurate timing observations from the NBs. With better TDoA observations from the NBs and additional ToA observations with surrounding UEs, the weighted least squares estimator will provide a better fix for the position sought. The improvement may also be associated with additional UEs available to assist in positioning. Figures 4.22a and 4.22b show that hearability improves at higher $\frac{E_c}{N_o}$, corresponds to additional ToA observations to assist in locating the target UE.

Additionally, the hearability conveyed in Figure 4.22a and 4.22b reveal that at $\frac{E_c}{N_o}$ of 10dB, with HAHCP more than 90% of the times the UEs could be located, as compared with 70% for OTDoA. These results clearly indicate the effectiveness of using nearby UEs as a PE, overcoming the hearability problem in the conventional fixed-based cellular positioning method. This will also mitigates difficulties usually came across in large cells or when the UE is locating at the centre of a cell, where the neighbouring NBs are usually out of the transmission range of the UE. Moreover, it is interesting to note that at low $\frac{E_c}{N_o}$, the hearability of urban environment is better than suburban environment. This clearly illustrates that UE residing in larger cell will have visibility problem with neighbouring NBs, hence, trilateration cannot be computed.

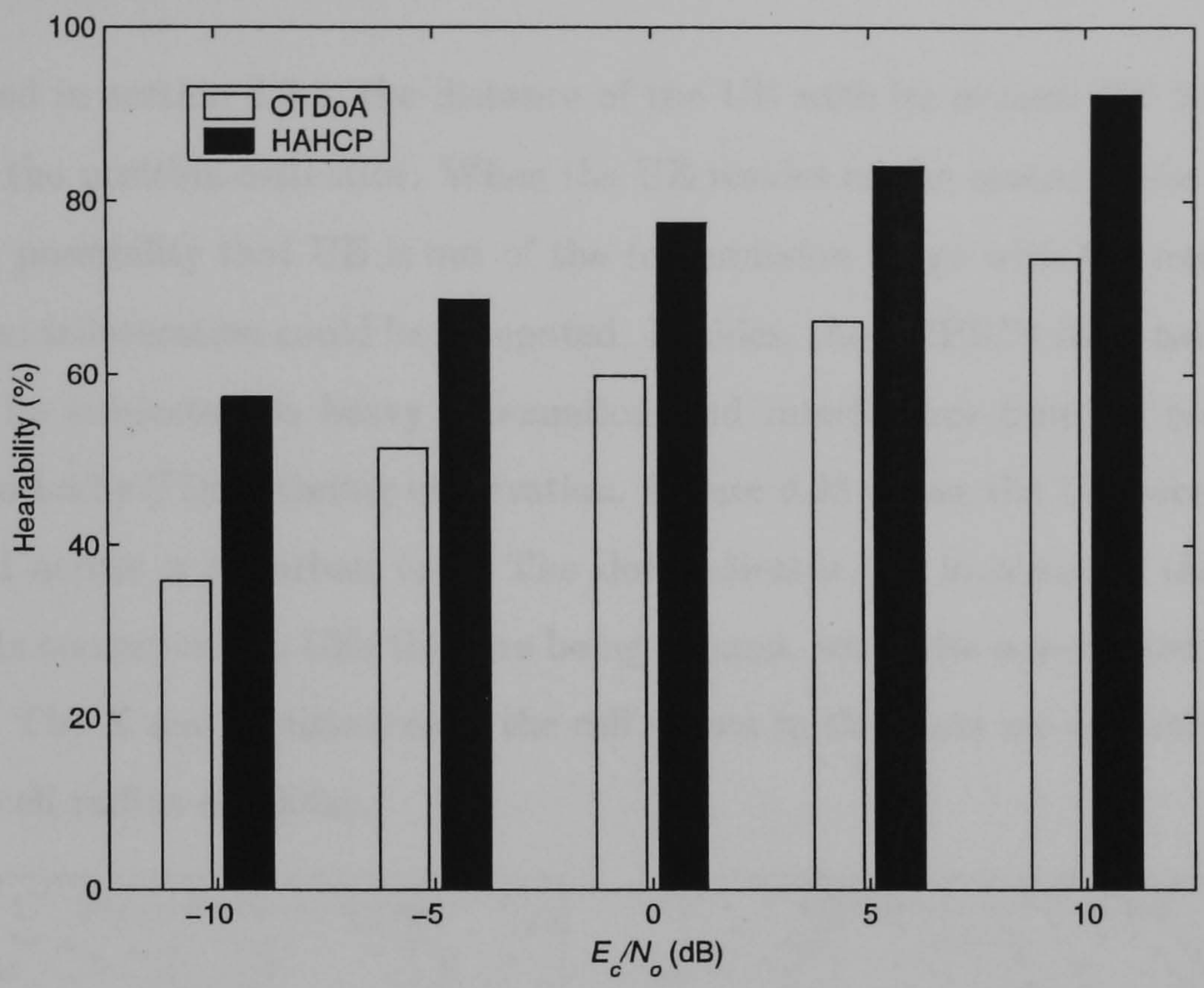

(a) Urban

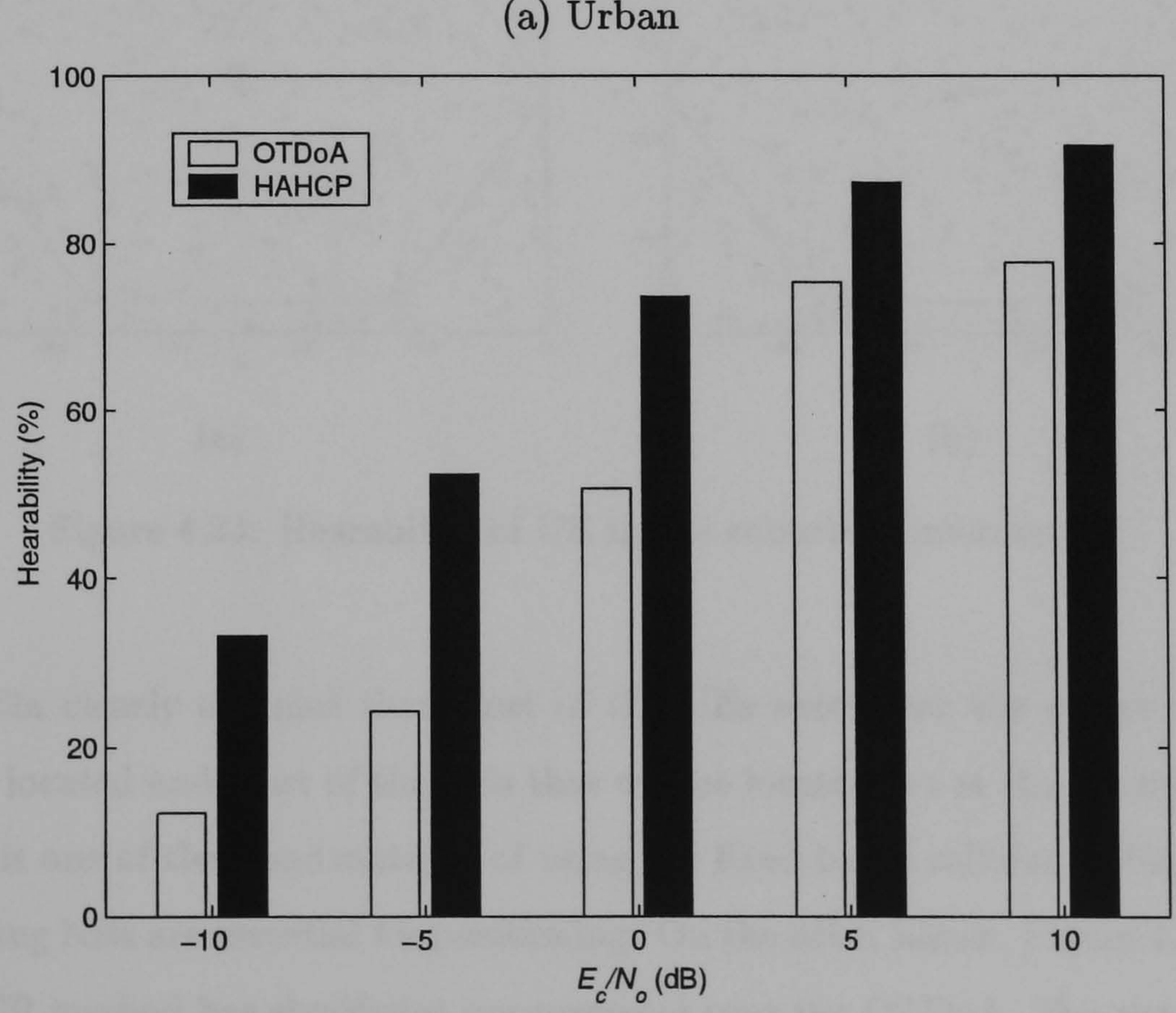

(b) Suburban

Figure 4.22: Hearability comparison of HAHCP with OTDoA at different levels of $\frac{E_c}{N_o}$

4.5.2 Effect of UE Location in a Cell

As discussed in section 4.3.4, the distance of the UE with its nearest NB has a direct impact on the position estimator. When the UE resides at the centre of the cell, there is a higher possibility that UE is out of the transmission range with the neighbouring NBs. So, no trilateration could be computed. Besides, the PCPICH from neighbouring NBs may be subjected to heavy attenuation and interference from its serving NB, resulting to badly TDoA timing observation. Figure 4.23 shows the UEs are randomly distributed across a suburban cell. The dot indicates the location of the UE, the shaded dots correspond to UEs that are being located, while the non-shaded dots show otherwise. The X and Y distances of the cell shown in the plots are normalised to the suburban cell radius of 2000m.

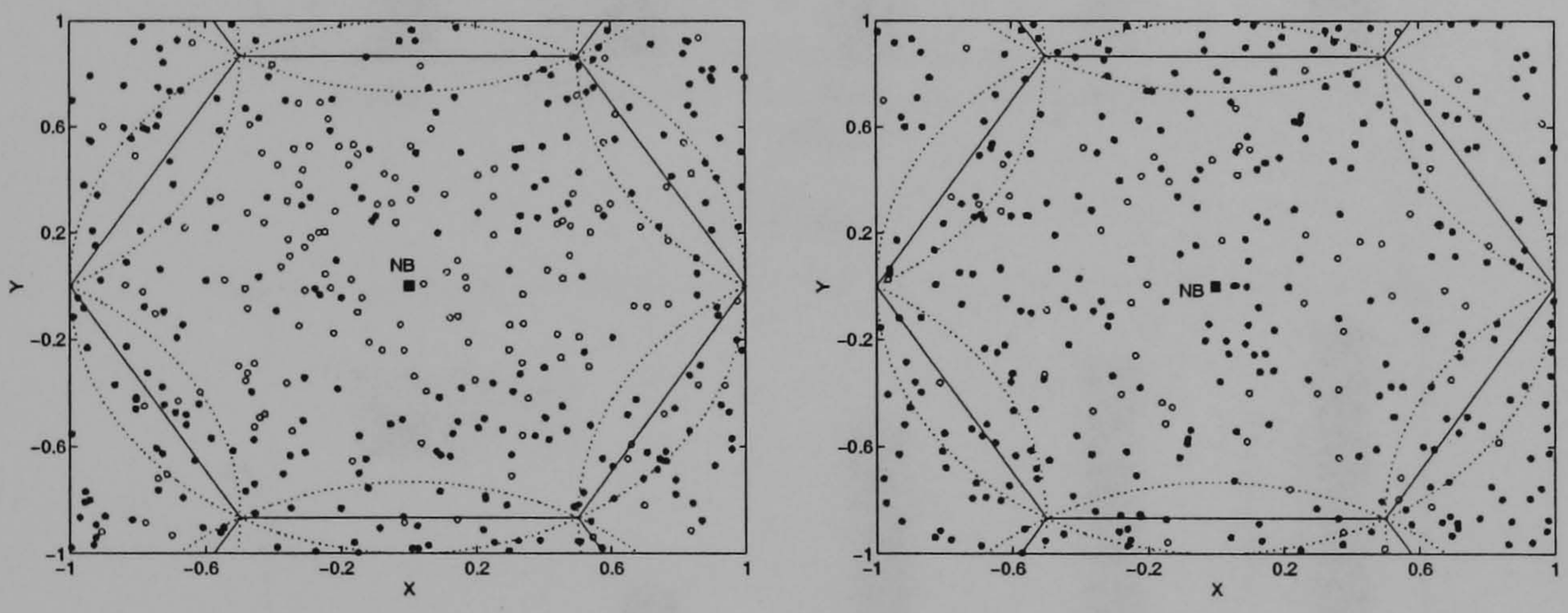

(a) (b)

Figure 4.23: Hearability of UE in the suburban environment

Figure 4.23a clearly explains that most of the UEs exist near the centre of the cell cannot be located and most of the UEs that can be located are at the boundary of the cell. This is one of the disadvantages of using the fixed-based cellular method because neighbouring NBs are essential for positioning. On the other hands, Figure 4.23b shows the HAHCP method has significant improvement over the OTDoA. The shaded circles are more evenly distributed throughout the cell area, revealing higher possibility that the UEs locating near the centre of the cell could be positioned. The results plotted in Figures 4.24a and 4.24b further defend this point.

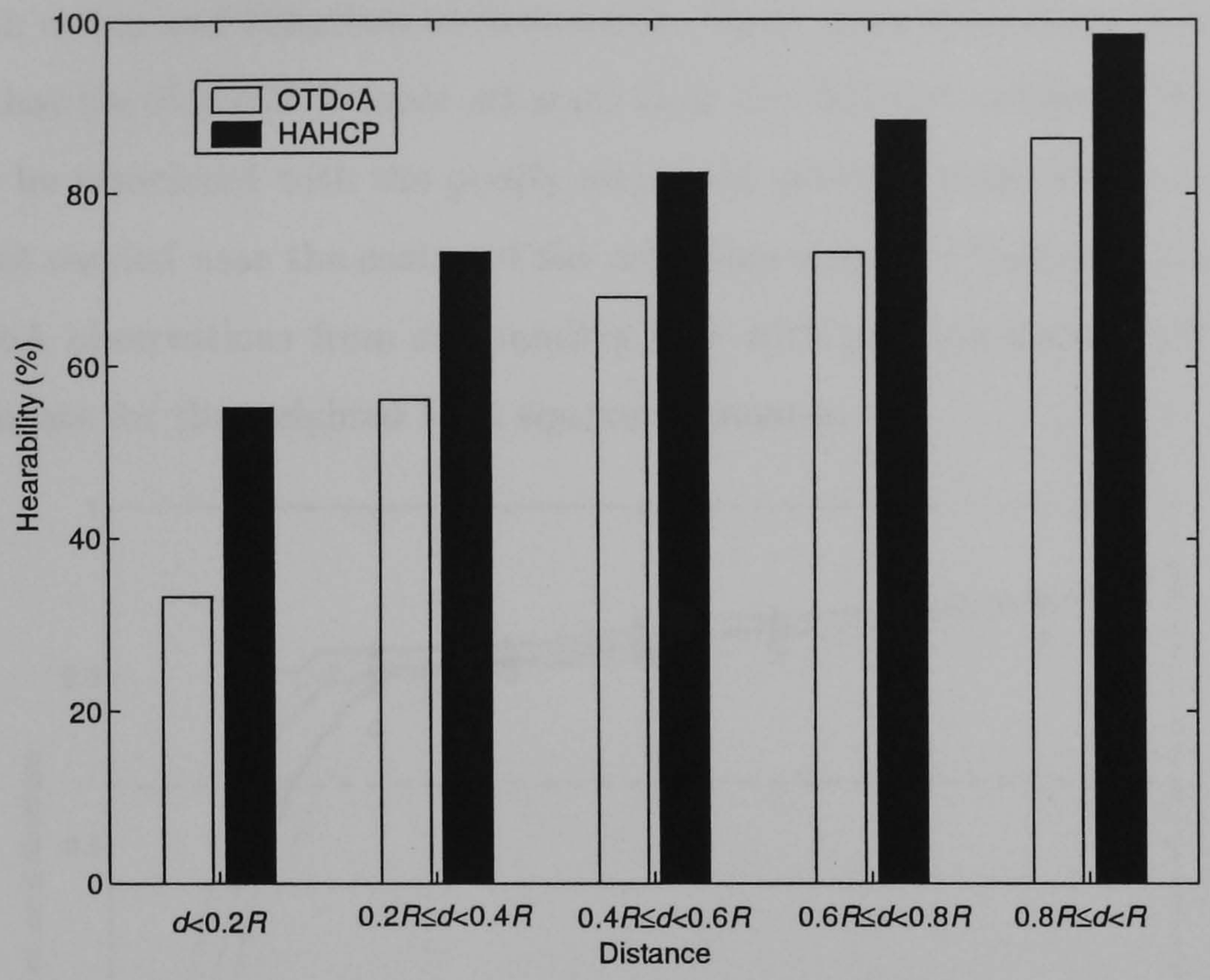

(a) Urban

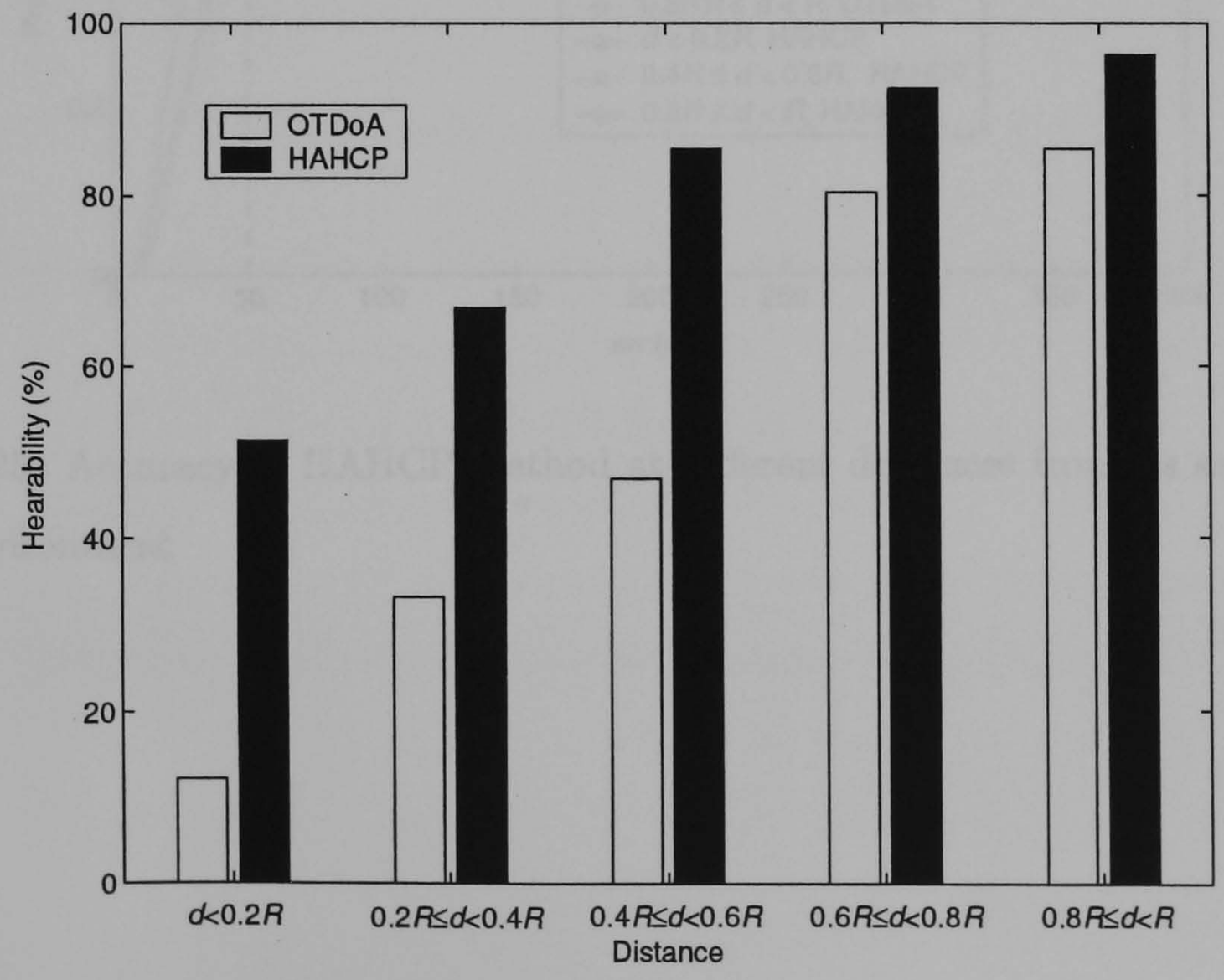

(b) Suburban

Figure 4.24: Hearability comparison of HAHCP with OTDoA at different distance, d

Figures 4.25 and 4.26 are the accuracy plots for both the HAHCP and OTDoA methods in both urban and suburban environments. Upon comparing the results, one may conclude that the HAHCP is more accurate than the OTDoA method. This improvement may be associated with the poorly estimated position using OTDoA, especially for UE that resided near the centre of the cell. One may also tempted to say the additional ToA observations from surrounding UEs with position known will provide a better estimate for the weighted least squares estimator.

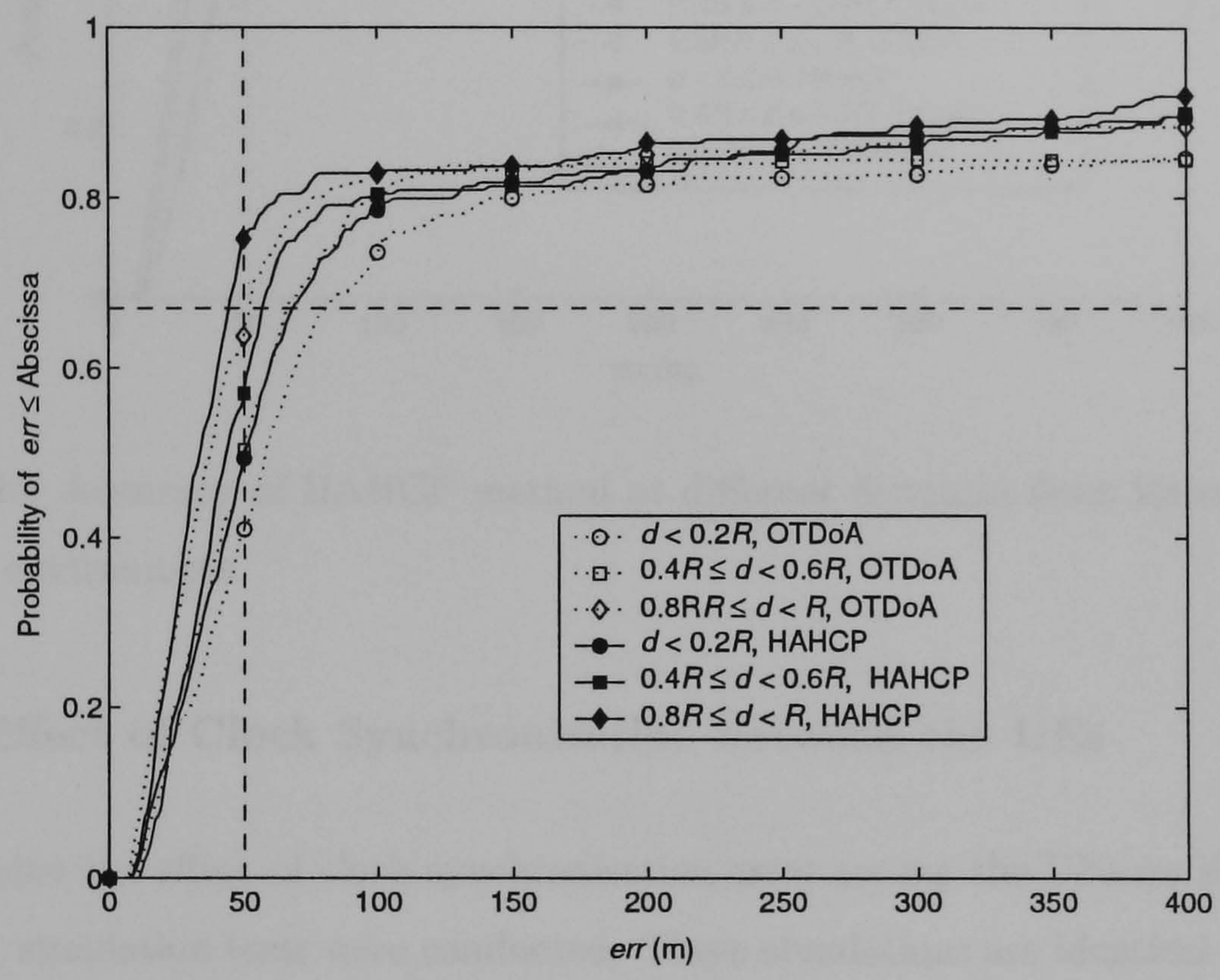

Figure 4.25: Accuracy of HAHCP method at different distances from its serving NB, urban environment

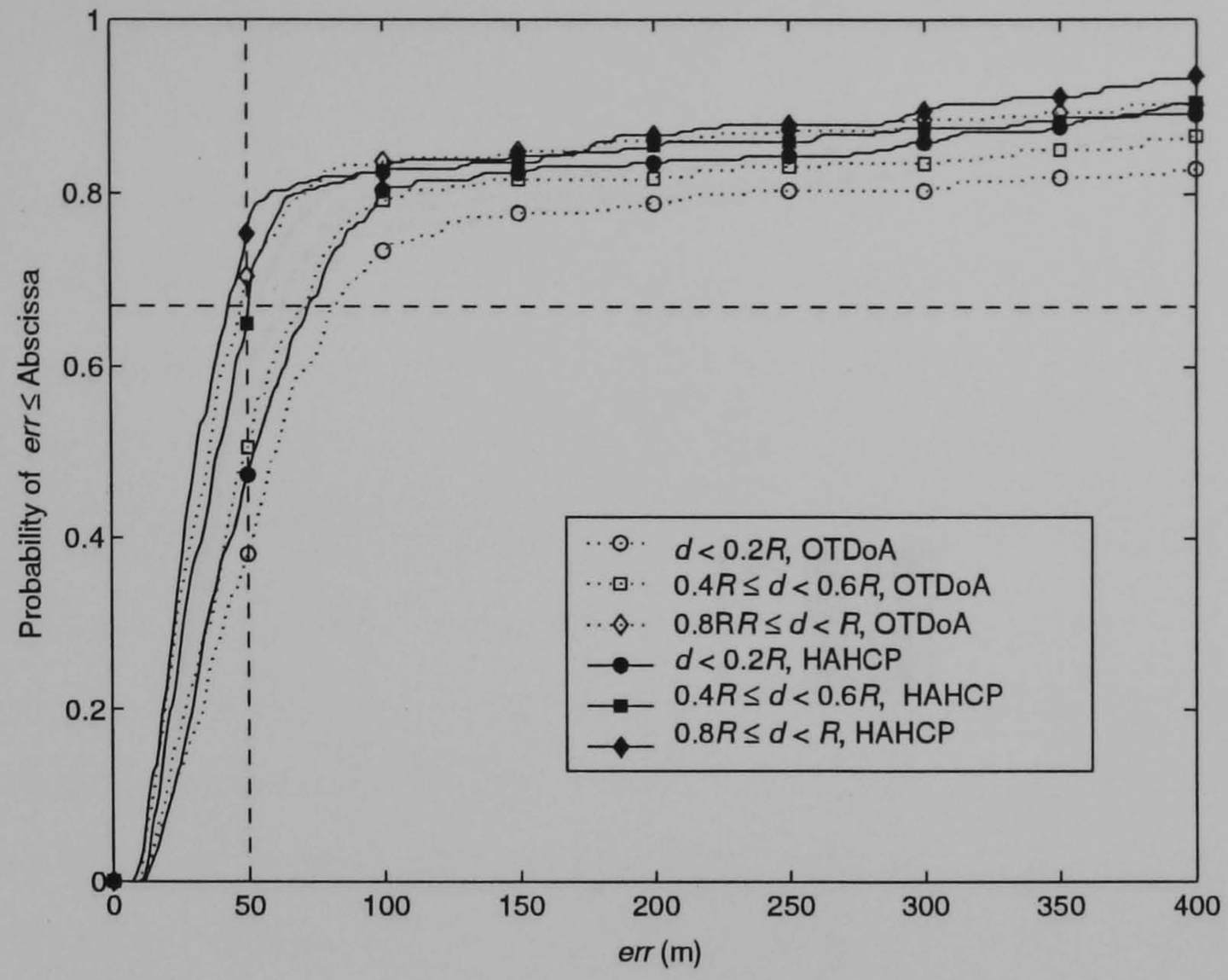

Figure 4.26: Accuracy of HAHCP method at different distances from its serving NB, suburban environment

4.5.3 Effect of Clock Synchronisation between the UEs

To determine the effect of clock synchronisation error among the UEs on the position estimator, simulation tests were conducted. These simulations are identical to those of section 4.5.1 with the following exceptions: the $\frac{E_c}{N_o}$ is set at 10dB and the synchronising error has a normal distribution with mean equal to zero and variances varied from 0.1μs to 0.7μs. As predicted, positioning accuracy worsens as the synchronising error increases. Surprisingly, Figure 4.27 shows that when synchronising error increases from N[0,0.1] μs to N[0,0.7] μs, within 50m error, the accuracy only drops from a probability of 0.62 to 0.50. This is probably due to the weighting factor considered in the least square estimator, where the variances of the ToA observation and assisting UEs estimates are considered.

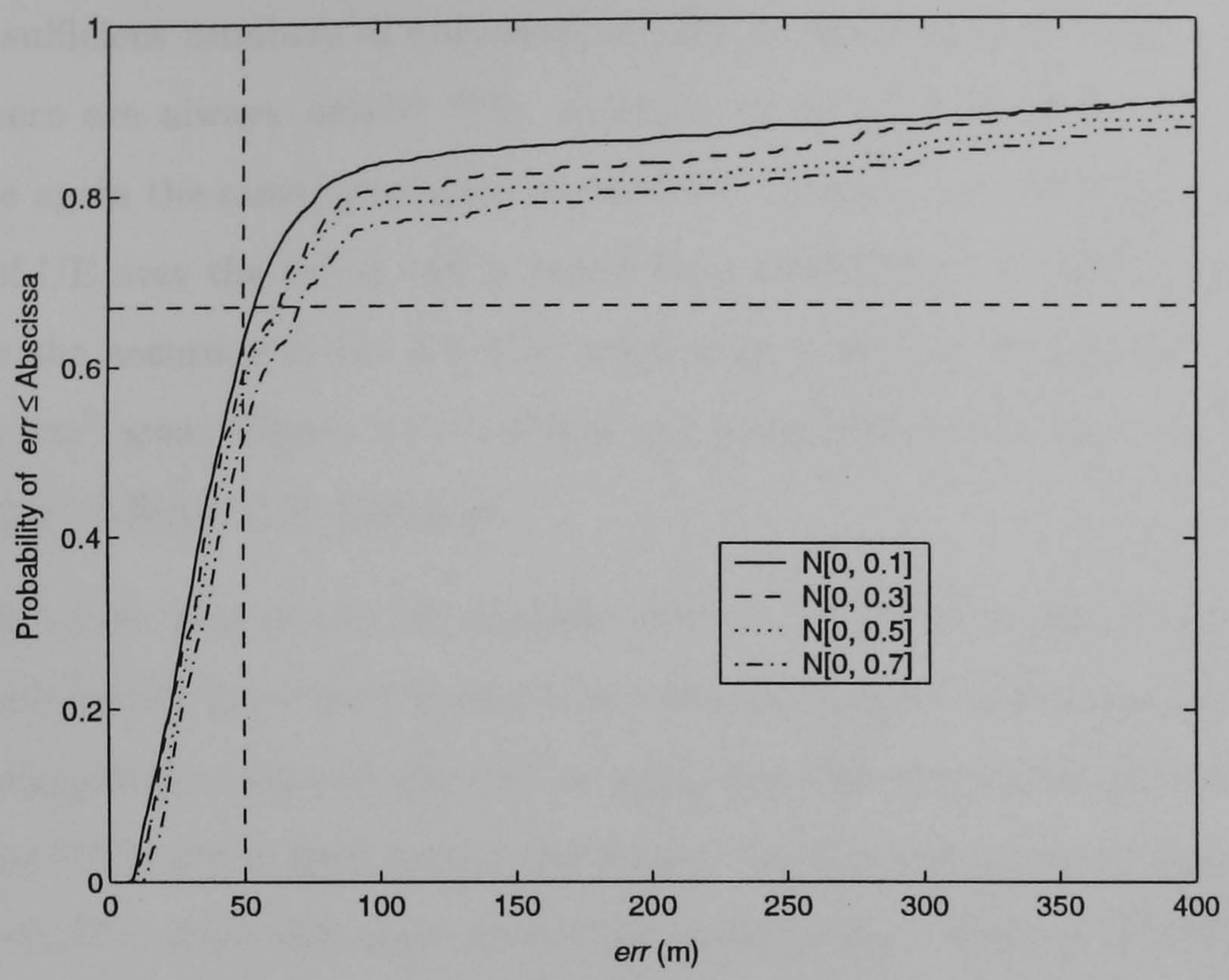

Figure 4.27: Clock synchronisation error among the UEs in urban environment

4.5.4 Effect of Nearby UEs Available to Assist in Positioning

Figures 4.28 and 4.29 demonstrate the effect of nearby UEs available to assist in geo-locating the UE. Simulation work on the urban and suburban environments were again chosen for this purpose. Both figures shows that the number of surrounding UEs used to assist in positioning, varied from 1 to 13. Comparing 1 with 13 UEs used to assist in positioning, one sees a significant improvement in the locating services. As conversed earlier, additional timing observations would improve the least squares estimator.

Results revealed in Figure 4.28 presents that with 13 surrounding UEs, approximately 73% of the estimates are within the 50m error. Moreover, Figure 4.29 also depicts that 81% of the estimates are within the 50m error. It is therefore more accurate than the E-911 required. Nevertheless, the performance is very similar when 9 to 13 UEs used for positioning are compared. The greatest difference is seen only in 1 to 9 UEs used for positioning. One may suspect, it perhaps owed to the ranging observation error between the UEs and the inaccuracy of the estimated position for the assisting UEs.

Although Figures 4.28 and 4.29 disclose that HAHCP method performs better when

there are sufficient numbers of surrounding UEs to assist in positioning, one cannot assume there are always nearby UEs available for locating services. To verify this point, once again the same simulation method was chosen. But, in this simulation, the numbers of UE over the urban cell is varied from 100UE/km^2 to 300UE/km^2. Figure 4.30 shows the accuracy of the HAHCP method as a function of different numbers of UE over a km^2 area. Figure 4.31 contains the probability of having 1 to 13 UEs for positioning at different UE densities.

Figure 4.30 shows that as the UE density reduces, the HAHCP performance also get worse. These results are closely linked to the results depicted in Figures 4.28 and 4.29. By decreasing the numbers of UE over an area, one also diminishes the availability of surrounding UE to aid in geo-locating the target UE. It is interesting to observe that at 300 UE/km^2, 72% of the estimates are within the 50m error. While at 100UE/km^2, only 52% of the estimates are within the E-911 requirement. This shows the dependency of HAHCP method on the surrounding UEs that are on hand for locating services.

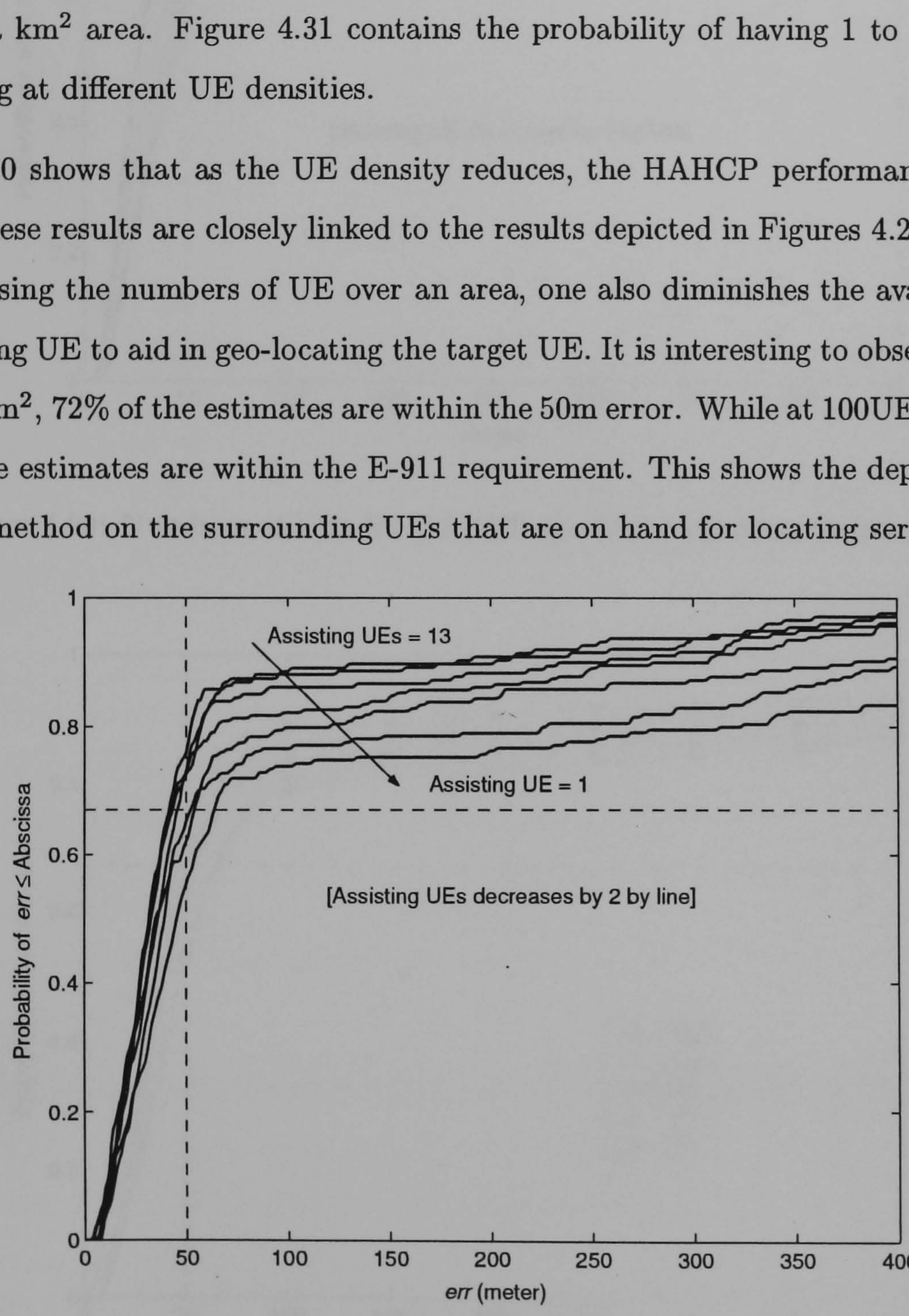

Figure 4.28: Numbers of UEs for HAHCP method, urban environment

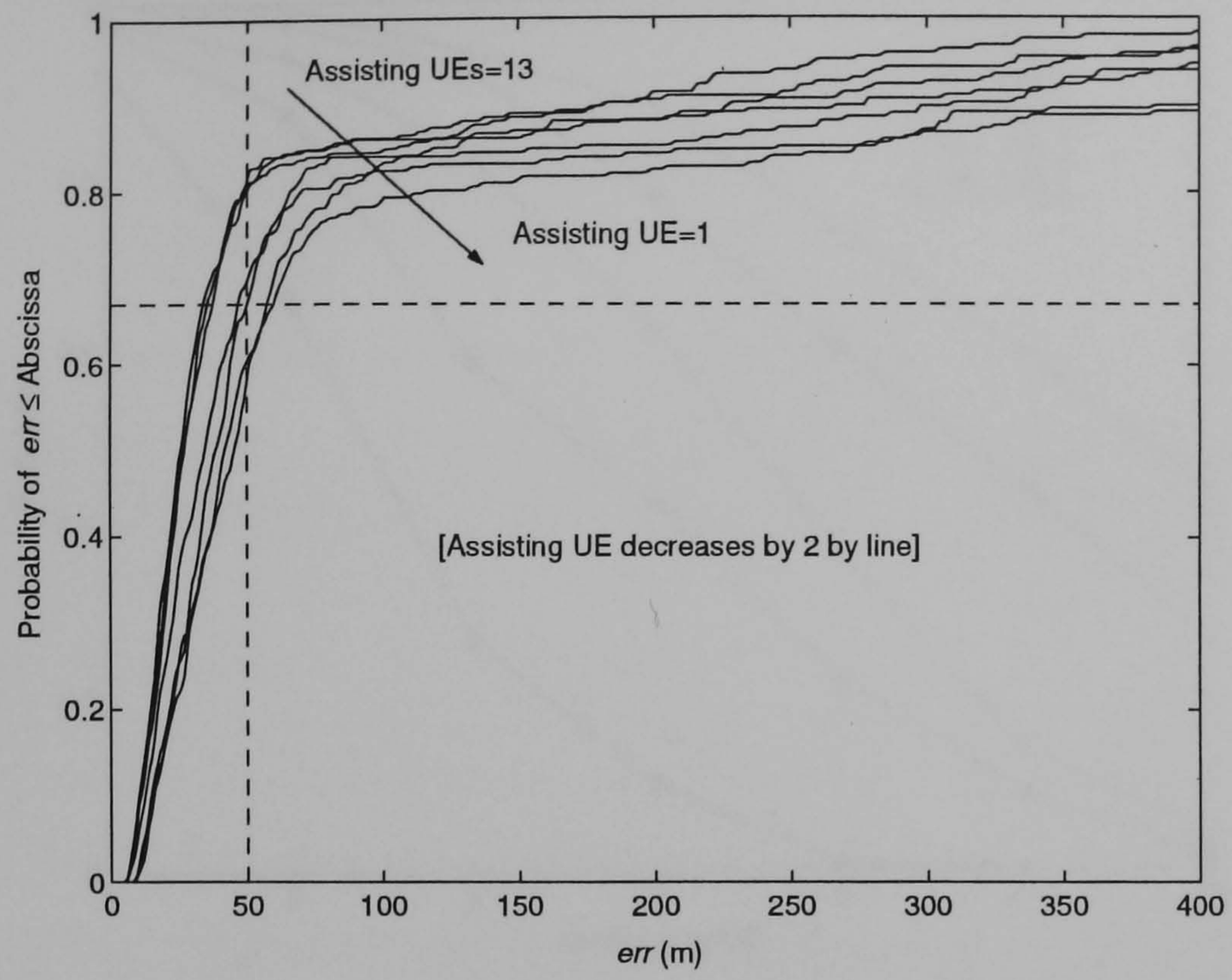

Figure 4.29: Numbers of UEs for HAHCP method, suburban environment

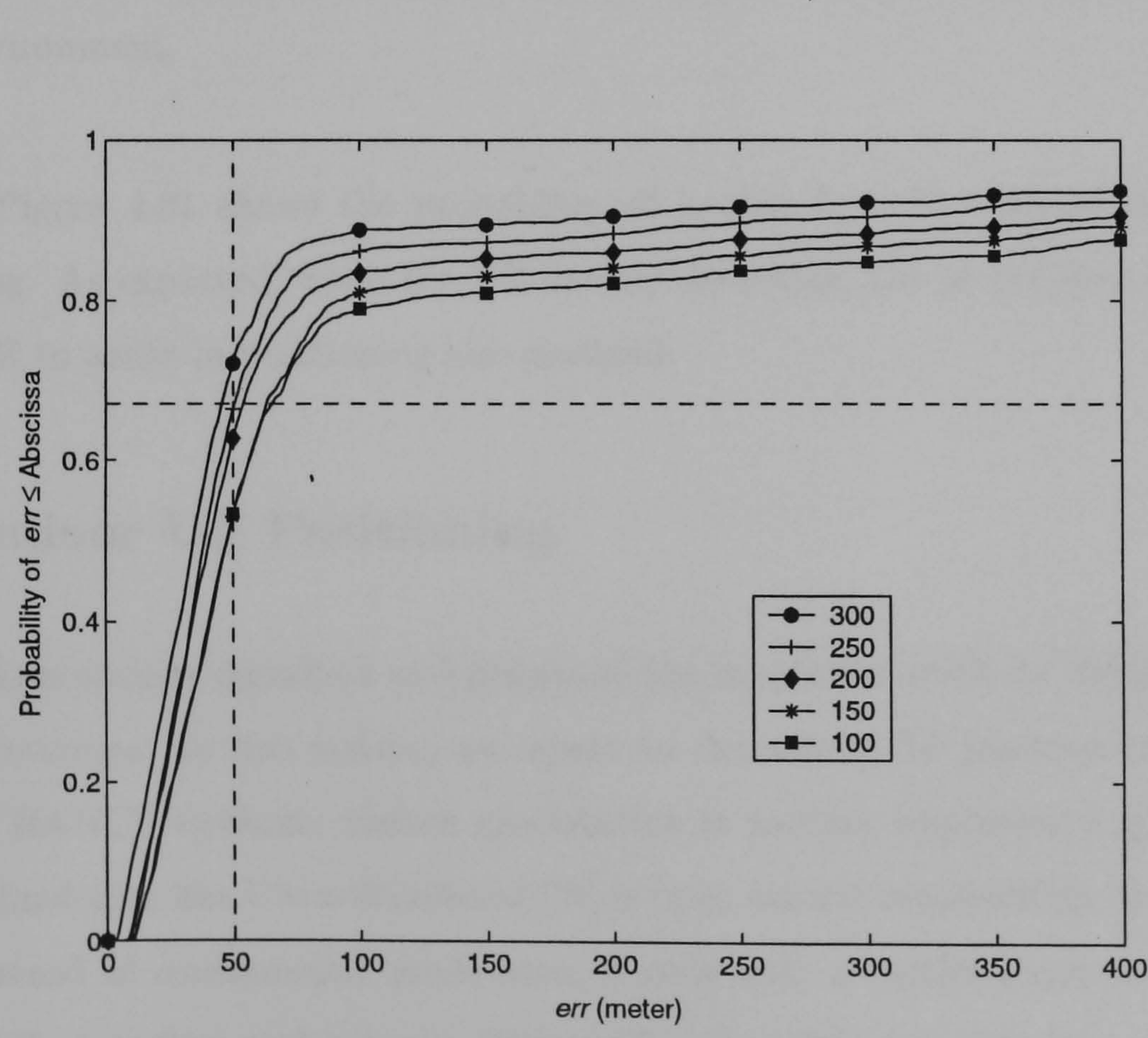

Figure 4.30: Performance evaluation of HAHCP method in difference UE density, urban environment

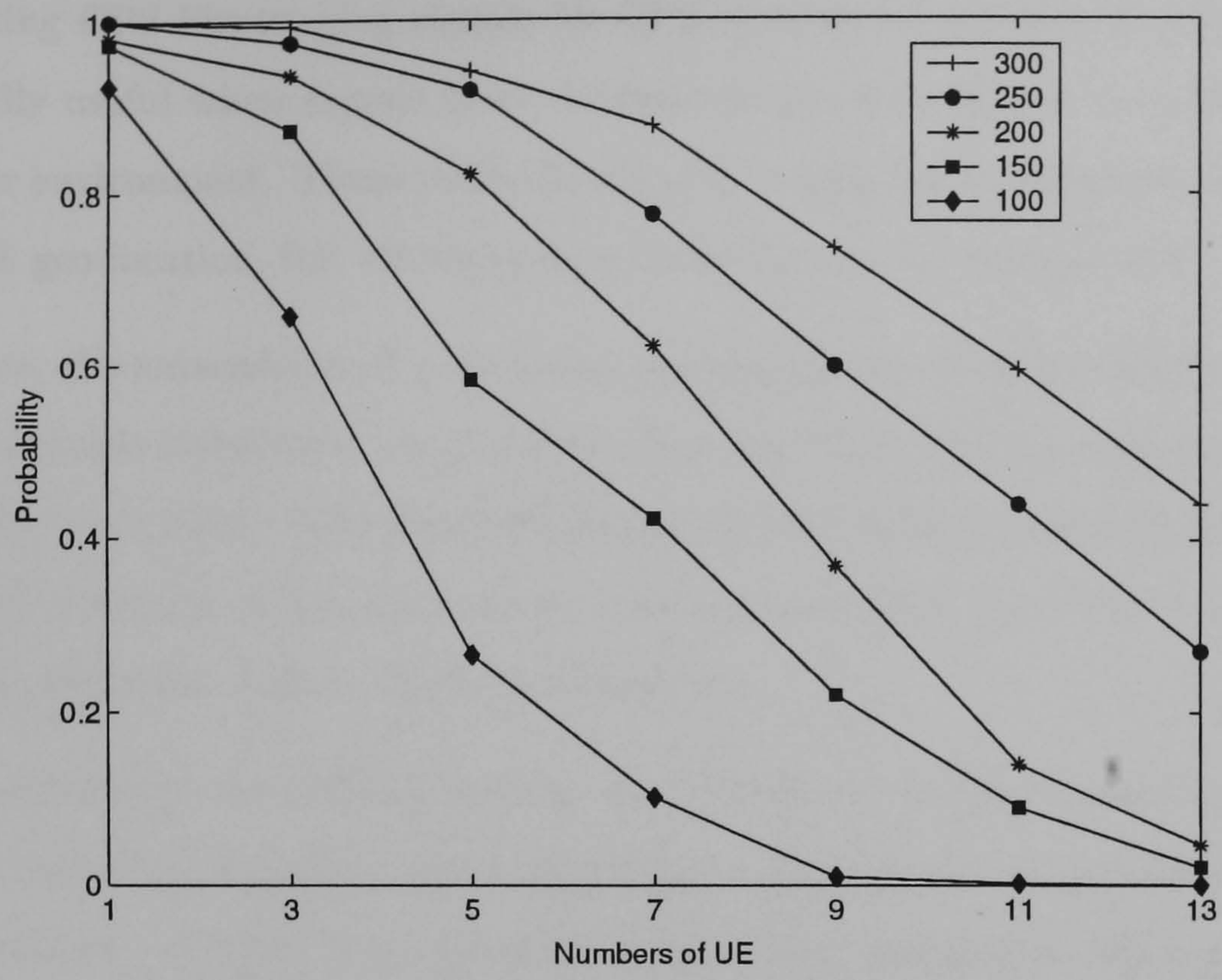

Figure 4.31: Probability of having nearby UE for positioning at difference UE density, urban environment

Besides, Figure 4.31 shows the probability of having 1 to 13 surrounding UEs for positioning. As expected, when the UE density decreases, the probability of having a nearby UE to assist in positioning also declined.

4.6 Indoor UE Positioning

The previous section described and presented the simulation work for HAHCP in outdoor environment. In this section, we report on the indoor UE geo-location using the proposed HAHCP method. Indoor geo-location is another important application for LCS. Technologies like Ultra-Wideband [73] is built around transmitting short discrete pulses instead of continuously modulating a code onto a carrier signal. Such pulses are typically 1 to 2ns, and one can distinguish pulses that are more than 0.3 to 0.6m apart. Thus, this makes Ultra-Wideband systems robust to multi-path delays of more than one pulse width. Another worth mentioning method that can be used indoor geo-location is Pseudolites [74]. They function like a GPS satellite on the ground,

broadcasting GPS-like ranging signals for GPS receiver to estimate its location. This is especially useful when signals from the space-borne satellite are completely lost in the indoor environment. These methods are able to provide considerable accuracy for indoor UE geo-location, but all requiring modification to the current UE.

In this case, the network-based positioning method like the Cell-ID or OTDoA will be the more suitable techniques. In situation when the UE is within a transmission range of one indoor or outdoor NB, then Cell-ID can be used to locate the UE. When higher accuracy than the resolution error of one cell size is preferred, the OTDoA trilateration positioning technique will be the better candidate.

As explained earlier, the OTDoA requires the UE to be within the transmission range of minimum three PEs if mathematical trilateration calculation is to be used to compute the UE position. Unless there are three indoor cells installed in the building, it is unlikely that the UE is able to receive signals from more than three outdoor PEs. The building external or internal walls will attenuate the ranging signal requisites for positioning, causing it to be lower than the acceptable threshold level. For this reason, the HAHCP method is used to eliminate the hearability problem encountered in indoor UE geo-location.

4.6.1 Indoor UE Positioning Simulation Results

In this part of work, a system level simulation is used to verify the performance of HAHCP method. Nine building blocks are placed at the inner most urban cell. Each block has an area of 100m by 100m, and 30m apart from each other. The path-loss between the outdoor UE and NB is determined by equation (4.9) and lognormal shadowing of N[0,10]dB is considered. If the UE is having a LOS link with the NB, the ranging error will be within one chip rate. However, if the UE is having NLOS link with the PE, the excess delay of first NLOS path, as summarised in Table 4.2, will be added to the timing observation.

A $\frac{E_c}{N_o}$ threshold of 10dB is set for the UE-to-NB and UE-to-UE. Any received signals lower than the threshold will not be considered. Under the HAHCP method, the

outdoor UEs will be used to assist in positioning the indoor UEs. The accuracy of the outdoor UE position is based on the work done in section 4.5.1, where the $\frac{E_c}{N_o}$ is 10dB.

The COST231 LOS and NLOS model will be employed for the path-loss between the outdoor and indoor transceivers [34]. Do note that the COST231 LOS model is valid for transmission within 500m and at a frequency range of 900MHz to 1800MHz. Figure 4.32 illustrates a scenario where a LOS transmitter is transmitting to an indoor receiver

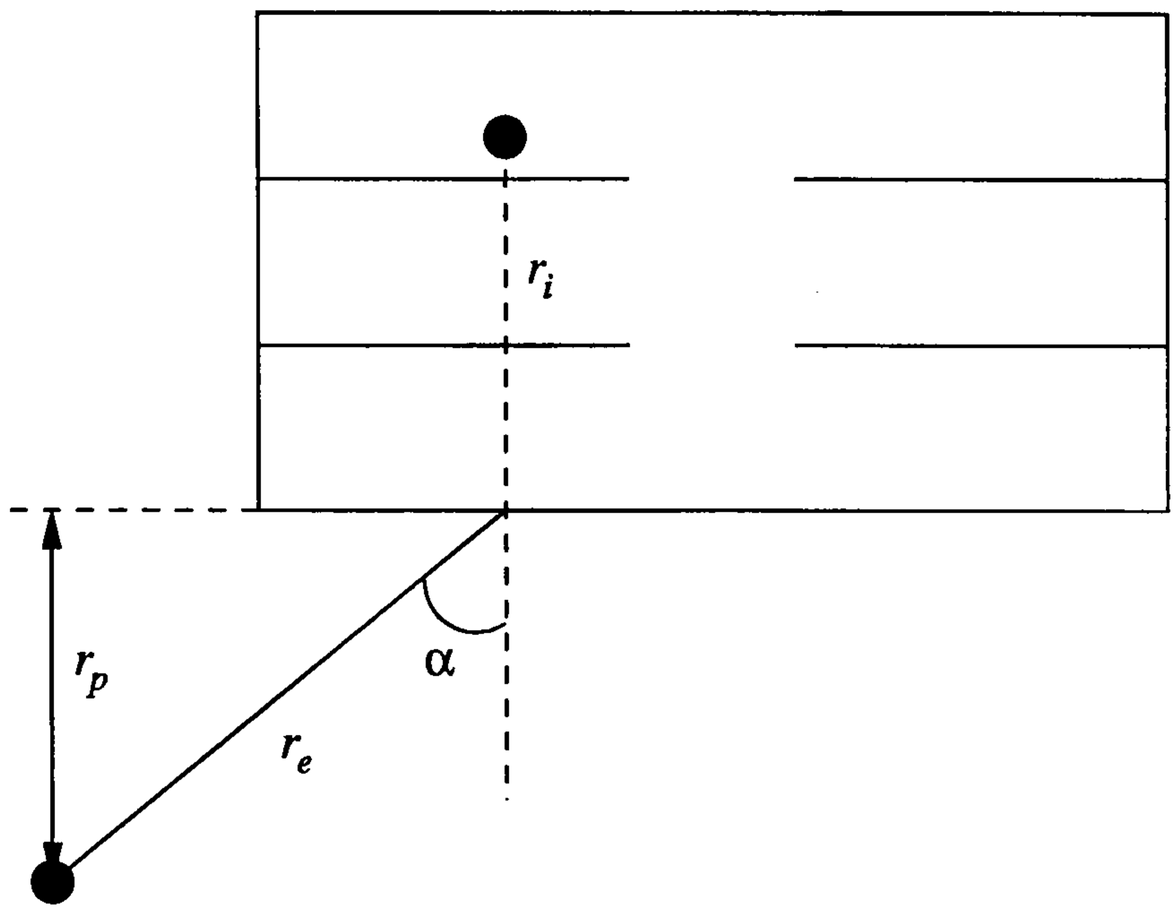

Figure 4.32: Geometry for COST231 LOS building penetration model

The path-loss mathematical model can be written as

$$PL = PL_F + PL_e + PL_g(1 - \cos\alpha)^2 + \max(PL_1, PL_2) \tag{4.15}$$

where $cos\alpha = \frac{r_p}{r_e}$, PL_F is the free space path-loss of total length of $(r_i + r_e)$, PL_e path-loss through the external wall at normal incidence ($\alpha = 0°$), PL_g is the additional external wall loss incurred at normal incidence ($\alpha = 90°$), and

$$\begin{cases} PL_1 = n_w PL_i \\ PL_2 = \kappa(r_i - 2)(1 - cos\alpha)^2 \end{cases} \tag{4.16}$$

where n_w is the number of walls crossed by the internal path r_i, PL_i is the loss per internal wall and κ is a specific attenuation [dBm^{-1}] which applies for unobstructed

internal paths. In this simulation no internal wall loss is considered, and κ is 0.6dBm^{-1}, PL_g is 20dB, and PL_e is 7dB.

The COST231 NLOS model is given by

$$PL = PL_{out} + PL_e + PL_{ge} + \max(PL_1, PL_3) - G_{fh} \tag{4.17}$$

where $PL_3 = \kappa r_i$ and r_i, κ and PL_1 are defined in the LOS model. The G_{fh} is the floor gain, which is not considered in the simulation. The PL_{ge} is chosen to be 6dB.

Figures 4.33 and 4.34 depict the comparison between the OTDoA and HAHCP methods. The results plotted in Figure 4.33 illustrates that the indoor UE suffered severe hearability problem when OTDoA method is used. Only 10% of the indoor UE is within the transmission range of three NBs. This is due to the penetration loss suffered by the indoor UE, so PCPICH from neighbouring NBs are too weak to be detected. However, if the nearby outdoor UEs with spatial information are allowed to assist in positioning, the hearability improves. Figure 4.33 shows that 66% and 28% of the indoor UEs are within the transmission range of three and seven PEs respectively.

Figure 4.34 depicts the accuracy of the location services for the two methods. Under the OTDoA method, only 24% of the estimates are within the 50m error. The main reason for such inaccuracy is because 55% of the estimates are determined by Cell-ID method. This method is used when UE is only within the transmission of one NB. Hence, the accuracy is within the cell radius, and the accuracy would deteriorate if the strongest NB is not the cell it resides in. Figure 4.34 also reveals that under the HAHCP method, 50 % of the estimates are within the 50m error. This is a noteworthy improvement over the OTDoA method. This is associated with better hearability of HAHCP method, for 66% of the indoor UEs can estimate their position using trilateration method.

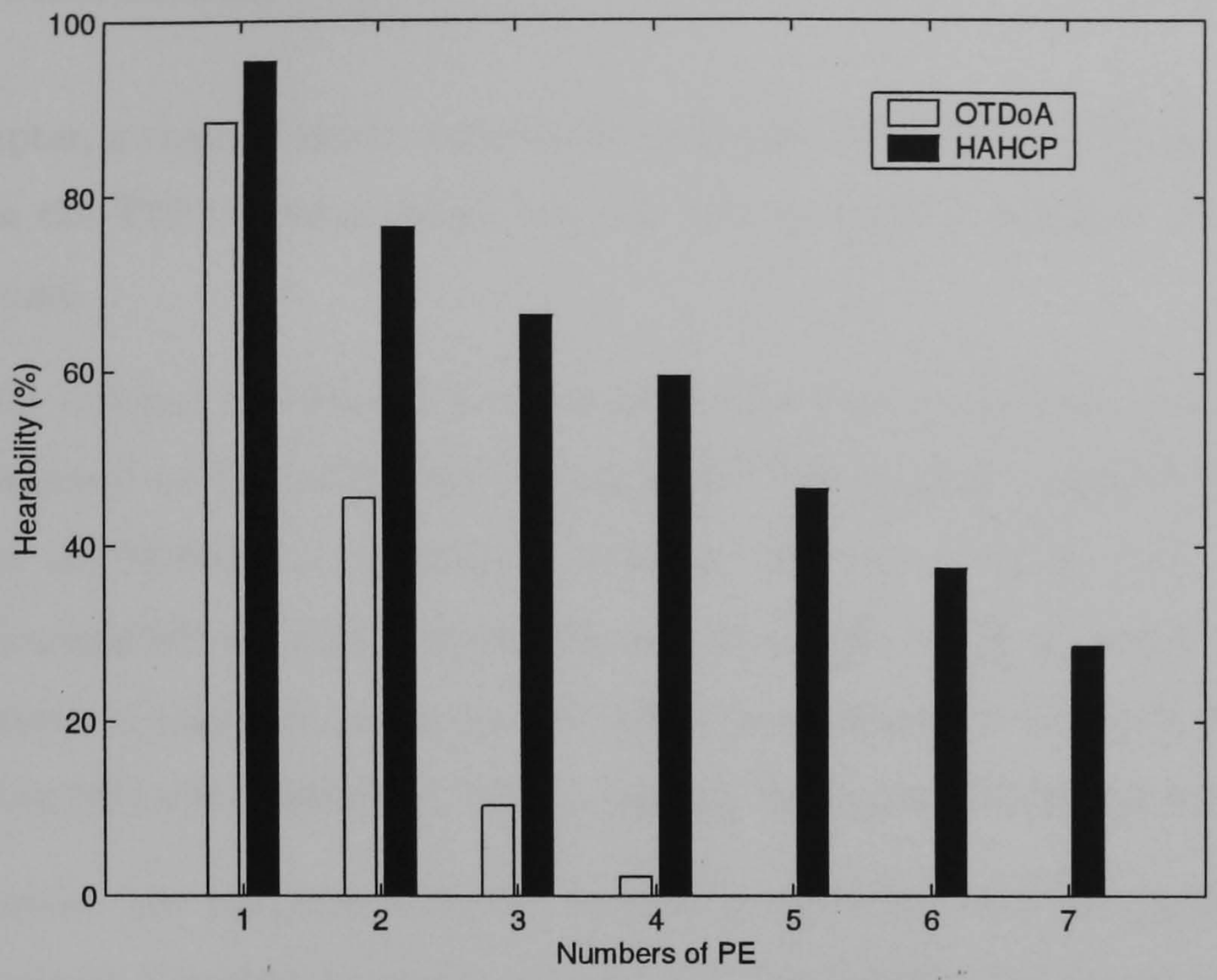

Figure 4.33: Hearability of indoor UE with OTDoA and HAHCP methods

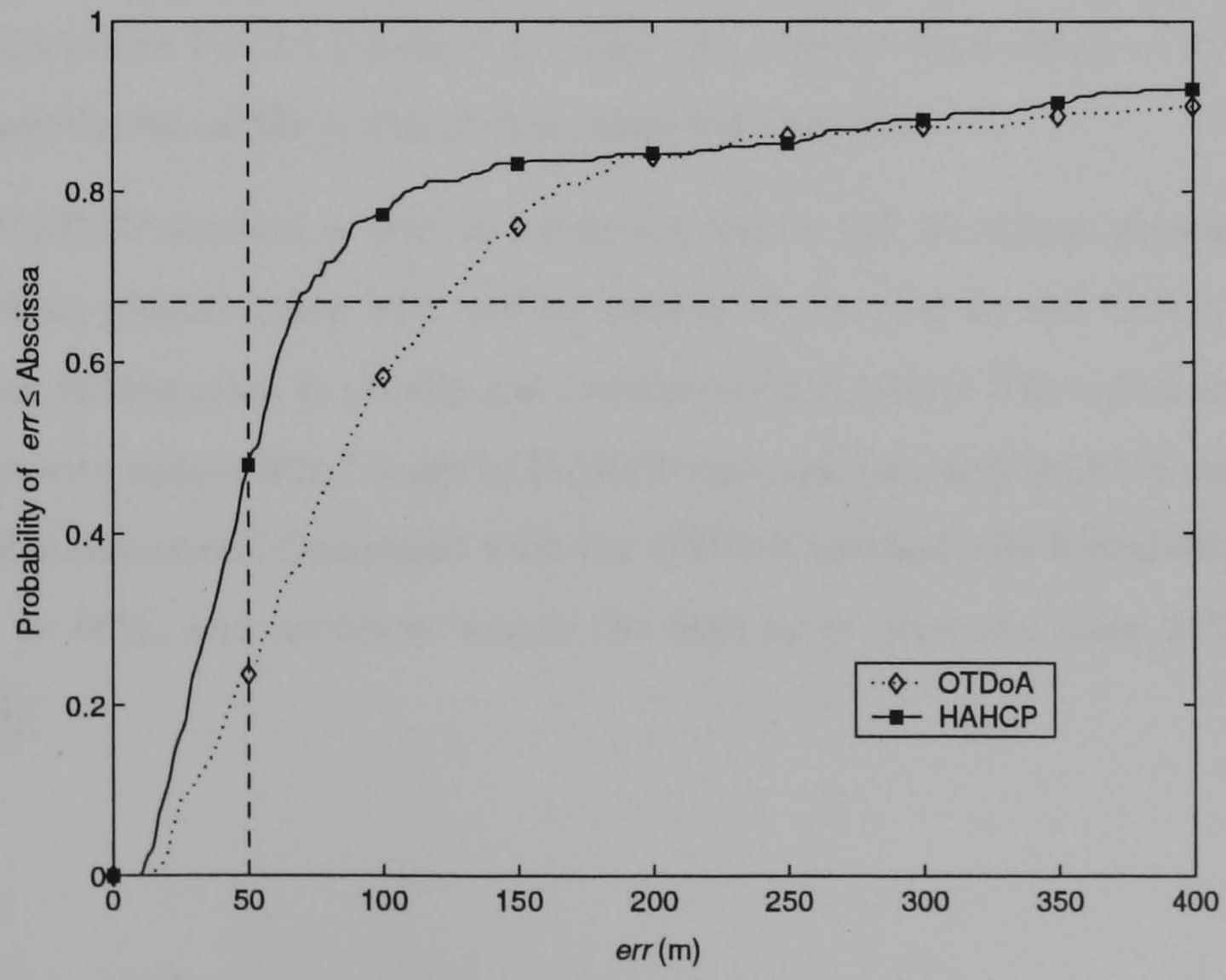

Figure 4.34: Accuracy of indoor UE positioning using OTDoA and HAHCP methods

4.7 Conclusions

In this chapter, a channel model suitable for evaluation of LCS has been developed. It is based on the T1P1 channel model and the LOS and NLOS model is added to the channel model.

The OTDoA method is evaluated and the different system parameters that will affect the performances of the LCS were investigated. The critical problems in OTDoA method are the NLOS and hearability problems. Simulation results show that when the neighbouring NB are fully obstructed, less than 10% of the estimates are within the 50m error. In addition, when the UE resides near the centre of a cell, visibility of neighbouring NBs will deteriorate. Hence, ranging observation would be badly affected.

In this chapter, the proposed HAHCP method is evaluated and compared with the OTDoA method. Simulations results revealed that the HAHCP has better performance than OTDoA method. The nearby UEs with spatial information will provide additional ToA observations to the least-squares estimator. That's why a better UE position is ensured. The hearability of the UE also improves with HAHCP method, for it is no longer restricted to NB for positioning. This will ease its dependency of remote NBs, which is usually out of the transmission range with the UE.

Also, the HAHCP method is used to locate the indoor UE. In indoor environment, the PCPICH from neighbouring NBs will be heavily attenuated by the building external walls. Thus, trilateration is usually not possible for the indoor UE, unless the building is equipped with indoor NB. Using the HAHCP method, hearability of UE and accuracy of the LCS is improved. Compared with the OTDoA method, the hearability improves from 10% to 66%, and accuracy within the 50m error improves from 24% to 50 %, respectively.

Chapter 5

Position Enhanced Soft Handover Algorithm

5.1 Introduction

In this chapter, the performance of the position enhanced SHO algorithm, which utilises the UE spatial information to assist in handover, is presented. The simulation work is based on the UTRA vehicular test environment, where the proposed SHO algorithm is studied and compared with the UTRA SHO. Additionally, UE position error and hearability are considered throughout the work. Different scenarios that affect the performance of the SHO algorithm are used to verify the performances of both algorithms. In particular, the shadowing, UE velocity, offered traffic loads and the accuracy of position estimated on the position enhanced SHO algorithm are looked into.

5.2 UE Geo-location in Handover

Location services will be available to all the cellular networks in near future, primarily as a requirement for the E-911 and value-added services. Also, the UE position estimate will be used to enhance mobility management schemes. In section 3.2.3, it is presented that the distance and UE angle of movement with the desired NB could

be determined by the UE spatial information. This supplementary information will be used to adaptively fine-tune the hysteresis margins, in turn to encourage or delay a handover. Then again, the performance of such an algorithm is limited by errors in the position estimated. Fortunately, inter-cell handovers usually occur at the boundary of the cell, where UE has better visibility with the neighbouring NBs, and so, making it favourable to use network-based positioning method to estimate the UE location for position enhanced SHO.

5.2.1 Adding a NB to the ActS

Figure 5.1 explains the NB is located at the central of each hexagonal cell with a radius of R, the UE is within the handover region (the intersection of the two circles), and moving towards NB_2. At time t_n, the UE is being served by NB_1. To add NB_2 into the UE's ActS, the following have to be determined. Firstly is to determine the location of the UE, which could be obtained by the network-based or A-GPS positioning method. With the location of UE known, the distance and direction of movement with desired NB can be calculated as the d and Θ, respectively. Besides, the spatial information also allows one to determine whether the UE is within the SHO region, where

$$SHO_{region} = \begin{cases} 1 & (d_1(t_n), d_2(t_n)) < R \\ 0 & otherwise \end{cases} \tag{5.1}$$

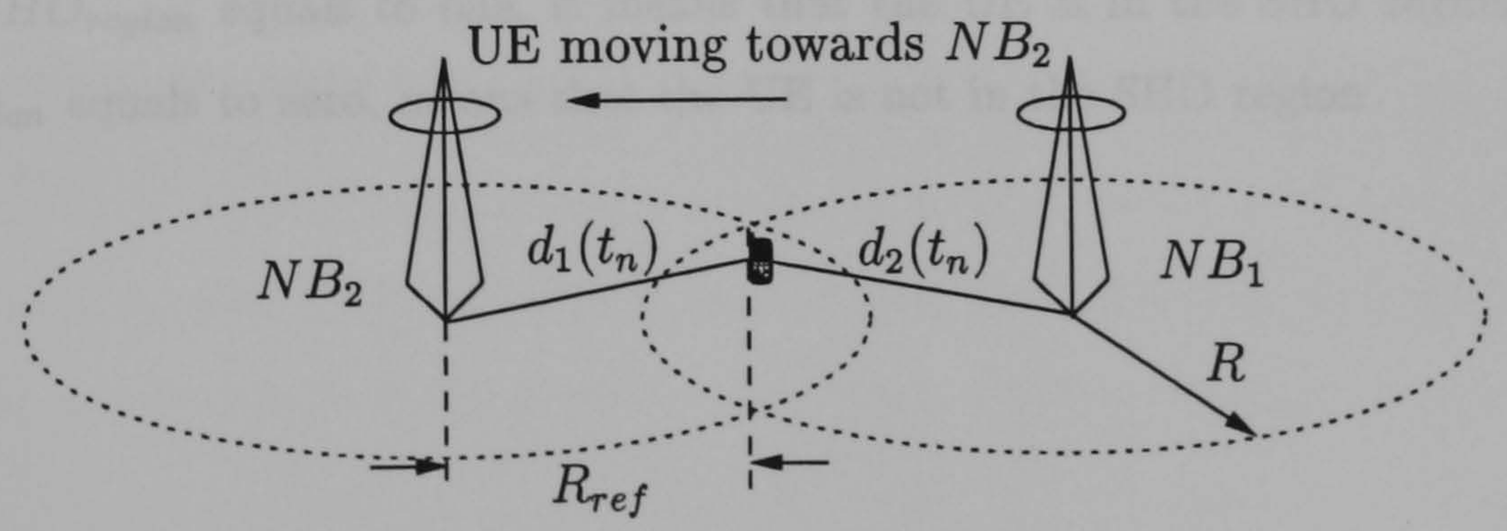

Figure 5.1: Position enhanced SHO

In order to act the NB_2 into UE's ActS, the measured and averaged PCPICH from NB_2 must be higher than the adding threshold Th_{ADD} (dB), and is modelled as

$$Th_{ADD} = Best\_ActS_{PCPICH} + Hyst_{ADD} + Hyst_d + Hyst_\Theta \tag{5.2}$$

where $Best\_ActS_{PCPICH}$ is the strongest NB in the ActS, $Hyst_{ADD}$ in dB is a fixed adding hysteresis value, $Hyst_d$ in dB is dependent to the distance between the UE and desired NB, and $Hyst_\Theta$ in dB is dependent to the bearing between the UE and desired NB. If the distance between the UE and NB_2 is shorter than R_{ref}, NB_2 will be encouraged to be added into the ActS, by reducing the $Hyst_d$ value. If the distance between the UE and NB_2 is longer than R_{ref}, NB_2 is prevented to be added into the ActS. This is done by raising the value of $Hyst_d$.

The increment and decrement of $Hyst_d$ with respect to the distance between the UE and desired NB, depends on the factor C_k (dB), where k=1 and 2. The factor C_1 is used when UE exists within the handover region, and otherwise C_2 is used, where $C_1 < C_2$. This is to ensure that changes in the $Hyst_d$ is marginal when UE resides within the handover region. UE that is within the handover region usually experiences from weak signal link with its serving NB and heavily interference from surrounding UEs. So, smaller variation of $Hyst_d$ is required. As illustrated in Figure 5.2, the $Hyst_d$ can be written as

$$Hyst_d = \begin{cases} \frac{d_2(t_n) - R_{ref}}{R_{ref}} C_1 & SHO_{region} = 1 \\ \frac{d_2(t_n) - R_{ref}}{R_{ref}} C_2 & SHO_{region} = 0 \end{cases} \tag{5.3}$$

When SHO_{region} equals to one, it means that the UE is in the SHO region. While SHO_{region} equals to zero, means that the UE is not in the SHO region

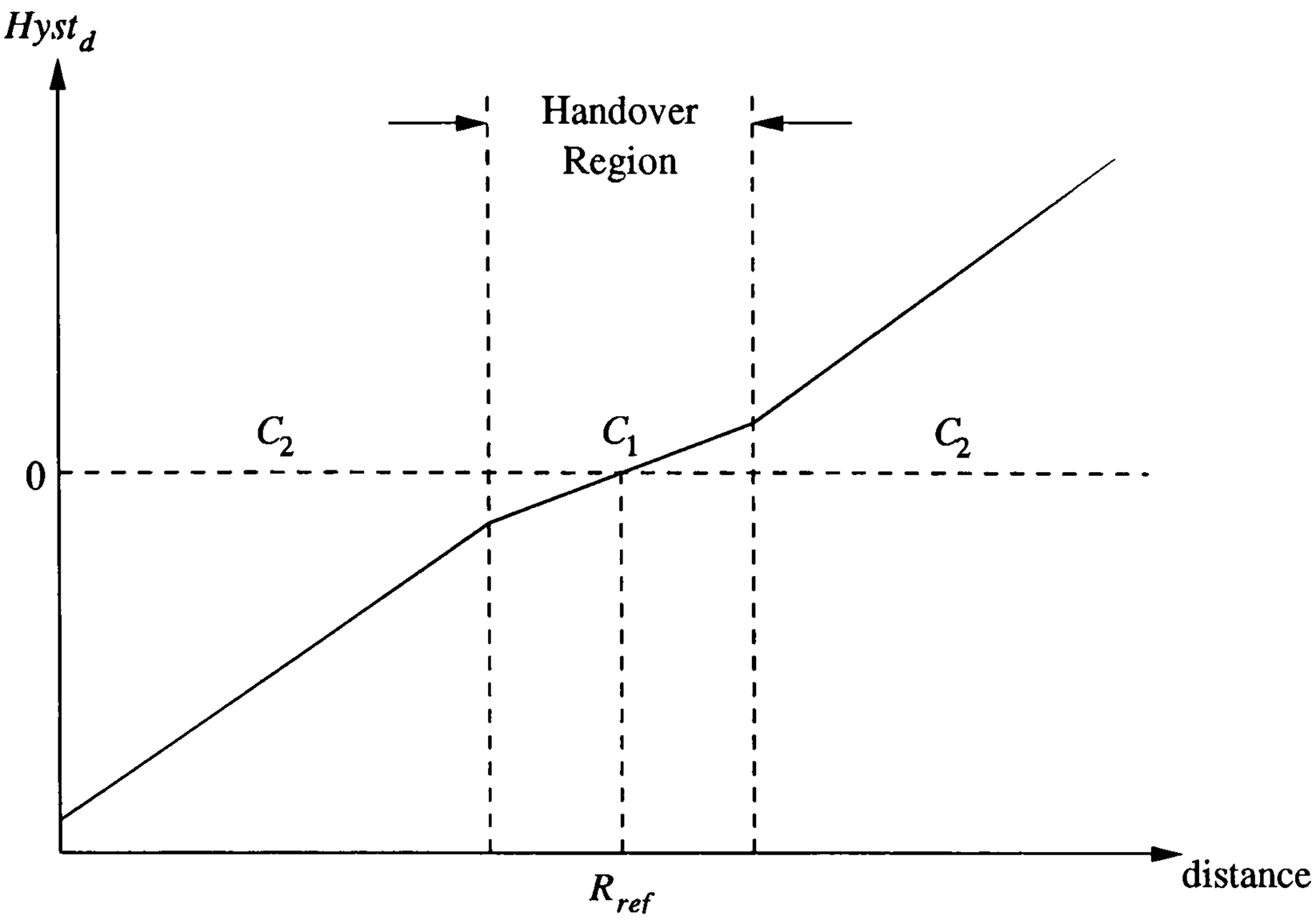

Figure 5.2: Changes of $Hyst_d$ with respect to the distance between UE and NB_2

The trajectory of the UE with respective to the NB is also considered in the position enhanced SHO algorithm. The hysteresis margin $Hyst_\Theta$ will be reduced or increased, if UE is approaching or residing from the NB_2 by a factor of C_Θ (dB), as illustrated in Figure 5.3. Then, the $Hyst_\Theta$ is written as

$$Hyst_\Theta = \left(\frac{\Theta - \frac{\pi}{2}}{\frac{\pi}{2}} \right) C_\Theta \tag{5.4}$$

where Θ is the calculated moving direction of UE with respect to NB_2.

In conclusion, the hysteresis margin is no longer a fixed value. It is adaptive to the mobility and spatial distance between the UE and NB. However, at time when UE geo-location information is not available, the hysteresis margins $Hyst_d$ and $Hyst_\Theta$ are zero.

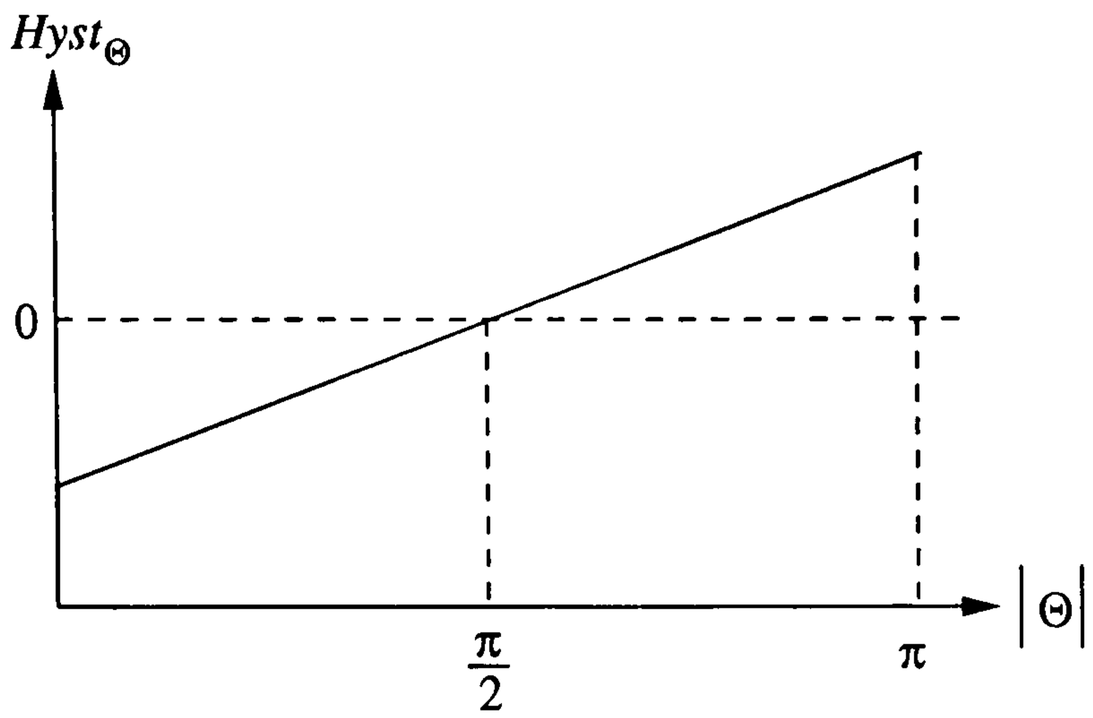

Figure 5.3: Changes of $Hyst_{\Theta}$ with respect to the UE direction of motion

5.2.2 Dropping a NB from the ActS

Similarly, to drop a NB from the UE's ActS, the $Worst\_NB\_ActS$ signal must be lower than the Th_{DROP} (dB) for a duration of T_{trig}, and more than one NB is serving the UE. It is written as

$$Th_{DROP} = Best\_ActS_{PCPICH} - Hyst_{DROP} + Hyst_{d} + Hyst_{\Theta} \tag{5.5}$$

where $Hyst_{DROP}$ (dB) is a fixed dropping hysteresis value, and $Hyst_{d}$ and $Hyst_{\Theta}$ are referred to equations (5.3) and (5.4).

5.2.3 Replacing a NB from the ActS with a NB from the MonS

On the other hands, to replace the weakest NB from the UE's ActS with the strongest NB from the MonS, the $Best\_NB\_MonS$ must be greater than the $Worst\_NB\_ActS$ for a period of T_{trig}. On top, the number of NBs serving the UE must be equals to the $ActS\_Max\_Size$. The replacement threshold Th_{REP} (dB) is written as

$$Th_{REP} = Worst\_ActS_{PCPICH} + Hyst_{REP} + Hyst_{d} + Hyst_{\Theta} \tag{5.6}$$

where $Hyst_{REP}$ in dB is a fixed replacing hysteresis value, and $Hyst_{d}$ and $Hyst_{\Theta}$ are referred to equations (5.3) and (5.4).

5.3 SHO Simulation Models

The simulation used a homogeneous cellular area consisting of three tiers of 19 hexagonal cells with identical radius of 2000m. To alleviate the boundary effect, only UEs in the inner 7 cells are considered for statistics collection. The cell loads is assumed to be uniform throughout the simulation area. The vehicular environment path-loss model is [35]

$$PL = 40\left(1 - 4 \times 10^{-3}\Delta h_b\right)\log(d) - 18\log\left(\Delta h_b\right) + 21\log(fc) + 80 \quad (dB) \qquad (5.7)$$

where d represent NB to UE separation in kilometres, Δh_b is NB antenna height measured from average roof top level (15m), and fc is the carrier frequency (2000MHz). The shadowing loss is considered as a lognormal random variable with de-correlation length d_{cor} of 20m. The standard deviation of shadowing σ_{sha} is set at 10 dB. Fast fading is not accounted as measurement interval to PCPICH is generally several miniseconds and the measured $\frac{E_c}{N_o}$ of PCPICH samples are averaged before they could trigger SHO. Therefore, the fast fading is assumed being averaged out due to its short correlated distance. The $Hyst_{ADD}$, $Hyst_{DROP}$, and $Hyst_{REP}$ are set to 2dB, 5dB, and 5dB respectively. For the position enhanced SHO algorithm, by simulation tests the C_1, C_2 and C_Θ for the proposed algorithm are set to 2dB, 4dB, 2dB, respectively. While R_{ref} is half the distance between two NBs.

A speech service of bit rate $R_{bit} = 8$ kbps is considered. Calls are generated according to a Possion process. The duration of a call follows an exponential distribution with mean of 100 second. Perfect power control is assumed for the uplink channels, while the transmitted power allocated to the downlink channels is fixed.

An active call is considered as in outage if received $\frac{E_b}{N_o}$ from corresponding traffic channel is below a threshold. In such system, the instantaneous PCPICH $\frac{E_c}{N_o}$ received from the i^{th} NB can be presented as

$$\left(\frac{E_c}{N_o}\right)_i = \frac{P_p 10^{-(PL_i - L_{sha_i})/10}}{\eta N_i P_t 10^{-(PL_i - L_{sha_i})/10} + \sum_{j \neq i}^{J}\left(P_p + N_j P_t\right) 10^{-(PL_i - L_{sha_i})/10} + n} \qquad (5.8)$$

where P_p(Watt) is the transmitted power allocated to PCPICH, P_t(Watt) is the power allocated to traffic channels, PL_i and L_{sha_i} is the path-loss and shadowing loss in dB from the i^{th} NB, and η is the orthogonality factor for intra-cell interference introduced by non-ideal orthogonality between channels in downlink. The N_j corresponds to the carried traffic in j^{th} cell, and n is the background thermal noise.

The instantaneous $\frac{E_b}{N_o}$ from a desired traffic channel in cell i^{th} thereafter can be presented as

$$\begin{aligned}\left(\frac{E_b}{N_o}\right)_i &= \frac{R_{chip}}{R_{bit}} \cdot \frac{S_t}{I_{own} + I_{other} + n} \\ &= \frac{R_{chip}}{R_{bit}} \cdot \frac{P_p L_{tot_i}}{\eta\left((N_i - 1)P_t + P_p\right) L_{tot_i} + \sum_{j \neq i}^{J} \left(P_p + N_j P_t\right) L_{tot_j} + n}\end{aligned} \tag{5.9}$$

where $L_{tot} = 10^{-(PL_i + L_{sha_i})/10}$.

The R_{chip} represents the UTRA chip rate of 3.84 Mcps. For an active UE in SHO, maximal ratio combining is assumed. Therefore, the received $\frac{E_b}{N_o}$ is the sum of $\frac{E_b}{N_o}$ from multiple traffic channels involved in SHO.

5.4 SHO Results and Discussion

To evaluate the performance of the position enhanced SHO algorithm, the vehicular environment was simulated and compared with the UTRA SHO algorithm. A uniformly distributed 25 Erlangs per cell offered traffic loads is provided. Each NB is limited to a maximum number of 30 active UEs. The transmitted powers of PCPICH and traffic channels are set to 33dBm and 30dBm, respectively. The thermal noise n is -118dBm and the orthogonality factor η is 0.68. The $\frac{E_b}{N_o}$ outage threshold for such a speech service is set to 7dB. The simulation interval step is 500ms. The velocity of the UE is fixed and set to 120km/h. The UEs move around the simulation area and their initial directions are uniformly distributed between 0 to 2π radian. The new direction is generated by a Gaussian distribution with mean equal to the UE's previous direction and standard deviation of $\frac{\pi}{6}$ radian.

In chapter 4, it was made known that network-based positioning method require strong visibility and LOS links with its surrounding PEs. Any NLOS errors and timing observations will result in position that is badly estimated. When UE is having LOS links with all its PEs, the error in the estimate is usually tens of meters away from its true value. Nonetheless, if there is NLOS errors or chips being wrongly estimated during cross-correlation, the error will be hundreds of meters. As well, the UE may not acquire its location at all time, especially when it resides near the centre or in a large cell. So, we suggest to model the accuracy and hearability as such

Distance	Hearability	Error err_a	Probability of position badly estimated	Error (Position badly estimated) err_b
$d < 0.2R$	12%	N[40, 45]m	0.20	U[0, R]m
$d \geq 1.8R$				
$0.2R \leq d < 0.4R$	33%	N[40, 45]m	0.20	U[0, R]m
$1.6R \leq d < 1.8R$				
$0.4R \leq d < 0.6R$	46%	N[35, 35]m	0.17	U[0, R]m
$1.4R \leq d < 1.6R$				
$0.6R \leq d < 0.8R$	80%	N[30, 30]m	0.15	U[0, R]m
$1.2R \leq d < 1.4R$				
$0.8R \leq d < R$	86%	N[25, 30]m	0.10	U[0, R]m
$R \leq d < 1.2R$				

Table 5.1: UE position estimated for position enhanced SHO algorithm

where R is the cell radius and d is the distance between the NB and UE.

The error err_a have a positive normal distribution with mean of 25m to 40m and σ of 30m to 45m. When the position is being badly estimated, the error err_b will have a positive uniform distribution of 0 to Rm. The error profile of the estimated UE positions is shown in Figure 5.4.

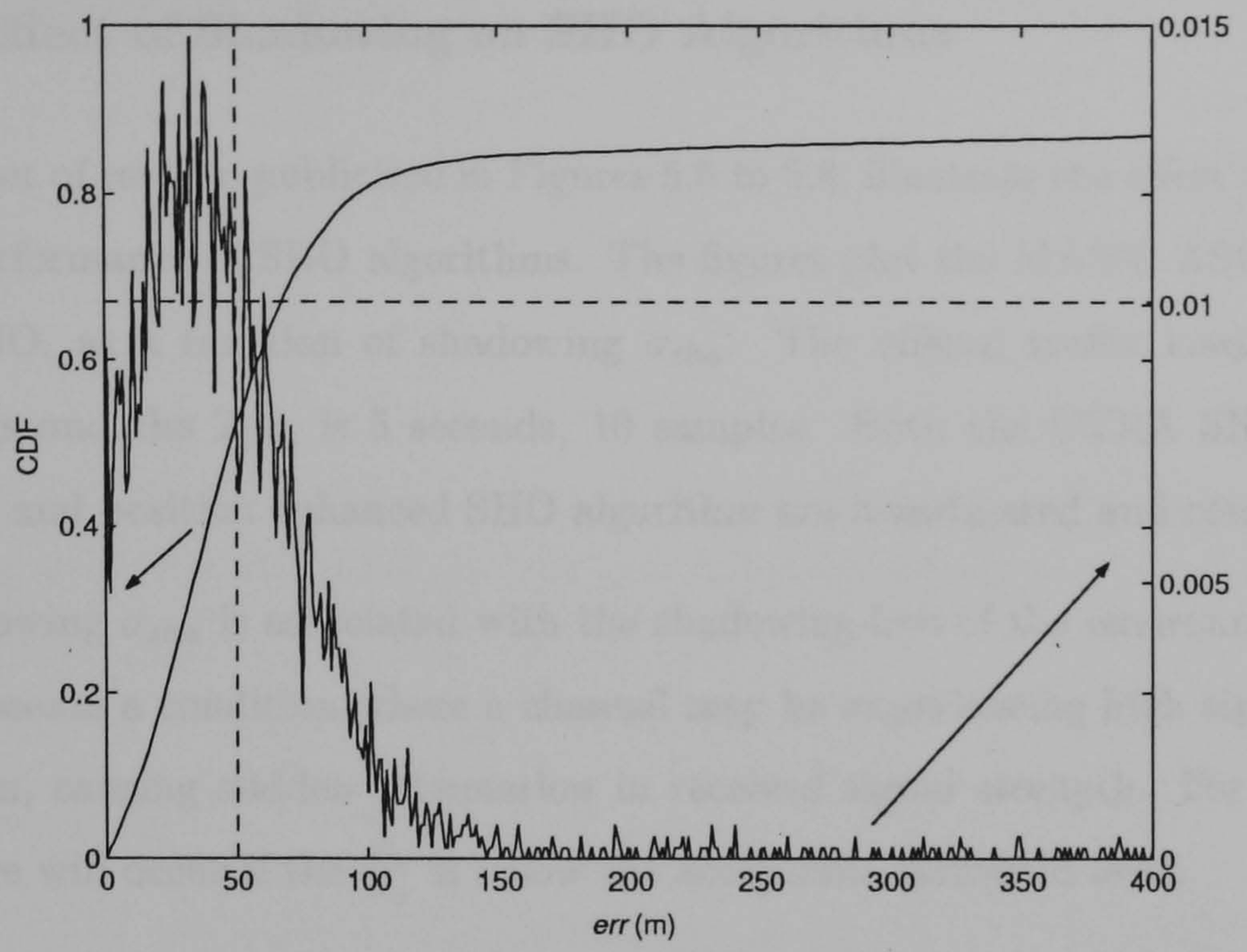

Figure 5.4: Error profile of estimated UE positions for position enhanced SHO algorithm

In principle, two types of indicator are defined to evaluate the performance of the algorithm. The indicators related to the QoS of the service are

- **Call blocking probability (BP)** is defined as the probability that a new call attempt is blocked.

- **Call Outage Probability (OP)** is defined as the probability that the maximal NB signal strength in the active set falls below an acceptable signal threshold. This indicator can be used to describe the QoS of the services.

The indicators related to the system resource efficiency are

- **Mean Active Set Number (MASN)** is defined as the average number of NB serving one active UE at a time. It represents the number of traffic channels supporting a single UE in a SHO system.

- **Active Set Update Rate (ASUR)** is defined as the number of changes in a UE's ActS per second. This indicator can represent the signalling load.

In a SHO algorithm, all these performance indicators should be as low as possible.

5.4.1 Effect of Shadowing on SHO Algorithms

The first set of results, publicised in Figures 5.5 to 5.8, illustrate the effect of shadowing on the performance of SHO algorithms. The figures plot the MASN, ASUR, OP, and BP of SHO, as a function of shadowing σ_{sha}. The offered traffic loads is fixed at 25 Erlangs and the T_{trig} is 5 seconds, 10 samples. Both the UTRA SHO handover algorithm and position enhanced SHO algorithm are investigated and compared.

The shadowing σ_{sha} is associated with the shadowing loss of the environment. Higher σ_{sha} represents a condition where a channel may be experiencing high signal strength fluctuation, causing sudden attenuation in received signal strength. For this reason, call outage will occur if the $\frac{E_b}{N_o}$ is below the acceptable threshold level.

Figure 5.5 depicts that as the σ_{sha} increases, the MASN increases. Clearly indicating that most of the time more than one NB are required to serve an active UE, and this will reduce the system capacity. With the addition of channels needed to serve the on-going calls, so lesser channels are reserved for new incoming calls, hence, higher probability of new calls would be blocked. This is conveyed in Figure 5.8, where new call BP enhances when the MASN is increased, as more channels are being reserved to serve the on going calls.

Figures 5.5 and 5.8 also show that the proposed algorithm is able to reduce the numbers of UE in the SHO stage. This perhaps direct to the $Hyst_d$ and $Hyst_\Theta$ in the proposed SHO algorithm. Under high σ_{sha} case, the handover decision that is based on signal strength criteria will be less reliable. A sudden rise in shadowing loss, might cause a false alarm and results a NB from the MonS added into the UE's ActS, even when the UE is spatially near to its current serving NB. This will be undesirable, as a sudden drop in the $\frac{E_b}{N_o}$ may only be temporary and $\frac{E_b}{N_o}$ higher than the threshold may still be achievable. In this circumstance, if the handover could be delayed by adding the $Hyst_d$ value to the hysteresis margin, then unnecessary handovers could be avoided as shown in Figure 5.6. On the other hand, if UE is located near the edge of the cell and the σ_{sha} is high, based on equation 5.4, handover is encouraged by reducing the hysteresis margin. Likewise, the handover could be further supported, by including the $Hyst_\Theta$ into the SHO algorithm. The $Hyst_\Theta$ will promote handover if the UE is approaching

the candidate NB, by further lowering the hysteresis margins. This will outcome in lesser call OP when compared with UTRA SHO, where the results are shown in Figure 5.7. As a result, the proposed SHO algorithm is able to reduce unnecessary handovers and additional NB added to UE's ActS. Furthermore, able to maintain a lower call outage than the UTRA SHO, hence, better QoS is achieved.

The results plotted in Figures 5.5 to 5.8 also demonstrate that when σ_{sha} is high (i.e., 16dB), the proposed algorithm out-performed the UTRA SHO. With high changing shadowing loss, algorithm that exclusively depends on the received signal quality will fail. Therefore, it is better to consist of multiple criteria like the distances between the UE and NBs (d) and UE direction of motion (Θ) to assist in handover.

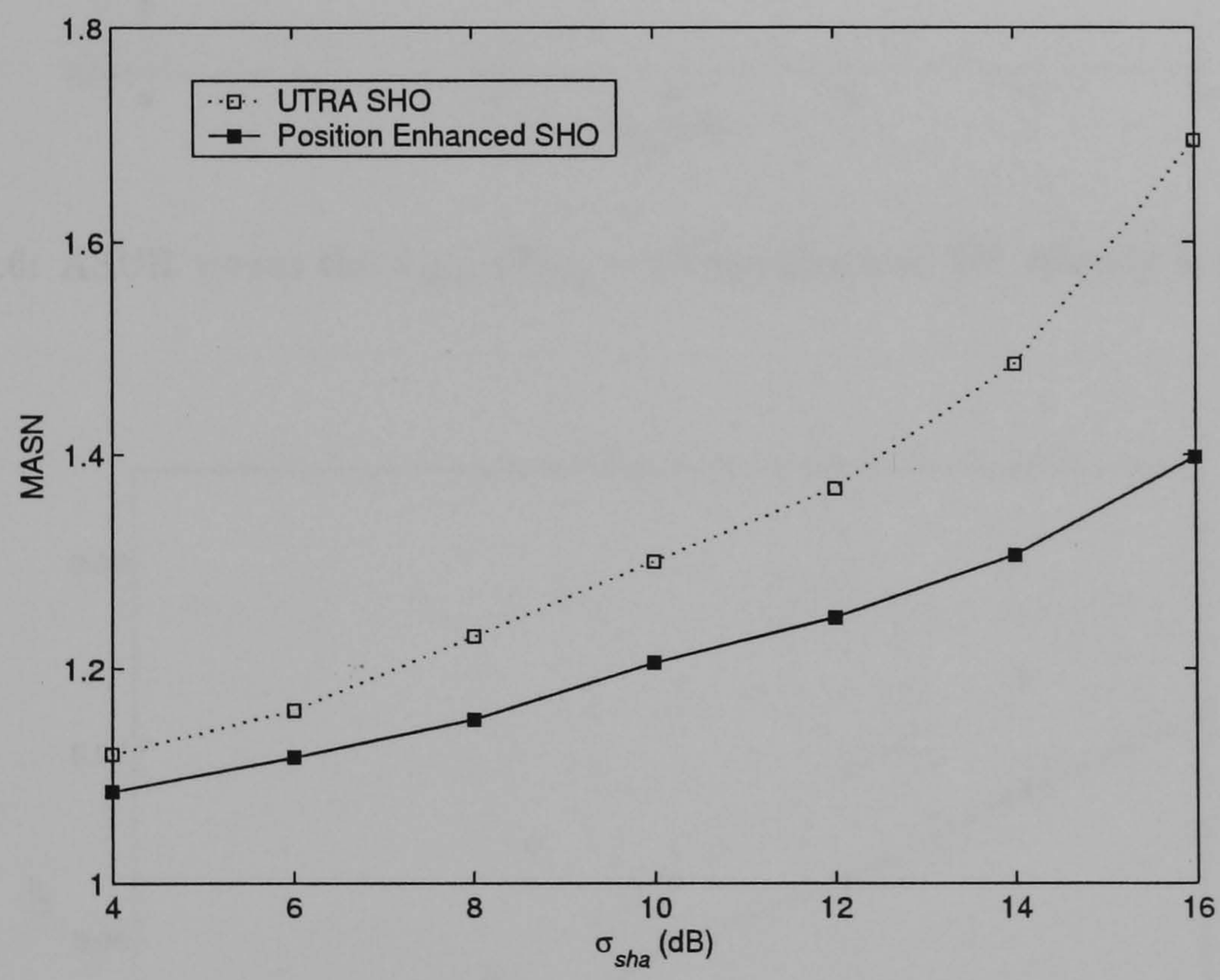

Figure 5.5: MASN versus the σ_{sha}, ($T_{trig} = 10$ samples and UE velocity is 120km/h)

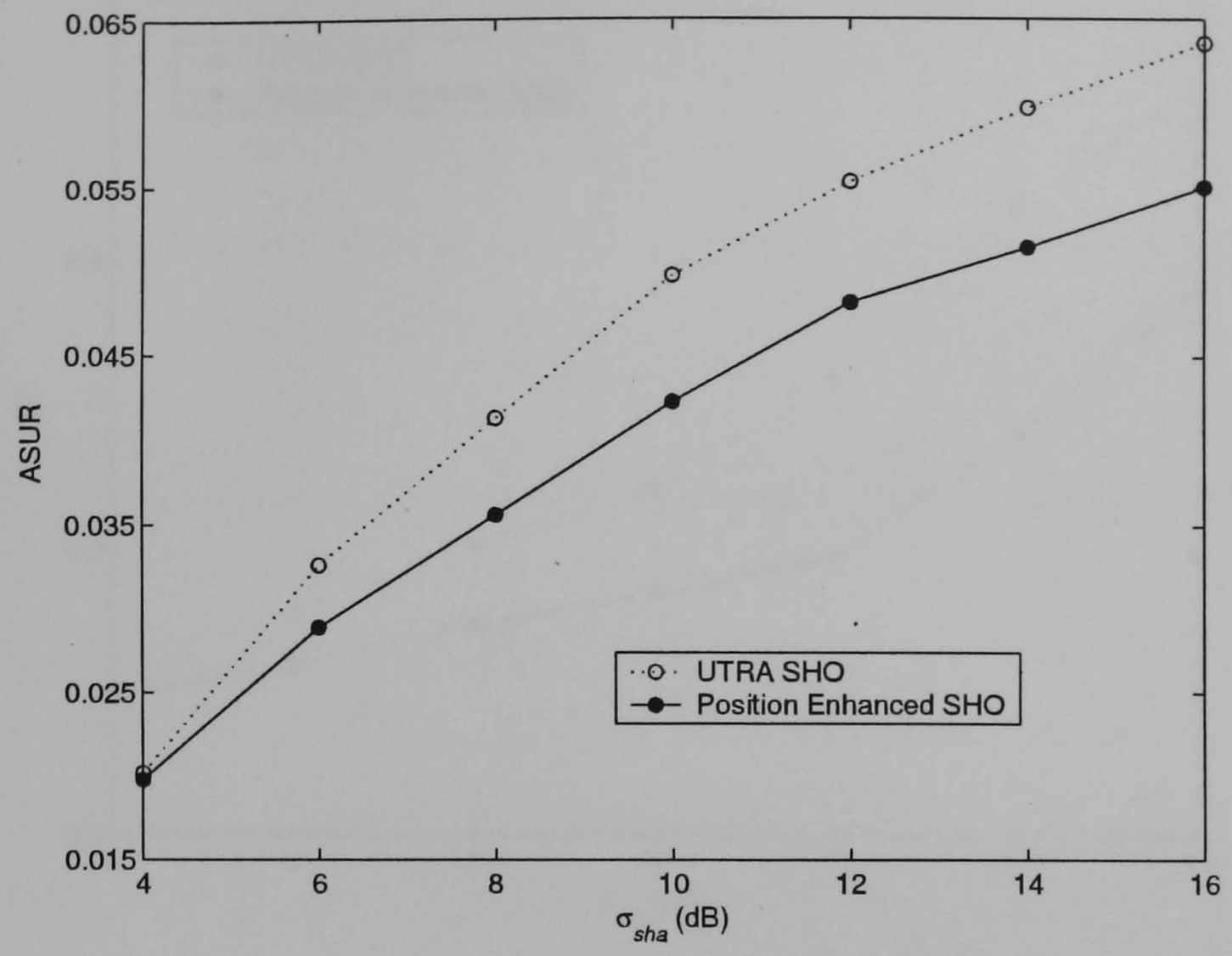

Figure 5.6: ASUR versus the σ_{sha}, ($T_{trig} = 10$ samples and UE velocity is 120km/h)

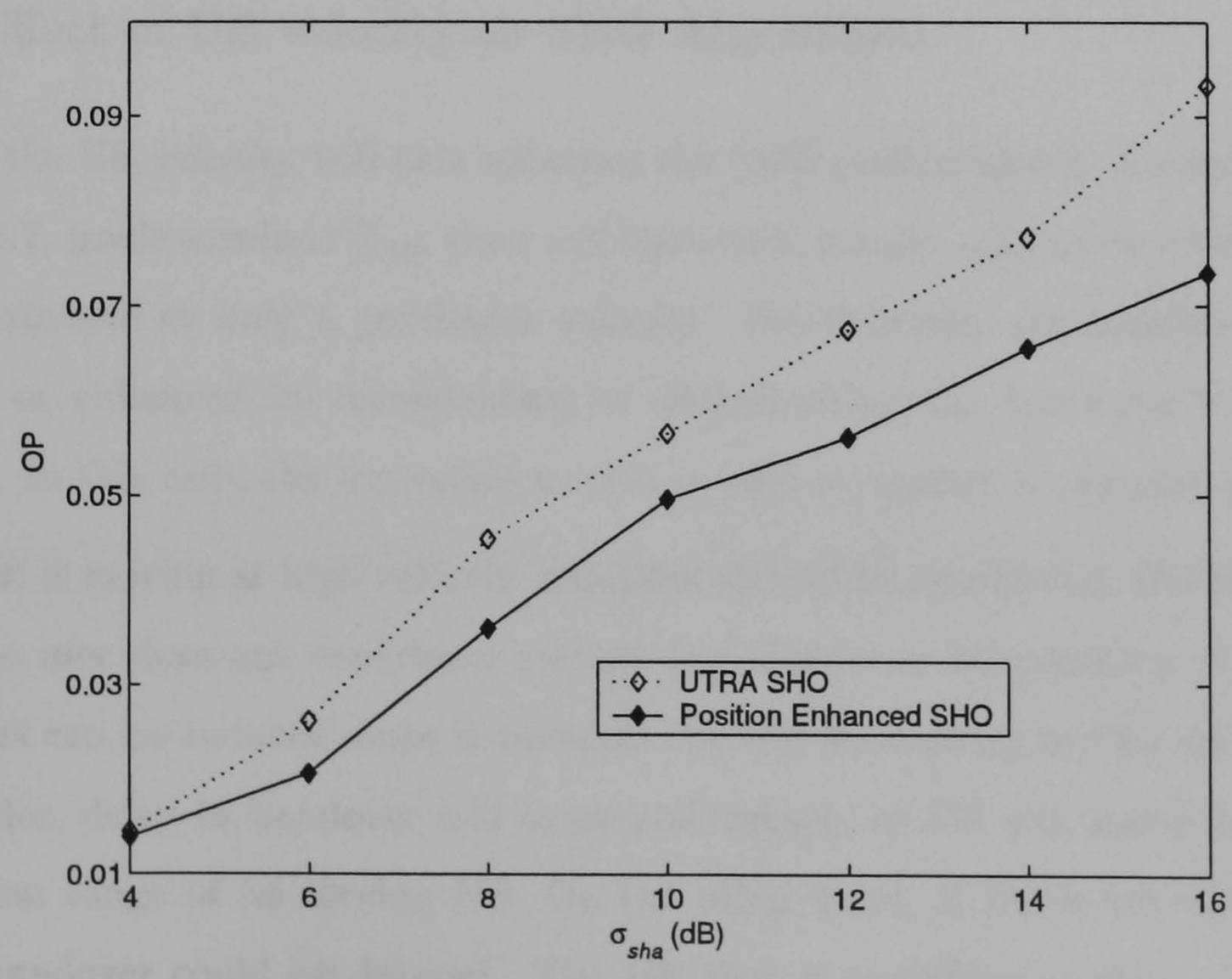

Figure 5.7: OP versus the σ_{sha}, ($T_{trig} = 10$ samples and UE velocity is 120km/h)

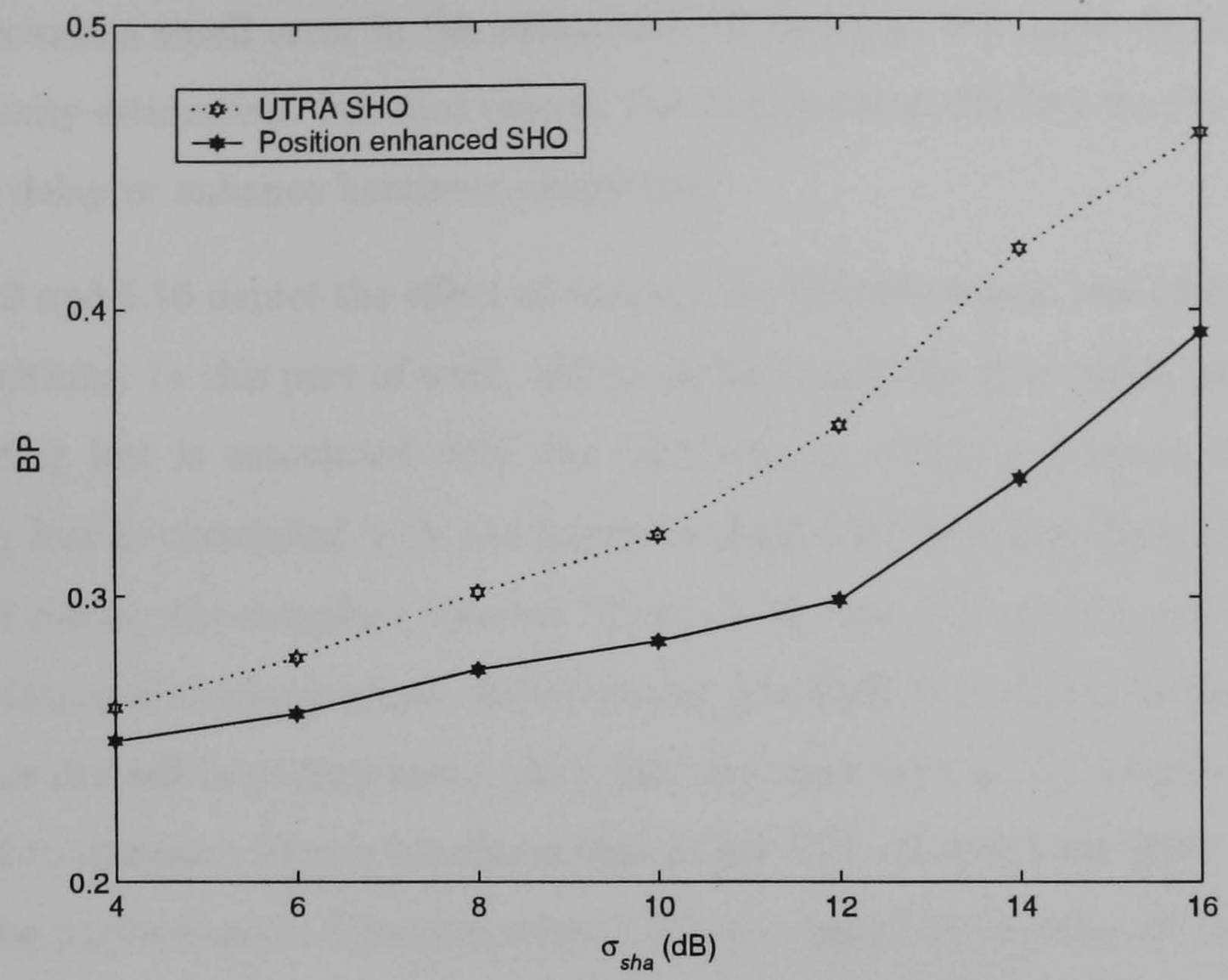

Figure 5.8: BP versus the σ_{sha}, ($T_{trig} = 10$ samples and UE velocity is 120km/h)

5.4.2 Effect of UE velocity on SHO Algorithms

Similarly, the UE velocity will also influence the SHO performances. As mentioned in section 3.2.2, predetermined T_{trig} time and hysteresis margin only makes the handover best performance at only a particular velocity. Nevertheless, the handovers can be dissuaded or enhanced by incrementing or decrementing the hysteresis margin and T_{trig} time. In this case, the hysteresis margin is used to oppose or support handover.

When a UE is moving at high velocity, handover should be executed at the fastest time so that the user does not experience service degradation or interruption. Co-channel interference can be reduced since it prevents the UE from going too far into the new cell. Besides, delay in handover will cause call outage, as UE will travel beyond the transmission range of its serving NB. On the other hand, if UE is travelling at low velocity, handover could be delayed. The UE that is travelling at slow velocity will reside within the transmission range of the serving NB longer than UE travelling at high velocity. So, if one knows the velocity of the UE, then the information can be used for handover. In the proposed SHO algorithm, the velocity of UE is not used for handover, although the UE spatial information allows one to determine the UE velocity.

This is because a small error in the estimated UE position will cause significant error in UE velocity estimation. For that reason, the distance and UE direction of movement is used to delay or enhance handover execution.

Figures 5.9 and 5.10 depict the effect of varying the UE velocity on the performance of SHO algorithms. In this part of work, although the σ_{sha} is fixed at 10dB, the variation of shadowing lost is associated with the UE velocity. This is because the current shadowing loss is correlated with the previous shadowing loss and distance travelled by the UE during the sampling interval. That's why high UE velocity will experience higher variation of shadowing loss. Additionally, when UE is travelling at high velocity, it will cross the cell boundary more often. So, the increment in UE velocity will cause the ASUR to increase. Figure 5.9 shows that at low UE velocity, both SHO algorithms have similar performances. However, when UE is moving at faster velocity, the proposed SHO algorithm starts to perform better than the UTRA SHO algorithm. Once again showing its ability to performance in condition where there high variation of shadowing loss. Furthermore, the call OP plotted in Figure 5.10 also depicts that the proposed SHO algorithm achieves better than UTRA SHO. At every cases of UE velocity, it has a lower call OP than the UTRA SHO.

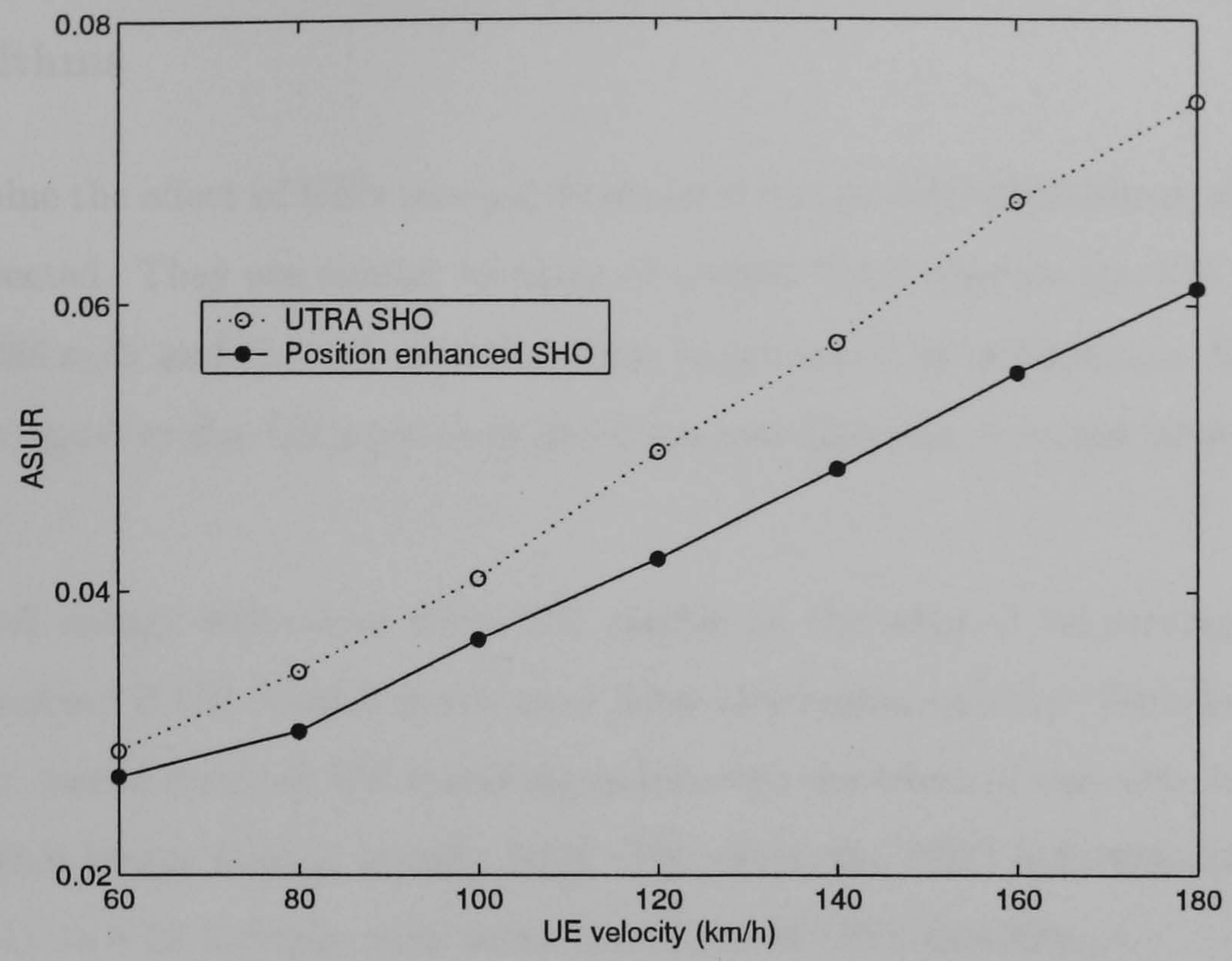

Figure 5.9: ASUR versus the UE velocity, ($T_{trig} = 10$ samples and σ_{sha}=10dB)

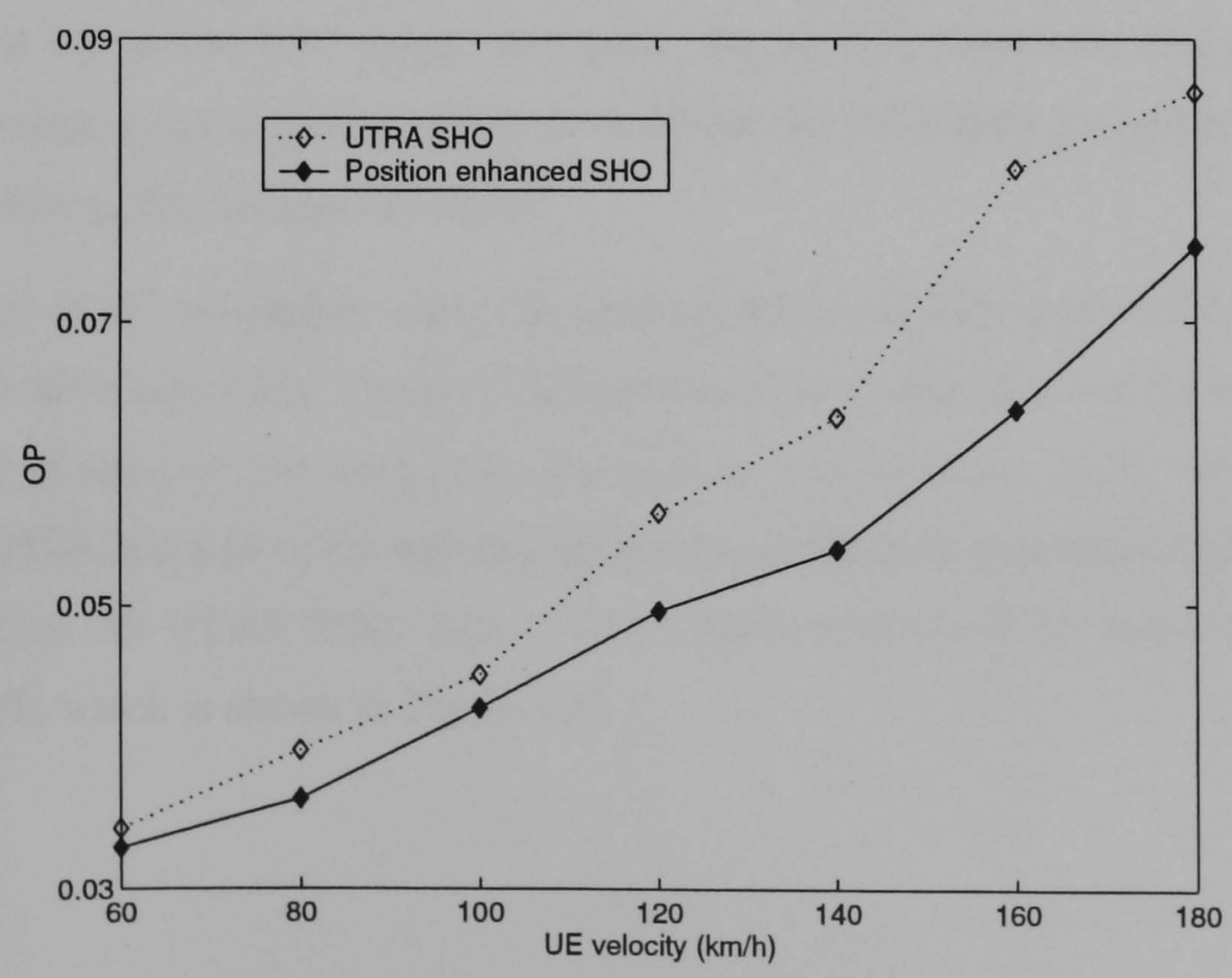

Figure 5.10: OP versus the UE velocity, (T_{trig}=10 samples and σ_{sha}=10dB)

5.4.3 Effect of UE's Direction Standard Deviation on SHO Algorithms

To determine the effect of UE's moving direction σ on the SHO algorithms, simulations were conducted. They are similar to those of section 5.4.2 whereas the UE velocity is fixed at 120km/h and the UE new direction is generated by a Gaussian distribution with mean equal to the UE's previous direction and direction σ varied between $\frac{\pi}{9}$ and $\frac{\pi}{3}$.

Usually call outage will occur when UE resides at the edge of its serving cell, and this is promoted if UE doesn't move away from this region quickly. With higher UE's direction σ, would result in UE travelling in between the edges of the cells, and staying in this region longer than it usually does. Therefore, the SHO indicators observed in Figures 5.11 to 5.13 increase with every increment of UE's direction σ.

In general, when the direction σ raises, all the SHO performance indicators increased. The increment in MASN and ASUR clearly indicate that the probability of UE existing at the edges of the cells is higher when direction σ increased. Hence, prolong the duration of UE in the SHO stage. Moreover, Figure 5.12 illustrates that additional adding, dropping and replacing of NBs to and from the UE's ActS are performed. This is also known as the 'ping-pong' effect.

In this part of the simulation work, the position enhanced SHO performs better than the UTRA SHO algorithm. Figure 5.13 illustrates that at direction σ of $\frac{\pi}{6}$, with UTRA SHO, 0.32 of the new incoming calls are blocked. On the other hand, with position enhanced SHO only 0.28 of the new incoming calls are blocked, possessing higher system capacity than the UTRA SHO. This is due to lower numbers of NB required to serve a single UE, which is shown in Figure 5.11.

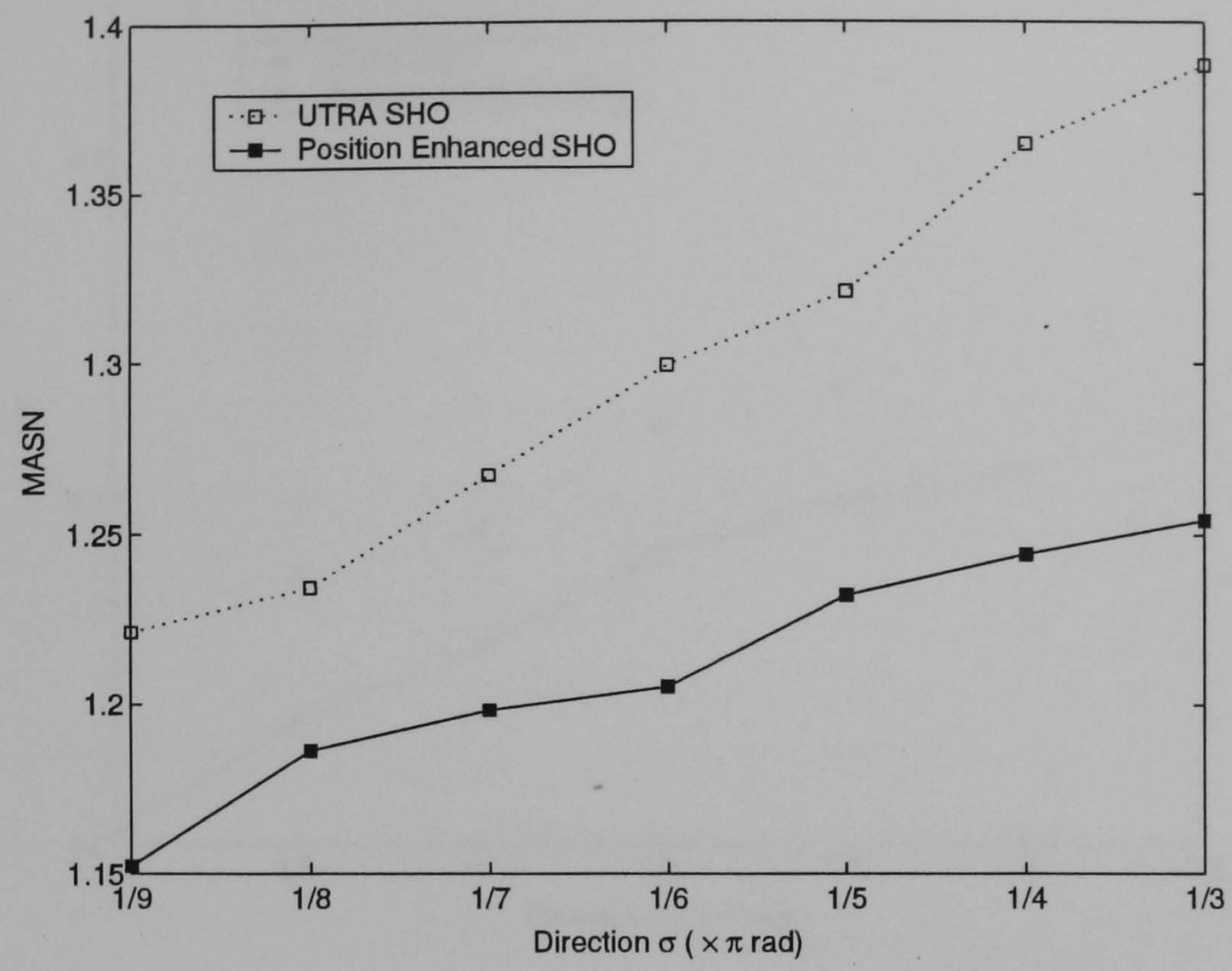

Figure 5.11: MASN versus the UE direction σ, (T_{trig}=10 samples and σ_{sha}=10dB)

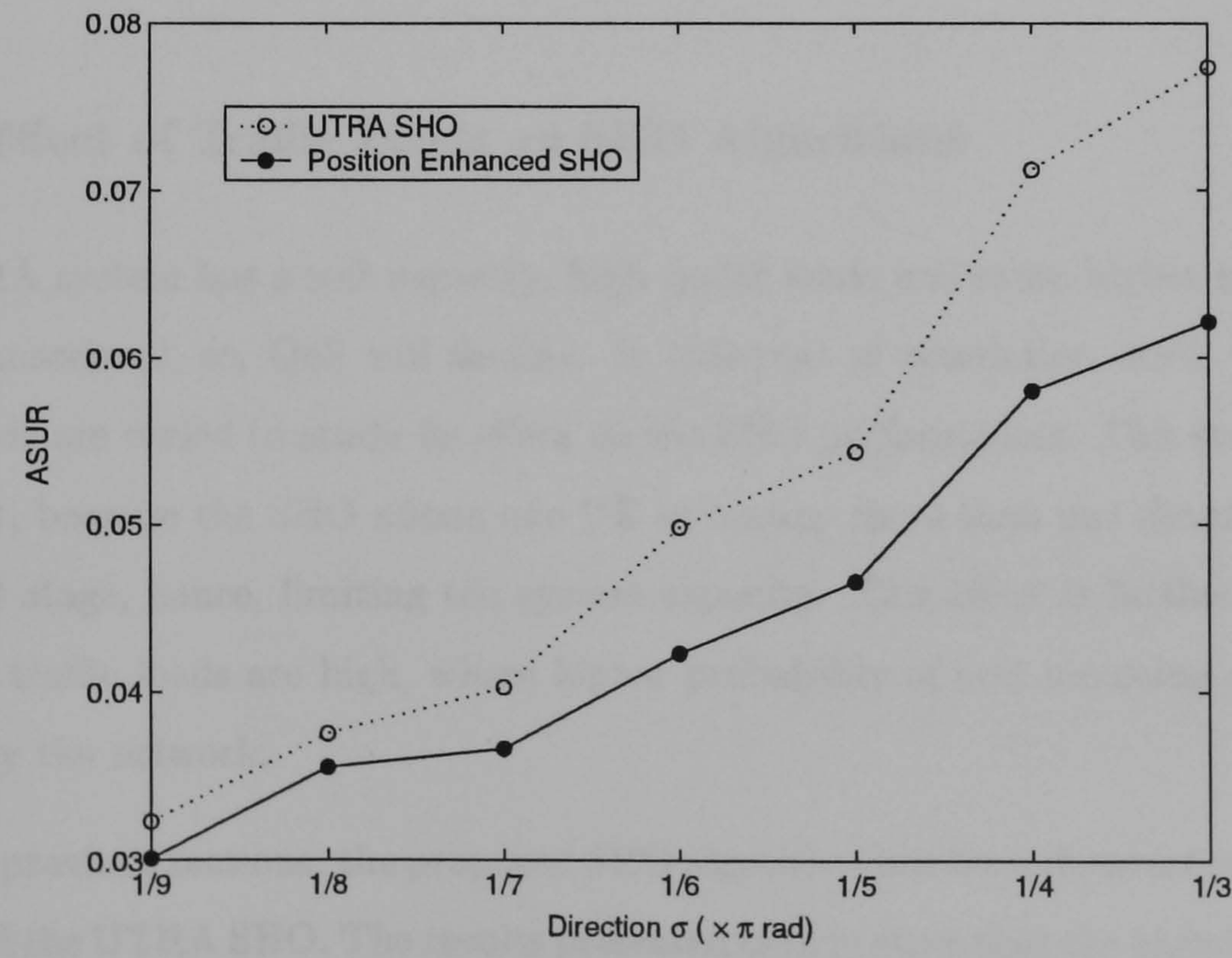

Figure 5.12: ASUR versus the versus the UE direction σ, (T_{trig}=10 samples and σ_{sha}=10dB)

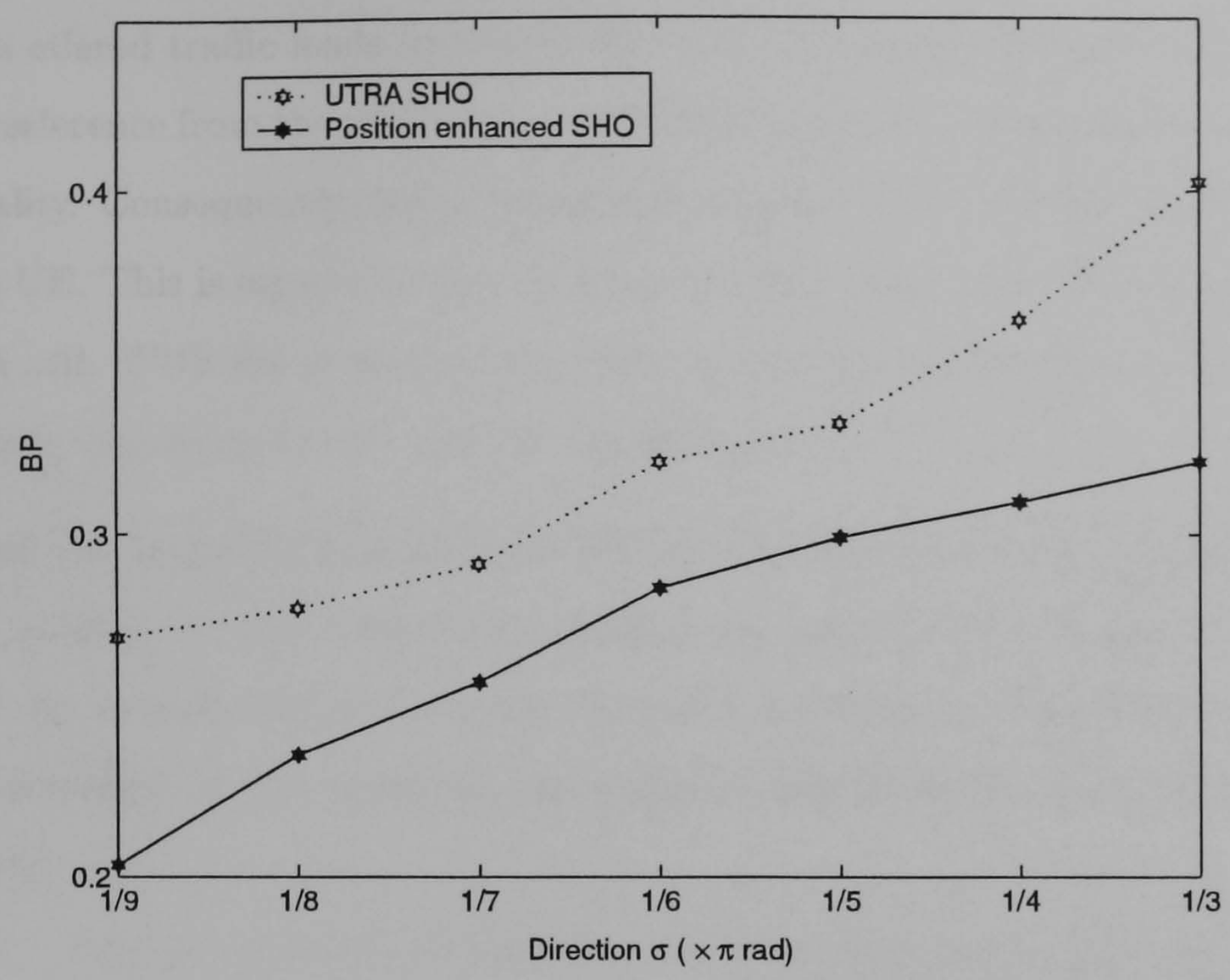

Figure 5.13: BP versus the versus the UE direction σ, ($T_{trig=10}$ samples and σ_{sha} = 10dB)

5.4.4 Effect of Traffic Loads on SHO Algorithms

The CDMA system has a soft capacity; high traffic loads will cause higher interference to the transceivers, so, QoS will decline. In this part of simulation work, the offered traffic loads are varied to study its effect on the SHO performances. This study is very important, because the SHO allows one UE to occupy more than one channel when it is in SHO stage, hence, limiting the system capacity. This effect is further magnified when the traffic loads are high, where higher probability of new incoming call will be blocked by the network.

From the previous sections, the proposed SHO algorithm has been demonstrated to outperformed the UTRA SHO. The results presented clearly show that the algorithm is able to achieve lower MASN and BP, and these are further proven in this part of simulation work. The offered traffic loads are varied from 10 Erlangs/cell to 50 Erlangs/cell, while keeping the σ_{sha}, direction σ, and UE velocity constant. Figures 5.14 and 5.15 show

that when offered traffic loads increases, the SHO indicators increased. This is due to higher interference from the additional traffic channels, and so, deteriorates the received signal quality. Consequently, higher transmission power or extras NBs may be required to serve a UE. This is especially true for circumstances where the UE is residing at the rim of the cell. With the proposed algorithm, handovers are executed at the optimum time. That's why lower MASN and BP are achieved.

Apart from the increased of MASN and BP, the OP also increased. As stated earlier, when the numbers of traffic channels increased, the interference power to each UE also increased. As a result, Figure 5.16 plots that with increases in offered traffic loads, the OP also increased. In this situation, the proposed algorithm has a lesser OP than the UTRA SHO.

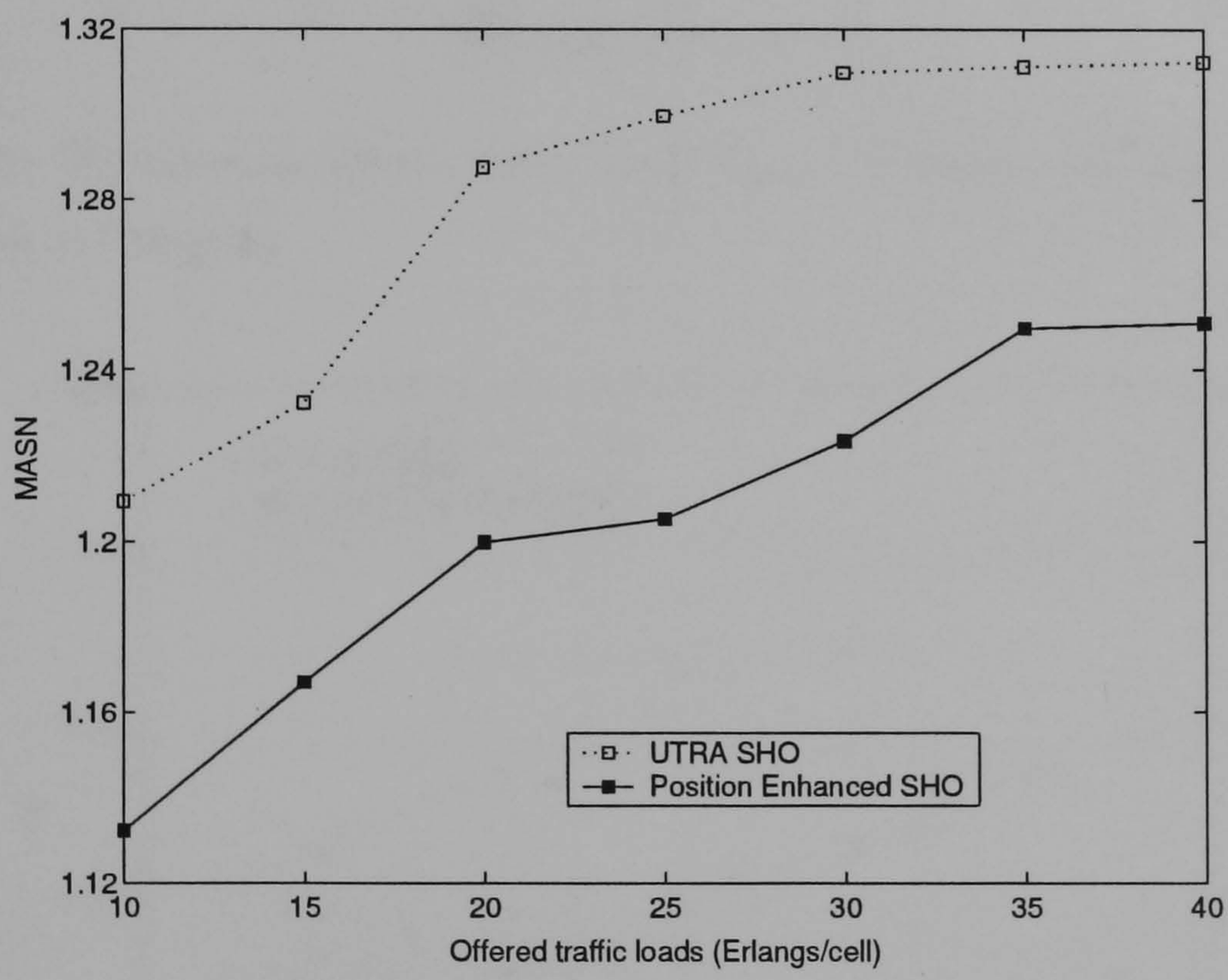

Figure 5.14: MASN versus the offered traffic loads, (T_{trig}=10 samples and σ_{sha}=10dB and UE velocity is 120km/h)

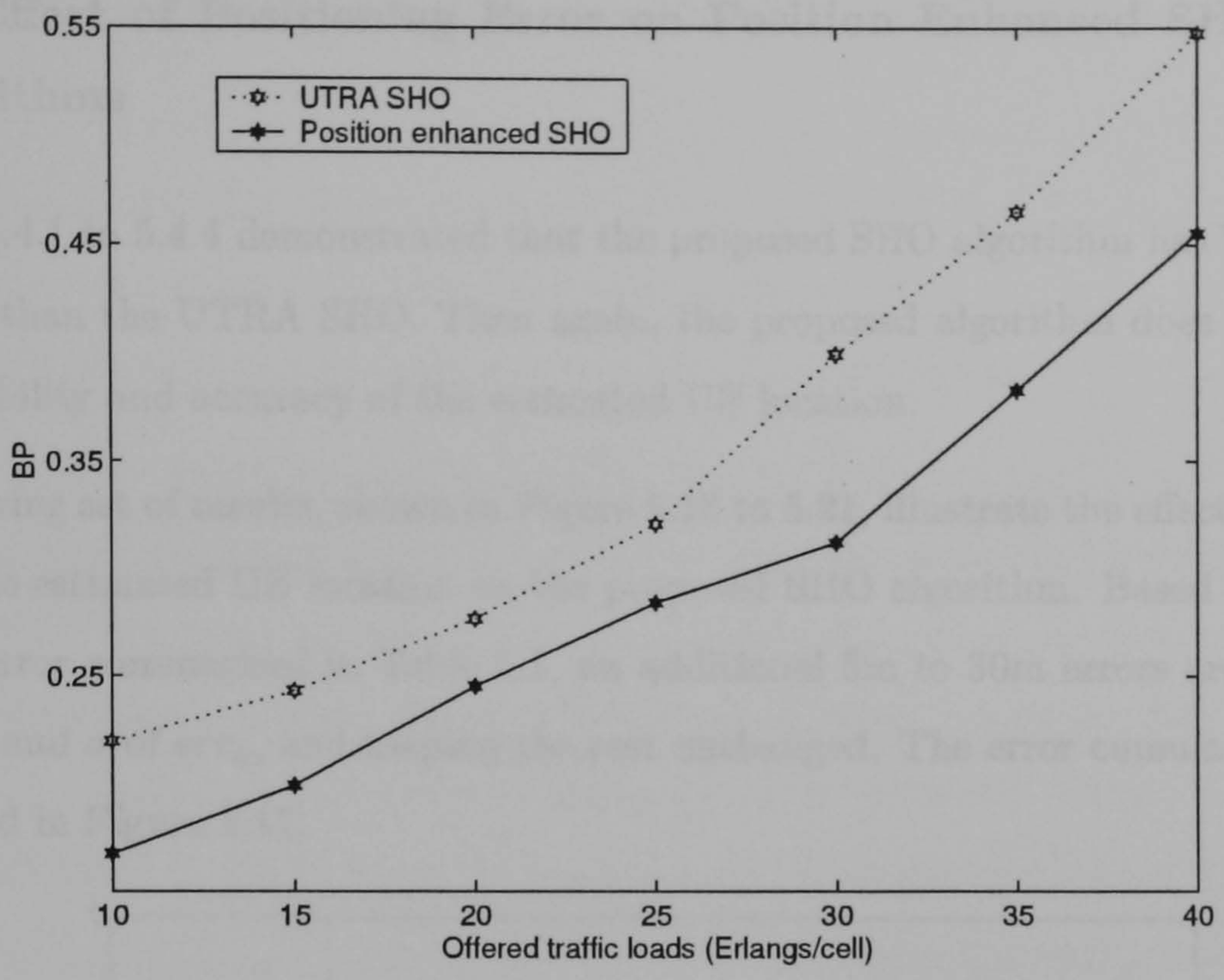

Figure 5.15: BP versus the offered traffic loads, (T_{trig}=10 samples and σ_{sha}=10dB and UE velocity is 120km/h)

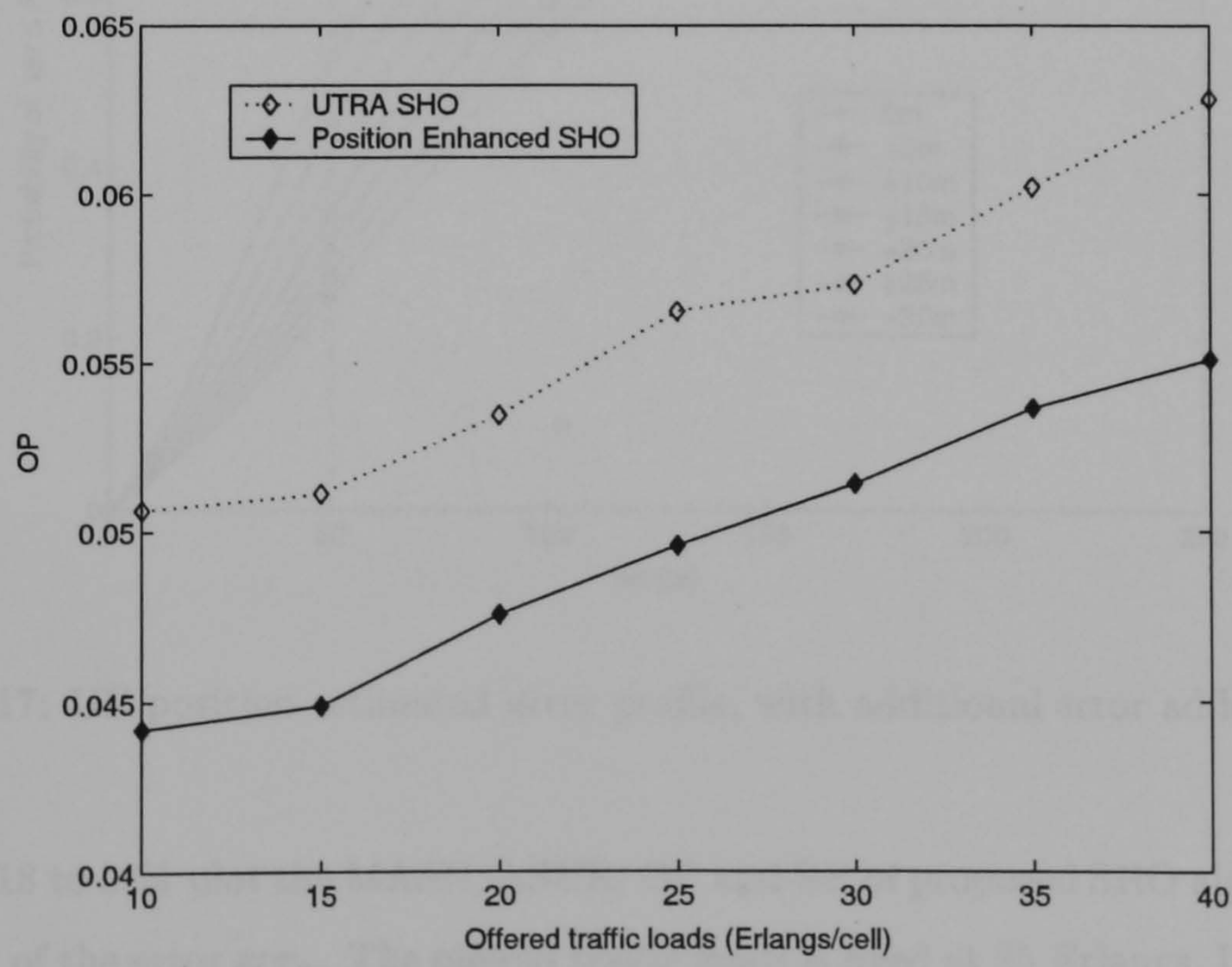

Figure 5.16: OP versus the offered traffic loads, (T_{trig}=10 samples and σ_{sha}=10dB and UE velocity is 120km/h)

5.4.5 Effect of Positioning Error on Position Enhanced SHO Algorithms

Sections 5.4.1 to 5.4.4 demonstrated that the proposed SHO algorithm has better performance than the UTRA SHO. Then again, the proposed algorithm does depend on the availability and accuracy of the estimated UE location.

The following set of results, shown in Figure 5.18 to 5.21, illustrate the effect of inaccuracy in the estimated UE location on the proposed SHO algorithm. Based on the UE position error summarised in Table 5.1, an additional 5m to 30m errors are added to the mean and σ of err_a, and keeping the rest unchanged. The error cumulative curves are plotted in Figure 5.17.

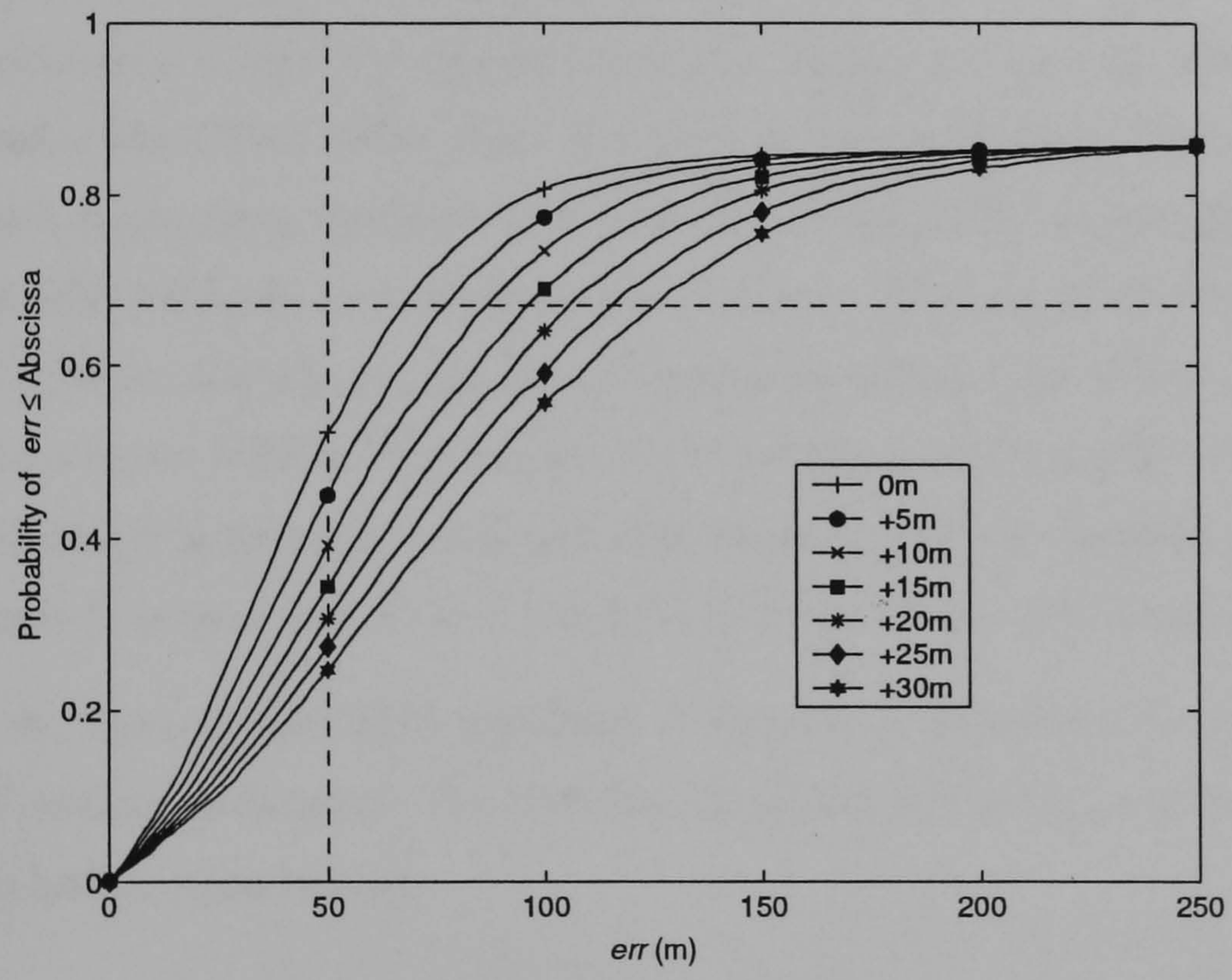

Figure 5.17: UE position estimated error profile, with additional error added to err_a

Figures 5.18 to 5.21 plot the MASN, ASUR, OP and BP of proposed SHO algorithm, as a function of the error err_a. The offered traffic loads is fixed at 25 Erlangs, UE velocity is 120km/h, σ_{sha} is 10dB, and T_{trig} is 5 seconds, 10 samples. In order to apprehend the effect of positioning accuracy on the SHO performance for each case of the simulation, an additional of 5m error is added to err_a. The err_a has a normal distribution, with

mean varied from 25m to 70m and σ varied from 30m to 75m, respectively.

When the UE position is poorly determined, UE that is near its serving NB may be apprehended as UE that is distance away or approaching UE may also be treated as residing from its serving NB. Then, handover is carried out when it is supposed to be opposed. On the other hand, handover is rejected when it is expected to be executed.

Referring to the results plotted in Figures 5.18 to 5.21, the performance starts to deteriorate when additional error is added to each position estimate. Figure 5.18 depicts that the MASN is actually higher than the UTRA SHO when an additional of 23m error is added to err_a. When UE position is inaccurately estimated, the $Hyst_d$ and $Hyst_\Theta$ will not adjust the hysteresis margins correctly. Instead of helping in handover, it causes problem in SHO and keeps unnecessary NBs in the ActS. Figure 5.21 shows that with increased MASN, the BP also increased. The system capacity actually starts to drop below the UTRA SHO when 15m error is added to err_a. Figure 5.19 also conveys that unnecessary handovers are executed. The handover probability is higher the UTRA SHO when the error of 19m is added to err_a. To make things worst, the OP depicted in Figure 5.20 shows that the call outage is greater than UTRA SHO, even when it has a higher MASN. This may be due to adding of additional NBs to the ActS, even when the UE is having a strong link with its serving NB. In the other case, UE is not handover to another NB when it is critical to do so. Hence, call outage may occur.

To conclude, the proposed SHO algorithm is very much dependent on the accuracy of the UE position estimated. The proposed algorithm will fail to perform when UE position is badly approximated.

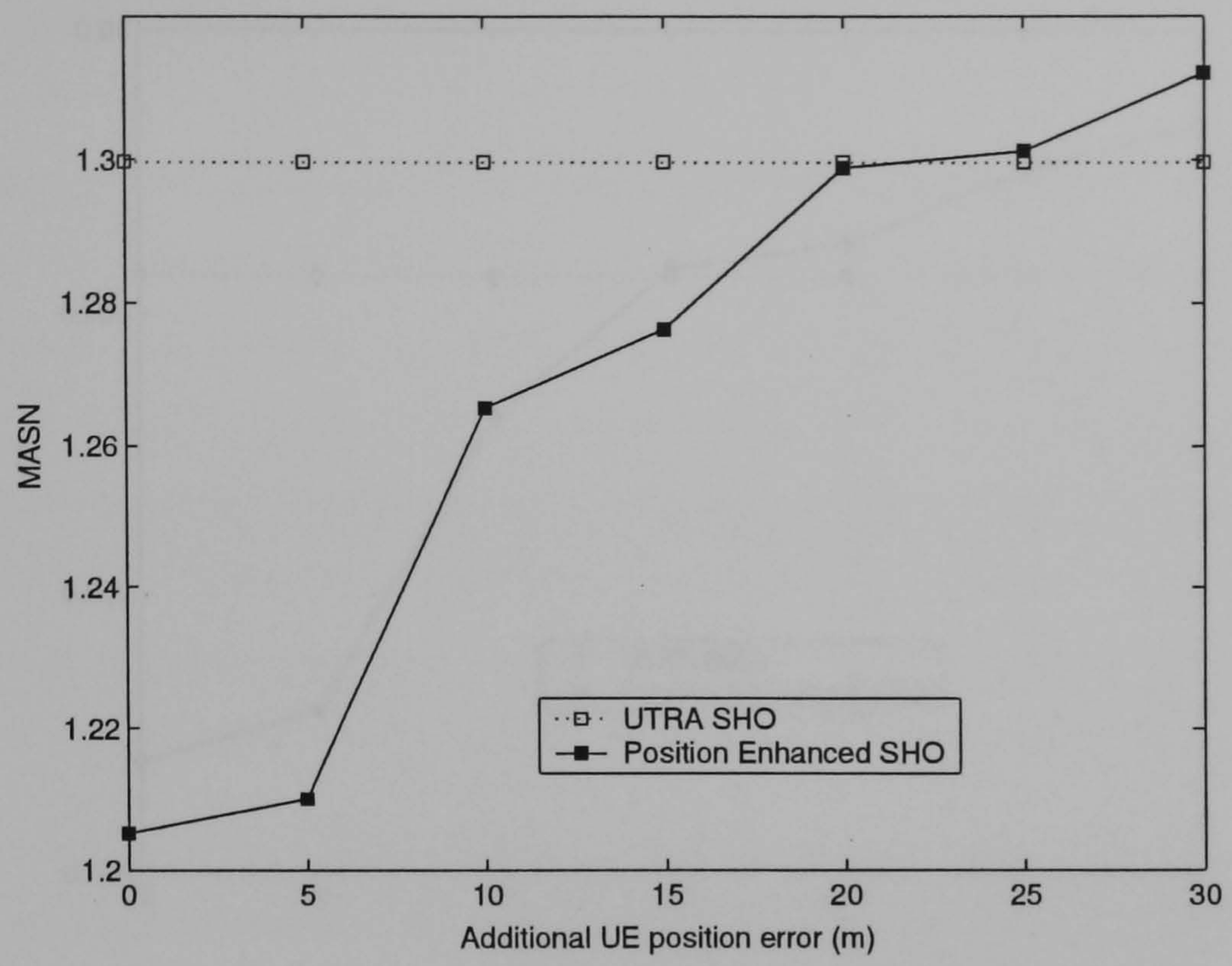

Figure 5.18: MASN versus the positioning error, (T_{trig}=10 samples and σ_{sha}=10dB and UE velocity is 120km/h)

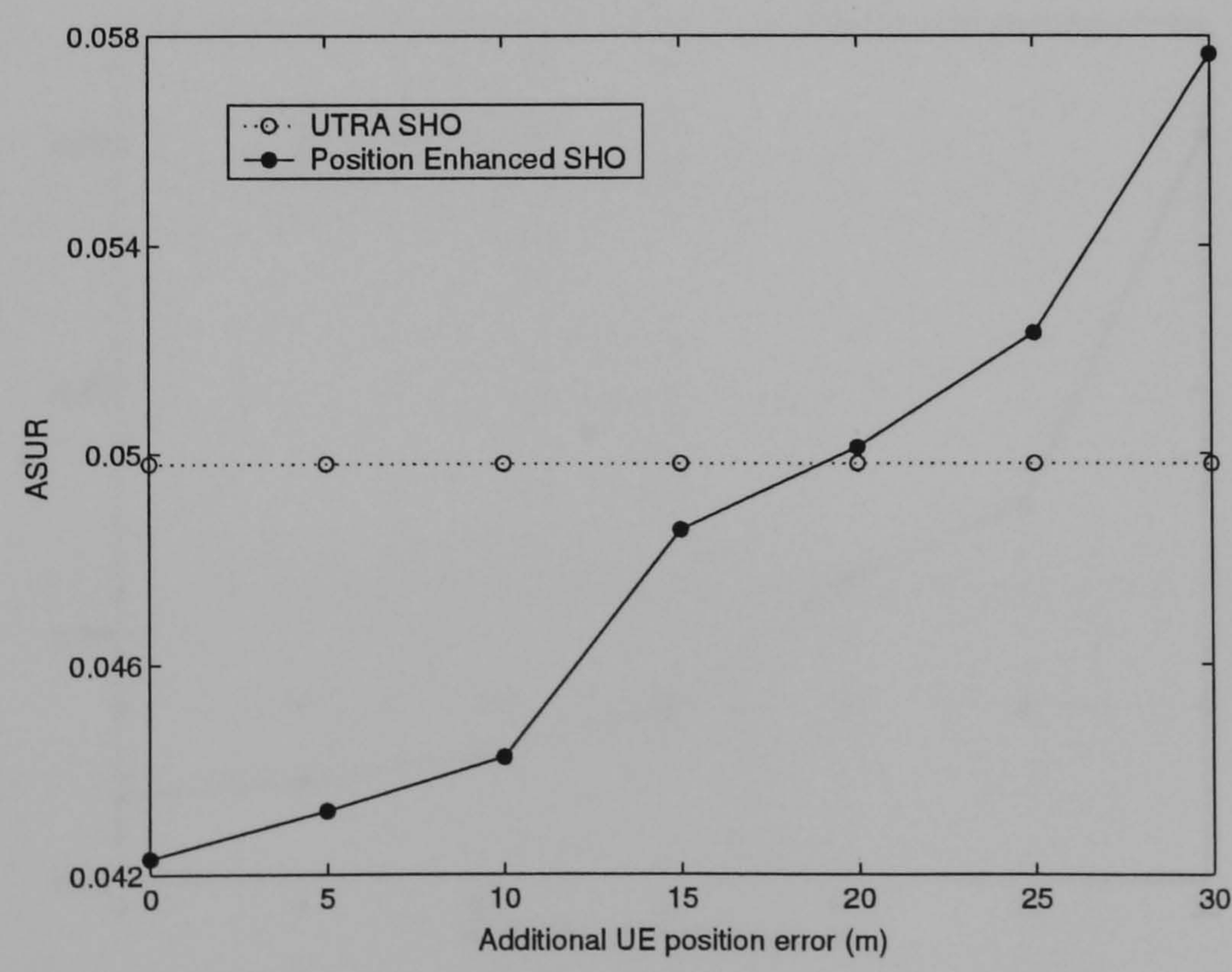

Figure 5.19: ASUR versus the positioning error, (T_{trig}=10 samples and σ_{sha}=10dB and UE velocity is 120km/h)

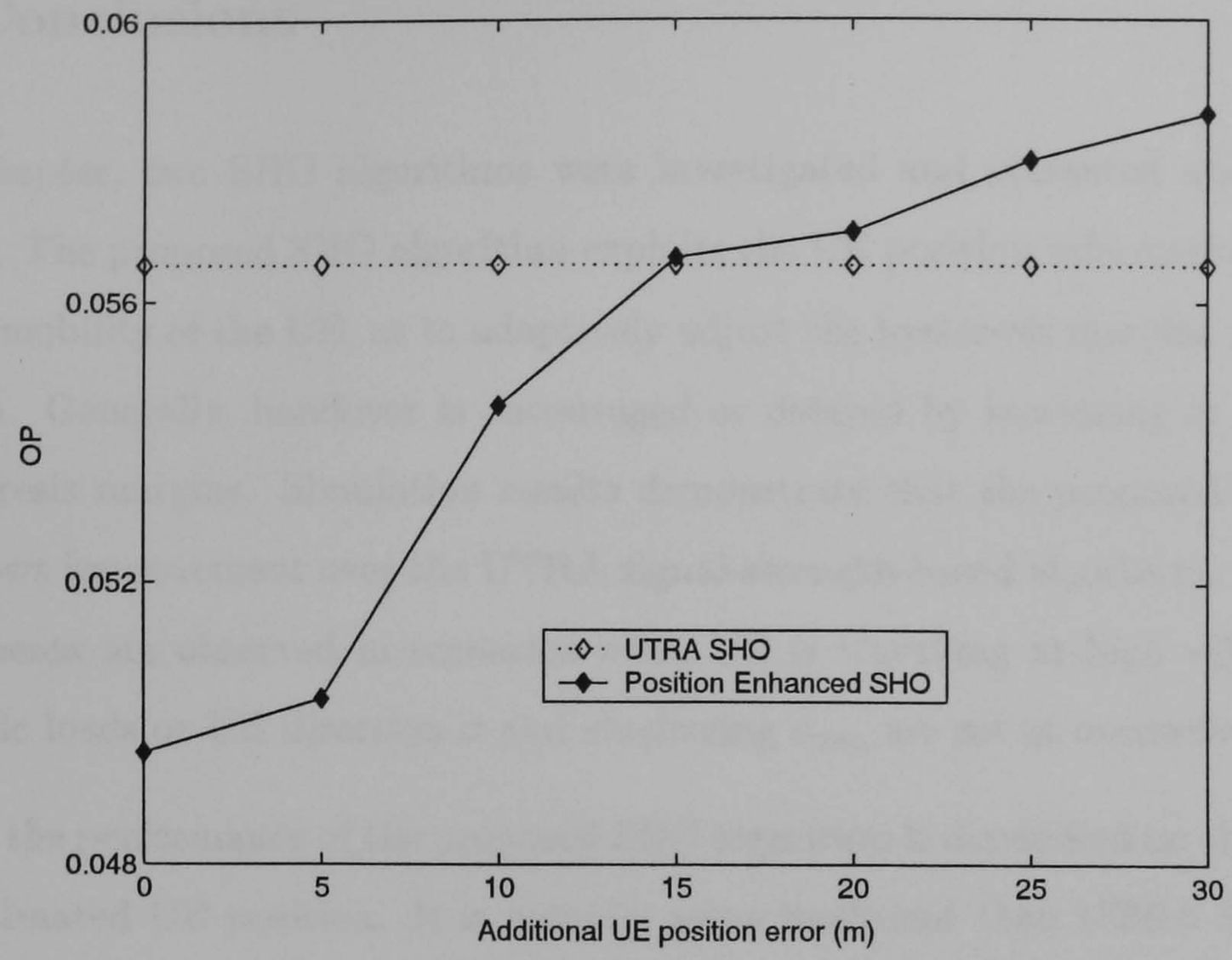

Figure 5.20: OP versus the positioning error, (T_{trig}=10 samples and σ_{sha}=10dB and UE velocity is 120km/h)

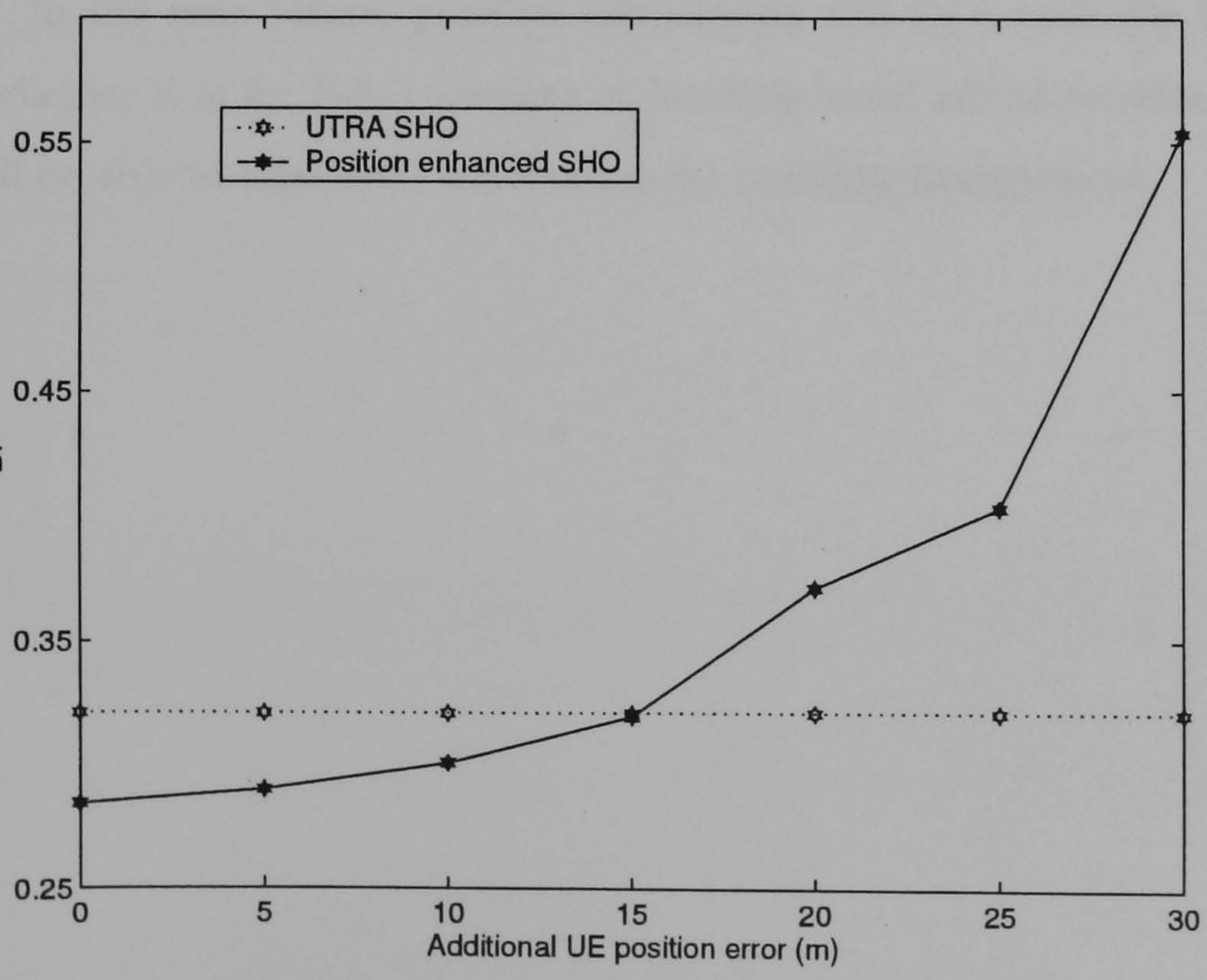

Figure 5.21: BP versus the positioning error, (T_{trig}=10 samples and σ_{sha}=10dB and UE velocity is 120km/h)

5.5 Conclusions

In this chapter, two SHO algorithms were investigated and presented under several scenarios. The proposed SHO algorithm exploits the UE position information to determine the mobility of the UE, as to adaptively adjust the hysteresis margins of the SHO algorithm. Generally, handover is encouraged or delayed by increasing or decreasing the hysteresis margins. Simulation results demonstrate that the proposed SHO algorithm shows improvement over the UTRA signal-strength-based algorithm. Significant improvements are observed in scenarios when UE is travelling at high velocity, high offer traffic loads or UE direction σ and shadowing σ_{sha} are set at excessive values.

However, the performance of the proposed SHO algorithm is dependent on the accuracy of the estimated UE position. It is actually more inefficient than UTRA SHO, when additional error of 20m is added to err_a. Nevertheless, it is envision that the LCS inaccuracy will be less than the errors introduced.

Finally, it should be noted that the proposed SHO algorithm is straight forward to implement. In the near future, position information will be a necessity to all UEs, regardless whether it is for E-911 services or location-based added services. Likewise, the LCS will be able to offer vital information for mobility management.

Chapter 6

Position Enhanced Relaying in the Heterogeneous Networks

6.1 Introduction

In the previous chapter, the UE spatial information is used to assist in handover, and the simulation results show significant improvement over the UTRA SHO. In this chapter, the UE position estimate will be used for mobility management in a hybrid *ad hoc* cellular system. The relaying concept is first introduced in Chapter 3, where the originating UE who is experiencing weak linkage with its serving NB would use nearby UE(s) to relay its data packet. Then again, unlike the fixed cellular system, relay UE would move out of the relaying network. Hence, link breakage would occur.

To make matter worst, the relay UE may not be willing to relay for the originating UE or battery failure during relaying process. For these reasons, it is essential to improve the path selection algorithm, to ensure that the most reliable candidate UE is used for relaying.

In this chapter, we put forward to use the UE spatial information to assist in path selection. The proposed algorithm will be investigated and compared with two other relaying algorithms that use only the received signal $\frac{E_b}{N_o}$ or UE spatial information for relaying decision-making. In addition, the conventional cellular network will be used

as a benchmark for the relaying network.

6.2 Relaying in Integrated *Ad Hoc* Cellular Network

As discussed in section 3.3, when it comes to coverage or capacity enhancement solution in a cellular network, relaying is one of the possible solutions to be considered. Since this form of relaying has not been implemented in the cellular networks before, significant research and understanding is expected before it can be fully implemented.

Following are some of the benefits that could be expected in the relaying cellular network

- Increased coverage
- Decreased peak and average power consumption
- Decreased Deployment period
- Increased spectral efficiency
- Increased node throughput (particular for those located near the edge of the cell)
- Decreased infrastructure requirement

This is especially true in a dense urban built up area, where the UE may experience NLOS link with the NB. When a UE turns into another street, the high-rise building blocks the sight between the UE and the serving NB, commonly known as the 'corner effect'. Under the NLOS condition, the strength of the received signal would drop, causing significant link quality degradation between the UE and serving NB. As a result, measures have to be taken to mitigate the problem in order to ensure a reliable service is delivered. Consider the scenario illustrated in Figure 6.1

The UE_1 is connected to NB_1 and makes a 90° turn into another street. The dashed arrow indicates the movement of UE_1. When this happens, the buildings along the streets will block the direct sight between the UE and its serving NB. If UE_1 is not handover to NB_2 before signal quality drops below the required $\frac{E_b}{N_o}$ threshold, call drop possibly will occur. An alternative solution is to use nearby UE such as UE_2 as a relayer to relay its data packets to NB_1 before it can be successfully handovered to NB_2.

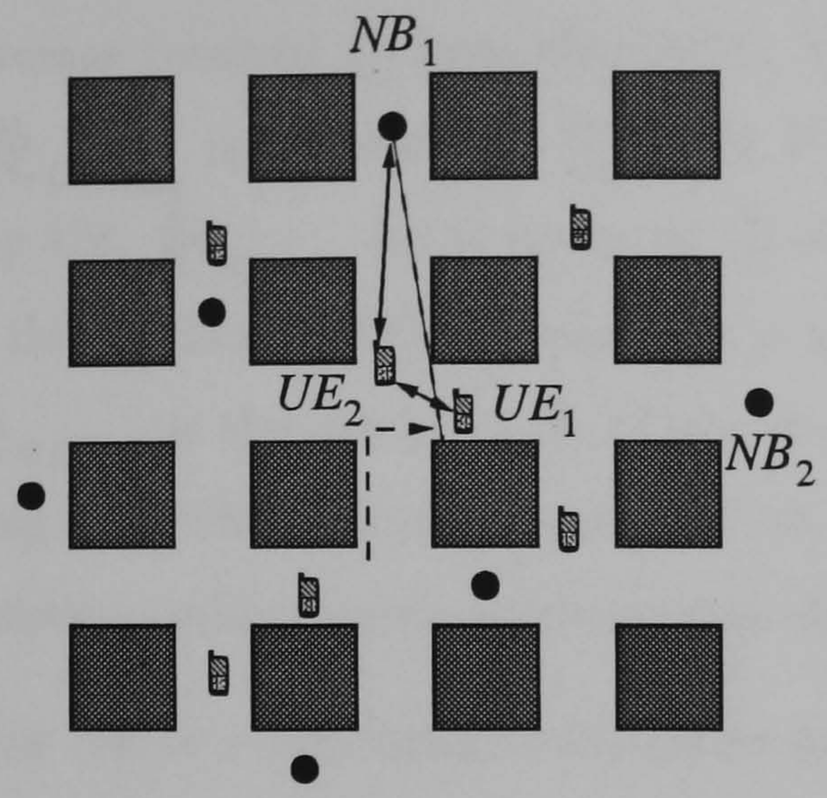

Figure 6.1: Relaying of data packets in a Manhattan type environment

The challenge now is to select the most reliable candidate UE for relaying and to handover between the UE-to-UE, UE-to-NB and NB-to-NB. The following sections will further explain each relaying and handover algorithms, as well the simulation work that was carried out to validate the proposed relaying algorithm.

6.3 Handover between the UE and NB in the Relaying Cellular Network

In this section, the handover between the UEs and NBs will be addressed. In section 3.3.1, it is already classified under three different types of handover for the relaying network. They are the handover between the originating UE to relay UE, relay UE to NB, and inter-relay UE handover.

A handover from the serving NB to a relay UE occurs if the following conditions are met

$$\begin{cases} \frac{E_b}{N_o}_{NB_{serv}} < \frac{E_b}{N_o}_{th} & \\ \frac{E_c}{N_o}_{UE_{relay}} > Th_{NB-UE}(= \frac{E_c}{N_o}_{NB_{serv}} + Hyst_{NB-UE}) & ; Handover = 1 \\ \frac{E_b}{N_o}_{NB_{neig}} < \frac{E_b}{N_o}_{th} & \\ otherwise & ; Handover = 0 \end{cases} \tag{6.1}$$

where $\frac{E_b}{N_o}_{NB_{serv}}$ is the average received $\frac{E_b}{N_o}$ from the serving NB, $\frac{E_b}{N_o}_{th}$ is the minimum $\frac{E_b}{N_o}$ threshold required, $\frac{E_c}{N_o}_{UE_{relay}}$ is the averaged $\frac{E_c}{N_o}$ of the PCPICH from the serving NB received by the relay UE, $\frac{E_c}{N_o}_{NB_{serv}}$ is the averaged $\frac{E_c}{N_o}$ of the PCPICH from the serving NB received by the originating UE, $Hyst_{NB-UE}$ is the hysteresis of the NB-to-UE handover and $\frac{E_b}{N_o}_{NB_{neig}}$ is the averaged $\frac{E_b}{N_o}$ of the strongest neighbouring NB received by the originating UE. When *Handover* equals to one, it means that handover is executed. While *Handover* equals to zero, it means that no handover is executed.

A handover from the relay UE to a NB occurs if the following conditions are met

$$\begin{cases} \frac{E_b}{N_o}_{NB_{serv}} > \frac{E_b}{N_o}_{th} \\ \frac{E_c}{N_o}_{NB_{serv}} > Th_{UE-NB}(= \frac{E_c}{N_o}_{UE_{curr}} + Hyst_{UE-NB}) & ; Handover = 1 \\ \frac{E_c}{N_o}_{NB_{serv}} > Th_{NB-NB}(= \frac{E_c}{N_o}_{NB_{neig}} + Hyst_{NB-NB}) \\ otherwise & ; Handover = 0 \end{cases} \tag{6.2}$$

where $\frac{E_c}{N_o}_{UE_{curr}}$ is the average $\frac{E_c}{N_o}$ of the PCPICH from the serving NB received by the current relay UE, $\frac{E_c}{N_o}_{NB_{neigh}}$ is the average $\frac{E_c}{N_o}$ of the neighbouring NB PCPICH received by the originating UE, and $Hyst_{UE-NB}$ is the hysteresis of the UE-to-NB handover.

Finally, an inter-relay UE handover occurs if the following conditions are met

$$\begin{cases} \frac{E_b}{N_o}_{NB_{serv}} < \frac{E_b}{N_o}_{th} \\ \frac{E_b}{N_o}_{UE_{curr}} < \frac{E_b}{N_o}_{th} \\ \frac{E_b}{N_o}_{NB_{neig}} < \frac{E_b}{N_o}_{th} & ; Handover = 1 \\ \frac{E_c}{N_o}_{UE_{new}} > Th_{UE-UE}(= \frac{E_c}{N_o}_{UE_{curr}} + Hyst_{UE-UE}) \\ otherwise & ; Handover = 0 \end{cases} \tag{6.3}$$

where $\frac{E_c}{N_o}_{UE_{new}}$ is the averaged $\frac{E_c}{N_o}$ PCPICH from the serving NB received by the new relay UE.

6.4 Path Selction for Relaying

Three path selection algorithms are considered in this work. They are the Signal Quality-based (SQRA), Position-based (PBRA), and Position Enhanced (PERA) relaying algorithms. The SQRA selects the path that has the strongest received signal, where the total $\frac{E_b}{N_o}$ between the originating UE, its serving NB, and relay UE is the highest. The PBRA only considered the spatial distances between the originating UE, its serving NB, and relay UE. The path with the shortest distance will be selected. Then again, due to fast fading and shadowing, signal may be heavily attenuated or interfered even when the transceivers are similar distance apart. That's why path selection based on geographical distance will never be the most advantageous solution. Then again, selection that is based on signal strength between the transceivers is also not sufficient to ensure the selected relay path is the most appropriate. The results presented in chapter 5 already established that handover algorithm that depend on signal quality will deteriorate when the wireless channel has high variation of shadowing loss or UE is having high mobility. Therefore, a signal quality and geographical distance based relaying algorithm (PERA) is proposed to enhance path selection.

6.4.1 Selection Based on Signal Quality, SQRA

Since the path-loss associated with each link varies from location to location, it would be desirable to have global signal quality information for different links in a given cell to have an efficient routing algorithm. Thus, for the following, let $\frac{E_b}{N_o}_{UE-UE_n}$ and $\frac{E_b}{N_o}_{NB-UE_n}$ be the $\frac{E_b}{N_o}$ of the originating UE with the candidate relay UE_n and the second hop candidate relay UE_n with the serving NB of originating UE. Then the selected route R_s, is determined as follows

$$R_s = \arg \max_{all n \in N} \left\{ \frac{E_b}{N_o}_{UE-UE_n} + \frac{E_b}{N_o}_{NB-UE_n} \right\} \tag{6.4}$$

where N is the total number of candidates UE that are within the transmitting range of originating UE and its serving NB.

6.4.2 Selection Based on Geographical Distance, PBRA

In the subsequent subsection, a two-hop relaying network based on the shortest relay hops is investigated. The first hop is the originating UE to the candidate relay UE_n and the second hop is the candidate relay UE_n to the serving NB of originating UE. Let d_{UE-UE_n} and d_{NB-UE_n} be the distances associated with the first and second hops, respectively, along the n^{th} route, $n \in N$. Then, the selected route R_s is determined as follows

$$R_s = \arg \min_{all n \in N} \{d_{UE-UE_n} + d_{NB-UE_n}\} \tag{6.5}$$

where d is obtained from the UE spatial information.

6.4.3 Selection based on signal quality and geographical distance, PERA

The position of the originating UE and candidate relay UE will determine the distances between the UEs and serving NB. The distance ratio between the UEs and serving NB will be summed, and is multiplied to the signal quality of originating UE with candidate relay UE and candidate relay UE with serving NB. The mathematical model is written as

$$R_s = \arg \max_{all n \in N} \left\{ \left(\frac{E_b}{N_{o\,UE-UE_n}} + \frac{E_b}{N_{o\,NB-UE_n}} \right) \left(\frac{d_{UE-NB}}{d_{UE-UE_n}} + \frac{d_{UE-NB}}{d_{NB-UE_n}} \right) \right\} \tag{6.6}$$

where d_{UE-NB} is the distance between the originating UE and its serving NB. This is different from PBRA, where the distances of the transceivers are used directly for path selection. Equation (6.6) promote the path selection when the distances between the NB, UE and UE_n are close to each other, otherwise the path is discouraged.

6.5 Simulation Model

It is envision that relaying would be more practical in an urban environment where the user population is dense. If a few sparse coverage holes existed, such that those located in these regions cannot get a good coverage from the NB, then there is a high probability that they will be relayed via those that have good communication with the NB. For this reason, for the simulation model that follows, the parameters are designed specifically towards those of an urban environment.

In this environment, the cell deployment model is of the Manhattan microcell type [35]. The area consists of 12 by 12 blocks with a total of 72 NBs, as depicted in Figure 6.1. The block size is 100m by 100m and the street width is 30m. The minimum distance between two street corners is 230m. The UE is uniformly distributed over the street area. In such a structure, the UE moves along streets and may turn at cross streets with a given probability. The UE's position is updated every 5m and velocity can be changed at each position update according to a given probability listed in Table 6.1.

Initial UE velocity	3km/h
UE minimum velocity	0km/h
UE maximum velocity	36km/h
UE velocity σ	0.3km/h
Probability to change speed at position update	0.2
Probability to turn at cross street	0.5
Shadowing σ_{sha}	10dB

Table 6.1: Manhattan simulation parameters

To evaluate the performance of the relaying cellular networks, a uniformly distributed 25 Erlangs per cell traffic loads is provided. The maximum transmitted powers of the PCPICH and traffic channels are set at 20dBm and 17dBm, respectively. The maximum transmitted power for UE-to-UE transmission is 14dBm. The thermal noise n is -118dBm and the orthogonality factor η is 0.68. The $\frac{E_b}{N_o}$ outage threshold for a speech service is set to 7dB. The simulation interval step is 500ms. Perfect power

control is assumed for the uplink and downlink channel. New call will be blocked if it causes any of the on going call to experience any outage. The relaying and non-relaying cellular network will be investigated and compared throughout the simulation work. The non-relaying cellular network will use the UTRA SHO algorithm presented in Chapter 5. Also, the SQRA, PBRA, and PERA will be studied and compared. The originating UE will initiate a relaying request when its $\frac{E_b}{N_o}_{th}$ is below 8dB. Additionally, the $Hyst_{NB-UE}$, $Hyst_{UE-NB}$, and $Hyst_{UE-UE}$ are fixed at 4dB.

A three-slope path-loss model is deployed [75] for the UE and NB transmission. The model is mathematically given by the following expressions

$$\begin{aligned} PL_{LOS_1} &= L_b + 20n_{LOS_1}\log\left(\frac{d}{R_b}\right) && dB \quad d \leq R_b \\ PL_{LOS_1} &= L_b + 40n_{LOS_2}\log\left(\frac{d}{R_b}\right) && dB \quad d > R_b \\ PL_{NLOS} &= PL_{LOS}(d_corner) + PL_{corner} + 10n_{NLOS}\log\left(\frac{d}{d_{corner}}\right) && dB \end{aligned} \tag{6.7}$$

$$\begin{aligned} R_b &= \frac{4h_b h_m}{\lambda} && m \\ L_b &= \left|20\log\left(\frac{\lambda^2}{8\pi h_{NB} h_{UE}}\right)\right| && dB \\ PL_{corner} &= -0.1w_S + 0.005d_{corner} + 20 && dB \\ n_{NLOS} &= -0.05w_s + 0.02d_{corner} + 4 && dB \end{aligned} \tag{6.8}$$

where d in meter is the distance from the transmitter to the receiver measured along the street path, h_{UE} is the height of the UE (2m), h_{NB} is the height of the NB (6m), λ is the wavelength (0.15m), d_{corner} is the distance from the transmitter to the corner (d_{corner}), PL_{corner} is the additional loss caused by the corner, w_s is 30m, and n_{LOS_1}, n_{LOS_2} are 2 and 4, respectively. The free space path-loss model is considered for UE-to-UE transmission. The UE-to-UE transmission has a lognormal shadowing of zero mean and σ of 4dB. Hence, there is no direct linkup between the UEs if the received signal quality falls below the $\frac{E_b}{N_o}$ threshold. It is also assumed that transmission between UE-to-NB and UE-to-UE has no interferences with each other.

The originating UE can only use idle UE as a relayer and relaying path will be broken if the relay UE becomes active. In this work, only a double hop will be considered. Therefore, the originating UE can only use one idle UE to relay its data to the serving NB. In addition, the relaying network considered only allows UE to be served by one NB at any time and handover decision between the NBs is made by the originating UE. The relay UE only acts as a relaying element, assuming that it is always willing to relay for other UE when it is in idle mode.

The UE positioning accuracy considered here is based on the work done by Berg [76]. UE positioning under the Manhattan microcell type environment was investigated and it showed that UE geo-locating under such environment is very accurate. For most of the time, UE is within the transmission range of 3 LOS NBs and more than 67% of the estimates are within the 50m error. Table 6.2 summarised the error profile of UE positioning that closely matched the results presented by Berg [76].

Hearability	Error err_a	Probability of position badly estimated	Error (Position badly estimated) err_b
100%	N[20, 30]m	0.05	U[0,500]m

Table 6.2: UE positioning parameters for Manhattan microcell type environment

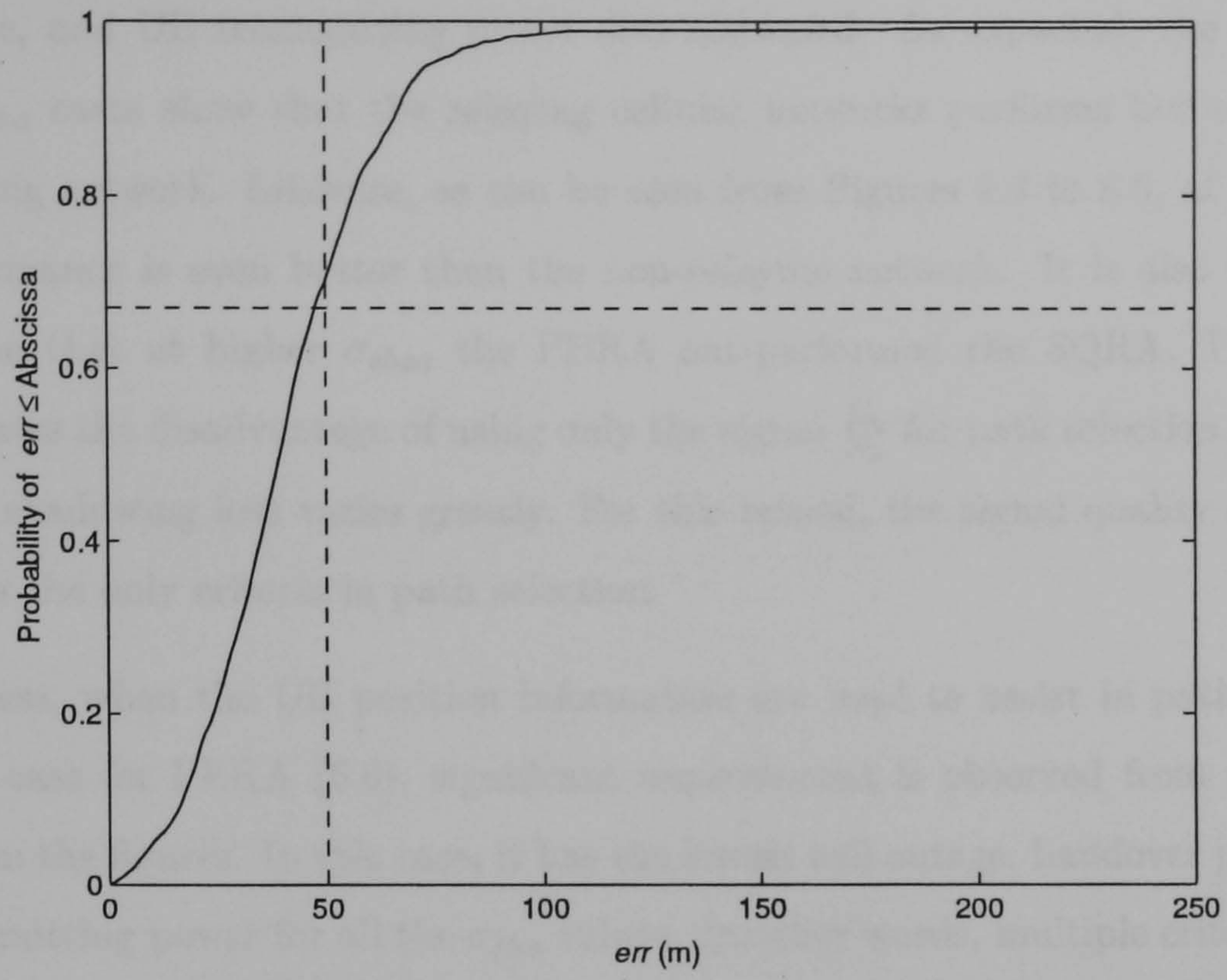

Figure 6.2: UE geo-locating error profile in Manhattan microcell type environment

6.6 Simulation Results and Discussion

6.6.1 Effect of Shadowing on Relaying Cellular Network

The relaying algorithms are tested for several shadowing σ conditions. It is assumed that UE is willing to relay for other UEs, given that it is idle and within the transmission range with the originating UE. Firstly, the shadowing σ_{sha} is chosen as 4dB, offered traffic load is 25 Erlangs per cell, and 250 numbers of UE per km^2. Three relaying algorithms, the SQRA, PBRA and PERA algorithms were tested and compared. The results are plotted in Figures 6.3 to 6.5. At low σ_{sha}, the relaying cellular network has shown significant improvement over the conventional cellular network. Figure 6.3 plots the relaying cellular networks having an averaged handover probability of 0.4, while the non-relaying cellular network has 0.5. Furthermore, Figure 6.4 shows the call outage dropped from 0.01 to 0.006, and Figure 6.5 reveals the averaged UE transmitting power is 4dB lower.

Then, the shadowing σ is increased to 16dB. In general, the handover probability,

call outage, and UE transmitting power also increased. As expected, the tests with all the σ_{sha} cases show that the relaying cellular networks performs better than the non-relaying network. Likewise, as can be seen from Figures 6.3 to 6.5, at high σ_{sha}, the performance is even better than the non-relaying network. It is also interesting to mention that at higher σ_{sha}, the PBRA out-performed the SQRA. This clearly demonstrates the disadvantage of using only the signal $\frac{E_b}{N_o}$ for path selection, especially when the shadowing loss varies greatly. For this reason, the signal quality should not be used as the only criteria in path selection.

Nevertheless, when the UE position information are used to assist in path selection, as in the case for PERA (6.6), significant improvement is observed from the results depicted in the figures. In this case, it has the lowest call outage, handover probability, and transmitting power for all the σ_{sha} values. In other words, multiple criteria should be used to aid in path selection and not based on only received signal strength or UE geographical location to decide the relaying path.

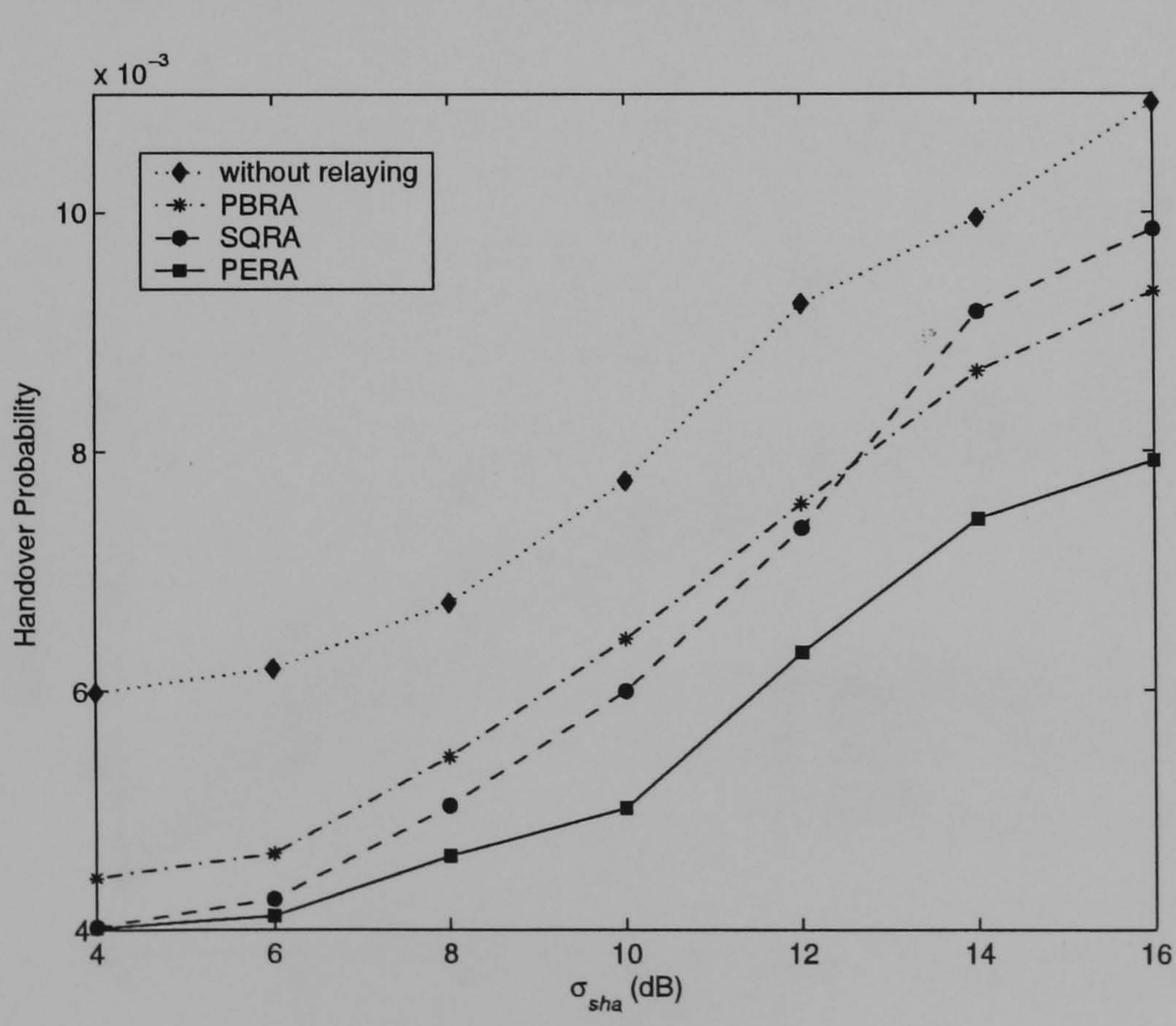

Figure 6.3: Handover probability versus the σ_{sha}, for relaying and non-relaying cellular network

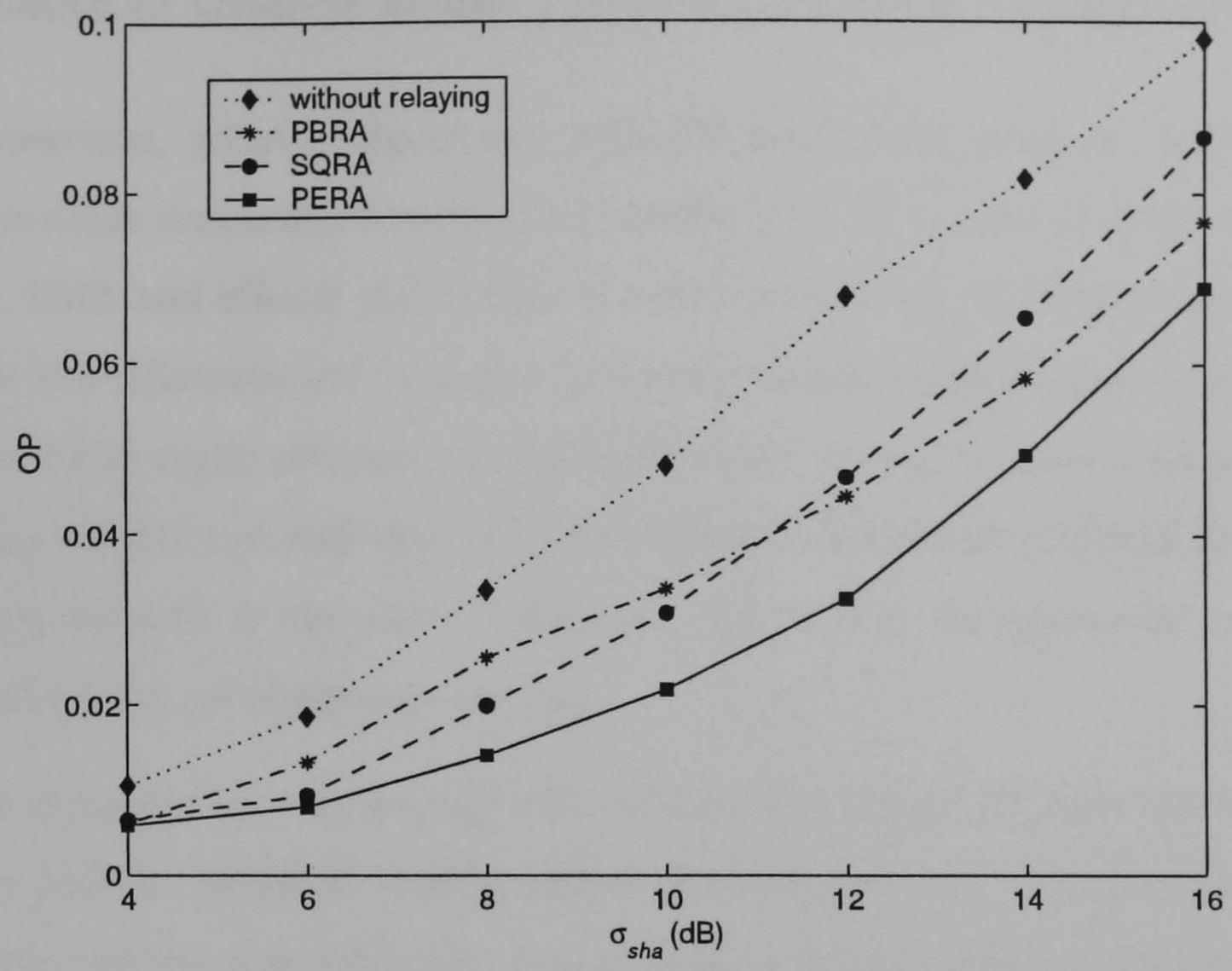

Figure 6.4: OP versus the σ_{sha}, for relaying and non-relaying cellular network

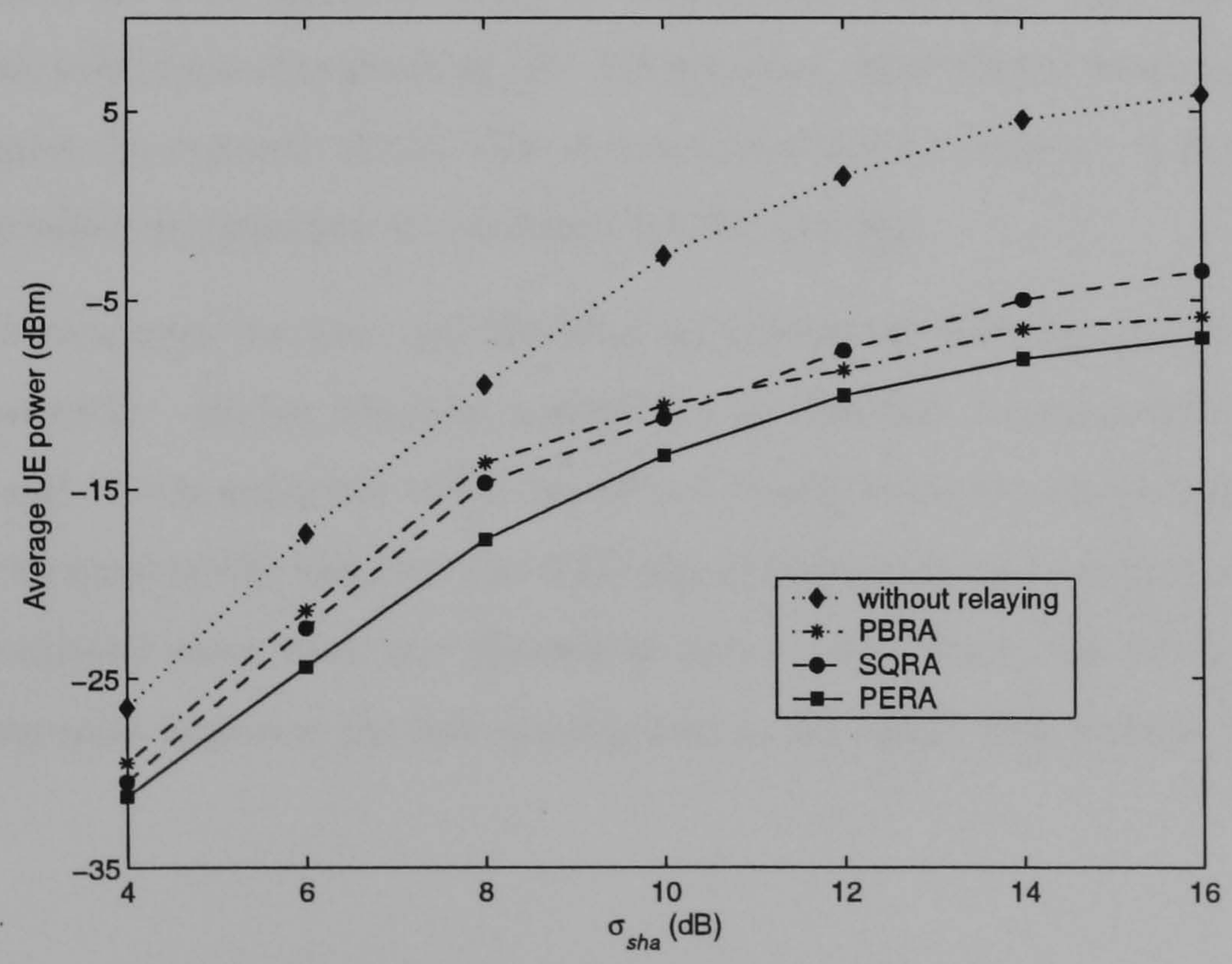

Figure 6.5: Average UE transmitting power versus the σ_{sha}, for relaying and non-relaying cellular network

6.6.2 Effect of Offered Traffic Loads on Relaying Cellular Network

In this subsection, relaying algorithms with different traffic loads are tested for efficiency. The same simulation condition for section 6.6.1 is considered, whereas the σ_{sha} is fixed at 10dB and offered traffic load is varied from 10 to 40 Erlangs per cell. Figures 6.6 to 6.8 illustrate and compare the performance of relaying and non-relaying cellular networks under different offered traffic load. As can be seen from the figures, the relaying cellular network that used the PERA has the best performance, and the non-relaying network is the worst. Moreover, this is fully demonstrated in test with offered traffic loads of 40 Erlangs per cell.

Figure 6.8 conveys that the average UE transmitting power for non-relaying cellular network is 10dBm, which is 15dBm higher than the relaying network that used the PERA. This justifies that relaying concept achieves better power efficiency. Also, the results plotted in the figures also exhibit that as the offered traffic loads raises, the performance of the relaying algorithms declines. This is perhaps due to the idle UEs that are used for relaying would have become active, causing sudden link breakage between the relaying and originating UE. What's more, high offered traffic loads would also minimise the numbers of idle UEs that are available for relaying, making it more difficult to select an appropriate candidate UE for relaying.

Figure 6.9 compares the new call blocking probability of relaying and non-relaying cellular networks. Higher blocking probability is observed for non-relaying cellular networks and this is enhanced when the offered traffic loads are set at higher values. This may be owed to the fact that the SHO algorithm used in the non-relaying cellular network occupied more than one channel to serve a UE. Thus, the relaying cellular network not only improves the link quality, and at the same time extends the system capacity.

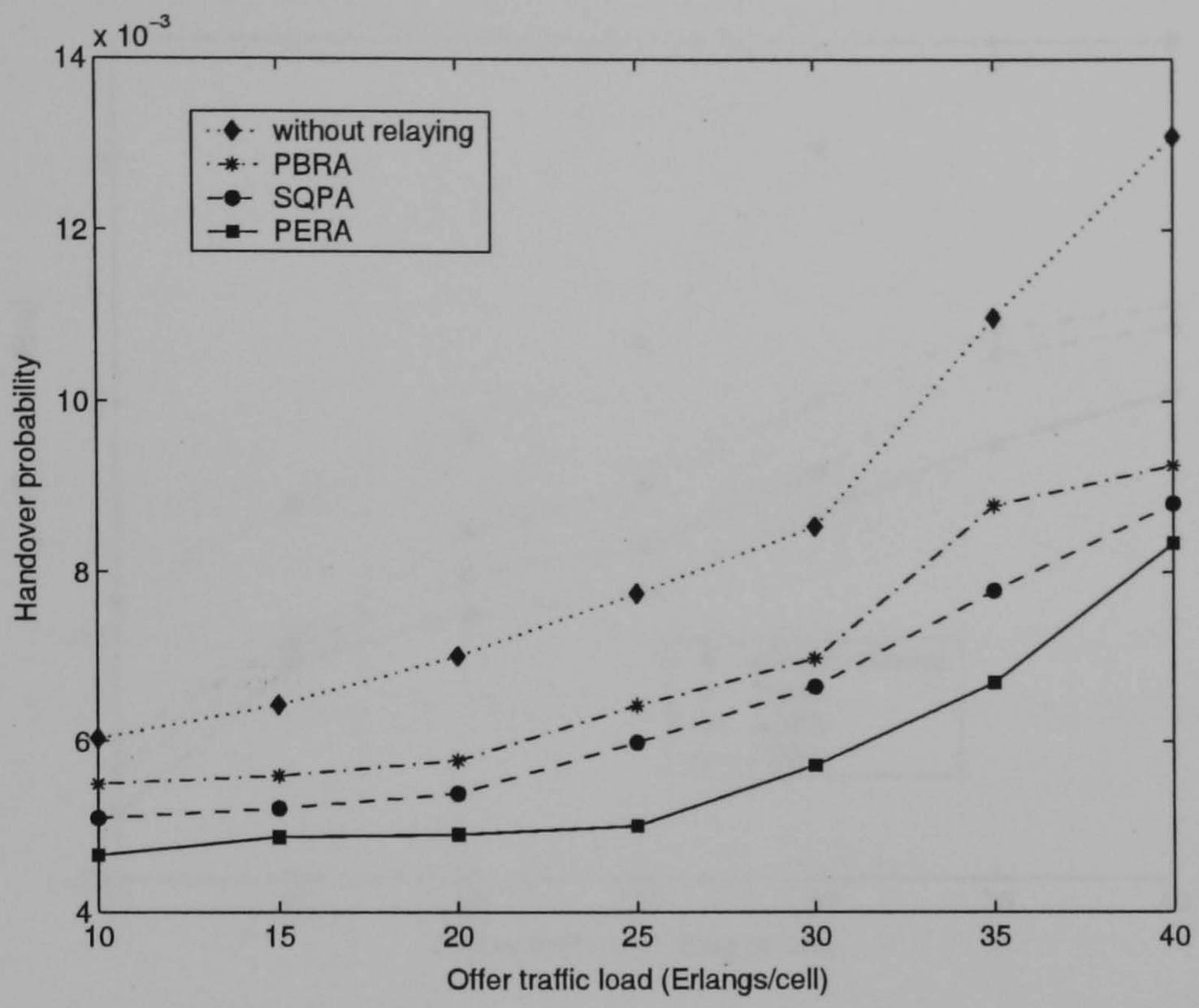

Figure 6.6: Comparison of handover probability for different cellular network

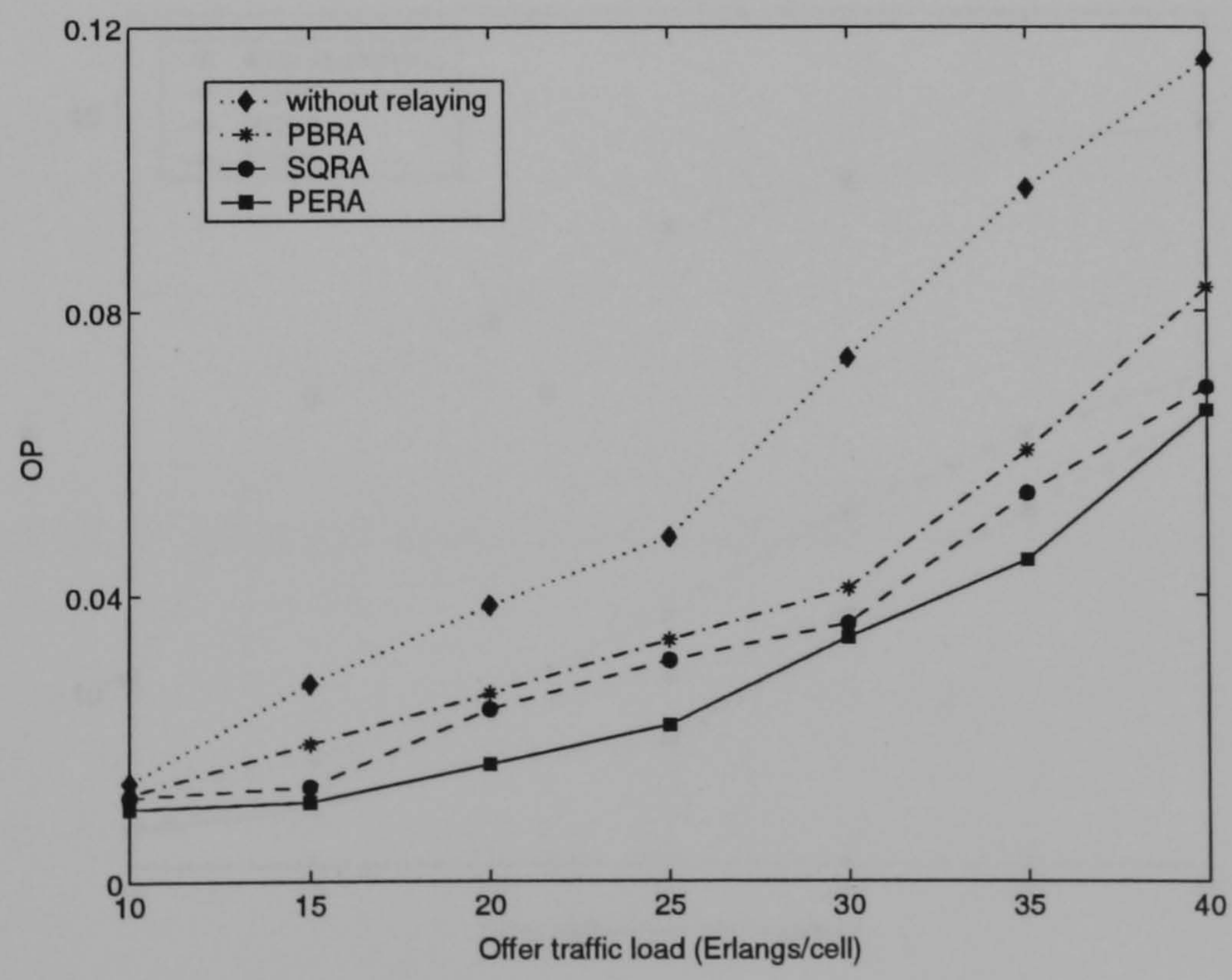

Figure 6.7: Comparison of OP for different cellular network

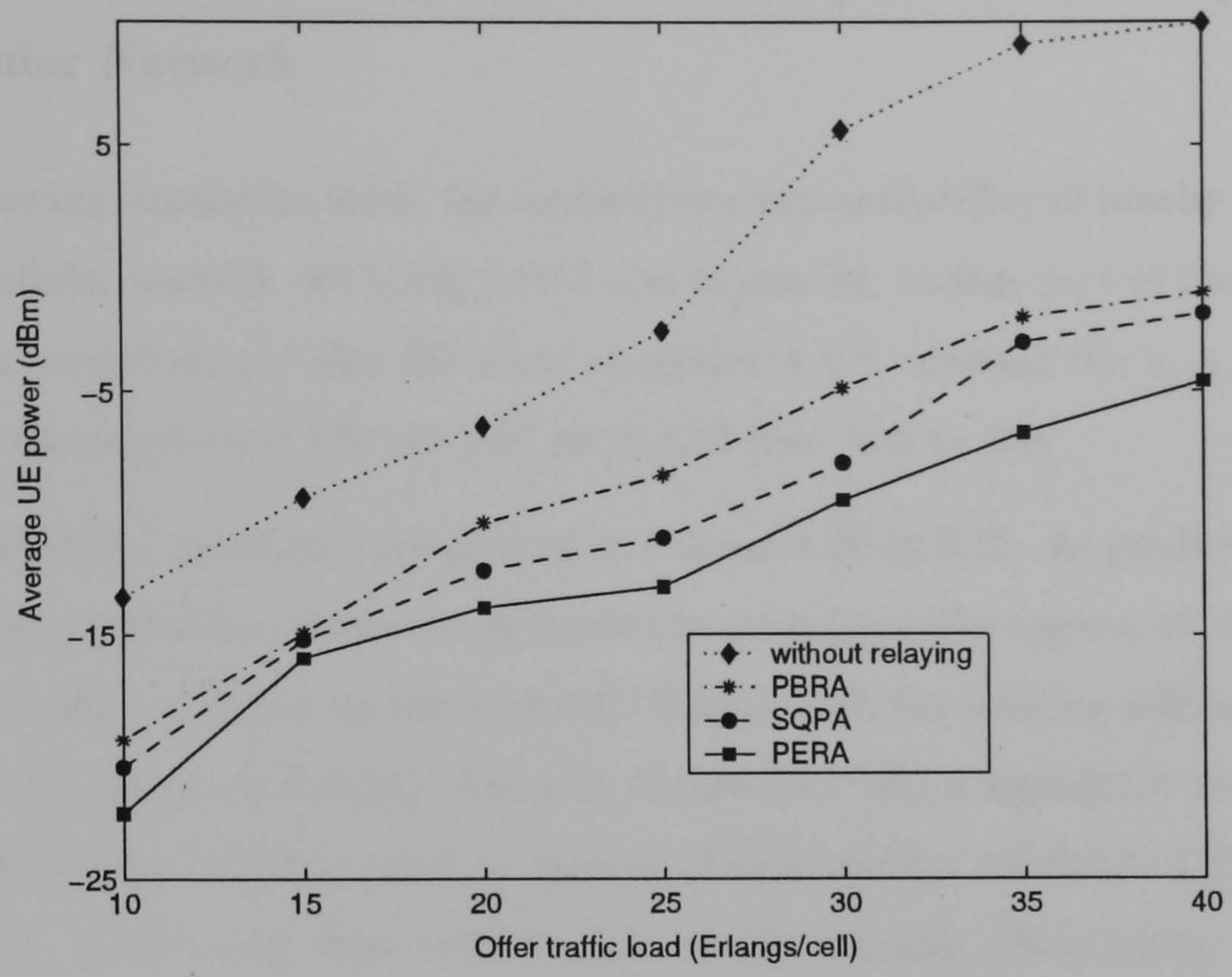

Figure 6.8: Comparison of average UE transmitting power for different cellular network

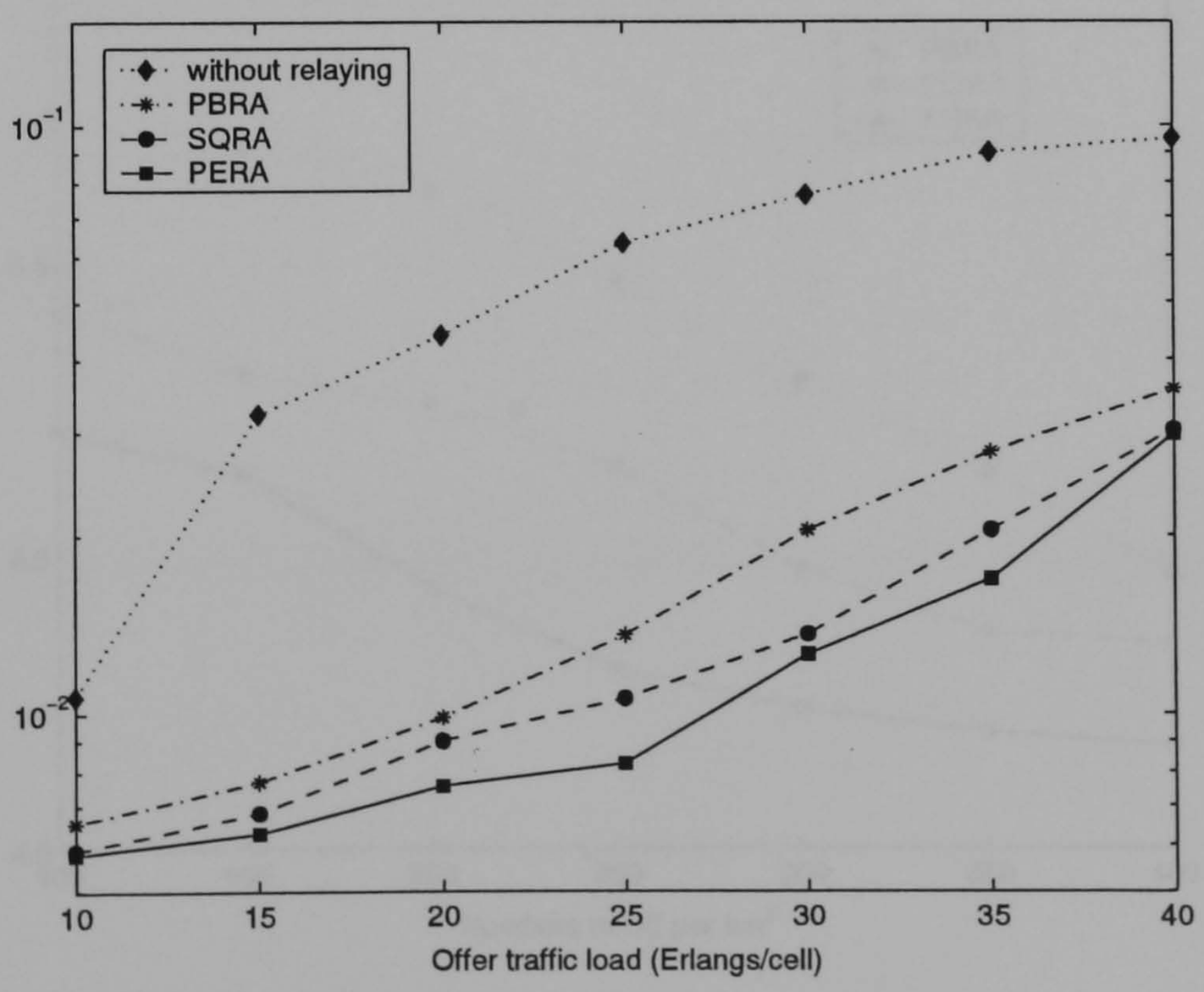

Figure 6.9: Comparison of BP for different cellular network

6.6.3 Effect of Availability and Connectivity of UEs on Relaying Cellular Network

In the following simulation work, the connectivity and availability of nearby UE on the relaying cellular network are being tested and evaluated. In this part of the work, the simulation conditions are also the same as section 6.6.1, whereas the σ_{sha} is fixed at 10dB and the numbers of UE per km^2 are varied from 100 to 400.

The results of the simulation are plotted in Figures 6.10 to 6.12. As predicted, the relaying cellular networks performances started to progress as the number of UEs over an area incremented. Comparing 100 with 400 UEs per km^2, the relaying cellular networks averaged call outage probability shown in Figure 6.11 had a significant improvement of 0.043 to 0.0066. This is owed to choices of surrounding candidate UEs available for relaying. That's why more reliable path could be made. Once again, the results revealed in Figures 6.10 to 6.12 depicts that the relay system that used the PERA, performs better than the other relaying algorithms.

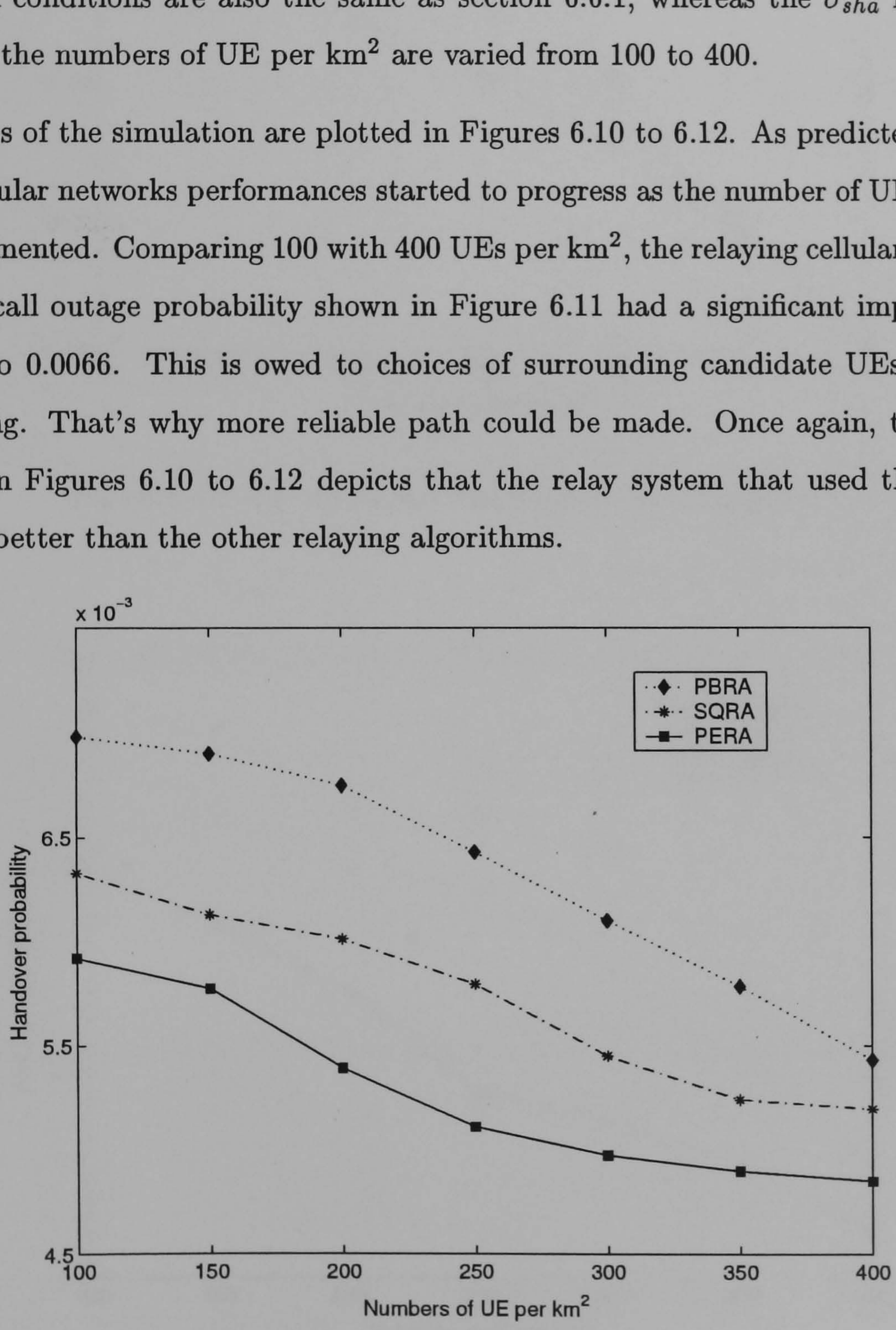

Figure 6.10: Handover probability versus the numbers of UE per km^2

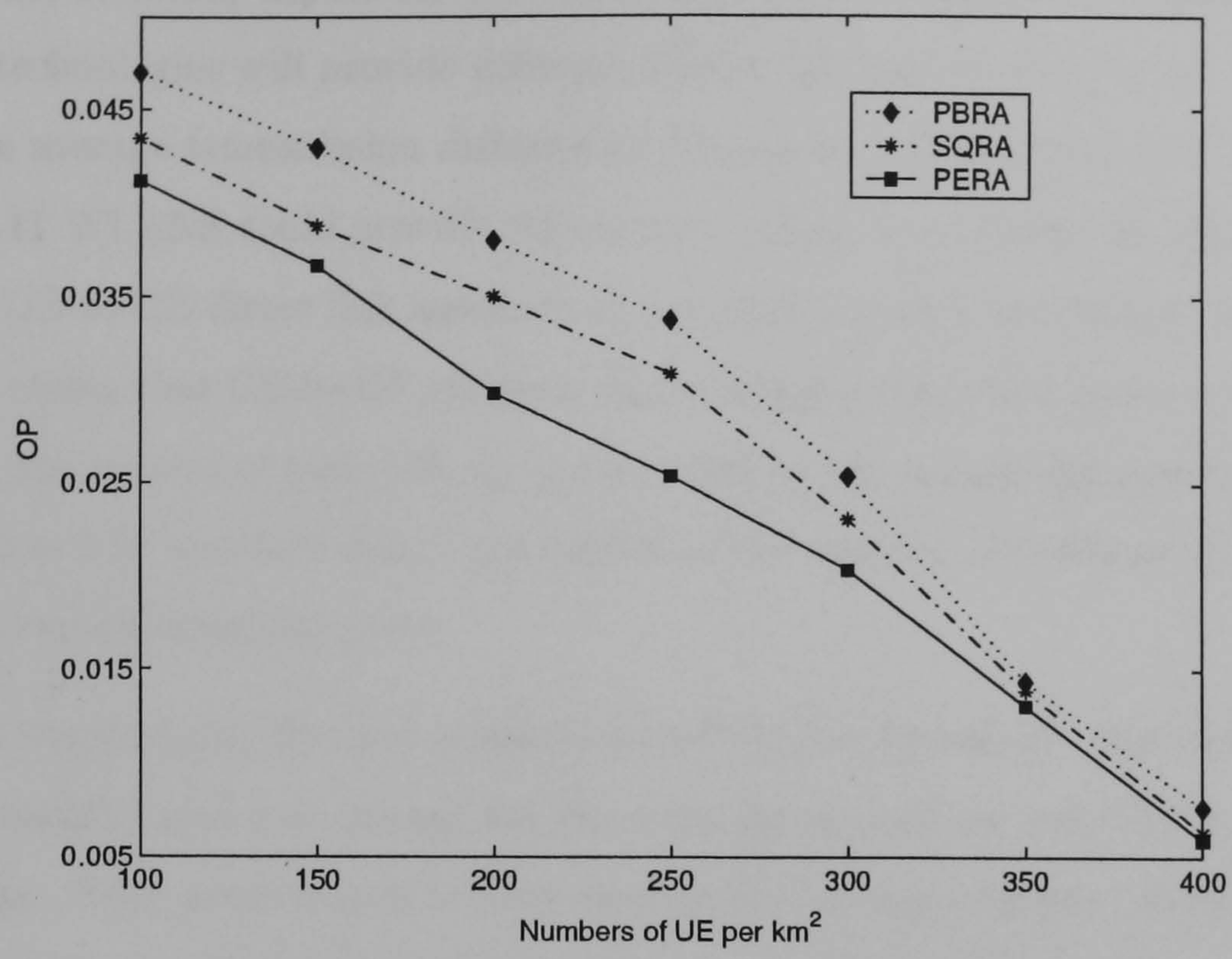

Figure 6.11: OP versus the the numbers of UE per km^2

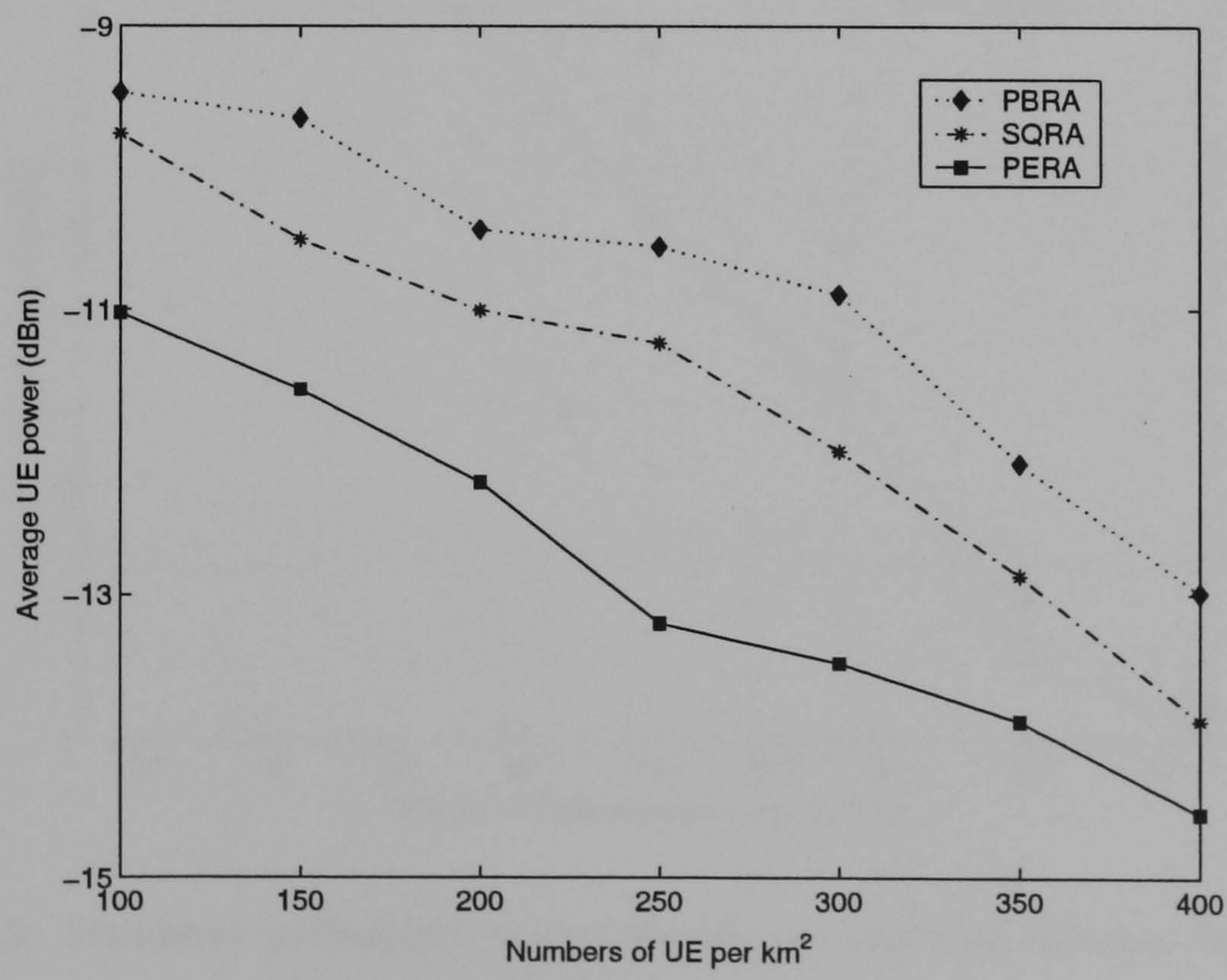

Figure 6.12: Average UE transmitting power versus the numbers of UE per km^2

As cited, the technical aspect for UE-to-UE direct link is still in an immature stage. Different technologies will provide different UE-to-UE transmission range. For an example, the average transmission distance for bluetooth technology is only 10m, while IEEE 802.11 WLANS could provide transmission range up to 100m. In order to investigate the UE-to-UE direct link issues, some simulation work is conducted. In this case, instead of saying that UE-to-UE can have direct link if the received signal is above a $\frac{E_b}{N_o}$ threshold, the success of each link up is restricted by the spatial distance between the UEs. Figures 6.13 and 6.14 depict the results of the relaying algorithms with different UE-to-UE transmission distances.

When the transmitting distance is restricted within the 10m range, the averaged handover probability and call outage for the relaying algorithms are 0.0075 and 0.047 respectively. This performance is very similar to the non-relaying cellular network, which are shown in Figure 6.3 and 6.4, with σ_{sha} equals to 10dB.

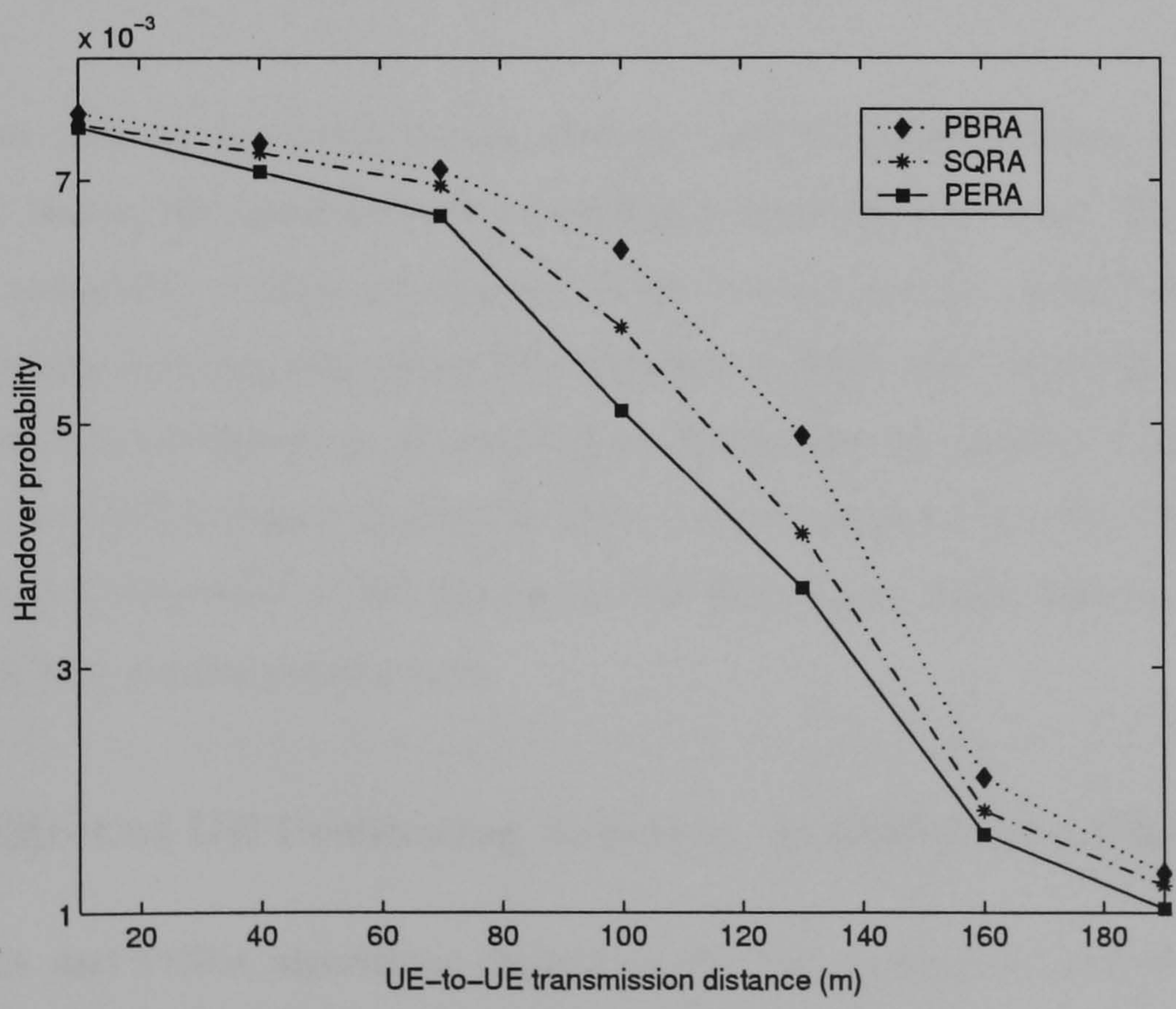

Figure 6.13: Handover probability versus the the connectivity distance between the UEs

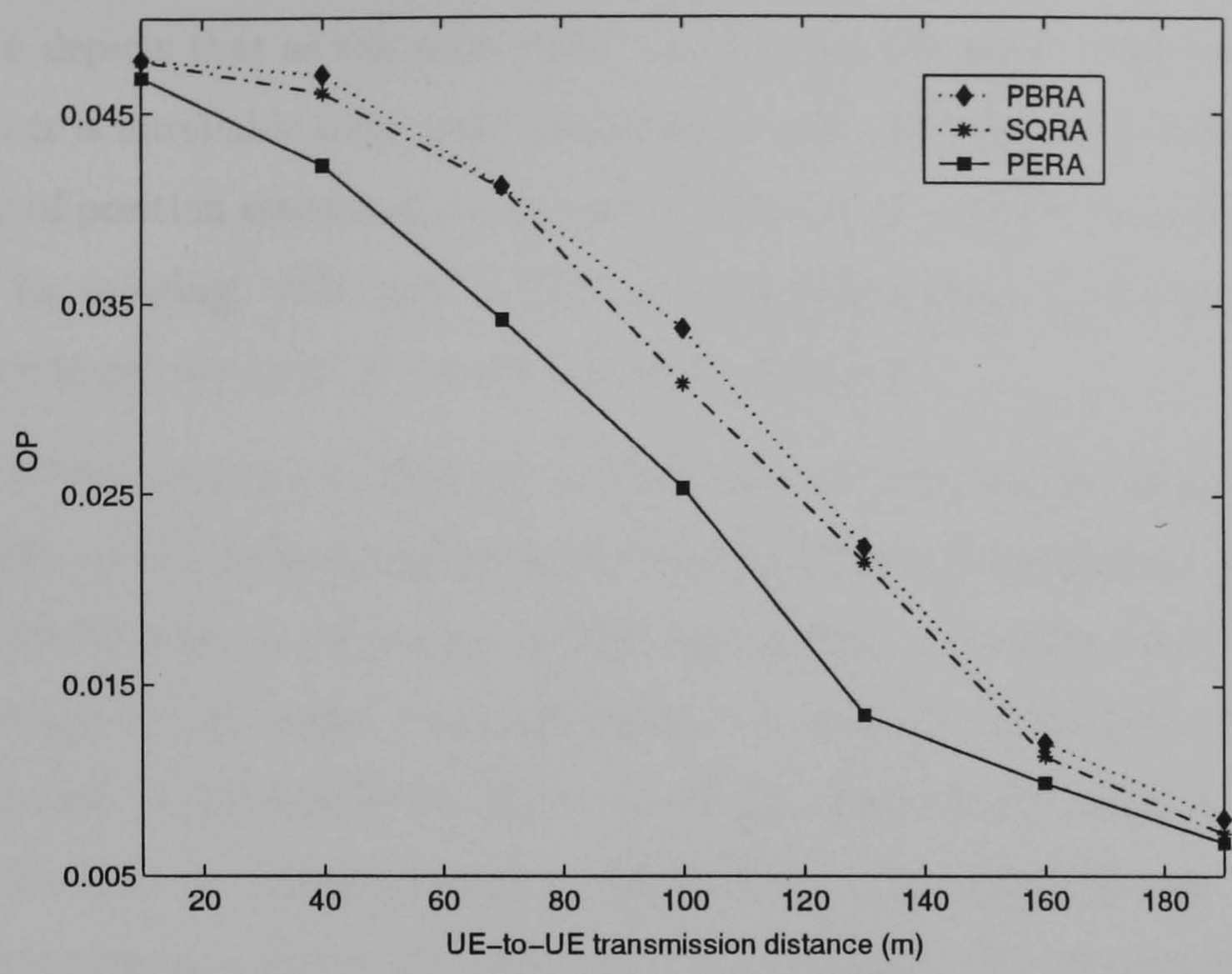

Figure 6.14: OP versus the connectivity distance between the UEs

In order to perk up the performance, the restricted distances between the UEs are increased. Hence, the handover and call outage probability decreased. This is due to the rising possibility of finding a nearby UE for relaying and also relay UE not losing its connectivity with the originating UE. Besides, at 190m, the results shown in both figures show the performances of the relaying algorithms are similar. This is mostly because of low link breakage among the UEs, for it is assumed that the UE will have direct linkup if they were within the 190m. For this reason, three relaying algorithms are able to have similar performance.

6.6.4 Effect of UE Positioning Accuracy on PBRA and PERA

The PBRA and PERA algorithms depend on the UE position to accurately predict its distance away from the NB and candidate relay UE. To validate its dependency on the distance predicted, simulations with additional UE positioning error are performed. Additional errors of 5m to 30m are added to err_a tabulated in Table 6.2. Figure 6.15 shows the UE positioning cumulative error curves, showing the estimates at 50m error drops from 69% to 30%, when additional errors increase from 0m to 30m.

Figure 6.16 depicts that as the error raises, the OP also increased. The reason for the deterioration is unreliable relay path being selected for relaying. This is linked to the inaccuracy of position estimated. In this case, distance UE may be treated as the best candidate for relaying, while nearby UEs are being dissuaded. That's why the relay path chosen is not the most favourable choice for relaying.

As likely, PBRA is severely affected by the inaccuracy of position estimated, as it only uses the spatial information for path selection. Figure 6.16 displays that at 30m error, the PBRA has an call outage of 19% higher than the SQRA, while PERA has an call outage of 10% higher than the SQRA. In addition, the PERA performance actually started to fall below the SQRA algorithm when an additional error of 18m is added to the err_a. When referred to Figure 6.15, approximately only 45% of the position estimates are within the 50m, when an additional of 18m error is added to err_a. In conclusion, if the position accuracy is able to meet the E-911 requirement, than the proposed PERA algorithm will perform better than the signal strength-based algorithm.

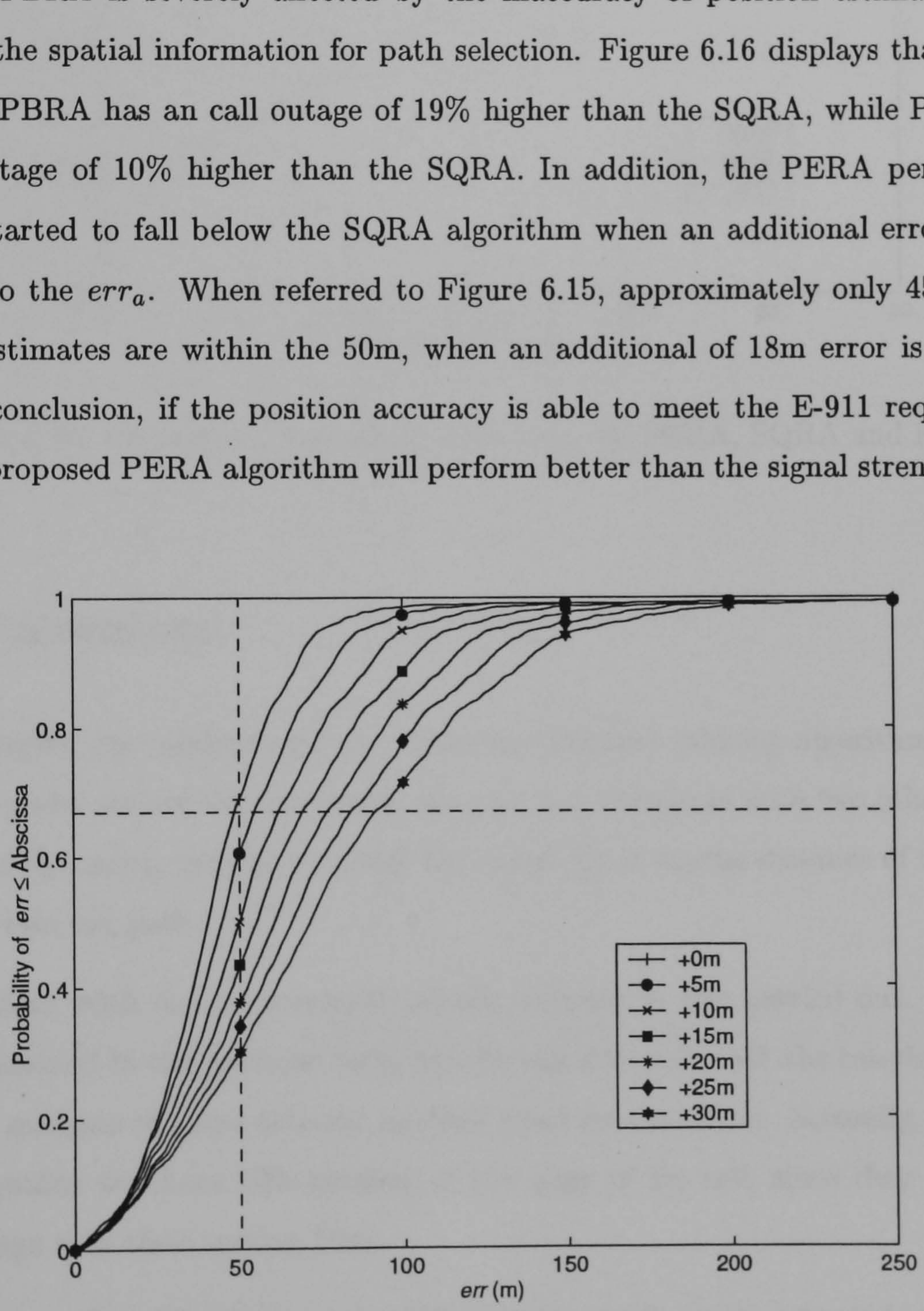

Figure 6.15: UE position estimates error profile, with additional error added to err_a

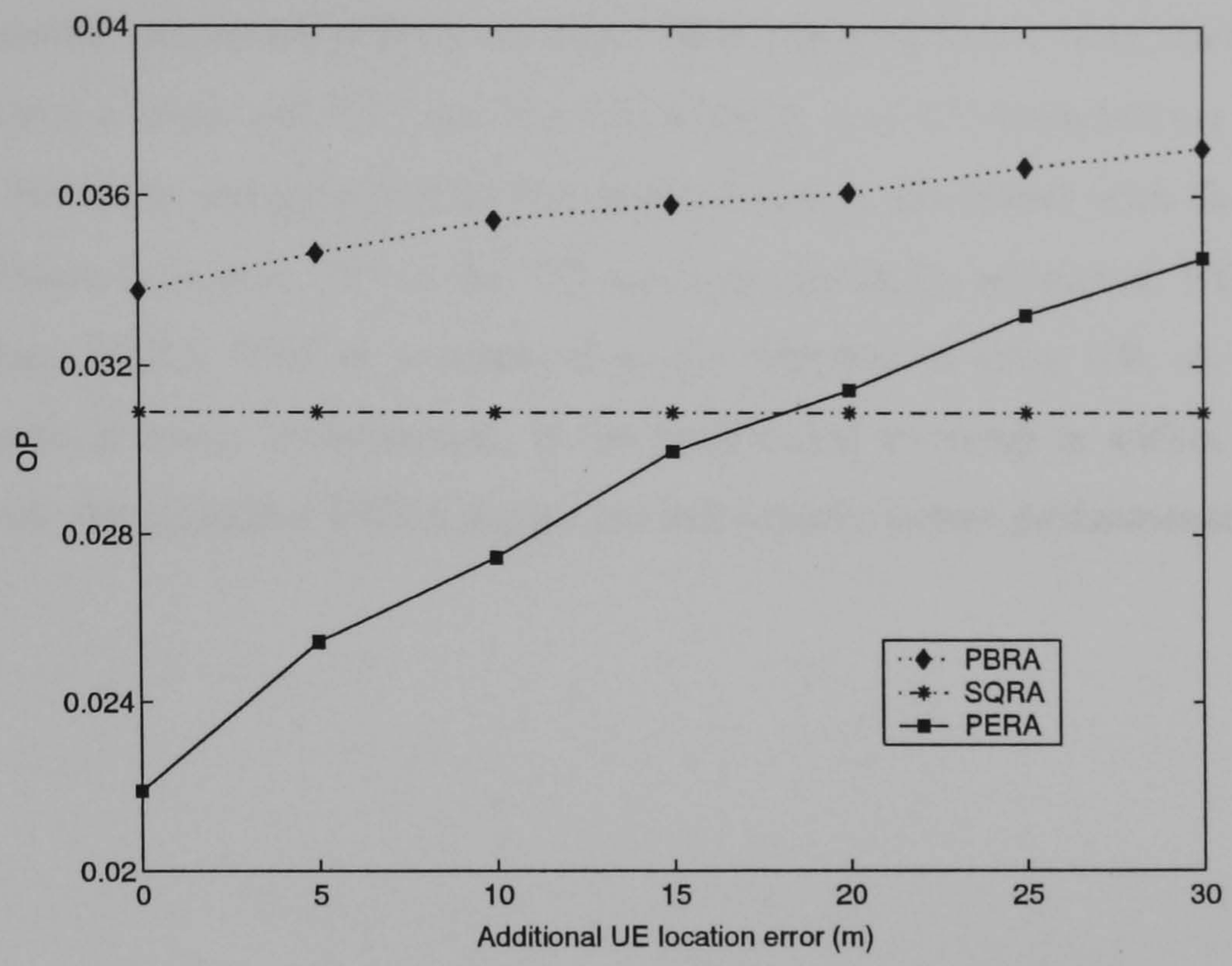

Figure 6.16: OP versus the position error err_a, for PERA, SQRA and PERA

6.7 Conclusions

In this chapter, the performance of a position enhanced relaying algorithm has been presented under several circumstances. On top, it is compared with two other relaying algorithms that solely depend on either the signal $\frac{E_b}{N_o}$ or spatial distance of the UEs to select the relaying path.

A comparison with the conventional cellular network is also carried out. From the results presented in the previous sections, one can conclude that the relaying network is able to mitigate the conventional network dead spot problem. Secondly, improving the link quality for those UEs residing at the edge of the cell, since they experience weak linkage with their serving NBs.

One of the benefits with relaying using UE is that it can be easily extended to multi-hop relaying; while using multi-hop relaying via fixed relay stations requires more stations to be installed, which may require long deployment period or incur more cost and overheads.

From the results presented, it is shown that PERA performs better than the SQRA and PBRA, where a lower call OP, handover probability and UE transmitting power are achieved. However, the proposed PERA performance is associated with the accuracy of the position estimated. When the UE positions are badly estimated, PERA is less efficient than SQRA. This as a result of wrong selection of relay UE, so, unreliable relaying path is used. Nevertheless, if the positioning accuracy is within the E-911 requirement, the proposed PERA algorithm will achieve better performance SQRA.

Chapter 7

Conclusions

Position estimation of the UE in the cellular networks is becoming important, because of the stringent requirement for meeting the E-911 standard and the value added location-based services of the future cellular networks. A precise position estimation capability will allow the service providers not only to satisfy the FCC requirements but also to offer new services to remain competitive. In addition, the LCS also provides useful information for network planning and mobility management schemes. This thesis has investigated the performance of an UE position method in a hybrid *ad hoc* cellular network. Firstly, the T1P1 channel model has been implemented to verify the performance of the location service. The OTDoA method has been presented with different channel scenarios. On top, the results obtained are used to compare with the proposed time-based HAHCP method. The use of UE spatial information to assist in mobility management is also being considered. A position enhanced SHO algorithm for the UMTS is proposed and simulation work was carried out to verify its performance. Furthermore, a relaying algorithm that uses the UE position to assist in path selection is suggested for the relaying cellular network. This chapter will give the conclusion of the work and suggestions for future work in this area are also presented.

7.1 Summary of Results

In chapter 2, the background of UE positioning is conversed, presenting an overview of terminal and network centric methods. The time-based methods are found to be the most attractive solutions since delay estimation can be done in the synchronisation phase. Secondly, the HAHCP method is introduced in this chapter. The HAHCP method uses the nearby UEs with positioning information to function as the PEs, to aid in positioning. This method requires the UE to have direct connectivity with other UEs, forming a temporary *ad hoc* network. The advantages of this method are to resolve hearability problem usually encountered in the fixed-based cellular locating method, where the UE is out of the transmission range of minimum 3 NBs. What's more, additional timing observations between the UEs will provide a better fix for the least square estimator.

Chapter 3 discussed the position enhanced SHO and relaying algorithms. It is known that SHO algorithms that use fixed hysteresis margins only make handover perform best at certain scenarios. Therefore, the UE position information is used to assist in handover. The geographical location of UE allows one to determine the mobility pattern of the UE, and in return, use to fine-tune the hysteresis margins of the SHO. Chapter 3 also introduced a relaying concept to resolve the coverage problem in conventional cellular network. UE that is having weak linkage with the serving NB may use nearby UE to relay its data packets to the NB. This will allow faster deployment and is more cost efficient than using relaying station. However, link breakage will occur if the relay UE moves out of the relaying network, causing call outage. As a result, the challenge is to find the best relaying path for the originating UE. In this part of our work, a position enhanced relaying algorithm is proposed to enhance the path selection process. Unfortunately, both the position enhanced SHO and relaying algorithms performance depend on the accuracy of the UE position estimated.

In Chapter 4, the T1P1 channel model is developed to verify the performance of the location service. The wideband channel model is based on the CoDiT channel model [70] and further modified by Lundqvist et al. [68]. Besides, the LOS and NLOS model by Thomas et al. [72] is implemented into the channel model. With the channel model

developed, different channel parameters that affect the accuracy of the position estimator can be investigated. During the course of the simulations it is found that the $\frac{E_b}{N_o}$ level in the received sequence, has a direct impact on the timing observation.

The effect of NLOS error on timing estimation is examined as a function of two NLOS parameters: LNLOS and CNLOS. As anticipated, when the probability of NLOS increases, the error in the timing estimation also increased. As the first arrival path will be the reflected or refracted path from the scatterers, travelling longer than the direct distance between the transceivers.

The location of UE that reside in a cell also affects the accuracy of the estimator. UE that exist at the rim of the cell have a better visibility with neighbouring NBs, compared with UE at the centre of the cell. For this reason, accuracy starts to deteriorate when UE moves to the centre of the cell. Therefore, the nearby UEs in a hybrid *ad hoc* cellular network is suggested to act as the PEs to resolve the hearability problem with remote NBs. Using this method, hearability improvement of 22% and 39% for urban and suburban environments are observed when UEs resided near the centre of the cell. Also, the accuracy of the estimates is also improved. Simulation results show that at $\frac{E_b}{N_o}$ of 0dB, 51% and 66% of the estimates are within the 50m error for urban and suburban, when the proposed HAHCP method is employed. While the conventional OTDoA method could only attain a 35% and 50% of estimates that are within the 50m error, which is 16% lower than the HAHCP method.

Nevertheless, the performance of the HAHCP depends on the availability of UEs that are nearby for positioning. As expected, when the numbers of UE over an area increases, the probability of having an extra UE to assist in positioning increased. Hence, this will provide additional timing observations to the least-squared estimator, and more accurate position could be calculated.

In Chapter 5, the performance of a position enhanced SHO is presented under several scenarios. When signal quality is used as the only criteria for handover, the performance of such a SHO algorithm will fail to perform in situations when UE is having high mobility or when the channel conditions vary greatly. Significant improvement is achieved if UE position is used to assist in handover. The distance of UE and direction

of movement with desired NB are used to adaptively adjust the hysteresis margins of the SHO algorithm. Handover is enhanced or delayed by decrementing or incrementing the $Hyst_d$ and $Hyst_\Theta$. But, when the position of UE is badly estimated, the performance of such a SHO algorithm can be worse than the UTRA SHO. Fortunately, the simulation results show that the position enhanced SHO algorithm starts to function underneath the UTRA SHO algorithm when an additional 15m error is added to err_a. This would correspond to 30% of the estimates within the 50m error, which is much lower than the OTDoA and HAHCP methods investigated in Chapter 4.

In Chapter 6, the performance of a position enhanced relaying algorithm is proposed. Simulation results have shown that the relaying concept could improve the coverage problem encountered in the conventional cellular network. In addition, the PERA are compared with the two other algorithms that are based on received signal quality (SQRA) and geographical distance between the transceiver (PBRA). Once again, multiple criteria algorithm performs better than algorithm that is based on single criteria. It is revealed from the simulation work that PERA achieves better performances than the latter two relaying algorithms. Regrettably, PERA starts to perform badly when the UE position is poorly estimated. Even so, if the location service is able to meet the E-911 requirement, than it is optimistic to say the proposed PERA will perform at optimum level.

7.2 Recommendations and Future Work

From this work, recommendations may be made for an operational system as well as for future work.

In this thesis, it is assumed that the UEs are able to communicate with one other if the received $\frac{E_b}{N_o}$ is above the threshold level. In particular the timing observation between the UEs is assumed to be within one chip period error, ignoring the level of $\frac{E_b}{N_o}$ and NLOS error on the ranging measurement. It will be useful to develop a wideband channel model that could verify the UE-to-UE timing observations. Taking into considerations like multi-path, $\frac{E_b}{N_o}$ and Doppler effect on the channel estimation.

The HAHCP positioning method studied is based on the WCDMA *ad hoc* cellular network. Further investigation can be conducted for other standards, like the CDMA IS-95 and Time Division Multiple Access (IS-136) in North America, and the European GSM network.

The variances of the timing observations are used to detect and weight the LOS and NLOS measurements. Performance could be enhanced with pre-filtering process and collateral information. NLOS error could be corrected as proposed by Wylie and Holtzman [77] and Kim et al. [78]. Although this will not give a completely accurate timing observation, it should gives a better timing estimate.

It is mentioned that the relaying technologies are still in an immature stage. In this thesis, it is assumed that the UTRA TDD is used for UE-to-UE communication. Candidate like the IEEE 802.11 [51] should be considered in the future investigation.

Lastly, in this work, we are only concerned with the received signal quality of the relaying cellular networks. The call outage, handover probability and UE transmitted power are used to verify the performance of the relaying algorithms. On the other hands, it is important to consider the overhead signalling required in establishing a relaying path. It can be foreseen that under such a network, will demand more from the UE. Consequently, an investigation on such an intelligent handset should be carried out.

Appendix A

Lists of Publication and Patent

A.1 Patent

J.H Yap, S. Ghaheri-Niri, R. Tafazolli, "Mobile Positioning using Integrated ad hoc Network", Patent Filed: GB 0027939.0

A.2 Publications

X Yang, J.H. Yap, S. Ghaheri-Niri and R. Tafazolli, "Enhanced positioning assisted handover algorithm for UTRA", IEEE VTC Fall, October 2001

J.H. Yap, X. Yang, S. Ghaheri-Niri and R. Tafazolli, "Dynamic hystersis values for position assisted soft handover", IEE 3G Conference, May 2002

J.H. Yap, S. Ghaheri-Niri and R. Tafazolli, "Accuracy and hearability in GSM and CDMA networks", IEE 3G Conference, May 2002

J.H. Yap, X. Yang, S. Ghaheri-Niri and R. Tafazolli, "Position assisted relaying and handover in hybrid ad hoc WCDMA system", IEEE PIMRC, September 2002

J.H. Yap and R. Tafazolli, "UE Positioning using Hybrid Ad Hoc Cellular Heterogeneous Network", WWRF7, December 2002, Eindhoven

Bibliography

[1] T.S. Rappaport, J.H. Reed, and B. D. Woerner. Position Location Using Wireless Communications on Highways of the Future. *IEEE Communications Magazine*, pages 33–41, October 1996.

[2] FCC. Enhanced 911 Emergency Calling Systems. Technical report, FCC Docket No 94-102, 1999.

[3] M_A. Dru and S. Saada. Location-based mobile services: the essentials. *Alcatel Telecommunication Review*, pages 71–76, 2001.

[4] J.H. Yap, S. Ghaheri-Niri, and R. Tafazolli. *Mobile Positioning using Integrated ad hoc Network.* CCSR, University of Surrey, U.K, GB 0027939.0, 2001.

[5] S Ghaheri Niri and R Tafazolli. Position assisted handover algorithm for multi layer cell architecture. In *IEEE Proceeding of Vehicular Technology Conference Fall*, pages 569–572, September 1999.

[6] Mark D. Austin and Gordon L. Stüber. Direction Biased Handoff Algorithm for Urban Microcells. In *IEEE Proceeding of Vehicular Technology Conference*, pages 101–105, July 1995.

[7] SA Patient. *Adaptive Communication System.* Salbu Research and Development (Proprietary) Ltd., 1978.

[8] W.G. Figel, N.H. Shepherd, and W.F. Trammel. Vehicle Location by a Signal Attenuation Method. *IEEE Transactions on Vehicular Technology*, 18:105–110, Nov 1969.

[9] Masaharu Hata and Takayoshi Nagatsu. Mobile Location Using Signal Strength Measurements in a Cellular System. *IEEE Transactions on Vehicular Technology*, pages 245–251, May 1980.

[10] Joseph Kennedy and Mark C. Sullivan. Direction Finding and "Smart Antennas" Using Software Radio Architectures. *IEEE Communication Magazine*, pages 62–68, May 1995.

[11] George P. Yost and Shankari Panchapakesan. Automatic Location Identification Using a Hybrid Technique. In *IEEE Proceeding of Vehicular Technology Conference*, pages 264–267, May 1998.

[12] Elliott D. Kaplan. *Understanding GPS : principles and applications.* Artech House Inc, 1996.

[13] B. Hofmann-Wellenhof. *Global positioning system : theory and practice.* Springer-Verlag Wien New York, 3 edition, 1994.

[14] Yilin Zhao. *Vehicle Location and Navigation Systems.* Artech House, Inc., 1997.

[15] Seymour H. Roth. History of Automatic Vehicle Monitoring (AVM). *IEEE Transactions on Vehicular Technology*, pages 2–6, February 1977.

[16] George L. Turin, William S. Jewell, and Tom L. Johnston. Simulation of Urban Vehicle-Monitoring Systems. *IEEE Transactions on Vehicular Technology*, pages 9–16, February 1972.

[17] George L. Turin, Fred D. Clapp, Tom L. Johnston, Stephen B. Fine, and Dan Lavry. A Statistical Model of Urban Multipath Propagation. *IEEE Transactions on Vehicular Technology*, pages 1–9, February 1972.

[18] W.T. Warren, James R. Whitten, Roy E. Anderson, and Miguel A. Merigo. Vehicle Location Experiment. *IEEE Transactions on Vehicular Technology*, pages 92–101, August 1972.

[19] Marko I. Silventoinen and Timo Rantalainen. Mobile Station Emergency Locating in GSM. In *International Conference on Personal Wireless Communications ICPWC*, pages 232–238, 1996.

[20] Christopher Drane, MAlcolm Macnaughtan, and Craig Scott. Positioning GSM Telephones. *IEEE Communications Magazine*, pages 46–59, April 1998.

[21] Jr. James J. Caffery and Gordon L. Stüber. Overview of Radiolocation in CDMA Cellular Systems. *IEEE Communications Magazine*, pages 38–45, April 1998.

[22] Erol Hepsaydir. Mobile Positioning in CDMA Cellular Networks. In *IEEE Proceeding of Vehicular Technology Conference*, pages 795–799, 1999.

[23] Muhammad Aatique. Evaluation of TDOA Techniques for Position Location in CDMA system. Master's thesis, Virginia Polytechnic Institute and State University, September 1997.

[24] S.S. Peter Wang, Marilynn Green, and Maged Malkawi. Analysis of Down-Link Location Methods for WCDMA and CDMA2000. In *IEEE Proceeding of Vehicular Technology Conference Spring*, May 2001.

[25] W.H. Foy. Position-Location Solutions by Taylor-Serirs Estimation. *IEEE Transactions on Areospace and Electronic Systems*, 12:187–194, March 1976.

[26] Julius O. Smith and Jonathan S. Abel. Closed-Form Least-Squares Source Location Estimation from Range-Difference Measurements. *IEEE Transactions on Acoustics, Speech, and Signal Processing*, 35(12):1661–1669, December 1987.

[27] Y.T. Chan and K.C. Ho. A Simple and Efficient Estimator for Hyperbolic Location. *IEEE Transactions on Signal Processing*, 42(8):1905–1915, August 1994.

[28] Cursor. *E-OTD for UE positioning in GSM networks.* on web page of Cursor^{TM}, www.cursor-system.com, 1995.

[29] Cellocate. *TDoA for locating UE.* on web page of Cellocate^{TM}, www.cell-loc.com, 1995.

[30] SnapTrack. *Wireless Assisted-GPS Technology for personalized, high-quality location services.* on web page of SnapTrack^{TM}, www.snaptrack.com, 1995.

[31] Simon R. Saunders. *Antennas and Propagation for Wireless Communication Systems.* John Wiley & Sons, Ltd., 1999.

[32] Y. Okumura, E. Ohmori, T. Kawano, and K. Fukuda. Field strength and its variability in VHF and UHF land mobile radio service. *Review of the Electrical Communications Laboratory*, 16:825–873, 1968.

[33] Masaharu Hata. Emprical Formula for Propagation Loss in Land Mobile Radio Services. *IEEE Transaction on Vehicular Technology*, VT-29(3):317–325, August 1980.

[34] COST 231 Final Report. Digital Mobile Radio: COST 231 View on the Evolution Towards 3^{rd} Generation Systems. Technical report, Commission of the European Communities and COST Telecommunications, Brussels, 1999.

[35] *UMTS; Selection procedures for the choice of radio transmission technologies of the UMTS.* 3GPP TR 101.112 version 3.2.0, April 1998.

[36] Jan-Erik Berg. A Recursive Method For Street Microcell Path Loss Calculation. In *IEEE PIMRC*, volume 1, pages 140–143, 1995.

[37] T.J. Harrold, A.R. Nix, and M.A. Beach. Propagation Studies for Mobile-to-Mobile Communications. In *IEEE Proceeding of Vehicular Technology Conference*, pages 1251–1255, 2001.

[38] M Gudmundson. Correlation Model for Shadow Fading in Mobile Radio Systems. *IEE Electronic Letters*, 27(23):1145–1146, 1991.

[39] Jr. Peyton Z. Peebles. *Probability, Random Variables, and Random Signal Principles.* McGraw-Hill, Inc, 3 edition, 1993.

[40] Roger L. Peterson, Rodger E. Ziemer, and David E. Borth. *Introduction to Spread Spectrum Communications.* Prentice Hall, 1995.

[41] Simon Haykin. *Communication Systems.* John Wiley and Sons, INC, third edition, 1994.

[42] John G. Proakis. *Digital Communications.* McGraw Hill, fourth edition, 2001.

[43] John Neter, Micheal H. Kutner, Christopher J. Nachtsheim, and William Wasserman. *Applied Linear Statistical Models.* McGraw-Hill, Inc, 4 edition, 1996.

[44] *UMTS; Stage 2 functional specification on UE positioning in UTRAN.* 3GPP TS25.305 version 5.4.0 Release 5, April 2002.

[45] Hongyi Wu, Chunming Qiao, Swades De, and Ozan Tonguz. Integrated Cellular and *ad hoc* Relaying systems. *IEEE on Selected Areas in Communications*, 19(10): 2105–2115, October 2001.

[46] T.J. Harrold and A.R. Nix. Intelligent Relaying for Future Personal Communication System. In *IEEE Proceeding of Vehicular Technology Conference Fall*, 2000.

[47] T Rouse, I Band, and S McLaughlin. Capacity and Power investigation of Opportunity Driven Multiple Access ODMA. In *IEEE International Conference on Communications*, 2002.

[48] Van Morning Sreng. Coverage Enhancement Through Two-hop Relaying in Cellular Radio Systems. Master's thesis, Carleton University, 2002.

[49] Ben Willis, Thomas Haslestad, Trond Friisø, and Olav Brôveit Holm. Exploiting Peer-to-Peer communications - mesh fixed and ODMA Mobile Radio. *Journal of the IBTE*, 2, April-June 2001.

[50] Harri Holma, Sanna Heikkinen, Otto-Aleksanteri Lethtinen, and Antti Toskala. Interference considerations for the time division duplex mode of the umts terrestial radio access. *IEEE Journal on Selected Areas in Communications*, 18(18):1386–1392, August 2000.

[51] *Wireless LAN Medium Access Control (MAC) and Physical Layer (PHY) specifications: Higher-Speed Physical Layer Extension in the 2.4 GHz Band*, IEEE Std 802.11b-1999 edition, 1999.

[52] G. Corazza, D. Giancristofaro, and F. Santucci. Characterization of Handover Initialization in Cellular Mobile Radio Networks. In *IEEE Proceeding of Vehicular Technology Conference*, pages 1869–1872, 1994.

[53] M. Anagnostou and G. C. Manos. Handover related Performance of Mobile Communication Networks. In *IEEE Proceeding of Vehicular Technology Conference*, pages 111–114, 1994.

[54] W. C. Y. Lee. *Mobile Cellular Telecommunications.* McGraw Hill, second edition, 1995.

[55] *UMTS; Technical Specification Group Radio Access Network; Radio Resource Management Strategies.* 3GPP TR 25.922 version 3.0.0, 1999.

[56] T. Kanai and Y. Furuya. A Handover Control Process for Microcellular Systems. In *IEEE Proceeding of Vehicular Technology Conference*, pages 170–175, 1988.

[57] Mark D. Austin and Gordon L. Stüber. Velocity Adaptive Handoff Algorithms for Microcellular Systems. *IEEE Transactions of Vehicular Technology*, 43(3): 549–460, August 1994.

[58] Kolio Ivanov and Gustav Spring. Mobile speed sensitive handover in a mixed cell environment. In *IEEE Vehicular Technology Conference*, pages 892–896, 1995.

[59] *3GPP; Technical Specification Group Radio Access Network; Opportunity Driven Multiple Access.* 3G TR 25.924 version 1.0.0, 1999.

[60] T.S. Rouse and S. McLaughlin. Coverage-capacity analysis of Opportunity Driven Multiple Access in UTRA TDD. In *IEE 3G Mobile Communication Technologies*, pages 252–256, March 2001.

[61] T.J. Harold and A.R. Nix. Capacity Enhancement Using Intelligent Relaying for Future Personal Communications Systems. In *IEEE Proceeding of Vehicular Technology Conference Fall*, pages 2115–2120, 2000.

[62] C. K. Toh. *Ad Hoc Mobile Wireless Networks: Protocols and Systems.* Prentice Hall, 2001.

[63] G. Aggelou and R. Tafazolli. On the relaying capability of next generation gsm cellular networks. *IEEE Personal Communications*, pages 40–47, February 2001.

[64] N. Vaidya Y. Ko. Location-Aided Routing (LAR) in Mobile Ad Hoc Networks. In *MOBICOM'98*, pages 66–75, October 1998.

[65] G. Aggelou and R. Tafazolli. Determining the Optimal Configuration for the Relative Distance Microdiscovery Ad Hoc Routing Protocol. *IEEE Transactions on Vehicular Technology*, 51(2):354–370, March 2002.

[66] *UMTS; Spreading and modulation (FDD).* 3GPP TS 125.213 version 5.1.0 Release 5, June 2002.

[67] *UMTS; UTRA (BS) FDD; Radio transmission and reception.* 3GPP TS 125.104 version 5.3.0 Release 5, July 2002.

[68] Patrick Lundqvist, Henrik Asplund, and Sven Fisher. Evaluation of positioning measurement systems. Technical Report T1P1.5/98-110, Ericsson, 1998.

[69] L.J. Greenstein, V. Erceg, Y.S. Yeh, and M.V. Clark. A new path-gain/delay-spread propagation model for digital cellular channels. *IEEE Transactions on Vehicular Technology*, 46(2):477–485, May 1997.

[70] Víctor Pérez and José Jiménez. Final propagation model. Technical Report R2020/TDE/PS/DS/P/040/a1, Telefónica, 1994.

[71] Ulrich Dersch amd Roland Rüegg. Simulations of the Time and Frequency Selective Outdoor Mobile Radio Channel. *IEEE Transactions on Vehicular Technology*, 42(3):338–344, August 1993.

[72] N.J. Thomas, D.G.M. Cruickshank, and D.I. Laurenson. Channel Model Implementation for Evaluation of Location Services. In *IEE 3G Mobile Communication Technologies Conference*, pages 446–450, March 2000.

[73] Kaveh Pahlavan, Prashant Krishnamurthy, and Jacques Beneat. Wideband Radio Propagation Modelling for Indoor Geo-location Applications. *IEEE Communications Magazine*, pages 60–65, April 1998.

[74] C. Kee, H. Jun, D. Yun, B. Kim, Y. Kim, B.W. Parkinson, T. Langestein, S. Pullen, and J. Lee. Development of indoor navigation system using asynchronous pseudolites. In *Institute of Navigation GPS-2000*, pages 1038–1045, September 2000.

[75] Tero Ojanperä and Ramjee Prasad. *Wideband CDMA for Third Generation Mobile Communications.* Artech House,, 1998.

[76] Miguel Berg. Performance of Mobile Station Location Methods in a Manhattan Microcellular Environment. In *Proceeding IEEE International Conference on Third Generation Wireless and Beyond, 3GW'01*, May 2001.

[77] Marilynn P. Wylie and Jack Holtzman. The Non-Line of Sight Problem in Mobile Location Estimation. In *IEEE 5th International Conference on Universal Personal Communication*, pages 827–831, 1996.

[78] Wuk Kim, Gyu-In Jee, and JangGyu Lee. Wireless Location with NLOS Error Mitigation in Korean CDMA System. In *3G Mobile Communication Technologies*, pages 134–138, March 2001.